

Studies on the Nucleophilic Aromatic ^{18}F -Fluorination

- From Model Compounds to Aromatic Amino Acids -

**Untersuchungen zur nucleophilen aromatischen
 ^{18}F -Fluorierung**

- Von Modellverbindungen zu aromatischen Aminosäuren -

DISSERTATION

**der Fakultät für Chemie und Pharmazie
der Eberhard-Karls-Universität Tübingen**

**zur Erlangung des Grades eines Doktors
der Naturwissenschaften**

2008

vorgelegt von

Bin Shen

Tag der mündlichen Prüfung: 17. Dezember 2008
Dekan: Prof. Dr. L. Wesemann
1. Berichterstatter: Prof. Dr. H.-J. Machulla
2. Berichterstatter: Prof. Dr. K.-P. Zeller

Diese Arbeit entstand im Zeitraum vom Feb. 2005 bis Mai. 2008 in der Sektion Radiopharmazie des Universitätsklinikums der Eberhard-Karls-Universität Tübingen unter Anleitung von Herrn Prof. Dr. H.-J. Machulla.

Acknowledgements

At first, I would like to thank Prof. Dr. Hans-Jürgen Machulla for suggesting the interesting subject of this thesis and for his constant guidance and support and in every way for the excellent working conditions.

This work was finished by cooperation with Prof. Dr. Klaus-Peter Zeller. I would like to thank for his steady and extensive support and his invaluable scientific assistance and discussions.

Dr. Michael Übele I thank for many discussions and his helpful advice, in particular, many thanks to Herren Dr. Roland Müller, Hans Bartholomä and Paul Schuler for recording MS and NMR spectra.

For the almost daily production of [^{18}F]fluoride ion, as well as excellent technical supports, I sincerely thank Dr. Gerald Reischl, Anke Stahlschmidt, Matthias Kuntzsch, Walter Ehrlichmann, Nadja Buckmüller, Denis Lamparter and Arzu Demir.

Adnan G. M. Al-Labadi, Uli Hagemann, Dirk Löffler, Dorothee Lutz, Noeen Malik and Hans Jörg Rahm, I would like to thank them for many scientific as well as non-scientific discussions and for the very pleasant atmosphere.

In general, I would like to thank all the people at Radiopharmacy PET Center, whose vital support made the whole time so convenient and my work a great experience.

for Haiping Wang

Contents

1	INTRODUCTION	1
1.1	BASIC ASPECTS OF POSITRON EMISSION TOMOGRAPHY (PET)	1
1.2	RADIONUCLIDES AND TRACERS FOR PET REGISTRATION	3
1.3	FLUORINE-18 AS A NUCLIDE FOR RADIOTRACERS	4
1.3.1	<i>Production pathway of fluorine-18.....</i>	6
1.3.2	<i>Type of radiosyntheses and specific activity of the radioactive product.....</i>	6
1.4	RADIOCHEMICAL SYNTHESSES FOR INCORPORATING ^{18}F INTO MOLECULES.....	7
1.4.1	<i>Electrophilic substitution.....</i>	8
1.4.2	<i>Nucleophilic substitution.....</i>	9
1.4.2.1	Addition of a cation	9
1.4.2.2	Water evaporation.....	9
1.4.2.3	Addition of the precursor solution	10
1.4.3	<i>Nucleophilic aromatic ^{18}F-fluorination.....</i>	10
1.4.4	<i>Indirect ^{18}F-labeling method.....</i>	11
1.5	AUTOMATIC TECHNOLOGY IN PET RADIOPHARMACEUTICALS	12
2	PROBLEM.....	14
3	RESULTS AND DISCUSSION.....	18
3.1	ORGANIC SYNTHESSES OF PRECURSORS FOR MODELING ^{18}F -LABELED AROMATIC AMINO ACIDS	18
3.1.1	<i>Model compounds as building blocks.....</i>	18
3.1.2	<i>Model compounds with a methyl substituent.....</i>	21
3.1.3	<i>The other precursors for systematic study of $S_{\text{N}}\text{Ar}$ reaction.....</i>	26
3.1.3.1	Precursor with differentially-protected hydroxyl group.....	26
3.1.3.2	Precursors with various numbers of methoxy substituents	27
3.1.3.3	Precursors with two formyl substituents.....	32
3.1.4	<i>The precursors of [^{18}F]fluoro-<i>m</i>-tyrosine containing protected 2-carboxy-2-aminoethyl substituents.....</i>	36
3.2	THE SYSTEMATIC STUDY ON THE NUCLEOPHILIC AROMATIC ^{18}F -FLUORINATION.....	39
3.2.1	<i>The principle of nucleophilic aromatic substitution.....</i>	39
3.2.1.1	Substitution pattern effect on RCY in the case of nitrobenzene derivatives.....	39
3.2.1.2	Formyl substituent as an EWG	40
3.2.1.3	Effect by LG	41
3.2.1.4	Solvent dependence	42

3.2.1.5	Effects of [¹⁸ F]nucleophile, concentration of precursor, temperature and reaction time	48
3.2.1.6	Analytical assay of ¹⁸ F-labeled product.....	48
3.2.2	<i>The effect of methoxy substituents on the S_NAr reaction.....</i>	50
3.2.2.1	Selection of protective groups for the hydroxyl group	50
3.2.2.2	Effect of methoxy groups	51
3.2.3	<i>The effect of methyl substituent on S_NAr reaction.....</i>	62
3.2.3.1	Dependence of RCY on LG.....	62
3.2.3.2	Influence of the methyl group.....	63
3.2.3.3	Attempts to improve the RCY of methyl-substituted precursors.....	67
3.2.4	<i>The effect of a second formyl substituent on the S_NAr reaction.....</i>	70
3.2.4.1	Effect of a second formyl substituent on the maximum RCY	70
3.2.4.2	Reaction Kinetics in ¹⁸ F-labeling of dialdehydic compounds.....	73
3.3	DECARBONYLATION OF THE ¹⁸ F-LABELED BENZALDEHYDES.....	76
3.3.1	<i>Decarbonylation of model compounds with monoaldehydic substituent.....</i>	76
3.3.1.1	Selection of catalyst.....	77
3.3.1.2	Solvent dependence	77
3.3.1.3	Influence of temperature.....	79
3.3.1.4	Effect of catalyst concentration	79
3.3.1.5	Decarbonylation of multiply-substituted model compounds under optimized condition	81
3.3.2	<i>Decarbonylation of model compounds with dialdehydic functions.....</i>	83
3.4	SYNTHESIS OF [¹⁸ F]FLUORO-M-TYROSINE BY A NEW DEVELOPED STRATEGY	84
3.5	AUTOMATED SYNTHESIS OF N.C.A. [¹⁸ F]FDOPA VIA NUCLEOPHILIC AROMATIC SUBSTITUTION.....	88
3.5.1	<i>Fluorination.....</i>	92
3.5.2	<i>Reductive iodination.....</i>	93
3.5.3	<i>Alkylation.....</i>	94
3.5.4	<i>Hydrolysis.....</i>	95
3.5.5	<i>Overall synthesis.....</i>	96
4	SUMMARY	98
5	EXPERIMENTAL	102
5.1	GENERAL.....	102
5.2	ORGANIC SYNTHESSES OF PRECURSORS AND STANDARDS FOR S _N AR WITH [¹⁸ F]FLUORIDE ION	104
5.2.1	<i>Model compounds as building blocks for ¹⁸F-labeled aromatic amino acids</i>	<i>104</i>
5.2.1.1	4-Formylphenyl-trimethylammonium triflate (2-N ⁺ Me ₃ TfO ⁻)	104
5.2.1.2	5-Methoxy-2-nitrobenzaldehyde (3-NO ₂).....	105
5.2.1.3	2-Chloro-5-methoxybenzaldehyde (3-Cl).....	106

5.2.1.4	2-Bromo-5-methoxybenzaldehyde (3-Br)	107
5.2.1.5	2-Iodo-5-methoxybenzaldehyde (3-I)	108
5.2.1.6	5-Methoxy-2-trimethylammoniumbenzaldehyde triflate (3-N ⁺ Me ₃ TfO ⁻)	109
5.2.1.7	4-Methoxy-2-nitrobenzaldehyde (4-NO ₂)	111
5.2.2	<i>Methyl-substituted model compounds</i>	112
5.2.2.1	3-Methyl-2-nitrobenzaldehyde (6-NO ₂)	112
5.2.2.2	2-Chloro-3-methylbenzaldehyde (6-Cl)	113
5.2.2.3	2-Bromo-3-methylbenzaldehyde (6-Br)	114
5.2.2.4	2-Fluoro-3-methylbenzaldehyde (6-F)	115
5.2.2.5	3-Methyl-4-nitrobenzaldehyde (7-NO ₂)	116
5.2.2.6	4-Bromo-3-methylbenzaldehyde (7-Br)	117
5.2.2.7	3-Methyl-4-trimethylammoniumbenzaldehyde triflate (7-N ⁺ Me ₃ TfO ⁻)	118
5.2.2.8	2-Fluoro-5-methoxy-3-methylbenzaldehyde (8-F)	120
5.2.2.9	5-Methoxy-3-methyl-2-nitrobenzaldehyde (8-NO ₂)	121
5.2.2.10	2-Bromo-5-methoxy-3-methylbenzaldehyde (8-Br)	127
5.2.2.11	2-Chloro-5-methoxy-3-methylbenzaldehyde (8-Cl)	129
5.2.3	<i>The precursors for further systematic study of nucleophilic aromatic ¹⁸F-fluorination</i> 131	
5.2.3.1	5-Ethoxy-2-nitrobenzaldehyde (12-C ₂ H ₅)	131
5.2.3.2	2-Nitro-5-propoxybenzaldehyde (12-C ₃ H ₇)	132
5.2.3.3	5-Butoxy-2-nitrobenzaldehyde (12-C ₄ H ₉)	133
5.2.3.4	5-(Benzyloxy)-2-nitrobenzaldehyde (12-Bn)	134
5.2.3.5	2-Nitro-5-(trifluoromethoxy)benzaldehyde (12-CF ₃)	135
5.2.3.6	2-Methoxy-6-nitrobenzaldehyde (13-NO ₂)	136
5.2.3.7	3,6-Dimethoxy-2-nitrobenzaldehyde (16-NO ₂)	137
5.2.3.8	3,5-Dimethoxy-2-nitrobenzaldehyde (17-NO ₂)	138
5.2.3.9	2-Bromo-3,5-dimethoxybenzaldehyde (17-Br)	139
5.2.3.10	3,4-Dimethoxy-2-nitrobenzaldehyde (18-NO ₂)	140
5.2.3.11	2,3,4-Trimethoxy-6-nitrobenzaldehyde (19-NO ₂)	141
5.2.3.12	6-Fluoro-2,3,4-trimethoxybenzaldehyde (19-F)	142
5.2.3.13	6-Bromo-2,3,4-trimethoxybenzaldehyde (19-Br)	144
5.2.3.14	2,3,4,5-Tetramethoxy-6-nitrobenzaldehyde (20-NO ₂)	145
5.2.3.15	2-Bromo-3,4,5,6-tetramethoxybenzaldehyde (20-Br)	148
5.2.3.16	2-Nitroisophthalaldehyde (21-NO ₂)	149
5.2.3.17	2-Fluoroisophthalaldehyde (21-F)	153
5.2.3.18	2-Nitroterephthalaldehyde (22-NO ₂)	156
5.2.3.19	2-Fluoroterephthalaldehyde (22-F)	158
5.2.3.20	5-Methoxy-2-nitroisophthalaldehyde (23-NO ₂)	160
5.2.3.21	2-Fluoro-5-methoxyisophthalaldehyde (23-F) and 2-fluoro-5-methoxyterephthalaldehyde (24-F)	163
5.2.3.22	5-Methoxy-2-nitroterephthalaldehyde (24-NO ₂)	168
5.2.4	<i>The precursors with protected glycine derivative</i>	172

5.2.4.1	Methyl N-(diphenylmethylene)-2-fluoro-3-formyl-5-methoxyphenylalaninate (27-F).....	172
5.2.4.2	2-(2-Fluoro-5-methoxybenzyl)-5-isopropyl-3,6-dimethoxy-2,5-dihydropyrazine (28-F) .	175
5.3	RADIOSYNTHESSES	178
5.3.1	<i>Production of [¹⁸F]fluoride ion</i>	<i>178</i>
5.3.2	<i>¹⁸F-labeling reaction</i>	<i>178</i>
5.3.3	<i>Decarbonylation of ¹⁸F-labeled product with (Ph₃P)₃RhCl</i>	<i>179</i>
5.3.4	<i>Synthesis of [¹⁸F]FDOPA by an automatic module.....</i>	<i>179</i>
5.4	ANALYTIC METHODS	181
5.4.1	<i>Analyses in ¹⁸F-labeling reaction and decarbonylation</i>	<i>181</i>
5.4.1.1	Radio thin layer chromatography	181
5.4.1.2	Radio high performance liquid chromatography	181
5.4.1.3	LC/MS	186
5.4.1.4	GC/MS.....	186
5.4.2	<i>Analyses in the automated synthesis of [¹⁸F]FDOPA.....</i>	<i>186</i>
6	REFERENCES	188
7	APPENDICES.....	194

Abbreviations

Å	angstrom (10^{-10} meter)
ACN	acetonitrile
ACPI	advanced configuration and power interface (LC/MS)
AIBN	2,2'-azobis-(2-methyl-propionitrile)
BMDAB	bromomethylenedimethylammonium bromide
Bn	benzyl group ($-\text{CH}_2\text{C}_6\text{H}_5$)
β^-	beta particle, electron
β^+	positron
c.a.	carrier-added (radiochemistry)
ca.	circa
CDCl_3	deuterium chloroform
Ci	curie (radiation)
δ	NMR chemical shift
d	days (time), doublet (NMR spectra)
d.c.	decay corrected
DCM	dichloromethane
dd	doublet of doublet (NMR spectra)
DEE	diethylether
DMAc	N,N-dimethylacetamide
DMF	N,N-dimethylformamide
DMPU	1,3-dimethyl-3,4,5,6-tetrahydro-2(1H)-pyrimidinon
DMSO	dimethylsulfoxide
DMSO-d_6	deuterium dimethylsulfoxide
EC	electron capture
EDG	electron donating group
EI	electron impact (mass spectrometry)
EOB	end of bombardment
EOS	end of synthesis
eV	electronvolt
EWG	electron withdrawing group
FAB	fast atom bombardment (mass spectrometry)
$[\text{}^{18}\text{F}]\text{FDG}$	2-deoxy-2- $[\text{}^{18}\text{F}]$ fluoro-D-glucose

[¹⁸ F]FDOPA or 6-[¹⁸ F]fluoroDOPA	3,4-dihydroxy-6-[¹⁸ F]fluoro-L-phenylalanine
g	gram
GBq	gigabecquerel
h	hour
HMTA	hexamethylenetetramine
HRMS	high-resolution mass spectrometry
HPLC	high performance liquid chromatography
Hz	hertz
IR	infrared
<i>J</i>	coupling constant (NMR spectra)
<i>k</i> *	¹⁸ F-labeling reaction rate constant (at 1 minute)
<i>k</i> '	selectivity (HPLC)
Kryptofix 222 / K2.2.2	4, 7, 13, 16, 21, 24-hexaoxa-1, 10-diazabicyclo[8.8.8]-hexacosane
LC/MS	liquid chromatography mass spectrometry
LG	leaving group
<i>m/z</i>	mass-to-charge ratio
<i>m</i>	multiplet (NMR spectra)
<i>M</i> ⁺	molecular ion (radical cation)
MBq	megabecquerel
Me	methyl
MeO	methoxy
MHz	megahertz
min	minute
mL	millimeter
m.p.	melting point (°C)
MPLC	middle-pressure liquid chromatography
MS	mass spectrometry
<i>n</i>	nano (10 ⁻⁹) or neutron
n.c.a.	no-carrier-added (radiochemistry)
NBS	N-bromosuccinimide
NMR	nuclear magnetic resonance
<i>p</i>	proton

Ph	phenyl
PCC	pyridinium chlorochromate
PDC	pyridinium dichlorochromate
PET	positron emission tomography
ppm	parts per million
PTSA	toluene-4-sulfonic acid
RCY	radiochemical yield (¹⁸ F-incorporation)
R _f	retention factor (TLC)
R _t	retention time (HPLC)
s	singlet (NMR spectra)
SD	standard deviation
S _N Ar	nucleophilic aromatic substitution
t	triplet (NMR spectra)
t _{1/2}	half life
THF	tetrahydrofuran
TLC	thin layer chromatography
TMEDA	N,N,N',N'-tetramethylethylenediamine
TMS	tetramethylsilane
UV	ultraviolet
$\bar{\nu}$	wavenumber
vs	versus
Y	yield

1 INTRODUCTION

1.1 Basic aspects of positron emission tomography (PET)

In contrast to the imaging techniques of magnetic resonance tomography (MRT) and X-ray computed tomography (CT), emission tomography technology shows the special advantage of visualising pathophysiological, physiological and metabolic processes. Emission tomography is possible as single photon emission tomography (SPECT) and positron emission tomography (PET). Both are routinely used in nuclear medicine and pharmacological research.¹ Although SPECT has become more developed in the past several years, PET is the more advanced technology, as PET shows a high sensitivity (more than 100-fold of SPECT) and its most important quantitation methods are well-elaborated.

Around the year 2000, PET had its international breakthrough as a method. This can clearly be seen by the broad application of PET/CT in clinical research and healthcare.²⁻⁴ Moreover, during the last three years animal PET has become available, allowing the determination of biochemical processes and biokinetics within small animals.⁵ In this unique international situation, radiopharmaceutical methods play a key role in PET applications since the spectrum of applications directly depends on the availability of compounds labeled with radionuclides appropriate for PET studies.

For labeling PET radiotracers, short-lived neutron-deficient positron emitters are of primary interest. The radioactive decay of the PET radionuclides gives rise to the emission of a positron. The positron loses its kinetic energy by collisions and interacts with matter over a short distance. The range depends on the β^+ -energy, which is specific for the employed isotope (Table 1-1),^{6,7} and reaches from less than 1 mm to several millimetres. When the positron is near rest, it interacts with an electron, its anti-particle. A positron and an electron compose an intermediary positronium, an exotic atom showing similarities to hydrogen. In the positronium, the particles “spiral” closer to each other until they are terminated by annihilation radiation. In a few microseconds, two gamma photons are released from the singlet state and show a nearly 180° emission. Each of them carries a characteristic energy of 511 keV (Figure 1-1).⁸

Table 1-1. Positron emitters used for PET and their important nuclear data

Nuclide	Half-life	Decay mode (%)	E _{β⁺, max} (keV)
¹¹ C	20.4 min	β ⁺ (99.8), EC (0.2)	960
¹³ N	9.96 min	β ⁺ (100)	1190
¹⁵ O	2.03 min	β ⁺ (99.9), EC (0.1)	1720
³⁰ P	2.5 min	β ⁺ (99.8), EC (0.2)	3250
¹⁸ F	109.6 min	β ⁺ (97), EC (3)	635
⁷⁵ Br	98 min	β ⁺ (75.5), EC (24.5)	1740
⁷⁶ Br	16.1 h	β ⁺ (57), EC (43)	3900
⁷³ Se	7.1h	β ⁺ (65), EC (35)	1320
¹²⁰ I	1.35 h	β ⁺ (64), EC (36)	4100
¹²⁴ I	4.18 d	β ⁺ (25), EC (75)	2140
³⁸ K	7.6 min	β ⁺ (100)	2680
⁶² Cu	9.7 min	β ⁺ (98), EC (2)	2930
⁶⁴ Cu	12.7 h	β ⁺ (18), β ⁻ (37), EC (45)	655
⁶⁸ Ga	68.3 min	β ⁺ (90), EC (10)	1900
⁸² Rb	1.3 min	β ⁺ (96), EC (4)	3350
⁸⁶ Y	14.7 h	β ⁺ (34), EC (66)	1300
^{94m} Tc	52 min	β ⁺ (72), EC (28)	2470
⁷² As	26 h	β ⁺ (88), EC (12)	2515

These resulting two body-penetrating gamma photons provide the basis for measurement by PET (Figure 1-1). The PET scanner (PET camera) consists of circular arrangement of scintillation detectors. In these rings of detectors, pairs of opposite detectors are connected for coincidence measurements. As a result, the two γ -rays of the annihilation process are detected if they hit both of the opposite detectors within a timeframe of a few nanoseconds. The visual field of the tomographic system is defined by the central area covered by all fan-shaped areas of coincidence. The body of the patient is placed in that visual field. If compounds labeled with positron-emitting isotopes are accumulated in certain regions of the body, an image of this region can be reconstructed with tomographic slices from the detected annihilation events. Computer-aided image reconstruction of the data from several transverse measurement planes allows the output of a 3D-image of the region of interest. The latest innovation is that modern scanners combine PET and MRT in one instrument, which leads to 3D-images with exact morphologic information as well as a physiological and biochemical assessment.⁹ Those procedures are highly relevant in the clinical management of oncologic therapy.

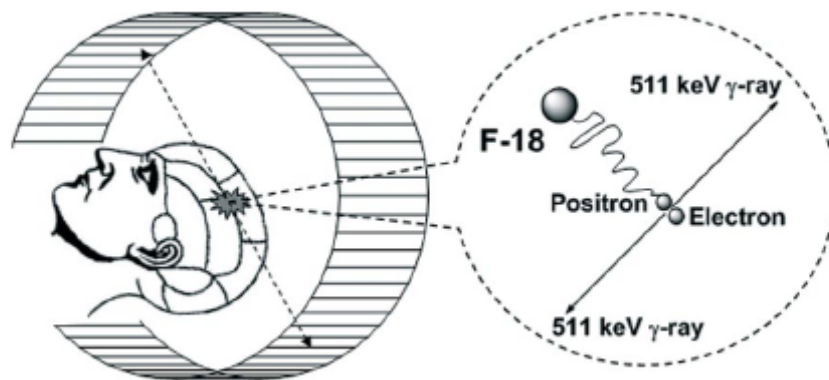


Figure 1-1. Radioactive decay by positron emission and annihilation coincidence detection in PET device ¹⁰

1.2 Radionuclides and tracers for PET registration

As mentioned before, PET is an excellent imaging technique with the advantages of very high sensitivity, good spatial resolution and the ability to assess (patho) physiological processes and functions in a highly-quantitative way. Therefore, the continuous improvement and advanced development of suitable and highly-specific radiotracers has been necessary for performing any type of PET investigation. The development of a radiotracer begins with the selection of an appropriate radionuclide (Table 1-1).

In general, radionuclides can be divided into three types: organic, analogous and metallic. The so-called “organic” PET nuclides, i.e. ^{11}C , ^{15}O , ^{13}N and ^{30}P , allow authentic labeling without any changes in the (bio)-chemical and physiological behaviour or properties of the labeled compounds. However, extremely short half-lives of those isotopes, from two to twenty minutes, limit their applicability. Only the half-life of ^{11}C ($t_{1/2} = 20.4$ min) provides the possibility of multi-step radiosyntheses and allows PET measurements of slower physiological processes. The so-called “analogous” radiotracers are commonly labeled with ^{18}F , $^{75,76}\text{Br}$, ^{73}Se and $^{120,124}\text{I}$. Their longer half-lives range from 1.35 h to 4.15 d, and allow more extensive radiosyntheses as well as PET studies of slower biochemical processes. Generally, analogous tracers make use of similarities in steric demand and/or in electronic character of the substituted atom or function. A third group of suitable positron emitters for PET is represented by the metallic isotopes. In contrast to the “organic” and “analogous” PET nuclides, a few metallic isotopes are achievable by generator systems (i.e. ^{82}Rb , ^{62}Cu and ^{68}Ga), so that they are available in places

without an on-site cyclotron.¹¹ For *in vivo* studies, they are applied as free cationic tracers or as metal complexes.

In the selection of the radionuclide, the following considerations are compulsory. The first is whether the physical half-life of the radioisotope matches the biological half-life of the process under investigation. The final radiotracer's achievable specific activity (see paragraph 1.3.2) is also a crucial point. In addition, the time necessary to perform the radiochemical reaction, manipulation through the subsequent synthetic pathways and/or purifications are influential in the decision. Furthermore, the type of information to be obtained from the PET measurement is also important in the selection of the radioisotope. Finally, the spatial distribution and regional concentrations of a target substance or neurotransmitter uptake site are also taken into consideration.

1.3 Fluorine-18 as a nuclide for radiotracers

At present, in the clinical application of PET, fluorine-18 is one of the most suitable nuclides for the syntheses of radiotracers, although it is not a significant element in the living system. As fluorine-18 (1.35 Å) has a very sterically similar size to hydrogen (1.20 Å) and shows extremely electronegative character, such substitution can often produce significant and useful changes in physicochemical and biological properties of radiopharmaceutical compounds. The most famous and most widely-used PET radiopharmaceutical is 2-deoxy-2-[¹⁸F]fluoro-D-glucose ([¹⁸F]FDG). For the first metabolic steps, [¹⁸F]FDG is accepted as a glucose analogue. It is taken up into cells by glucose transporters. In cells, it is metabolised by the enzyme hexokinase to 2-[¹⁸F]fluorodeoxyglucose-6-phosphate, but ¹⁸F- for -OH substitution in the original glucose molecule leads to a blockage of the metabolism and leaves the phosphorylated FDG in the cell unaltered. Thus, FDG accumulates and gives rise to a PET signal which can very well be registered. Active cancer tissue can be detected because of its elevated glucose metabolism.¹² On the other hand, the success of cancer chemotherapy results in the death of the cancer cells and, consequently, in low or no accumulation of [¹⁸F]FDG. Another typical application of [¹⁸F]FDG is the investigation of the biodistribution of drugs in the body or the detection of receptors for certain biomolecules. In recent years, the number of newly-developed ¹⁸F-labeled pharmaceuticals has increased rapidly, such as 6-[¹⁸F]FluoroDOPA, [¹⁸F]Fluoro- α -methyltyrosine and [¹⁸F]Fluoromisonidazole. They are widely used in research on

dopamine metabolism, tumor imaging and hypoxia imaging. Table 1-2 shows a list including a couple of important ^{18}F -labeled radiotracers and their applications.¹³

Table 1-2. Fluorine-18 labeled radiopharmaceuticals in clinical use¹³

Compound	Common synthesis	Clinical utility
6- ^{18}F FluoroDOPA	Electrophilic fluoro-demetalation; nucleophilic aromatic substitution	Dopamine metabolism
6- ^{18}F Fluoro-m-tyrosine	Fluorodestannylation	Dopamine metabolism
6- ^{18}F Fluorophenylalanine	Electrophilic fluorination with ^{18}F AcOF	Neutral amino acid transport
2- ^{18}F Fluoro-4-boronophenylalanine	Electrophilic fluorination with ^{18}F AcOF	Neutron capture therapy titration
^{18}F Fluoroethyltyrosine	O-alkylation with ^{18}F fluoroethyl tosylate	Tumor imaging
^{18}F Fluoro- α -methyltyrosine	Electrophilic fluorination with ^{18}F AcOF	Tumor imaging
6- ^{18}F Fluorodopamine	Nucleophilic aromatic substitution	Cardiac sympathetic innervation
(-)-6- ^{18}F Fluoronorepinephrine	Nucleophilic aromatic substitution	Cardiac sympathetic innervation
6- ^{18}F Altanserin	Nucleophilic aromatic substitution	5HT _{2A} receptors
^{18}F Fluoroethylspiperone	N-alkylation with ^{18}F fluoroethyltosylate	D ₂ receptor
^{18}F Fluoromisonidazole	N-alkylation using ^{18}F epifluorohydrin	Hypoxia imaging
5- ^{18}F Fluorouracil	Direct electrophilic fluorination with ^{18}F F ₂	Tumor imaging
16 α - ^{18}F Fluoroestradiol	Nucleophilic displacement of aliphatic cyclic sulfone	Estrogen receptor positive tumors
^{18}F Fleroxacin	Nucleophilic displacement of mesylate	Antibiotic pharmacokinetics
^{18}F CFT	Fluorodestannylation with high spec. act. ^{18}F AcOF	Dopamine transport

The success of fluorine-18 as a routine PET nuclide in diagnosis and pharmacological research is based on its chemical and nuclear properties. Fluorine-18 can be produced in good yields, even with low-energy cyclotrons. As mentioned above, the half-life of 109.7 min allows both time-consuming multi-step radiosyntheses up to 3 h and extended PET studies of slower biochemical processes. In addition, this half-life makes shipment within a range of at least 200 km possible. In the so-called satellite concept, the supply of clinics without an on-site cyclotron can be ensured.¹⁴ The ^{18}F has a low β^+ -energy of 635 keV that provides a very high resolution for PET images and guarantees minor radiation doses to the patients. In terms of chemistry, several facile labeling reactions and methods are known for ^{18}F -introduction into organic molecules.

1.3.1 Production pathway of fluorine-18

The PET nuclides are generally produced by the bombardment of stable isotopes by small charged particles in accelerators. Protons, deuterons and alphas are predominately employed. The final chemical form of the product depends on the type of nuclear reaction and even more on the target, the aggregate state (i.e. gas, liquid, solid) and the chemical form of the target material.

Fluorine-18 can be produced for nucleophilic and electrophilic labeling reaction by using various types of nuclear reactions. The most common forms of fluorine-18 are listed in Table 1-3.^{6, 15-17} Currently, the use of the $^{18}\text{O}(p,n)^{18}\text{F}$ reaction on ^{18}O -enriched water is the most effective and reliable for the production of [^{18}F]fluoride ion with high specific activity. Thus, under optimised conditions, high amounts of [^{18}F]fluoride ion can easily be achieved from cyclotrons, even with low-energy machines, within less than one hour of irradiation time. In the case of electrophilic radiolabeling reactions, fluorine-18 can be produced as [^{18}F]F₂ or [^{18}F]acetylhypofluorite in a neon target. In that method, the major problem is the deposition of the produced fluorine-18 on the target walls. Therefore, the target has to be treated in advance with a 1 % fluorine/neon gas mixture in order to coat the target walls with F₂. The fluorine acts as a kind of “carrier gas” by facilitating the transport of fluorine-18 from the target to the laboratory. The addition of non-radioactive fluorine to the target results in a lower specific activity of the produced fluorine-18, so this production method is not applicable for the syntheses of radiotracers that require a high specific activity.

Table 1-3. Most common nuclear reactions for production of fluorine-18^{6, 15-17}

Reaction	$^{18}\text{O}(p,n)^{18}\text{F}$	$^{16}\text{O}(^3\text{He},p)^{18}\text{F}$	$^{20}\text{Ne}(d,\alpha)^{18}\text{F}$	$^{18}\text{O}(p,n)^{18}\text{F}^c$
Target	H ₂ ¹⁸ O ^a	H ₂ O	Ne _(0.1-0.2 % F₂) ^b	¹⁸ O ₂ , Kr _(1 % F₂) ^b
Particle energy [MeV]	16→3	36→0	14→0	10→0
Main product form	¹⁸ F _{aq} ⁻	¹⁸ F _{aq} ⁻	[¹⁸ F]F ₂	[¹⁸ F]F ₂
Yield [GBq/μAh]	2.22	0.26	0.37-0.44	~0.37
Specific activity [Bq/mmol]	≤ 3.7×10 ¹⁵	≤ 3.7×10 ¹⁵	≤ 3.7×10 ¹⁰⁻¹¹	≤ 3.7-185×10 ¹⁰

a Ti-target with Ti-window. **b** passivated Ni-target. **c** two steps process.

1.3.2 Type of radiosyntheses and specific activity of the radioactive product

In principle, radiosyntheses can be classified as: carrier-free, no-carrier-added (n.c.a.) and carrier-added (c.a.). Ideally, carrier-free systems are only achieved when artificial

radioelements (i.e. astatine) are used and the presence of non-radioactive isotopes of the element is excluded. Nevertheless, in radiosyntheses with cyclotron-produced radionuclides of naturally-occurring elements, tracers of stable isotopes of these elements are omnipresent and act as isotopic carriers. Even the most accurate operation methods can not circumvent this effect. Under those conditions radiosyntheses are referred to be performed as no-carrier-added (n.c.a.) processes. In contrast, some circumstances require the addition of weighable quantities of stable isotopes. In the case of [^{18}F]F₂ production, fluorine gas is added because n.c.a. [^{18}F]F₂ is too reactive to be removed from the walls of targets and tube lines. These methods are termed as carrier-added (c.a.).

The extent to which a compound labeled with a radionuclide is diluted with the non-radioactive isotopic compound is referred to as the specific activity. The specific activity is calculated from the ratio of the amount of radioactive compound (Becquerel, Bq or Curie, Ci) and the molar concentration of the compound (mol), and is usually expressed in GBq/ μmol or Ci/mmol.¹⁸ The maximum theoretical specific activity of fluorine-18, with a half-life of 110 min, is 63,000 GBq/ μmol (1.7×10^6 Ci/mmol). In practice, much lower specific activities are obtained due to the unavoidable dilution with the ubiquity of the stable element (i.e. ^{19}F). PET investigations using labeled biomolecules with very low concentrations in the destined tissue (i.e. substrates of enzymes, receptor ligands and reuptake inhibitors) demand radiotracers of very high specific activities. Therefore, n.c.a. ^{18}F -fluorination has been taken under more intensive consideration for the radiosyntheses of ^{18}F -labeled radiopharmaceuticals.

1.4 Radiochemical syntheses for incorporating ^{18}F into molecules

In general, fluorination is more difficult than other halogenations, because most fluorinating reagents are either very toxic, corrosive to glass and metals or too reactive. Fluorination with fluorine-18 is also different from fluorine-19. First, this work is related to the decay in the case of radioactive ^{18}F and the need to conduct all of the work, including the syntheses of reagents *in situ* and the fluorination reaction, within a limited time. In addition, in ^{19}F -fluorination reactions, the product can be identified by the usual spectroscopic techniques (^1H NMR, ^{13}C NMR, ^{19}F NMR, MS, etc.), but it is difficult in ^{18}F -fluorination reactions unless a standard is available for quick comparison by TLC and HPLC. In contrast to equimolar ratios in classic reactions, radiochemical reactions on the n.c.a. scale are performed at a

subnanomolar level. Such reactions under non-equilibrium conditions generally proceed according to pseudo-first-order kinetics, since the concentration of the precursor to be labeled is in very high excess to the n.c.a. radionuclide and can approximately be considered to be constant. Therefore, many ^{18}F -labeling reactions are successful, although the same ^{19}F -fluorination reactions fail.

Fluorine-18 can be incorporated into organic compounds using a variety of methods, which can generally be divided into direct methods (electrophilic substitution and nucleophilic substitution) and indirect methods (^{18}F -fluorination via prosthetic groups or build-up procedures).¹⁹ Owing to the development of PET and the requirement for new radiopharmaceuticals (especially ^{18}F -labeled aromatic amino acids), there has been extensive research on the field of aromatic fluorination. However, the introduction of fluorine atoms onto an aromatic ring can be realized by only a small number of reactions, and remains an active area of research.

1.4.1 Electrophilic substitution

These methods rely on $^{18}\text{F}]\text{F}_2$ or reagents that can supply electrophilic fluorine.²⁰ The normally used ^{18}F -sources in electrophilic fluorination are $^{18}\text{F}]\text{F}_2$,²¹ $^{18}\text{F}]\text{CF}_3\text{OF}$,²² $^{18}\text{F}]\text{CH}_3\text{COOF}$,²³ $^{18}\text{F}]\text{FCIO}_3$,²⁴ $^{18}\text{F}]\text{XeF}_2$ ²⁵ and ^{18}F -labeled N-fluoropyridinium triflate.²⁶ These reagents create a chemical environment in which the fluorine atom is highly polarized with a partial positive charge.¹³ Hence, it is possible to fluorinate a variety of electron-rich substrates (e.g. alkenes, aromatic molecules, carbanions, etc.). On the basis of the high reactivity of the electrophilic ^{18}F -labeling reagents, the selectivity is rather low, so that undesired radical side reactions and reactions with the solvent can take place. To increase the regioselectivity on arenes, demetallation reactions of organometallic precursors can be used (Figure 1-2). The substituent **X** deactivates the arene, but for the ^{18}F -fluorodemetallation reaction, the effect is less strong than in direct electrophilic ^{18}F -labeling reactions. Thus, side reactions and consecutive fluorination are decreased and the purification is simplified. However, due to carrier addition in $^{18}\text{F}]\text{F}_2$ production, only half of the fluorine atoms are radioactive, hence the theoretical achievable maximum RCY in electrophilic ^{18}F -labeling reactions is limited to 50 %. Recent attempts were made to reduce the amount of fluorine-19 carriers in the syntheses of electrophilic ^{18}F -species in order to get higher specific activities, but lower radiochemical yields were an undesired drawback of this work.²⁷ As a result, electrophilic ^{18}F -labeling routes are restricted to

radiopharmaceuticals, where high specific activities are not compulsory and the chemical species in question are not toxic.

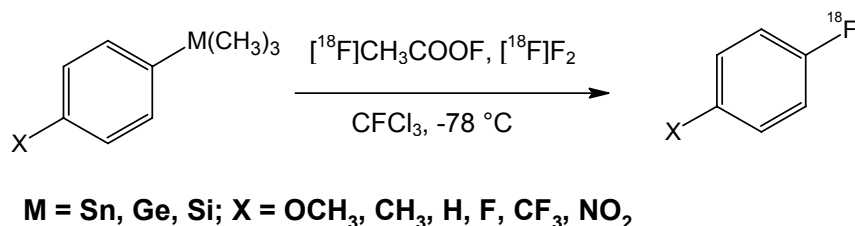


Figure 1-2. Regioselective ¹⁸F-labeling via electrophilic fluorodemetalation reactions²⁸

1.4.2 Nucleophilic substitution

In general, the most important route to synthesize ¹⁸F-labeled compounds is nucleophilic substitution based on n.c.a. [¹⁸F]fluoride ion, which is directly available from the target without any carrier addition. Thus far, this is the only method to obtain n.c.a. ¹⁸F-radiopharmaceuticals with high specific activity. [¹⁸F]Fluoride ion is mainly obtained as an aqueous solution and, due to its high electronegativity, it is strongly hydrated and inactivated for nucleophilic reactions. In the presence of proton donors, the fluoride anion is deactivated by solvation effects or even the formation of [¹⁸F]hydrogen fluoride. Therefore, some simple but very important manipulations are required to provide a reactive nucleophilic reagent. The steps in preparing for reactive [¹⁸F]fluoride ion follow.¹³

1.4.2.1 Addition of a cation

After irradiation of an [¹⁸O]H₂O target, the [¹⁸F]fluoride ion must be accompanied by a positively charged counterion. This is mainly solved by the addition of a cationic counterion (mostly potassium complexed by a cryptand such as Kryptofix 222 or tetraalkylammonium salts) prior to the evaporation of the water. Many syntheses now utilize the potassium/Kryptofix system, although examples of the use of tetraalkylammonium salts are frequently encountered in the literature.²⁹ The carbonate ion CO₃²⁻ is mostly used as the counter ion because it has low nucleophilicity and moderate basicity.

1.4.2.2 Water evaporation

Water is removed by the use of a relatively volatile solvent such as acetonitrile (azeotropic distillation) under a mild stream of an inert gas like argon at 140 °C. This method provides practically anhydrous and, thus, reactive [¹⁸F]fluoride ion.

1.4.2.3 Addition of the precursor solution

After the two steps described above, [^{18}F]fluoride ion is provided in a dry and “naked” form, suitable for substitution reactions. Because of the strong basicity of fluoride ion, all reactions performed in polar protic solvents (such as methanol and ethanol) fail. In general, nucleophilic substitution reactions are favourable in dipolar aprotic solvents such as acetonitrile (ACN), dimethyl sulphoxide (DMSO), *N,N*-dimethylformamide (DMF) and dimethylacetamide (DMAA), which are inert towards [^{18}F]fluoride ion. In addition, organic compounds and [^{18}F]fluoride ion (particularly the K^+ /Kryptofix pair) show good solubility in these dipolar aprotic solvents. The choice of solvent also depends on the type of chemical reaction being performed, potential side reactions with the precursor and the simplification of the subsequent workup and product isolation.

In the last few years, ionic liquids have been successfully applied³⁰ as a medium to carry out nucleophilic fluorination. The big advantage of ionic liquids is the fact that they tolerate the presence of water up to 20 % in solution. The use of ionic liquids as a media for ^{18}F -fluorinations³¹⁻³³ has been extended to the important tracers like [^{18}F]FDG and [^{18}F]FLT.

1.4.3 Nucleophilic aromatic ^{18}F -fluorination

Nucleophilic aromatic ^{18}F -fluorination is of great importance in the development of ^{18}F -labeled radiopharmaceuticals, which generally show good stability in the metabolic pathways of organisms. This reaction is activated by electron withdrawing groups *ortho* and/or *para* to the leaving group (Figure 1-3)

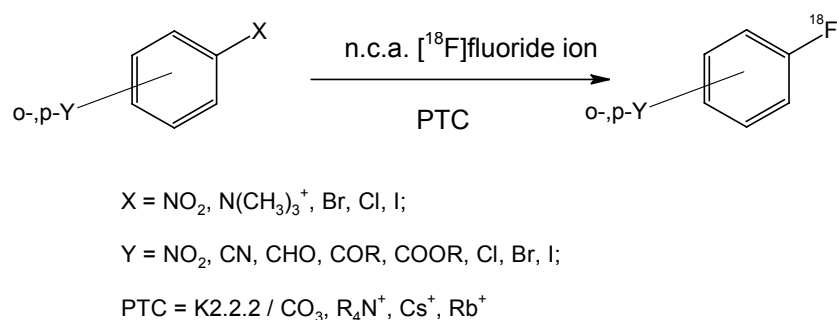


Figure 1-3. Nucleophilic ^{18}F -fluorination with activated arenes¹⁹

A good leaving group on the benzene ring is needed, and nitro ($-\text{NO}_2$) and trimethylammoniumtriflate ($-\text{NMe}_3\text{OTf}$) groups are widely used in $\text{S}_{\text{N}}\text{Ar}$ reactions. Halogens are used less frequently. A recent study shows that the diphenyliodonium

(Ar-I⁺-Ar') group has the advantage of unnecessary electron withdrawing groups on the ring, but problems are associated with undesired radioactive byproducts.³⁴ Simple isotopic substitution, ¹⁸F for ¹⁹F, mostly shows very high radiochemical yield. However, the lower specific activity from these isotopic substitutions makes this process less practiced.

As an activating group, functions with high positive Hammett constants, such as nitro, cyano and carbonyl groups, are suitable for activating S_NAr reactions. The choice of activating group depends on the structure of the desired final product, or the sequence of synthetic steps to be followed after the introduction of ¹⁸F. The best case is that the activating group is a part of the desired product. Otherwise, the activating group needs to be conveniently transformed into the structural component after ¹⁸F-fluorination. In some cases, such a group can temporarily be placed on the aryl ring and subsequently removed. An example here is the aldehydic function, which can be removed by catalytic decarbonylation (using Wilkinson's catalyst i.e. Rh[PPh₃]₃Cl).³⁵

1.4.4 Indirect ¹⁸F-labeling method

The methods mentioned above are direct ¹⁸F-labeling methods. In some cases, indirect ¹⁸F-labeling methods are applied. These methods mean that a primary ¹⁸F-labeled prosthetic group or synthon is coupled with a second molecule to form the product. Important procedures via prosthetic groups are ¹⁸F-fluoroalkylation,^{36, 37} ¹⁸F-fluoroacylation^{38, 39} and ¹⁸F-fluoroamidation.⁴⁰ (Figures 1-4)

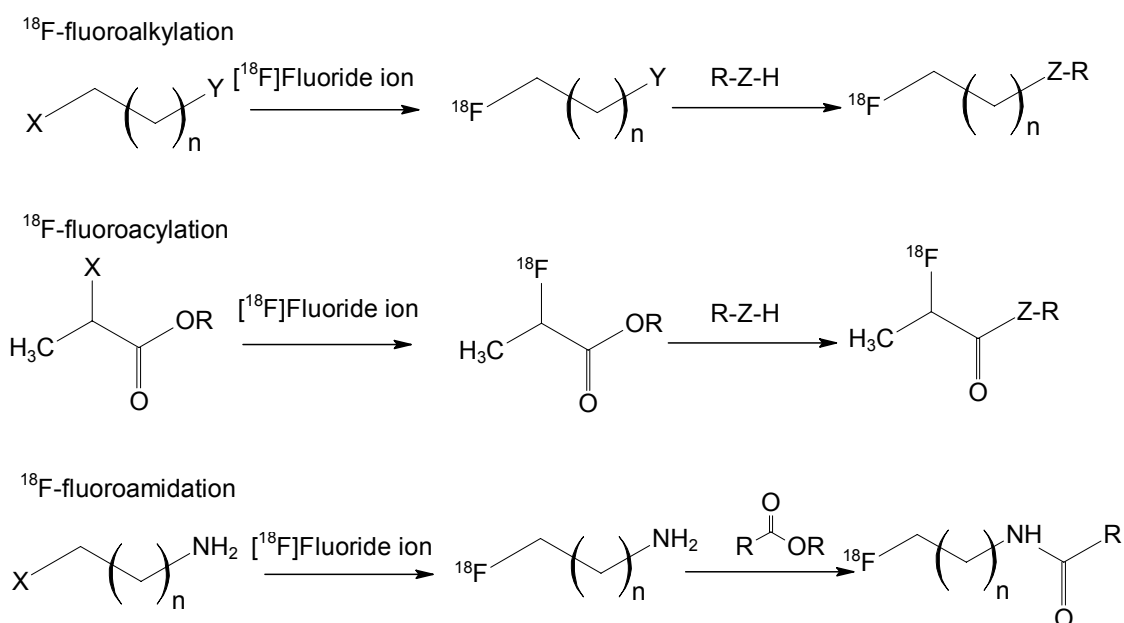


Figure 1-4. ¹⁸F-fluorination via prosthetic groups

In addition, the various ^{18}F -synthons used for indirect ^{18}F -labeling methods are 4- ^{18}F fluorophenyl lithium,⁴¹ 1- ^{18}F fluoro-4-haloarenes,⁴² 4-cyano-1- ^{18}F fluorobenzene,⁴³ 4- ^{18}F fluorophenol⁴⁴ and 4- ^{18}F fluorobenzaldehyde.⁴⁵

1.5 Automatic technology in PET radiopharmaceuticals

In order to produce reliable, cost-effective commercially available PET radiopharmaceuticals and to facilitate the application of these radiotracers, the development of automated systems has been an important focus for researchers.

In principle, the design and development of automated radiotracer synthesis systems follow the organic synthetic practices, but there is clear difference between the development of automated machines for PET radiotracer synthesis and organic synthesis. Radiotracer synthesis is more often carried out in volume range of 5 μL to 5 mL (comparing with 50 mL to 5 L in organic synthesis), and has special time constraints (often limited to 2 or 3 half-lives of the radioactive isotope) and shielding requirements defined by the short-lived isotopes that PET exploits. All these limitations make automatic radiochemical processes and equipment difficult or impossible.

In radiotracer syntheses, an automatic system is composed of the modular design concept of laboratory unit operations and feedback control.^{46, 47} Those general-purpose unit operations include manipulations common to the organic chemist like transferring reagents, evaporating solvents, regulating vessel temperature and solid phase extraction (SPE). In addition, the use of appropriate sensors and feedback controls are necessary for building more robust, general-purpose modules.

The earliest fully automated production systems for PET radiotracers appeared in the early 1980's. These pioneering systems included hard-wired automatic syntheses of ^{11}C -glucose⁴⁸ and $^{13}\text{NH}_3$,⁴⁹ a microprocessor based syntheses of $^{13}\text{NH}_3$ and L- ^{13}N -glutamate⁵⁰ and an automatic production system for syntheses of ^{75}Br -labeled radiopharmaceuticals.⁵¹ By 1990, automated systems were common in many PET research facilities due to the reliable, high yield, one-pot syntheses of ^{18}F FDG reported by Hamacher et al..⁵² This synthesis of ^{18}F FDG by nucleophilic substitution using Kryptofix 222 not only provided a simple, efficient, stereospecific route for radiotracer production, but also allowed the utilization of new high yield cyclotron targets for the production of ^{18}F fluoride ion from H_2^{18}O .^{53, 54}

Currently, due to the rapid development of radiochemistry and PC technology, more and more examples illustrate the diversity of engineering solutions to the problem of

automated PET radiotracer syntheses, such as automated syntheses of 6- ^{18}F fluoro-L-DOPA by electrophilic substitution⁵⁵ and robot syntheses of ^{11}C flumazenil.⁵⁶

Except for the automated syntheses of PET radiotracers, the automatic application of PET radiotracers is also important in basic and drug research and development. These systems include automated quality control of radiotracers,⁵⁷ computer controlled infusion systems for the automated injection of radiopharmaceuticals,⁵⁸ automated dose dispensing systems⁵⁹ and the automated delivery of radiotracers using pneumatic transport systems.⁶⁰

Along with the rapid development of PET technology, more and more new strategies for the radiolabeling, purification and formulation of PET radiopharmaceuticals are likely to be utilized in automated systems. In particular, PET radiochemists have exploited captive solvent techniques and solid phase reactions to create very simple high yielding radiochemical systems that are amendable to automation.^{61, 62} The development trend of automation in PET technology is that the latest technologies in personal computers, industrial controls, and laboratory robots will be used to implement more reliable and flexible automated radiosynthesis systems.

2 PROBLEM

The successful application of molecular imaging with positron emission tomography (PET) directly depends on the availability of selective molecular probes labeled with positron-emitters, i.e. radiotracers. The crucial role of the radiotracers is due to the fact that the primarily-registered physical signal can be selectively correlated to a particular metabolic function. For imaging dopamine metabolism and neutral amino acid transport, new interest in ^{18}F -labeled phenolic amino acids (i.e. [^{18}F]FDOPA, [^{18}F]fluoro-*m*-tyrosine) is apparent in PET and recent PET/MRI studies.

Commonly, fluorinated aromatic amino acids are synthesized by electrophilic substitutions using [^{18}F]F₂, ^{18}F -acetylhypofluorite etc. as reagents. The limitation of these electrophilic methods is the low specific activity (ratio of ^{18}F -compound (in Bq) to ^{18}F - plus ^{19}F -compound (in mol)) of the radiotracer. This is due to the type of nuclear process that is used at the cyclotron. However, high specific activities are important for following metabolic processes without altering the biochemical processes that are on-going *in vivo*. Therefore, the incorporation of ^{18}F into the tracer is to be carried out with no-carrier-added fluorination reagents. Since [^{18}F]fluoride ion can be produced at a cyclotron efficiently and, most importantly, without any carrier addition, fluorination by nucleophilic substitution results in high specific activities.

For this reason, nucleophilic aromatic substitution (S_NAr) is considered to be the reaction type of choice in order to introduce ^{18}F at aryl carbons. However, due to high electron density of aromatic compounds, that approach has become a challenging task to radiopharmaceutical research groups.⁶³

Aiming at syntheses of ^{18}F -labeled aromatic amino acids via S_NAr, two different synthetic strategies were studied in this work. One of them is an existing synthetic strategy for [^{18}F]FDOPA that includes four steps: fluorination, reductive iodination, alkylation and hydrolysis (Figure 2-1). It has been developed by several groups.⁶⁴⁻⁶⁶ However, this complicated multi-step synthesis is not suitable for routine production. Therefore, in order to realize the reliable automated synthesis of [^{18}F]FDOPA for the multi-patient-dose routine production, the reaction conditions and operating system for the entire synthesis should be improved.

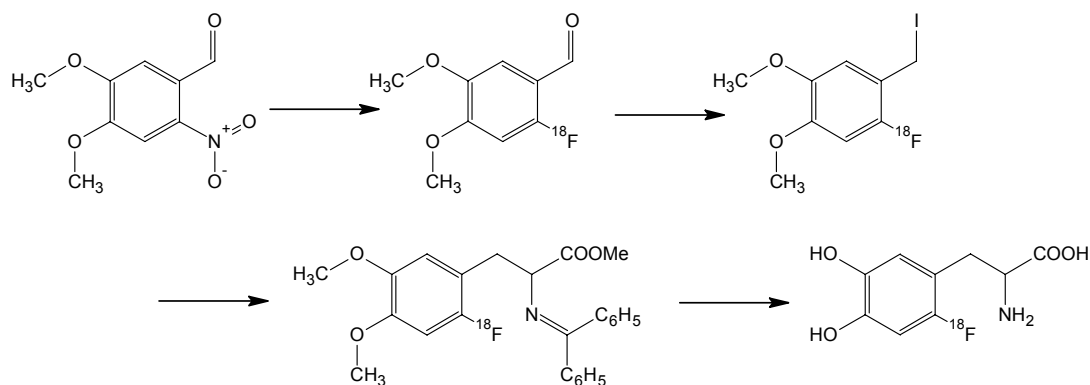
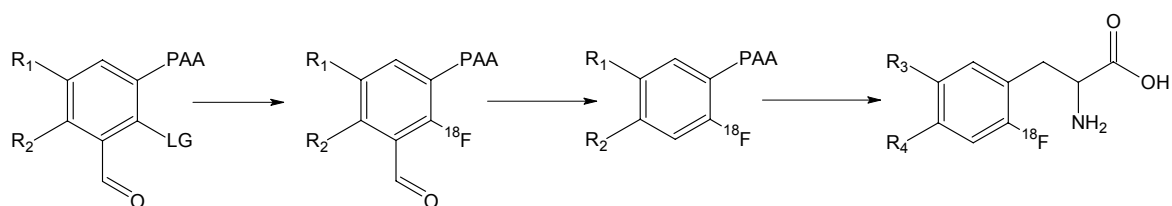


Figure 2-1. An existing synthetic strategy for [^{18}F]FDOPA (^{18}F -labeling and subsequent addition of the amino acid residue)⁶⁴

Another synthetic process with less and more simple radioactive synthesis steps has been under consideration for a long time. In this work, a three-step synthetic strategy is developed. The precursor would contain a protected glycine residue and, thus, would be ready for ^{18}F -labeling by nucleophilic substitution followed by removal of the assisting electron withdrawing group and the protective groups (Figure 2-2).



PAA = Protected amino acid residue

$\text{R}_1, \text{R}_2, \text{R}_3, \text{R}_4 = \text{H}$, [^{18}F]fluorophenylalanine

$\text{R}_1, \text{R}_3 = \text{H}$, $\text{R}_2 = \text{OMe}$, $\text{R}_4 = \text{OH}$, [^{18}F]fluoro-*p*-tyrosine

$\text{R}_2, \text{R}_4 = \text{H}$, $\text{R}_1 = \text{OMe}$, $\text{R}_3 = \text{OH}$, [^{18}F]fluoro-*m*-tyrosine

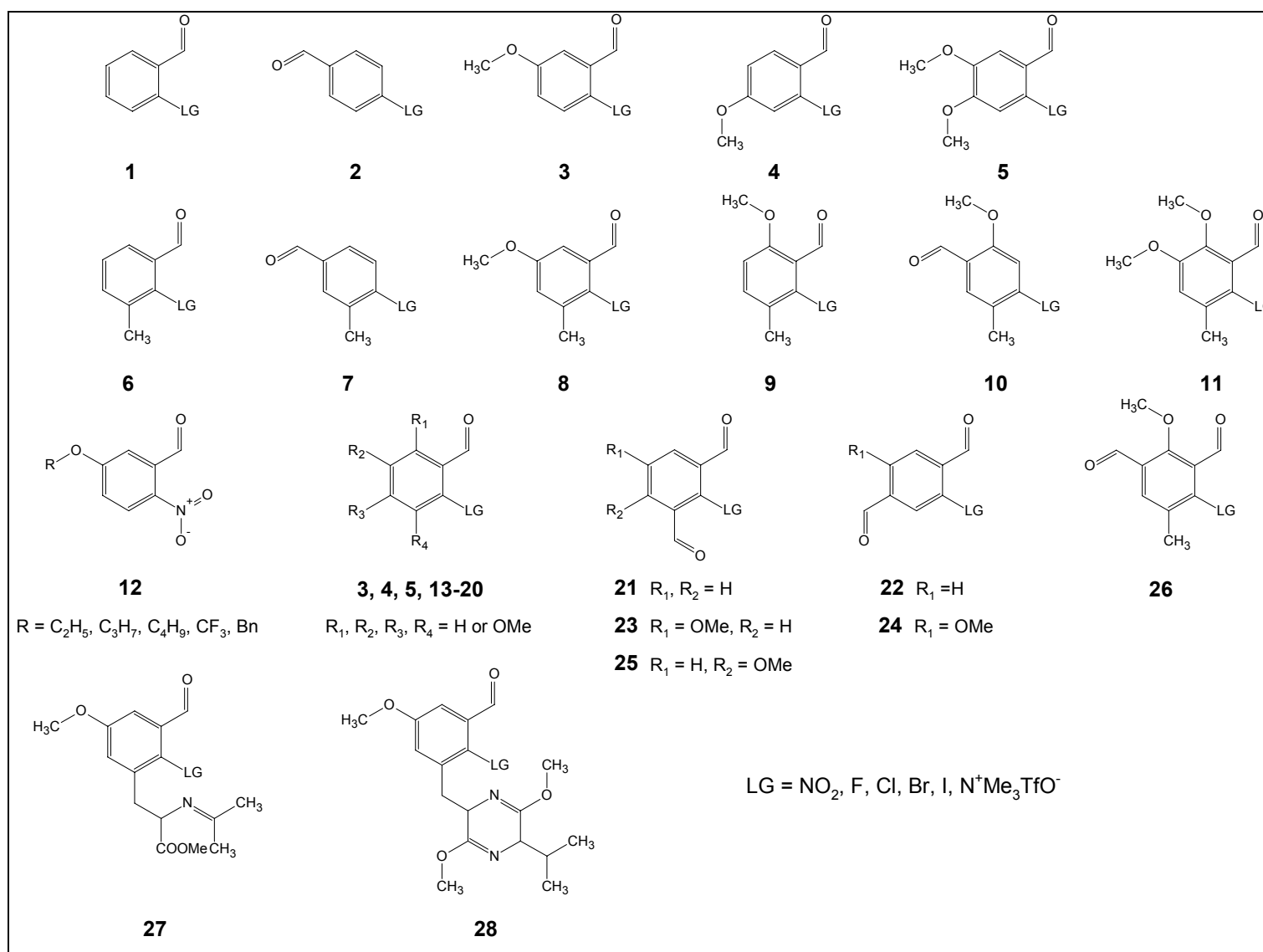
$\text{R}_1, \text{R}_2 = \text{OMe}$, $\text{R}_3, \text{R}_4 = \text{OH}$, [^{18}F]FDOPA

Figure 2-2. The synthetic strategy to be developed for syntheses of ^{18}F -labeled aromatic amino acids via $\text{S}_{\text{N}}\text{Ar}$

For both strategies, it is essential to gain more information about nucleophilic aromatic ^{18}F -fluorination with model compounds. Therefore, a systematic investigation of $\text{S}_{\text{N}}\text{Ar}$ with a broad variation of the substitution pattern (modeling ^{18}F -labeled aromatic amino acids, Figure 2-3) has to be performed. When both electron donating and electron withdrawing groups exist in the precursor molecule, the contradictory influence of these substituents on the $\text{S}_{\text{N}}\text{Ar}$ reaction will be discussed.

In order to understand the $\text{S}_{\text{N}}\text{Ar}$ reaction in more detail, the labeling reaction must be monitored by sensitive and precise analytic methods (i.e. HPLC, LC/MS), and the potentially competitive side reactions during $\text{S}_{\text{N}}\text{Ar}$ should be checked.

Additionally, one of the goals in this work is to prove the feasibility of the newly-developed synthetic strategy (Figure 2-2). Therefore, the crucial intermediate step (decarbonylation) should be tested with model compounds and a suitable protected glycine residue (stable against the synthesis conditions) should be chosen.

Figure 2-3. Model compounds for systematic study on S_NAr reaction with $[^{18}F]$ fluoride ion

3 RESULTS AND DISCUSSION

3.1 Organic syntheses of precursors for modeling ^{18}F -labeled aromatic amino acids

For the systematic study on nucleophilic aromatic substitution aiming at ^{18}F -labeled aromatic amino acids, a series of model compounds had to be synthesized. These compounds can be divided into four groups.

1) Model compounds that can be used as building blocks for ^{18}F -labeled aromatic amino acids (see paragraph 3.1.1).

2) Model compounds with methyl substituents that mimic ^{18}F -labeled aromatic amino acids (see paragraph 3.1.2). In these precursors, the methyl group is in the position of the glycine residue.

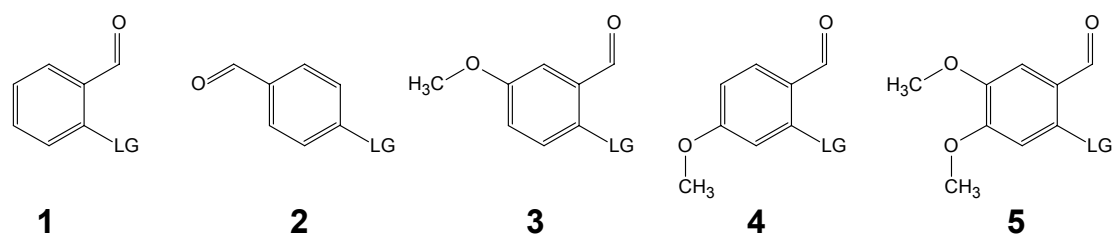
3) A series of precursors multi-substituted with methoxy groups, two formyl substituents or differentially-protected hydroxyl groups that is used for a broad investigation of $\text{S}_{\text{N}}\text{Ar}$ (see paragraph 3.1.3).

4) Compounds with protected glycine derivatives that are suitable for the synthesis of [^{18}F]fluoro-*m*-tyrosine via $\text{S}_{\text{N}}\text{Ar}$ (Figure 2-2) (see paragraph 3.1.4).

In the following, the organic synthetic paths are shown, and the details of the available compounds, synthetic procedures and the characterization data of products are included in the experimental section.

3.1.1 Model compounds as building blocks

In this work, model compounds that can be building blocks for ^{18}F -labeled aromatic amino acids have five basic substitution patterns (Figure 3-1).



LG = F, NO₂, Cl, Br, I, N⁺Me₃TfO⁻

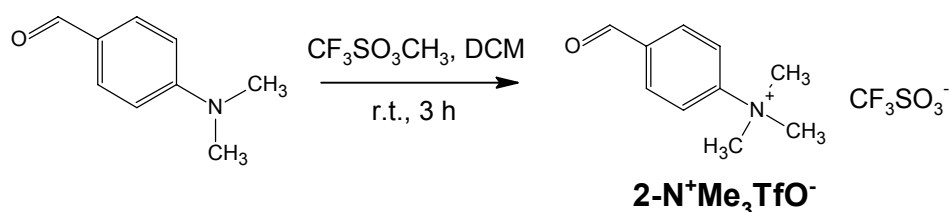
Figure 3-1. Model compounds as building blocks for ^{18}F -labeled aromatic amino acids

In case of substitution patterns 1 and 2, most model compounds are commercially available except 4-formylphenyl-trimethylammonium triflate ($2\text{-N}^+\text{Me}_3\text{TfO}^-$).

Compounds with substitution pattern **5** were synthesized in a previous work,⁶⁷ while all of the other compounds were synthesized.

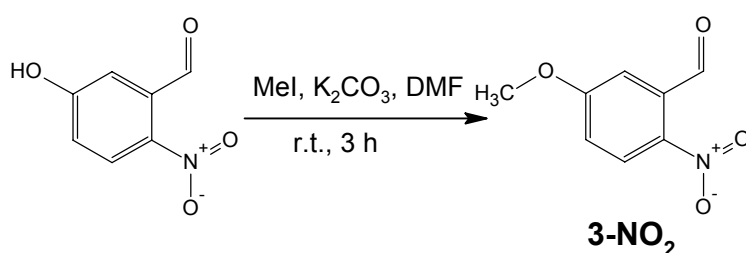
4-Formylphenyl-trimethylammonium triflate (**2-N⁺Me₃TfO⁻**)

Following the method in the literature,⁶⁸ **2-N⁺Me₃TfO⁻** was synthesized by quaternisation of *p*-dimethylaminobenzaldehyde with methyl trifluoromethanesulfonate (Y = 39 %).



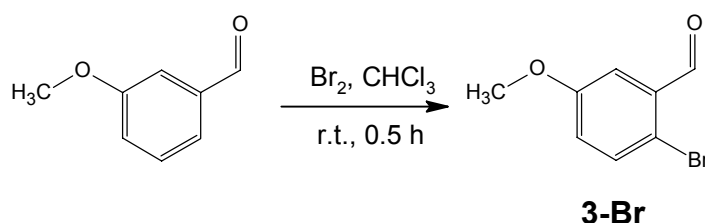
5-Methoxy-2-nitrobenzaldehyde (**3-NO₂**)

3-NO₂ was synthesized by methoxylation according to the literature.⁶⁹ Treatment of 5-hydroxy-2-nitrobenzaldehyde with methyl iodide under basic conditions afforded **3-NO₂** (Y = 87 %).



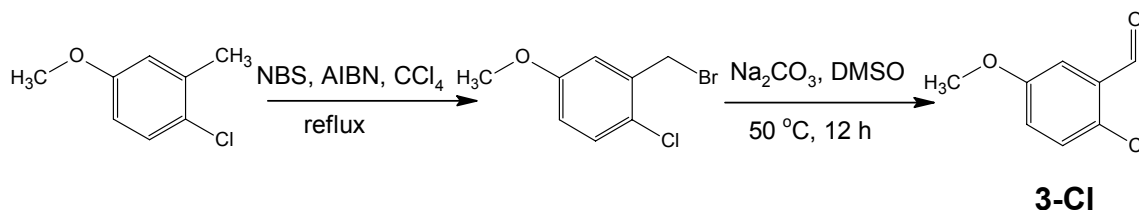
2-Bromo-5-methoxybenzaldehyde (**3-Br**)

Following the literature,⁷⁰ **3-Br** was synthesized by bromination of 3-methoxybenzaldehyde with bromine in CHCl₃. A mixture of monobromo compound and dibromo compound was obtained and **3-Br** was isolated by using flash chromatography (Y = 82 %).



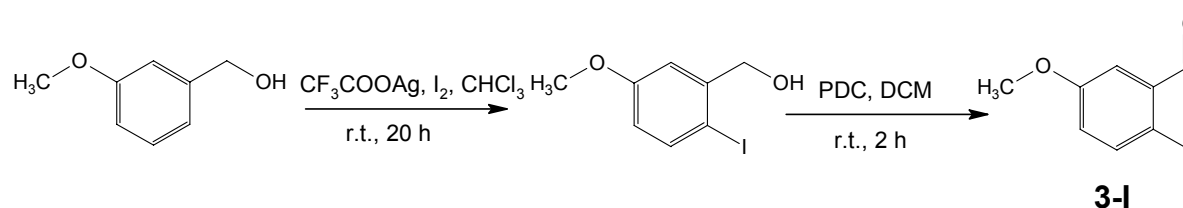
2-Chloro-5-methoxybenzaldehyde (**3-Cl**)

2-Chloro-5-methoxytoluene was brominated with NBS (N-bromosuccinimide) and a catalytic amount of AIBN in CCl₄ to provide 4-chloro-3-bromomethylanisole, and this intermediate product was oxidized in DMSO in presence of potassium carbonate to **3-Cl** (Y = 36 % based on 2-chloro-5-methoxytoluene).



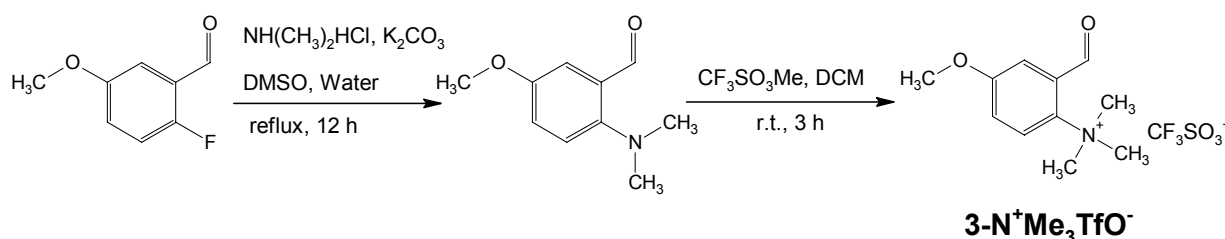
2-Iodo-5-methoxybenzaldehyde (3-I)

Following the literature,⁷¹ 3-methoxybenzyl alcohol was iodinated with iodine and silver trifluoroacetate in CHCl_3 , and 2-iodo-5-methoxybenzyl alcohol was formed in 48 % yield. This intermediate product was oxidized by using PDC in DCM to **3-I** (Y = 84 %).



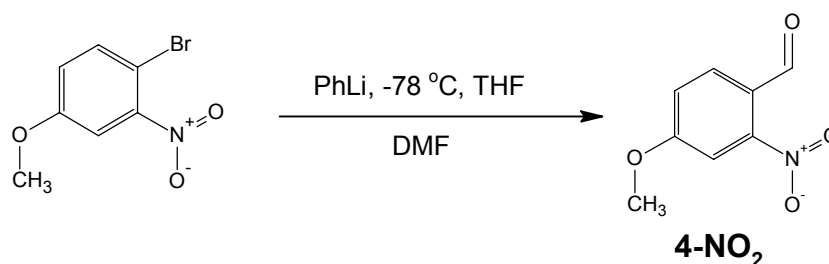
5-Methoxy-2-trimethylammoniumbenzaldehyde triflate (3-N⁺Me₃TfO⁻)

According to the literature,⁷² 5-methoxy-2-dimethylaminobenzaldehyde was prepared by nucleophilic substitution with $\text{NH}(\text{CH}_3)_2 \cdot \text{HCl}$ and potassium carbonate on 2-fluoro-5-methoxybenzaldehyde. The reaction proceeded under reflux in a mixture of DMSO and water (Y = 59 %). After quaternisation of this dimethylamino compound with methyl trifluoromethanesulfonate in DCM, **3-N⁺Me₃TfO⁻** was obtained (Y = 78 %).



4-Methoxy-2-nitrobenzaldehyde (4-NO₂)

4-Bromo-3-nitroanisole was lithiated with phenyllithium at $-78\text{ }^\circ\text{C}$ for 2 h and consecutively formylated by the addition of DMF to give **4-NO₂** (Y = 65 %).



3.1.2 Model compounds with a methyl substituent

Similar to compounds (see paragraph 3.1.1), the methyl-substituted compounds had five different basic substitution patterns (Figure 3-2), which can also be used to mimic [^{18}F]fluorophenylalanine (substitution patterns **6** and **7**), [^{18}F]fluoro-*m*-tyrosine (substitution pattern **8**), [^{18}F]fluoro-*p*-tyrosine (substitution pattern **9**) and [^{18}F]FDOPA (substitution pattern **10**).

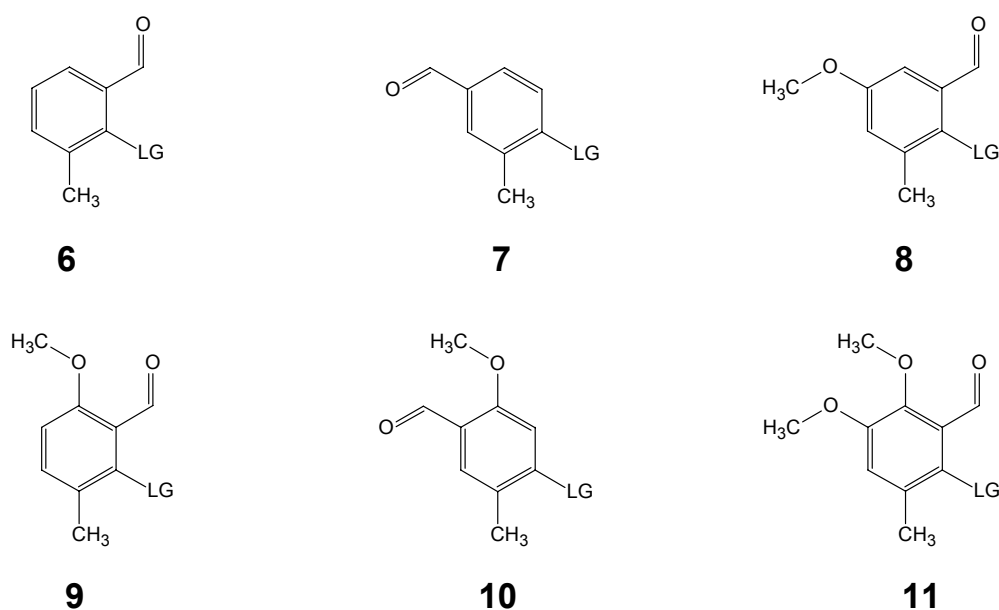
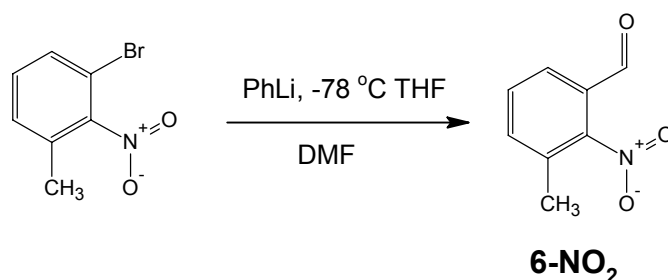


Figure 3-2. Methyl-substituted compounds mimicking ^{18}F -labeled aromatic amino acids

In case of substitution patterns **9**, **10** and **11**, all of these compounds were synthesized elsewhere.⁷³ For the substitution patterns **6** and **7**, all compounds were synthesized by the following pathways.

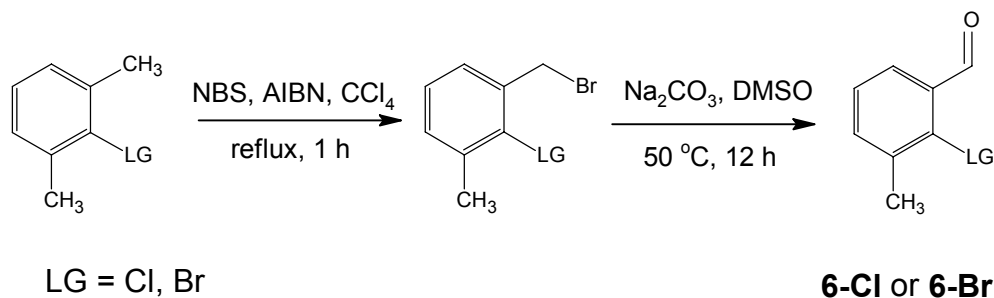
3-Methyl-2-nitrobenzaldehyde (6-NO₂)

6-NO₂ was prepared in the same manner as **4-NO₂**. 1-Bromo-3-methyl-2-nitrobenzene was lithiated with phenyllithium and consecutively formylated by the addition of DMF to give **6-NO₂** (Y = 66 %).



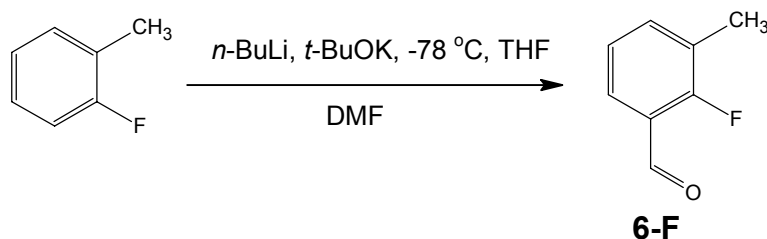
2-Chloro-3-methylbenzaldehyde (**6-Cl**) and 2-bromo-3-methylbenzaldehyde (**6-Br**)

6-Cl and **6-Br** were synthesized analogous to the way described in the preparation of **3-Cl**. The starting compound (2-chloro-1,3-dimethylbenzene or 2-bromo-1,3-dimethylbenzene) was brominated with NBS in CCl_4 to afford the intermediate product, which was oxidized to **6-Cl** (Y = 33 % based on 2-chloro-1,3-dimethylbenzene) and **6-Br** (Y = 53 % based on 2-bromo-1,3-dimethylbenzene).



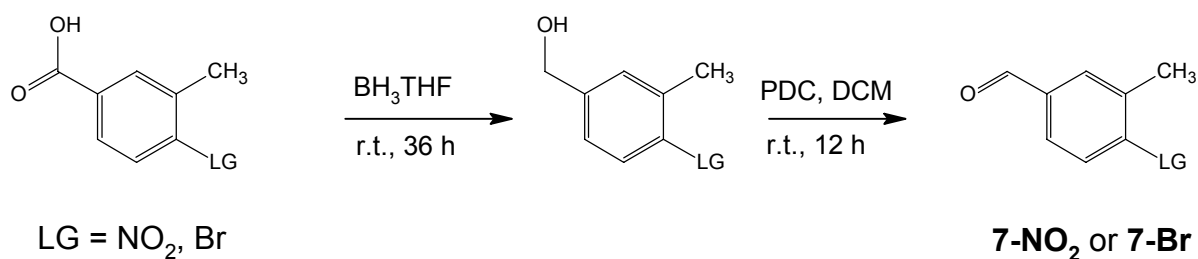
2-Fluoro-3-methylbenzaldehyde (**6-F**)

6-F was synthesized from 1-fluoro-2-methylbenzene by formylation with *n*-BuLi and DMF (Y = 62 %).



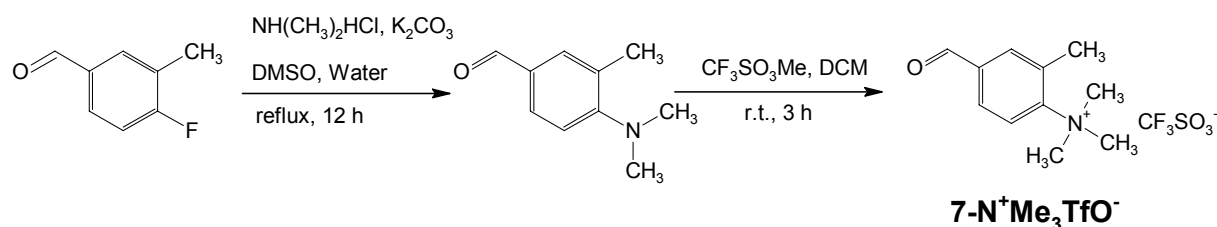
3-Methyl-4-nitrobenzaldehyde (**7-NO₂**) and 4-bromo-3-methylbenzaldehyde (**7-Br**)

3-Methyl-4-nitrobenzoic acid or 4-bromo-3-methylbenzoic acid was stirred in a $\text{BH}_3 \cdot \text{THF}$ solution to yield 3-methyl-4-nitrobenzyl alcohol or 4-bromo-3-methylbenzyl alcohol, and these intermediate products were directly oxidized with PDC to the final products. (**7-NO₂**, Y = 76 % based on 3-Methyl-4-nitrobenzoic acid; **7-Br**, Y = 58 % based on 4-bromo-3-methylbenzoic acid).



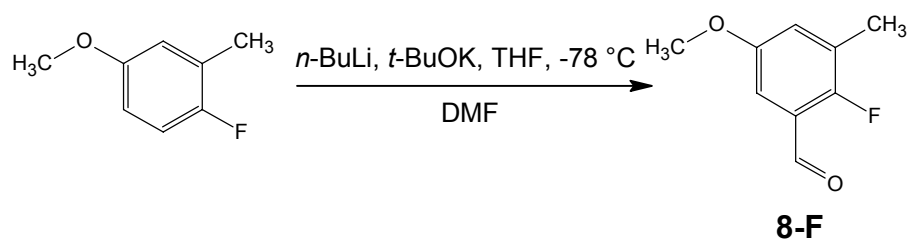
3-Methyl-4-trimethylammoniumbenzaldehyde triflate (**7-N⁺Me₃TfO⁻**)

The synthesis of **7-N⁺Me₃TfO⁻** was the same as for **3-N⁺Me₃TfO⁻**. The dimethylamino compound was prepared by a nucleophilic substitution with $\text{NH}(\text{CH}_3)_2\text{HCl}$ on 4-fluoro-3-methylbenzaldehyde ($Y = 68\%$). The ammonium triflate **7-N⁺Me₃TfO⁻** was obtained by quaternisation of the dimethylamino compound ($Y = 74\%$).



2-Fluoro-5-methoxy-3-methylbenzaldehyde (**8-F**)

8-F was synthesized by formylation of 2-fluoro-5-methoxytoluene with *n*-BuLi and DMF ($Y = 70\%$).



In the first phase of this reaction, the lithium ion could be introduced in the *ortho* position to the methoxy substituent or *ortho* to the fluoro substituent. However, when the *n*-BuLi and *t*-BuOK (or TMEDA) are used as reagents in the reaction, lithiation *ortho* to the fluoro substituent is the predominant reaction.⁷⁴

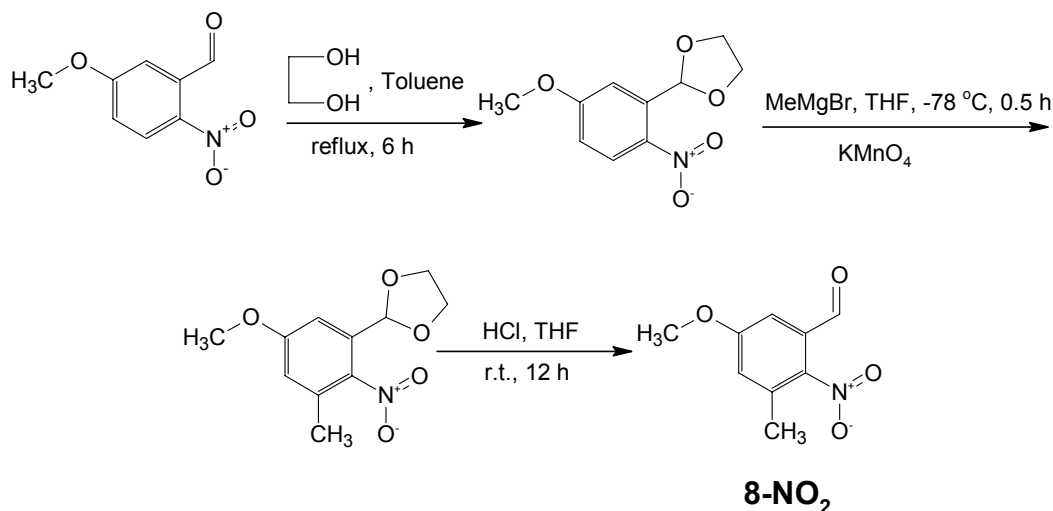
5-Methoxy-3-methyl-2-nitrobenzaldehyde (**8-NO₂**)

In order to reduce the risk of unknown impurities in **8-NO₂** by organic synthesis, this compound was prepared by three different synthetic pathways. In the preparation, the **synthetic pathway 1** needed less synthetic steps and had the highest overall yield compared to the other two synthetic pathways.

Synthetic pathway 1

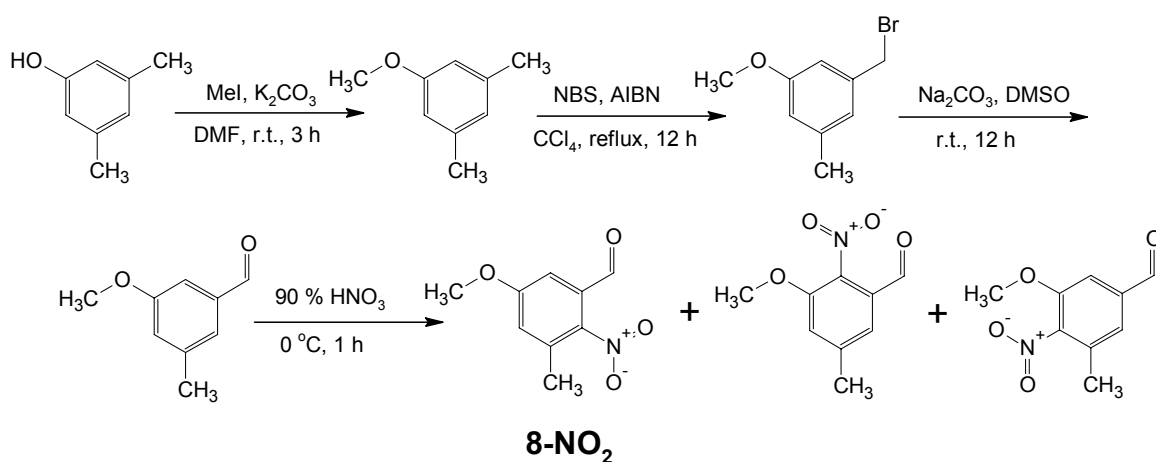
Reaction of 5-methoxy-2-nitrobenzaldehyde in presence of toluene-4-sulfonic acid with ethylene glycol provided 2-(5-methoxy-2-nitrophenyl)-1,3-dioxolane ($Y = 71\%$). This intermediate product was treated with MeMgBr at $-78\text{ }^\circ\text{C}$ in THF to form a Meisenheimer adduct, which was oxidized with KMnO_4 to 2-(5-methoxy-3-methyl-2-nitrophenyl)-1,3-dioxolane ($Y = 39\%$). In this nucleophilic alkylation of nitroarenes, the methyl group is selectively introduced at the *ortho* position of the nitro group.⁷⁵

After cleavage of the 1,3-dioxolane group under acidic conditions, **8-NO₂** was obtained (Y = 70 %).



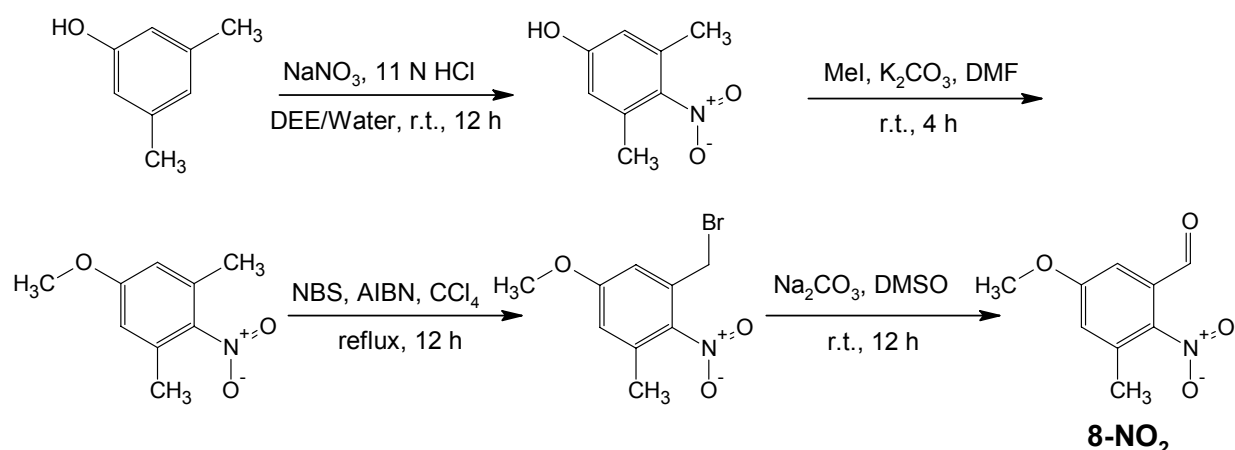
Synthetic pathway 2

Methoxylation of 3,5-dimethylphenol afforded 3,5-dimethylanisole, which was brominated with NBS and consecutively oxidized in DMSO (Y = 30 %) to provide 3-methoxy-5-methylbenzaldehyde. Following, it was nitrated by using 90 % HNO₃ at 0 °C and three different isomers were obtained. The desired product **8-NO₂** was obtained by using flash chromatography (Y = 30 %).



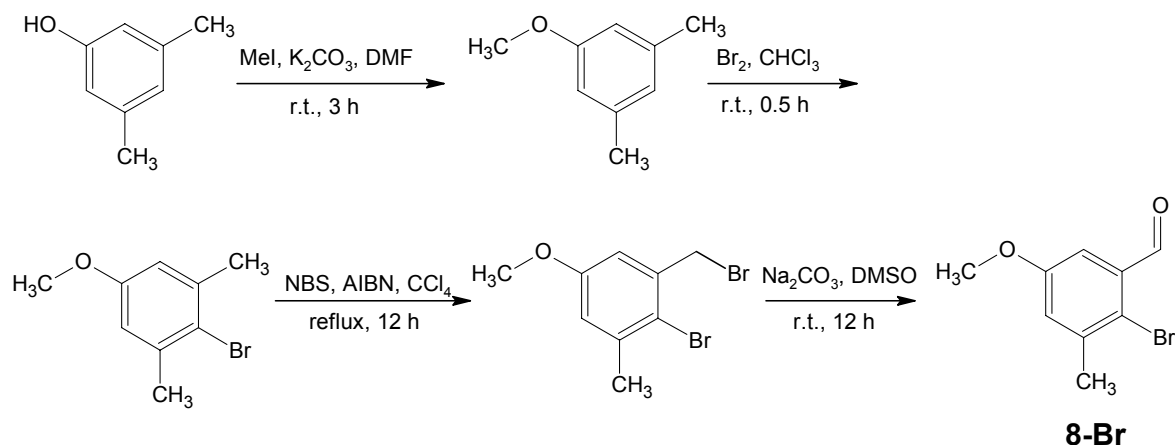
Synthetic pathway 3

According to the method described in the literature,⁷⁶ 3,5-dimethylphenol was nitrated with NaNO₃ and 11 N HCl in the mixture of water and diethylether (1:1, v/v) to furnish 3,5-dimethyl-4-nitrophenol (Y = 29 %). Following, this was methoxylated to 3,5-dimethyl-4-nitroanisole (Y = 81 %). After bromination with NBS and oxidation in DMSO, **8-NO₂** was obtained (Y = 30 % based on 3,5-dimethyl-4-nitroanisole).



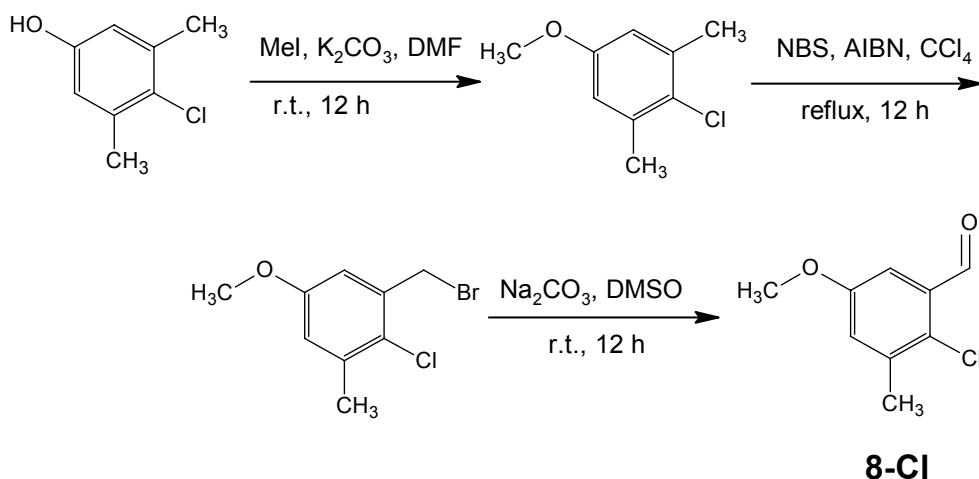
2-Bromo-5-methoxy-3-methylbenzaldehyde (8-Br)

8-Br was synthesized from 3,5-dimethylphenol. Methoxylation of 3,5-dimethylphenol yielded 3,5-dimethylanisole, which was brominated with bromine in CHCl_3 to 2-bromo-5-methoxy-1,3-dimethylbenzene ($Y = 85\%$ based on 3,5-dimethylphenol). This intermediate product was subjected to bromination with NBS and oxidation in DMSO to afford **8-Br** ($Y = 39\%$ based on 2-bromo-5-methoxy-1,3-dimethylbenzene).



2-Chloro-5-methoxy-3-methylbenzaldehyde (8-Cl)

8-Cl was synthesized from 3,5-dimethyl-4-chlorophenol, and the synthetic route was similar to that described in the synthesis of **8-Br**. After methoxylation of the hydroxyl group ($Y = 94\%$), bromination of the methyl group and oxidation of bromomethyl group, **8-Cl** was obtained ($Y = 15\%$ based on 2-chloro-5-methoxy-1,3-dimethylbenzene).

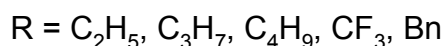
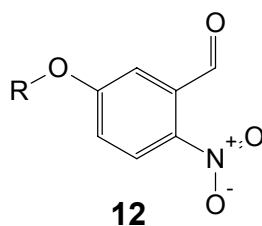


3.1.3 The other precursors for systematic study of S_NAr reaction

In order to perform the systematic study on S_NAr for the syntheses of ^{18}F -labeled aromatic amino acids, a broad variety of model compounds with different ether functions as a protection for phenol, varying numbers of methoxy substituents or dialdehydic functions were synthesized.

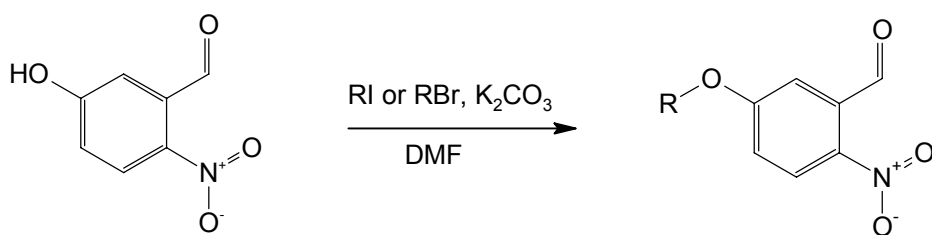
3.1.3.1 Precursor with differentially-protected hydroxyl group

The $^{18}F^-$ ion is deactivated by proton donors, therefore the phenolic hydroxyl group in the precursor molecule has to be protected. In this work, based on the structure of 5-hydroxy-2-nitrobenzaldehyde, -OH group was protected as different types of ethers, and these derivatives were used for studying the influence of different alkyl groups on the RCY (see paragraph 3.2.2.1). For substitution pattern **12**, all compounds were synthesized by the following pathways.



Compounds **12-C₂H₅**, **12-C₃H₇**, **12-C₄H₉**, **12-Bn**

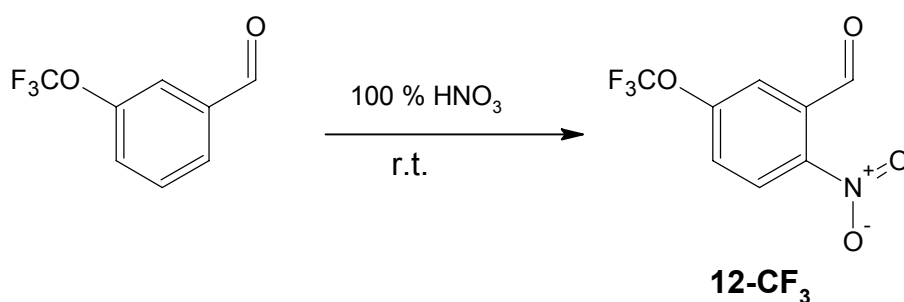
5-Hydroxy-2-nitrobenzaldehyde, K_2CO_3 and the iodoalkane (or BnBr) were stirred in DMF (or mixture of MeOH and $CHCl_3$). The products were produced in good yields (**12-C₂H₅**, Y = 95 %; **12-C₃H₇**, Y = 72 %; **12-C₄H₉**, Y = 70 %; **12-Bn**, Y = 70 %).



R = C_2H_5 (**12-C₂H₅**); C_3H_7 (**12-C₃H₇**); C_4H_9 (**12-C₄H₉**); Bn (**12-Bn**)

2-Nitro-5-(trifluoromethoxy)benzaldehyde (**12-CF₃**)

3-(Trifluoromethoxy)benzaldehyde was nitrated with 100 % HNO_3 at room temperature to yield **12-CF₃** (Y = 81 %).



3.1.3.2 Precursors with various numbers of methoxy substituents

In this work, a study was also performed to determine the dependency of the RCY on the number and positions of methoxy groups present in *o*-nitrobenzaldehydes or *o*-bromobenzaldehydes (Figure 3-3) (see paragraph 3.2.2.2).

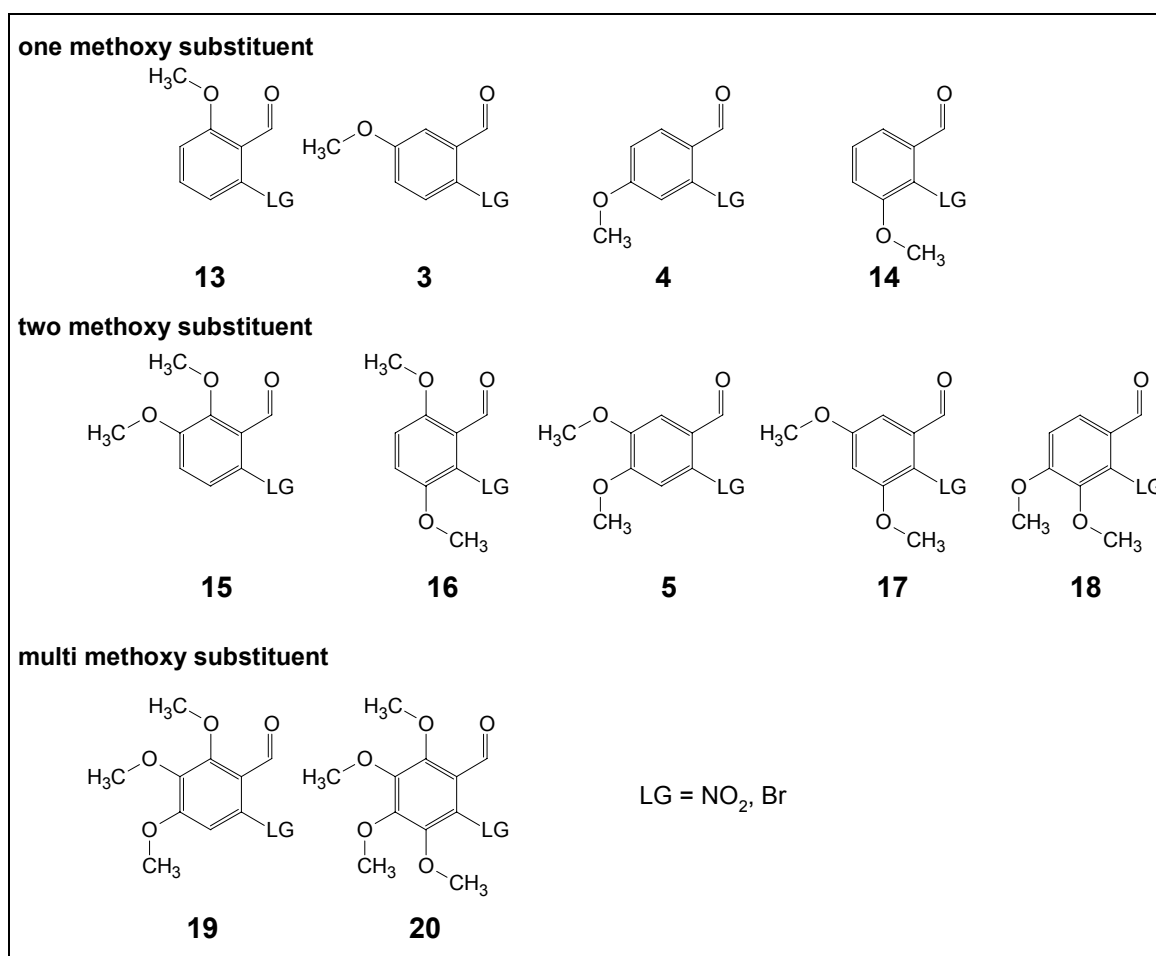
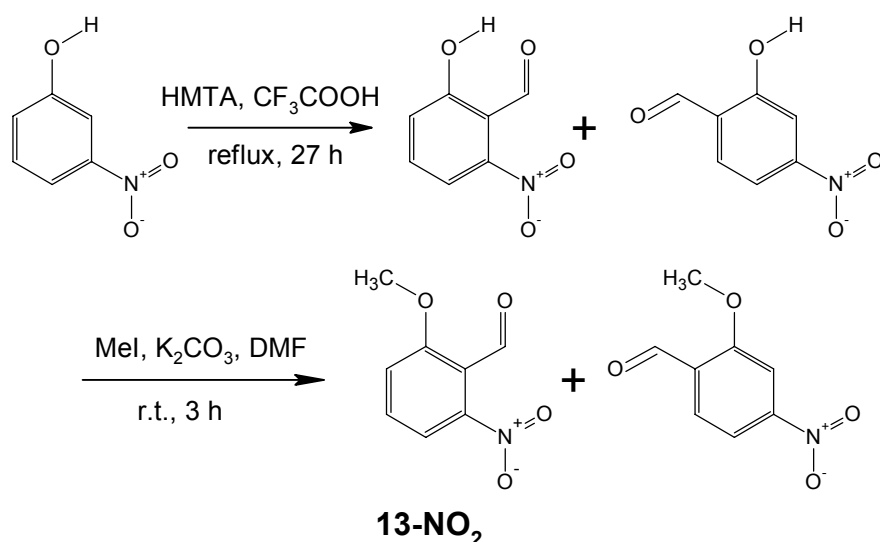


Figure 3-3. Precursors with different number of methoxy substituents

In Figure 3-3, **14-NO₂** and **14-Br** are commercially available; **15-NO₂** and **15-Br** were prepared previously,⁶⁷ in addition, **3-NO₂**, **4-NO₂** and **5-NO₂** have already been synthesized as model compounds (see paragraph 3.1.1). All the other *o*-nitrobenzaldehyde or *o*-bromobenzaldehyde derivatives were synthesized by the following methods.

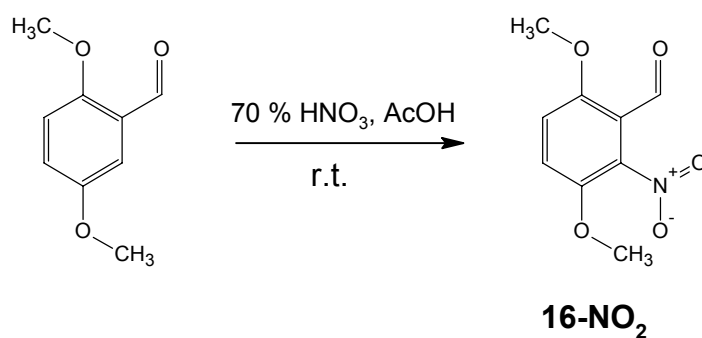
2-Methoxy-6-nitrobenzaldehyde (13-NO₂)

Following the method in the literature,⁷⁷ formylation of 3-nitrophenol by the DUFF reaction led to a mixture of 2-hydroxy-6-nitrobenzaldehyde and 2-hydroxy-4-nitrobenzaldehyde. These crude intermediate products were directly methoxylated by the same method used in the synthesis of **3-NO₂**, and **13-NO₂** was isolated by using flash chromatography (Y = 16 % based on 3-nitrophenol).



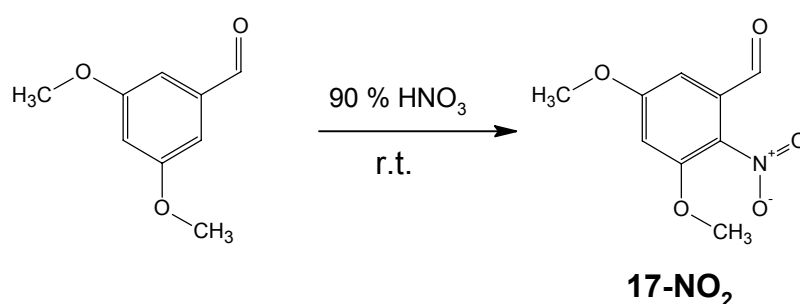
3,6-Dimethoxy-2-nitrobenzaldehyde (16-NO₂)

2,5-Dimethoxybenzaldehyde was nitrated with a mixture of AcOH and 70 % HNO₃ at room temperature for 1 h, and **16-NO₂** was formed (Y = 42 %).



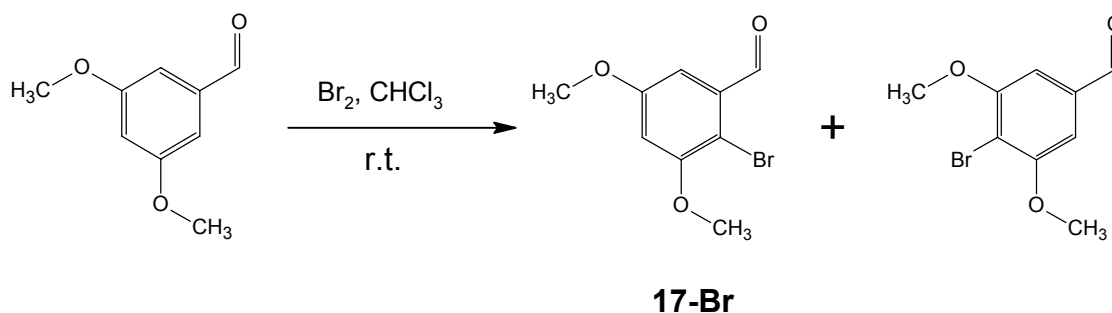
3,5-Dimethoxy-2-nitrobenzaldehyde (17-NO₂)

3,5-Dimethoxybenzaldehyde was treated with 90 % HNO₃ at 0 °C to give **17-NO₂** (Y = 17 %).



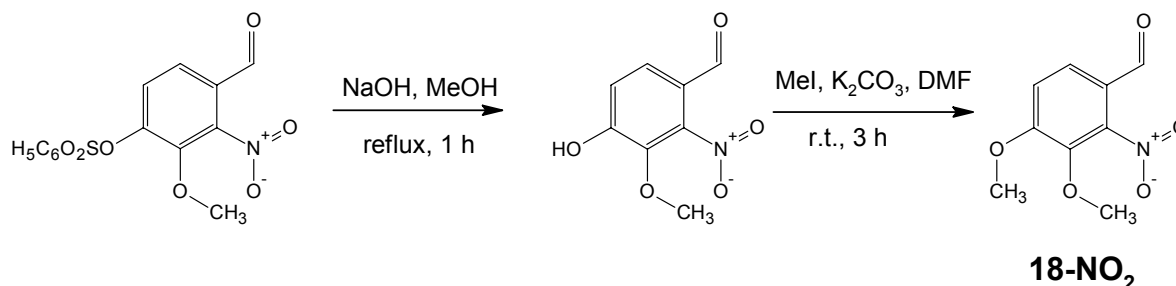
2-Bromo-3,5-dimethoxybenzaldehyde (17-Br)

In the bromination of 3,5-dimethoxybenzaldehyde with bromine in CH₃Cl, **17-Br** was obtained after purification by using flash chromatography (Y = 84 %).



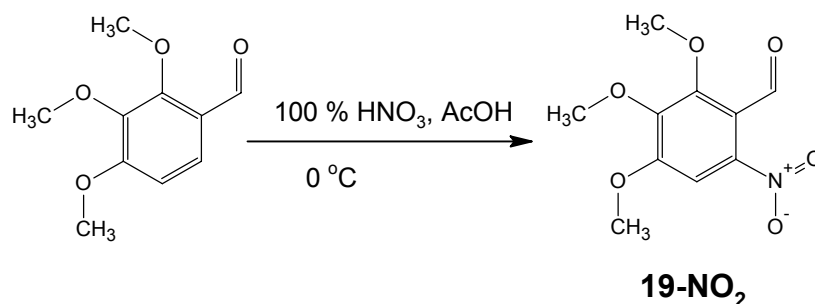
3,4-Dimethoxy-2-nitrobenzaldehyde (**18-NO₂**)

The synthesis of **18-NO₂** started from phenyl-4-formyl-2-methoxy-3-nitrobenzenesulfonate, which was readily obtained in previous work.⁶⁷ It was hydrolyzed under basic conditions to give 4-hydroxy-3-methoxy-2-nitrobenzaldehyde. Methoxylation of this intermediate product afforded **18-NO₂** (Y = 46 % based on phenyl-4-formyl-2-methoxy-3-nitrobenzenesulfonate).



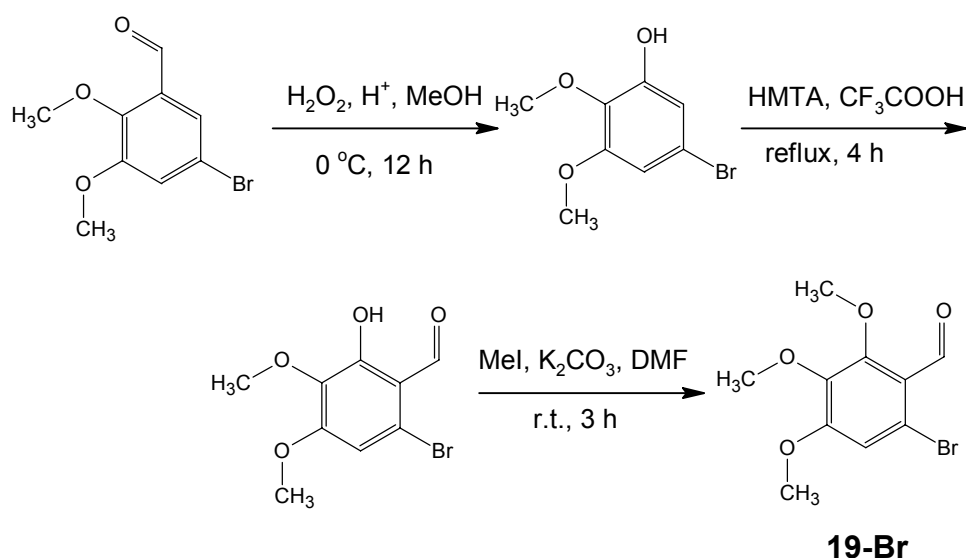
2,3,4-Trimethoxy-6-nitrobenzaldehyde (**19-NO₂**)

19-NO₂ was directly synthesized by nitration with a mixture of 100 % AcOH and 100 % HNO₃ at 0 °C for 10 min (Y = 66 %).



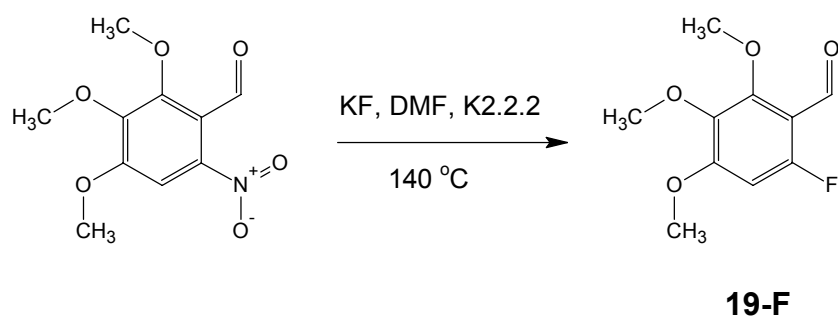
6-Bromo-2,3,4-trimethoxybenzaldehyde (**19-Br**)

The synthesis of **19-Br** was started from 5-bromo-2,3-dimethoxybenzaldehyde, which was prepared in previous work.⁶⁷ This compound was converted to 5-bromo-2,3-dimethoxyphenol by a Baeyer-Villiger reaction. Following, the formyl group was introduced into the molecule by the DUFF reaction. Finally, **19-Br** was obtained after methoxylation (Y = 13 % based on 5-bromo-2,3-dimethoxybenzaldehyde).



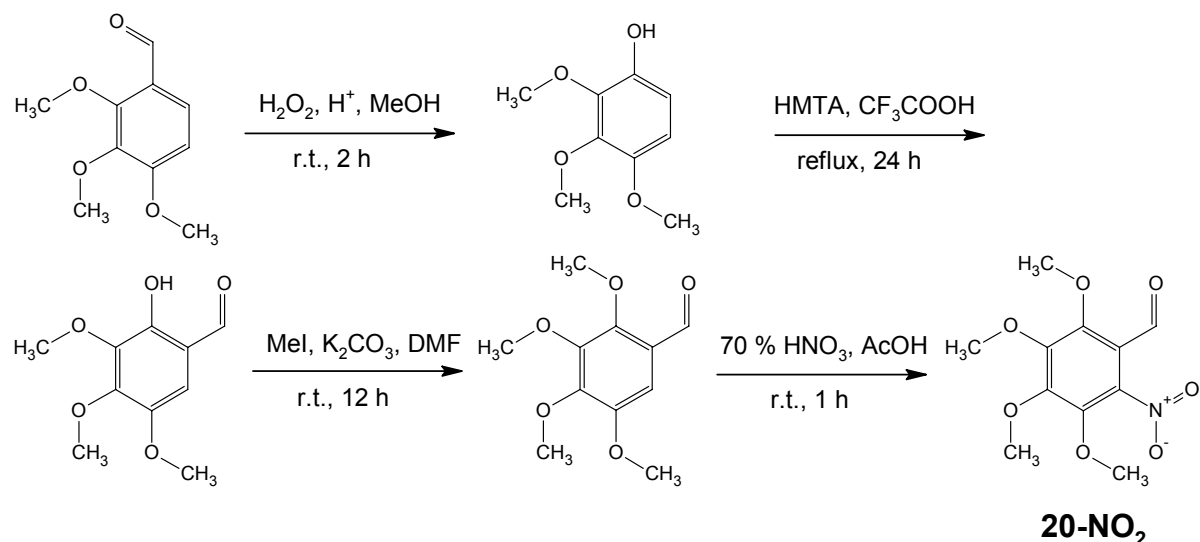
6-Fluoro-2,3,4-Trimethoxybenzaldehyde (19-F)

19-F was synthesized by fluorination of **19-NO₂** with KF in DMF in presence of K2.2.2, and the synthetic procedure was analogous to that described in fluorination with the ¹⁸F nucleophile (Y = 1.3 %).



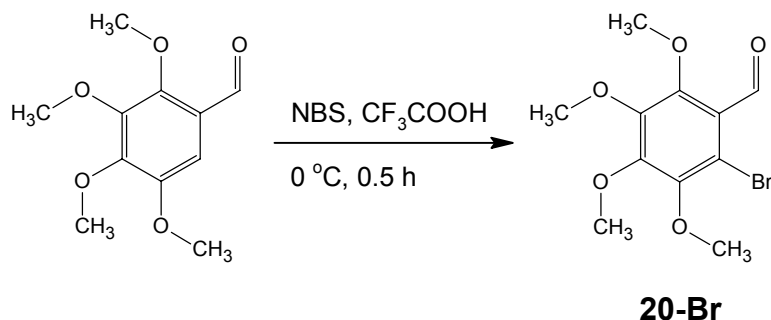
2,3,4,5-Tetramethoxy-6-nitrobenzaldehyde (20-NO₂)

2,3,4-Trimethoxybenzaldehyde was converted into 2,3,4-trimethoxyphenol by the Baeyer-Villiger reaction. Following, formylation of 2,3,4-trimethoxyphenol by the DUFF reaction afforded 2-hydroxy-3,4,5-trimethoxybenzaldehyde (Y = 51 %), which was methoxylated to 2,3,4,5-tetramethoxybenzaldehyde (Y = 80 %). This intermediate was nitrated with a mixture of 100 % AcOH and 70 % HNO_3 to give **20-NO₂** (Y = 39 %).



2-Bromo-3,4,5,6-tetramethoxybenzaldehyde (**20-Br**)

20-Br was prepared by the bromination of 2,3,4,5-tetramethoxybenzaldehyde (intermediate product in the synthesis of **20-NO₂**) with trifluoroacetic acid and NBS (Y = 75 %).



3.1.3.3 Precursors with two formyl substituents

In order to improve the RCY of precursors modeling ¹⁸F-labeled aromatic amino acids, the model compounds with two aldehydic functions (Figure 3-4) were synthesized.

Substitution patterns **25** and **26** used in this work were synthesized elsewhere.⁷³ All of the other compounds were synthesized by the following synthetic pathways.

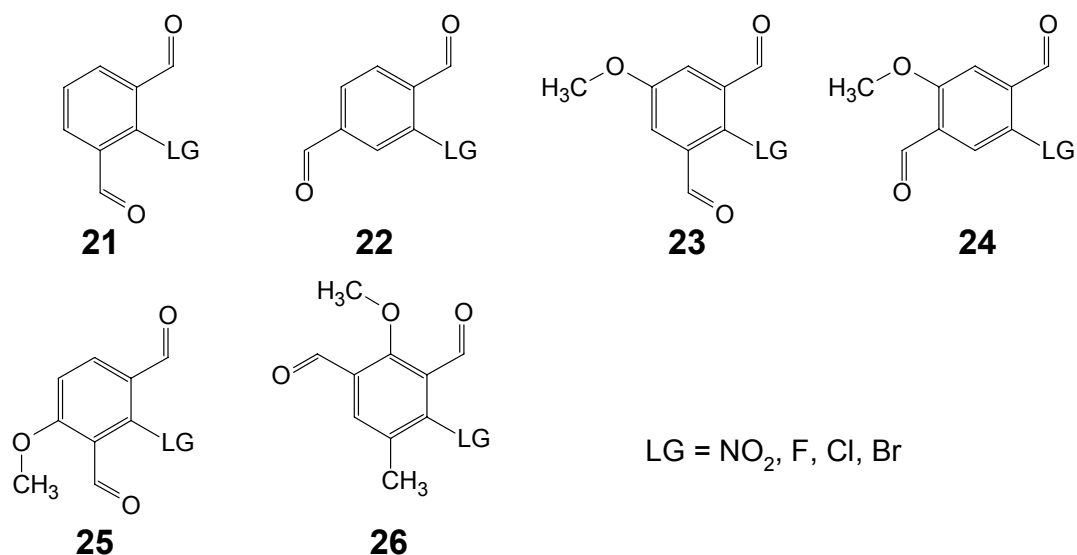
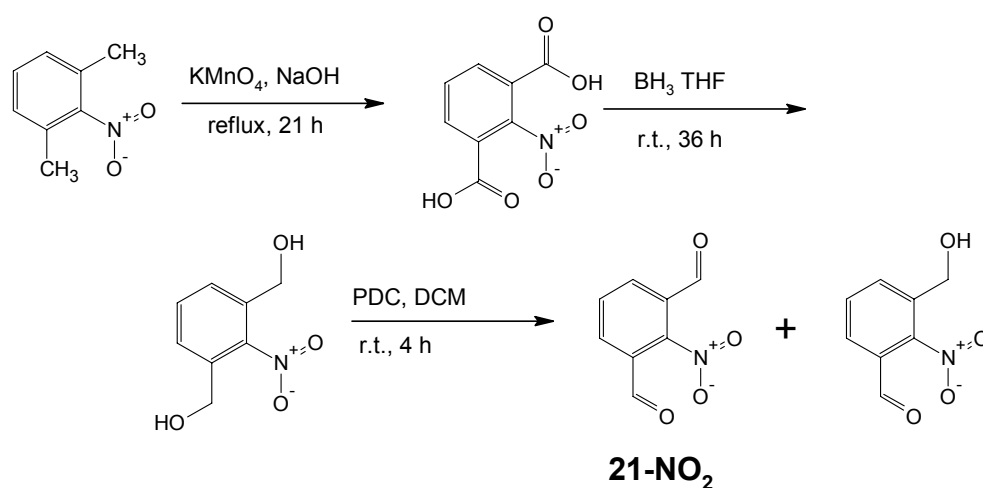


Figure 3-4. Model compounds with two formyl substituents

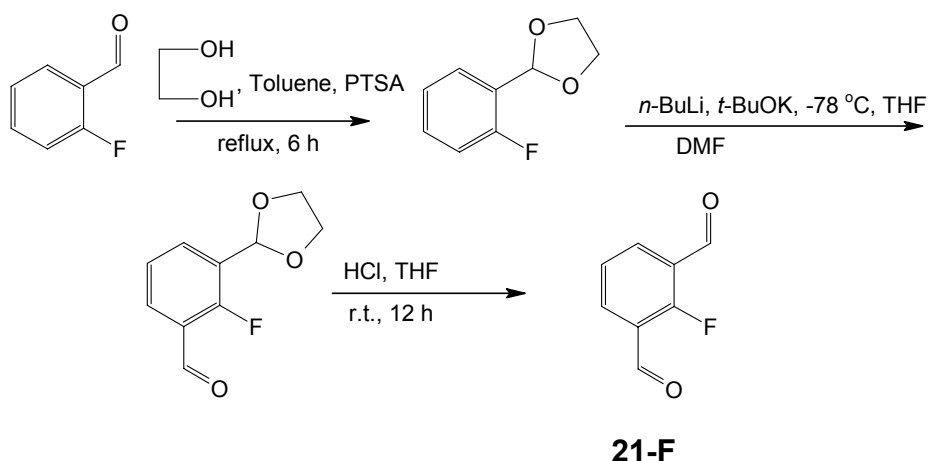
2-Nitroisophthalaldehyde (21-NO₂)

The synthesis of 2-nitroisophthalaldehyde began with the oxidation of 1,3-dimethyl-2-nitrobenzene with KMnO_4 ⁷⁸ to provide 2-nitroisophthalic acid (Y = 63 %). Following, it was reduced using $\text{BH}_3 \cdot \text{THF}$ to 1,3-dihydroxymethyl-2-nitrobenzene (Y = 90 %). The oxidation of this benzyl alcohol led to the mixed products (monoaldehyde and dialdehyde), which were isolated by using flash chromatography (21-NO₂, Y = 23 %; 3-(hydroxymethyl)-2-nitrobenzaldehyde, Y = 54 %).



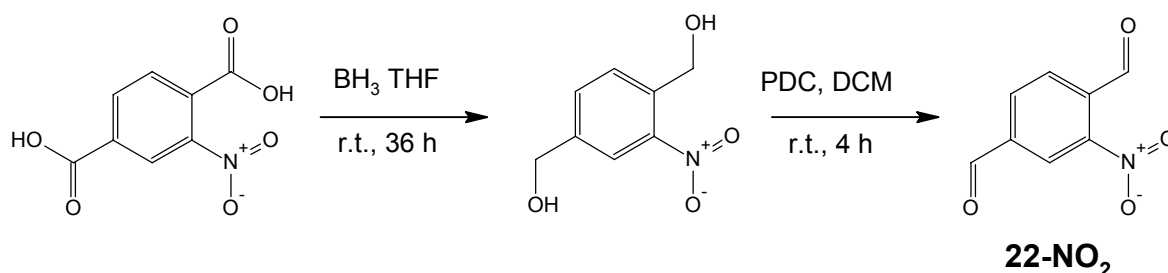
2-Fluoroisophthalaldehyde (21-F)

2-Fluorobenzaldehyde was treated with ethylene glycol in toluene to provide 2-(2-fluorophenyl)-1,3-dioxolane (Y = 81 %), which was subjected to formylation with *n*-BuLi and DMF to give 3-(1,3-dioxolan-2-yl)-2-fluorobenzaldehyde (Y = 37 %). This intermediate was deprotected under acidic conditions to yield **21-F** (Y = 61 %).



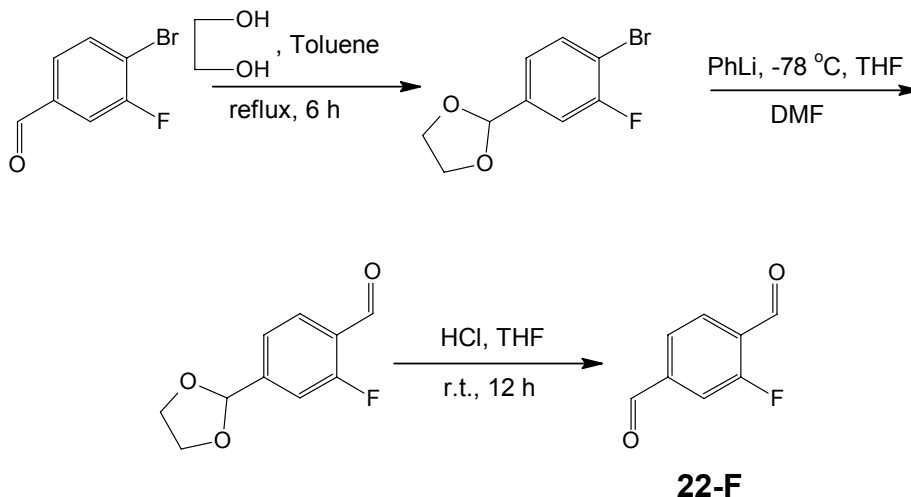
2-Nitroterephthalaldehyde (**22-NO₂**)

This synthesis of **22-NO₂** started from 2-nitroterephthalic acid, and the synthetic procedure was the same as described in the preparation of **21-NO₂**. After reduction with $\text{BH}_3 \cdot \text{THF}$ ($Y = 96\%$) and oxidation with PDC ($Y = 64\%$), **22-NO₂** was produced.



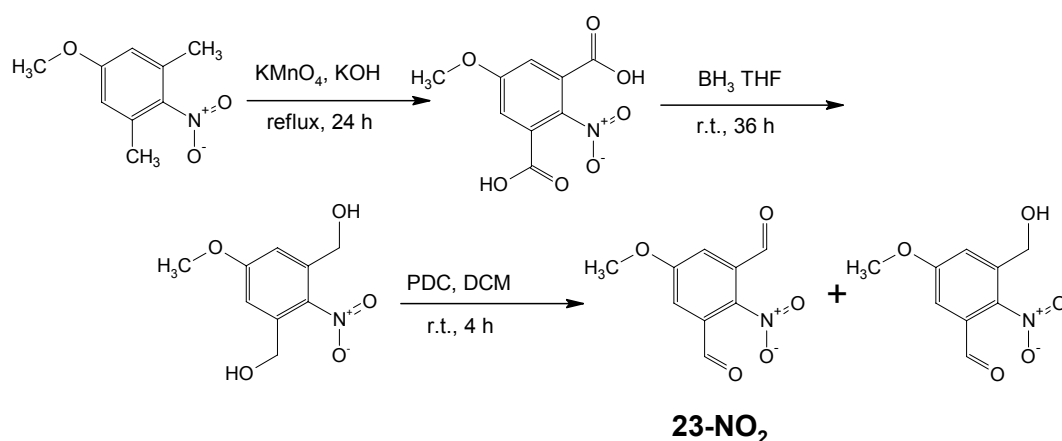
2-Fluoroterephthalaldehyde (**22-F**)

4-Bromo-3-fluorobenzaldehyde was treated with ethylene glycol in toluene to provide 2-(4-bromo-3-fluorophenyl)-1,3-dioxolane ($Y = 92\%$). This intermediate was converted to 4-(1,3-dioxolan-2-yl)-2-fluorobenzaldehyde by formylation with phenyllithium and DMF. The crude product was directly subjected to the deprotection to afford **22-F** ($Y = 77\%$ based on 2-(4-bromo-3-fluorophenyl)-1,3-dioxolane).



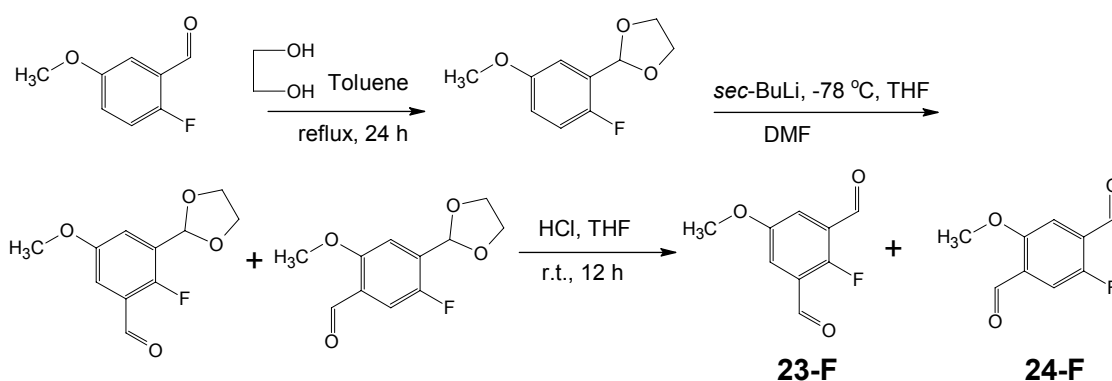
5-Methoxy-2-nitroisophthalaldehyde (**23-NO₂**)

The synthesis of **23-NO₂** began with 1,3-dimethyl-5-methoxy-2-nitrobenzene (intermediate product in the synthesis of **8-NO₂**), and the synthetic procedure was the same as described in the preparation of **21-NO₂**. After oxidation with KMnO₄ (Y = 41 %), reduction with BH₃·THF (Y = 53 %) and oxidation with PDC, a mixture of 5-methoxy-2-nitroisophthalaldehyde and 3-(hydroxymethyl)-5-methoxy-2-nitrobenzaldehyde was obtained. **23-NO₂** was isolated by using flash chromatography (Y = 22 % based on 5-methoxy-1,3-dihydroxymethyl-2-nitrobenzene).



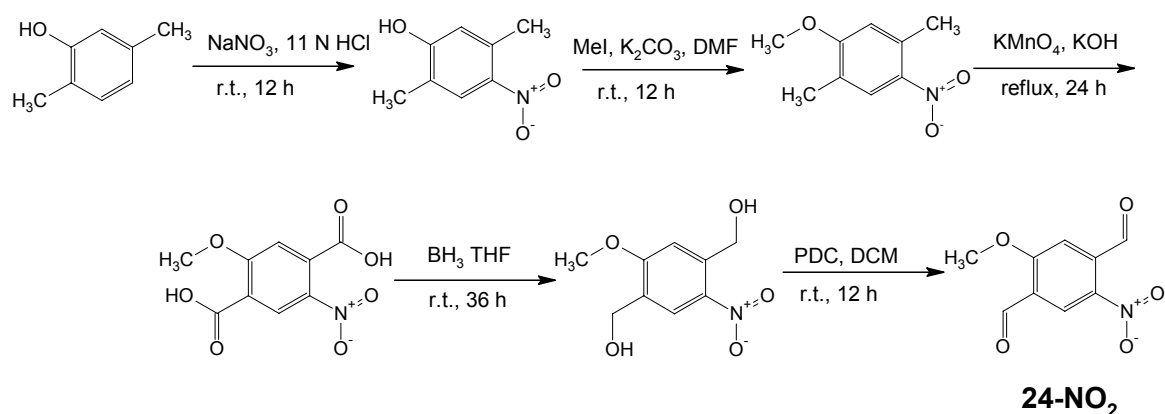
2-Fluoro-5-methoxyisophthalaldehyde (**23-F**) and 2-fluoro-5-methoxyterephthalaldehyde (**24-F**)

2-Fluoro-5-methoxybenzaldehyde was treated with ethylene glycol in toluene to provide 2-(2-fluoro-5-methoxyphenyl)-1,3-dioxolane (Y = 90 %). The formylation of this protected aldehyde with *sec*-BuLi and DMF led to a mixture of two important intermediates, which were isolated by using flash chromatography (4-(1,3-dioxolan-2-yl)-5-fluoro-2-methoxybenzaldehyde, Y = 10 %; 3-(1,3-dioxolan-2-yl)-2-fluoro-5-methoxybenzaldehyde, Y = 37 %). After deprotection under acidic conditions, **23-F** (Y = 88 %) and **24-F** (Y = 80 %) were obtained.



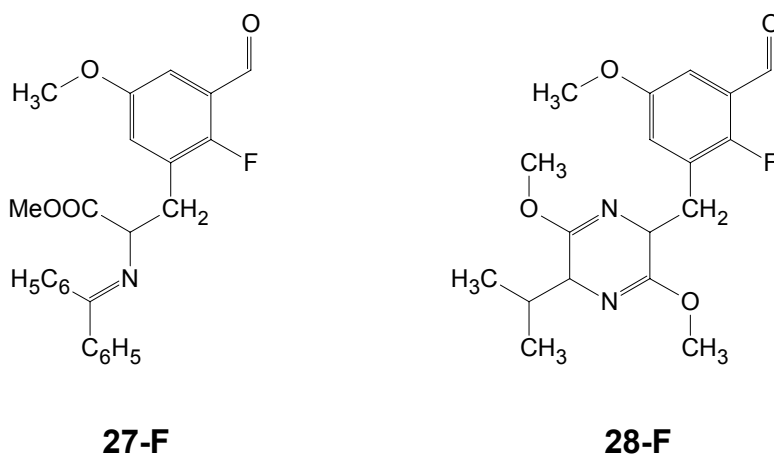
5-Methoxy-2-nitroterephthalaldehyde (**24-NO₂**)

2,5-Dimethylphenol was nitrated with NaNO₃ and 11 N HCl (Y = 36 %), and consecutively methoxylated with MeI to give 2,5-dimethyl-4-nitroanisole (Y = 85 %). This intermediate product was subjected to oxidation with KMnO₄ to provide 2-methoxy-5-nitroterephthalic acid (Y = 40 %). The following synthesis was analogous to that used in the preparation of **22-NO₂**. After reduction with BH₃·THF and oxidation with PDC, **24-NO₂** was obtained (Y = 44 % based on 2-methoxy-5-nitroterephthalic acid).



3.1.4 The precursors of [¹⁸F]fluoro-*m*-tyrosine containing protected 2-carboxy-2-aminoethyl substituents

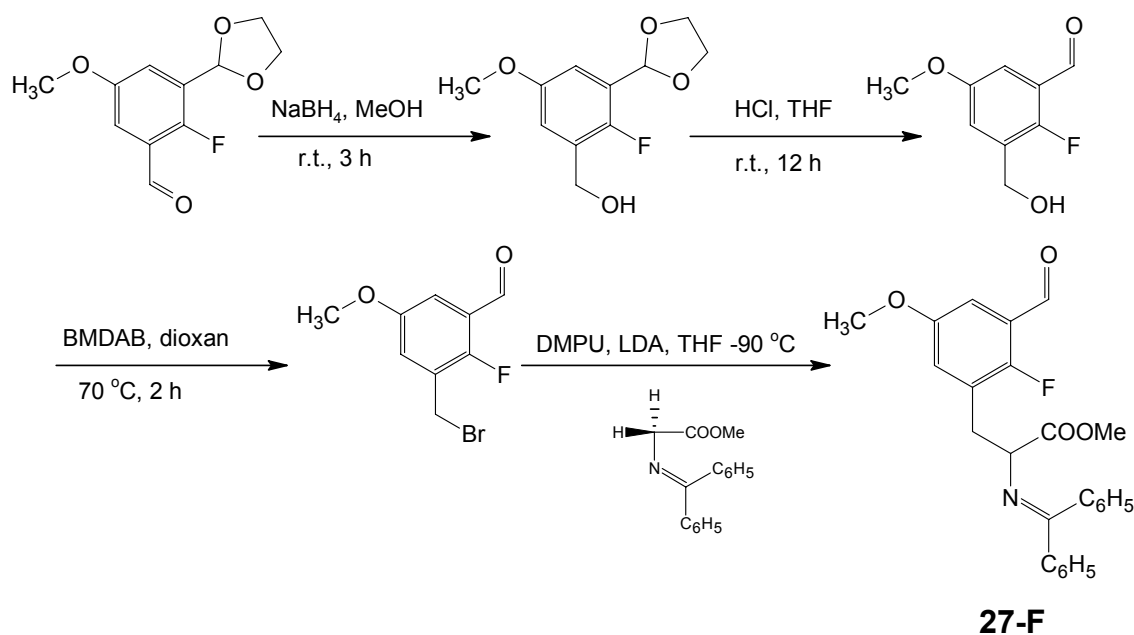
For the preparation of [¹⁸F]fluoro-*m*-tyrosine via a newly-developed strategy (Figure 2-2), precursors with protected glycine residues were synthesized by the following routes.



Methyl N-(diphenylmethylene)-2-fluoro-3-formyl-5-methoxyphenylalaninate (**27-F**)

The synthesis of **27-F** was started from 3-(1,3-dioxolan-2-yl)-2-fluoro-5-methoxybenzaldehyde (see synthesis of **23-F**). It was reduced with NaBH₄ (Y = 76 %)

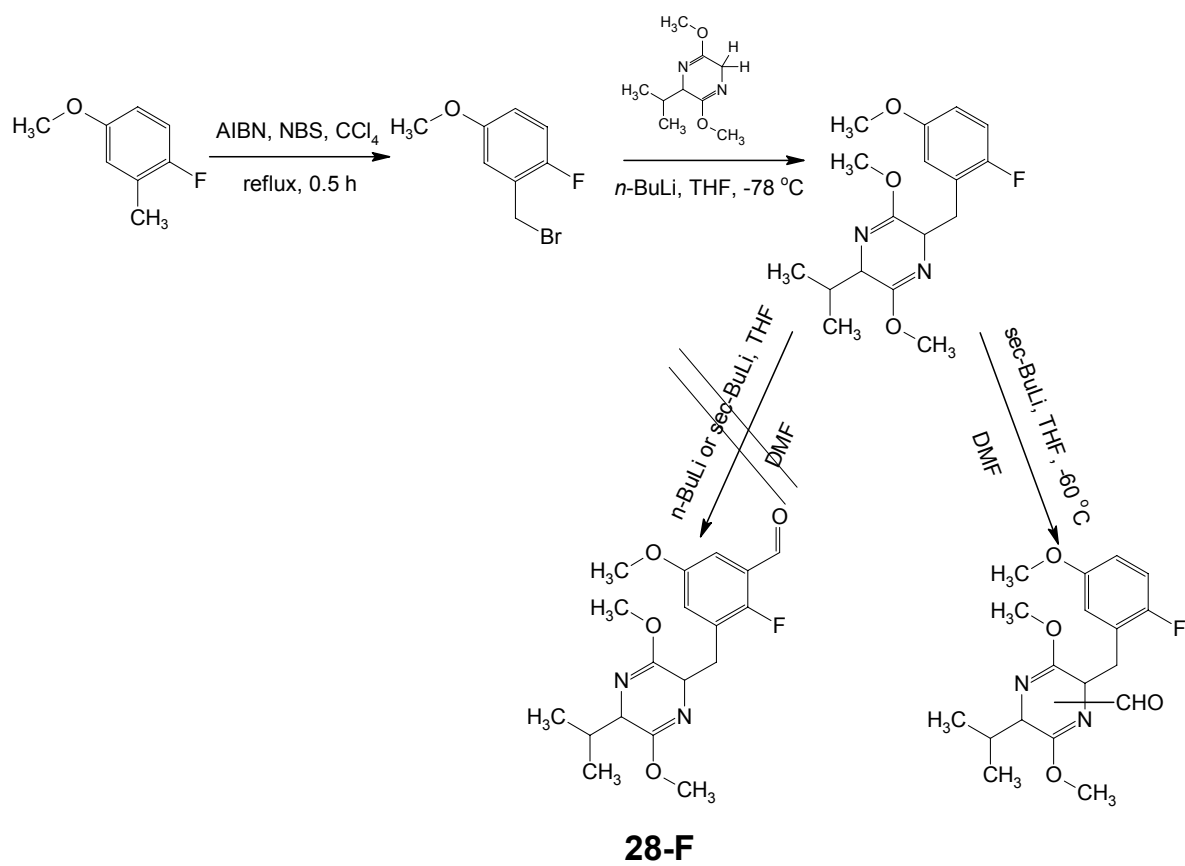
and deprotected under acidic conditions to provide 2-fluoro-3-(hydroxymethyl)-5-methoxybenzaldehyde. This intermediate product was subjected to bromination with BMDAB,^{73, 79} and 3-(bromomethyl)-2-fluoro-5-methoxybenzaldehyde was obtained (Y = 76 % based on 3-(1,3-dioxolan-2-yl)-2-fluoro-5-methoxybenzyl alcohol). After incorporation of N-(diphenylmethylene)glycine methylester into this benzyl bromide by a coupling reaction, **27-F** was prepared in a yield of 44 %.



2-Fluoro-3-[(5-isopropyl-3,6-dimethoxy-2,5-dihydropyrazin-2-yl)methyl]-5-methoxybenzaldehyde (**28-F**)

4-Fluoro-3-methylanisole was brominated by the method used in the synthesis of **3-Cl** to afford 3-(bromomethyl)-4-fluoroanisole (Y = 55 %). Following, it was coupled with (2R)-(-)-2,5-dihydro-3,6-dimethoxy-2-isopropylpyrazine in presence of *n*-BuLi in THF to provide 2-(2-fluoro-5-methoxybenzyl)-5-isopropyl-3,6-dimethoxy-2,5-dihydropyrazine (Y = 91 %).

The last step was to introduce the formyl group *ortho* to the fluoro substituent by formylation with BuLi and DMF. However, several attempts failed. The reaction was performed in the presence of *n*-BuLi or *sec*-BuLi in the range of -78 °C to -60 °C. After the addition of DMF, the reaction solution was monitored by LC/MS. When using *sec*-BuLi, a new compound with the correct mass peak of **28-F** (ACPI (+) mode, $[M+H]^+$, m/z 351) was observed, but the NMR analysis of the raw product showed that the formyl group was introduced on the dihydropyrazine ring, so that particular synthesis remains under development.



3.2 The systematic study on the nucleophilic aromatic

¹⁸F-fluorination

3.2.1 The principle of nucleophilic aromatic substitution

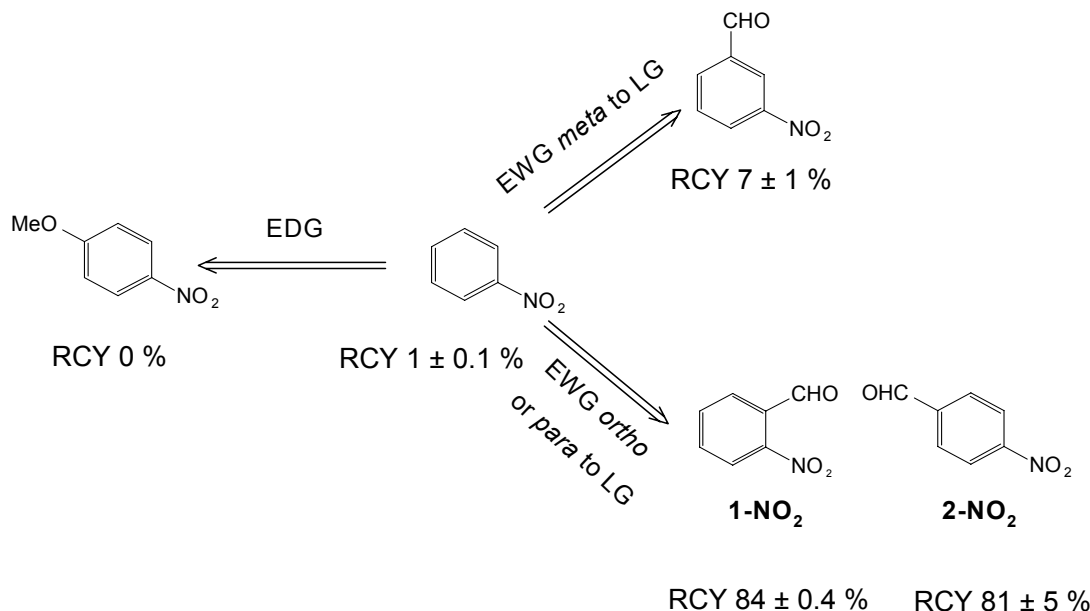
In aromatic compounds such as phenolic derivatives, nucleophilic substitution cannot occur because the electron density on the ring is too high so that a nucleophile is repulsed. In order to realize this reaction with a nucleophile such as [¹⁸F]fluoride ion, different factors have to be taken into consideration. Most importantly, the aromatic compounds should have a type of chemical structure in which the electron density of the reactive center is decreased. For that reason the compound must have a leaving group (LG) with an electron withdrawing effect. To achieve a good substitution yield, another electron withdrawing substituent (EWG) is necessary as an auxiliary activating group. Moreover, these substitution reactions exhibit strong dependencies on solvent, reaction temperature, reaction time, amount of base and precursor concentration. In this paragraph, all these effects on the S_NAr reaction are discussed on the basis of compounds modeling aromatic amino acids. Additionally, two more different methods are developed for analyzing the ¹⁸F-labeled products.

3.2.1.1 Substitution pattern effect on RCY in the case of nitrobenzene derivatives

In the nucleophilic aromatic ¹⁸F-fluorination, the effect of the substitution pattern on the radiochemical yield was studied with nitrobenzene and its derivatives (only including one EWG or one EDG). The results are presented in Figure 3-5.

The effect of substitution pattern can be illustrated starting with nitrobenzene, which showed a low RCY of 1 %. This is due to the electron withdrawing ability of the nitro group, which can reduce the electron density of the reactive center to a certain extent. Based on this structure, if one electron donating group (-MeO) was introduced in the *para* position to the leaving group (4-nitroanisole), the electron density of the reactive center would be increased by the +M-effect. Therefore, an RCY of 0 % was observed after 30 min. If an electron withdrawing group (-CHO) was introduced onto the ring, RCYs were improved (3-nitrobenzaldehyde, 7 ± 1 %; **1-NO₂**, 84 ± 0.3 %; **2-NO₂**, 81 ± 5 %). This RCY increase was the result of two different effects, the I-effect and M-effect. In the case of 3-nitrobenzaldehyde, the electron density of the reactive center was decreased by the inductive effect, which slightly improved the RCY but

not remarkably. In the case of **1-NO₂** and **2-NO₂**, the carbon bearing the leaving group had a relatively low electron density because of the direct -M-effect and I-effect in the *ortho* or *para* positions. This results in an easier replacement of the LG by a nucleophile, hence the RCY was increased significantly.



Labeling condition: precursor (10 mg), DMF (1 mL), 3.5 % K₂CO₃ (100 μL) and K2.2.2 (15 mg), at 140 °C, within 30 min.

Maximum RCY is presented.

Figure 3-5. The effect of substitution pattern of nitrobenzene derivatives on RCY in S_NAr

In summary, the radiochemical yield in the nucleophilic aromatic ¹⁸F-fluorination is strongly dependent on the substitution pattern of the precursor. When the LG and EWG are *ortho* or *para* to each other, the nucleophilic substitution reaction is accelerated. In this study, the model compounds for the ¹⁸F-labeled aromatic amino acids were designed to contain an EWG *ortho* or *para* to the LG.

3.2.1.2 Formyl substituent as an EWG

In this work, the choice of EWG was dependent on the structure of the desired final product or the sequence of synthetic steps following the introduction of ¹⁸F. The formyl substituent was chosen as an activating group in the syntheses of ¹⁸F-labeled aromatic amino acids because it can easily be removed in a decarbonylation reaction (see paragraph 3.3), or in the further steps of the synthesis, this formyl substituent can be used as starting point for the connection of the amino acid residue to the aromatic part (see paragraph 3.5).

3.2.1.3 Effect by LG

The leaving group quality has an effect on the RCY in the S_NAr reaction. In the case of model compounds with different substitution patterns, the RCY dependence on the leaving group quality was studied (Table 3-1).

In all of the structures, $^{18}F/^{19}F$ isotopic exchange always gave high RCY (> 75 %); however, only low specific activity can be reached by this isotopic exchange, which limits its utility in clinical applications.

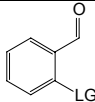
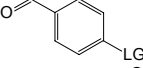
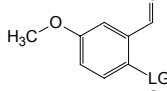
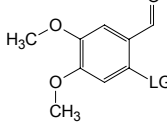
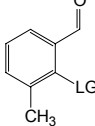
For no-carrier-added S_NAr reactions, the nitro group or the trimethylammonium triflate group are usually used as LGs. In Table 3-1, high RCYs (substitution patterns **1**, **2** and **5**) were obtained for both LGs. However, due to the difficult syntheses of trimethylammonium triflate precursors, especially for the precursor including the amino acid residue, this LG is not the first option. Interestingly, in the case of **2-NO₂**, when the scale of [^{18}F]fluoride ion in the labeling reaction was increased from 300 MBq to 60 GBq, the RCY was decreased from 81 % to 0 %; however, this unusual result was not observed for **1-NO₂**.

As a general tendency, bromo and chloro precursors give similar RCYs, and are usually lower than the nitro precursor. However, this is not always observed. In Table 3-1, when the precursor molecule did not include electron donating groups, the RCYs of bromo and chloro precursors were close to that of nitro precursors (substitution patterns **1** and **2**). On the contrary, the bromo and chloro precursors showed lower RCYs than nitro precursors when methoxy groups were present (substitution patterns **3** and **5**). In addition, in the case of substitution pattern **6**, the RCYs of bromo and chloro precursors were even a little bit higher than that of the nitro precursors because there was a side reaction competing with S_NAr during the labeling reaction for the nitro-precursor. An approach to explain this result is given in paragraph **3.2.3**. The iodo precursor, as the most inactive LG mentioned in the literature, showed the lowest RCY.

As expected, the leaving group quality in S_NAr reaction generally follows the order: $F > [N^+Me_3OTf] \approx NO_2 > Br \approx Cl > I$. However, this order is not always mirrored by the detected RCYs, because competitive reactions coexist during the nucleophilic aromatic substitution reaction. Even though, the nitro derivatives are the most promising precursors because they show good RCYs in most cases and can easily be separated from the ^{18}F -labeled products to give products with high specific activity. Furthermore, the synthesis of the nitro precursors is usually straightforward.

Therefore, the precursors in the further work, modeling different aromatic amino acids, derive from 2-nitrobenzaldehyde or 4-nitrobenzaldehyde.

Table 3-1. RCYs in model compounds with different LGs

Substitution pattern	RCY (%)					
	F	NO ₂	Cl	Br	I	N ⁺ Me ₃ OTf ⁻
1 	75 ± 1 ⁶⁷	84 ± 0.3	65 ± 1 ⁶⁷	73 ± 0.2 ⁶⁷	--	--
2 	78 ± 0.5 ⁶⁷	81 ± 5 ⁶⁷	67 ± 3 ⁶⁷	75 ± 0.5 ⁶⁷	--	88 ± 1
3 	83 ± 3	57 ± 1	31 ± 4	28 ± 4	18 ± 2	35 ± 4
5 	88 ± 1 ^{*, 67}	87 ± 2	57 ± 6 ^{*, 67}	36 ± 2	--	--
6 	79 ± 3	48 ± 5	62 ± 8	52 ± 2	--	--

Labeling condition: precursor (10 mg), DMF (1 mL), 3.5 % K₂CO₃ (100 μL) and K2.2.2 (15 mg), at 140 °C, within 30 min.

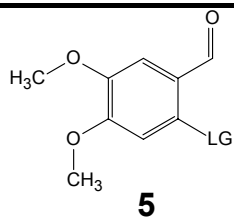
*: precursor (20 mg).

Maximum RCY is presented.

3.2.1.4 Solvent dependence

Solvents have great effects on the nucleophilic aromatic fluorination reaction. This type of reaction is favoured in dipolar aprotic solvents, where the suppression of the nucleophilicity of the ¹⁸F⁻ ion by solvation is smallest. A commonly used solvent is DMSO.^{80, 81} However, in a previous report^{82, 83} (Table 3-2), compounds presenting substitution pattern **5** with different leaving groups were labeled in different solvents (DMSO, DMF, DMAc, Sulfolane). The results showed that the best RCY was always obtained in DMF, whereas with bromo or chloro as the LG, the RCYs in DMSO were extremely low.

Table 3-2. Dependence of the RCY on Solvent for substitution pattern **5**^{82, 83}

 5	RCY (%)		
	LG = NO ₂	LG = Br	LG = Cl
Solvent = DMF	89 ± 2	45 ± 4*	57 ± 6*
Solvent = DMAc	76 ± 2	27 ± 0.2*	12 ± 4*
Solvent = Sulfolane	40 ± 2	13 ± 3*	9 ± 0.3*
Solvent = DMSO	71 ± 2	4 ± 1*	4 ± 1*

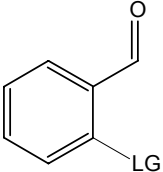
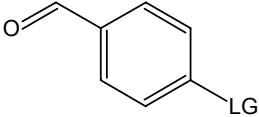
Labeling condition: precursor (20 mg), solvent (1 mL), 3.5 % K₂CO₃ (100 μL) and K2.2.2 (15 mg), at 140 °C, within 30 min.

*: at 160 °C.

Maximum RCY is presented.

For better monitoring of the labeling reaction, model compounds which have fewer substituents on the benzene ring were used (Table 3-3). Similar to the previous results of substitution pattern **5**, the influence of the solvent on the radiochemical yields was strongly dependent on the leaving group. With the fluoro or nitro group as a substituent (**1-F**, **2-F**, **1-NO₂**, **2-NO₂**), the radiochemical yield was reduced from 75 ~ 82 % in DMF to 40 ~ 68 % in DMSO. In the case of the chloro or bromo precursors (**1-Cl**, **2-Cl**, **1-Br**, **2-Br**), in DMSO the radiochemical yield decreased to less than 2 %, whereas yields of 65 ~ 75 % were obtained in DMF.

Table 3-3. RCY for benzaldehydes only with one leaving group in DMF or DMSO

Leaving group	 1			 2		
	RCY (%)			RCY (%)		
	DMF	DMSO		DMF	DMSO	
		This study	Literature		This study	Literature
F	75 ± 1	64 ± 4	--	78 ± 0.5	56 ± 4	--
NO₂	84 ± 0.3	68 ± 0.4	53-78 ^{35, 80, 84-88}	81 ± 5	40 ± 3	53-75 ^{35, 80, 85-89}
Cl	65 ± 1	0.6 ± 0.3	--	67 ± 3	1 ± 0.8	1-6 ^{80, 89}
Br	73 ± 0.2	1 ± 0.5	--	75 ± 0.5	1 ± 0.6	3-7 ^{80, 89}

Labeling condition: precursor (10 mg), solvent (1 mL), 3.5 % K₂CO₃ (100 μL) and K2.2.2 (15 mg), at 140 °C, within 30 min.

Maximum RCY is presented.

In order to better understand the labeling reactions in DMF and DMSO, the case of **1-Br** versus a possible effect of oxidation was examined. HPLC analysis showed the formation of the corresponding substituted benzoic acid as result of the oxidation of the aldehydic group (Figure 3-6). In DMSO, more than 90 % of **1-Br** was oxidized within 3 min. In DMF, less than 5 % of benzoic acid was formed and after 1 min the amount of benzoic acid did not change. These results show oxidation proceeds rapidly in DMSO resulting in low labeling yields. Interestingly, no ^{18}F -labeled benzoic acid derivatives were observed.

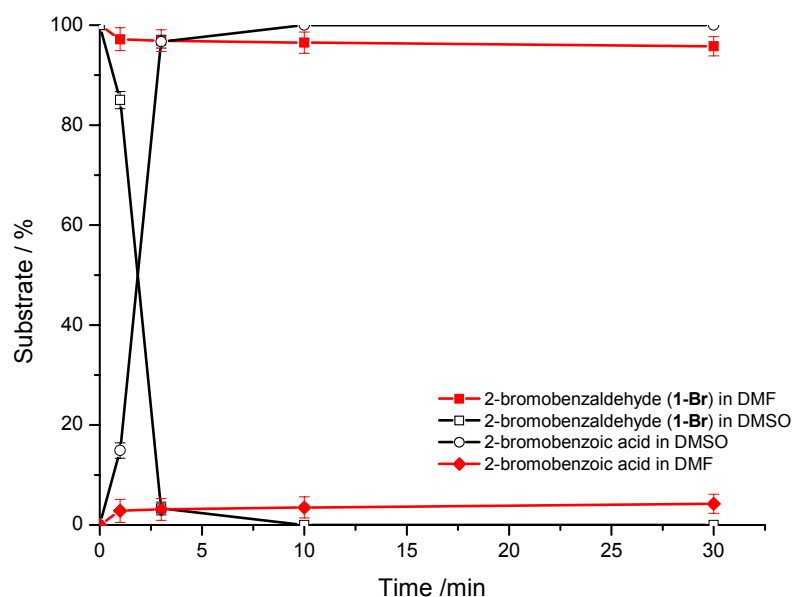


Figure 3-6. Oxidation of 1-Br to 2-bromobenzoic acid during labeling reactions in DMF or DMSO

The effect of the carbonyl group *para* or *ortho* to the LG should be similar when substituent effects are considered on the basis of mesomeric interactions. In DMF, *ortho* and *para* isomers were similarly substituted by $[^{18}\text{F}]$ fluoride ion independent of the LG (Table 3-3). In DMSO, no differences between *ortho* and *para* isomers were noted except in the case of the nitro group as the LG. The *ortho* isomer (**1-NO₂**) showed a radiochemical yield of 68 ± 0.4 %, the *para* isomer (**2-NO₂**) only 40 ± 3 %. For **1-NO₂** and **2-NO₂**, the labeling reactions in both solvents were also analyzed by HPLC.

In DMF, the formation of oxidation products was always much slower and the concentration of benzoic acid remained below 10 % (Figure 3-7 and Figure 3-8) and good labeling yields, i.e. 84 ± 0.3 % and 81 ± 5 %, for **1-NO₂** and **2-NO₂** were observed, respectively.

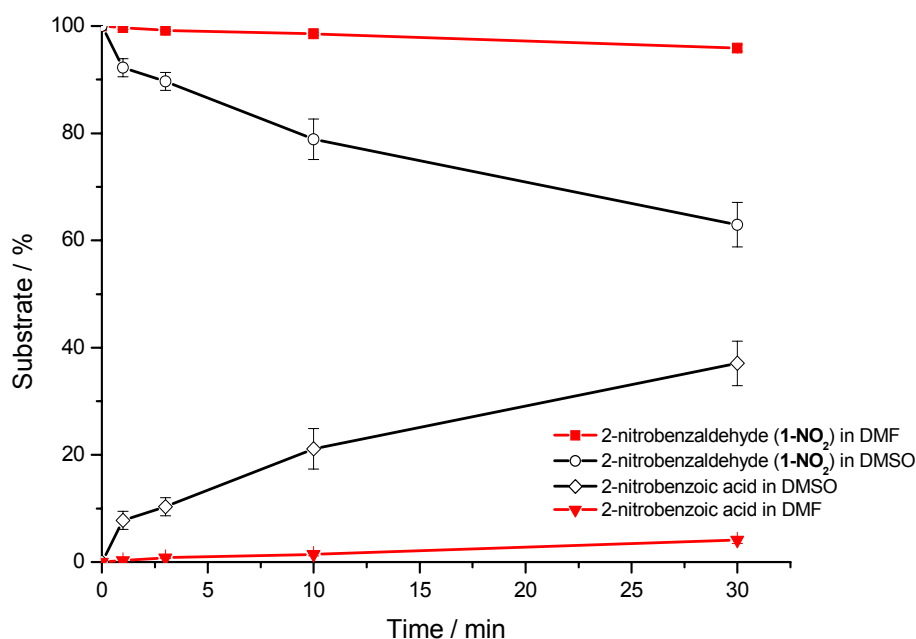


Figure 3-7. Formation of 2-nitrobenzoic acid by oxidation of 1-NO₂ during labeling reactions in DMF or DMSO

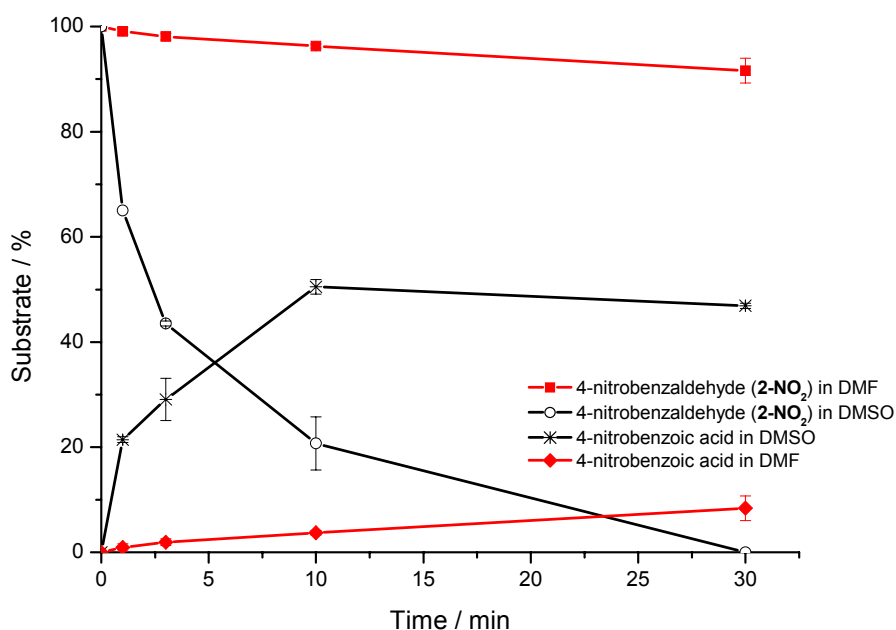


Figure 3-8. Conversion of 2-NO₂ during labeling reactions in DMF or DMSO

In DMSO, almost 40 % of 1-NO₂ was oxidized to benzoic acid within 30 min. The oxidation proceeded faster than in DMF without giving rise to any other by-products (Figure 3-7). Therefore, the radiochemical yield (68 ± 0.4 %) was lower than in DMF (84 ± 0.3 %). Labeling of 2-NO₂ in DMSO was accompanied by a high degree of

oxidation. After 30 min there was almost no precursor left due to the conversion to benzoic acid (ca. 50 % of the precursor) and an unidentified by-product (Figure 3-8), but the radiochemical yield (40 ± 3 %) did not decrease significantly. Neither benzoic acid nor the other by-product were detected as radioactively labeled products.

The small amount of oxidation of bromo and nitrobenzaldehyde (Figure 3-6 – Figure 3-8) in DMF observed at the beginning of the reaction may be due to dissolved oxygen. The high oxidation rates observed in DMSO, however, seem to be the result of an oxidation process mediated by this solvent. DMSO is known to be a superior reagent for the oxidation of alcohols to carbonyl compounds when it is activated by an electrophile.⁹⁰⁻⁹² The oxidation of benzaldehydes substituted with electron-withdrawing groups by DMSO in the presence of K_2CO_3 can be rationalized as an electrophilic addition of the aldehyde to the nucleophilic oxygen in DMSO, followed by deprotonation of the resulting sulfonium intermediate. The sulfur ylide, thus formed, may finally decompose under internal hydrogen abstraction into the anion of the benzoic acid and dimethylsulfide (Figure 3-9). In this study, benzoic acid was detected by HPLC and dimethylsulfide by GC/MS analysis.

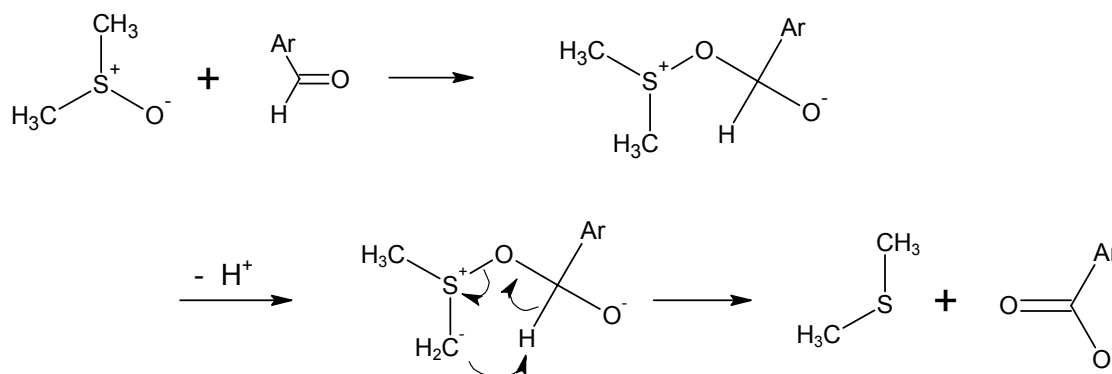


Figure 3-9. Suggested mechanism for the oxidation of substituted benzaldehydes in DMSO

In the case of isomers **1** and **2**, substitution by [¹⁸F]fluoride ion was reduced because the Cl and Br groups are poorer LGs (Table 3-3). In these cases, the competing oxidation prevailed. As already pointed out, the radiolabeled benzaldehydes formed by nucleophilic displacement by [¹⁸F]fluoride ion did not suffer from subsequent oxidation by DMSO. In all cases the fluorine was introduced either *ortho* or *para* to the aldehydic function. Despite its strong electron-withdrawing character, fluorine is also a strong +M-donor. This mesomeric effect lowers the electrophilic character of the aldehydic carbon and may protect the aldehyde from oxidation.

In conclusion, DMF is superior to DMSO as a solvent in the labeling reaction of benzaldehydes by S_NAr . Benzaldehydes with bromo or chloro substituents as leaving groups give very low radiochemical yields in DMSO due to rapid oxidation.

3.2.1.5 Effects of [^{18}F]nucleophile, concentration of precursor, temperature and reaction time

In order to achieve “naked” [^{18}F]fluoride ion of high nucleophilicity, the tetraalkylammonium carbonates (hydrogen carbonates) or the aminopolyether Kryptofix 222 in combination with potassium carbonates or oxalate ($TBA^{+18}F^-$ or $[K2.2.2-K]^{+18}F^-$) are widely adapted in the literature.^{10, 13, 19} In this work, the Kryptofix system was used for all radiofluorination reactions.

In a previous report,⁸² the influence of the concentration of the precursor and reaction temperature effects were studied in detail with substitution pattern **5**. It was found that the RCY was improved by increasing the concentration of the precursor, but when this concentration was higher than 10 mg/mL, the RCY reached a plateau. In addition, the optimum temperature for labeling with [^{18}F]fluoride ion was 140 °C (tests were carried out in the range of 100 - 160 °C).

In this study, the RCY for the labeling reaction was investigated at different time points, and kinetic curves were plotted. In most cases, the nucleophilic aromatic fluorination proceeded quickly and the maximum RCY was reached after 10 - 20 min. In order to systematically study the nucleophilic aromatic ^{18}F -fluorination, the following experiments were carried out under optimized conditions which were determined as: 10 mg precursor is labeled with $[K/2.2.2-K]^{+18}F^-$ in DMF (1 mL) at 140 °C within 30 min.

3.2.1.6 Analytical assay of ^{18}F -labeled product

In analytical radiochemistry, the standard protocol for checking the identity and purity of ^{18}F -labeled products is carried out by radio-TLC and radio-HPLC (**Method 1**).⁹³ In this work, however, a few of the fluoro reference compounds were not available and could not be synthesized. In this case, only the purity of product could be checked by **Method 1**, and the identity of product was assured by **Method 2** or **Method 3**.

Method 1: The solutions of labeling reactions are analyzed by TLC and an Instantimager using the fluoro reference compounds as standards. Due to the lower resolution of TLC or the volatility of ^{18}F -labeled products (i.e. [^{18}F]fluorobenzene, [^{18}F]fluoroanisole), HPLC equipped with a NaI(Tl)-scintillation detector is used for

additional identification. ^{18}F -labeled products are identified in the radio-HPLC by the nonradioactive reference standards via comparison of their UV signal with the radioactive signal. The fraction of radioactive product is collected and measured by a gamma-counter to give the RCY in the labeling reaction. In order to avoid error by coincidence in the HPLC retention time, the ^{18}F -labeled product could be verified by using another different characteristic column i.e. a reverse phase C18 column and a phenyl hexyl column. In this study, most precursors (in the case of availability of reference standards) were analyzed by this standard method (radio-TLC accompanied by radio-HPLC analysis).

Method 2: Labeling reactions are performed in the presence of a K^{19}F (spray-dried) carrier (c.a. reaction, see paragraph 5.3.2). In this case, the carrier-added nucleophilic fluorination allows analyses by LC/MS in addition to detection by Radio-HPLC. Thus, by finding the mass of the ^{19}F -product within the fraction of the eluted ^{18}F -labeled product characterised by the retention time, the identification is independently assured.

Because the concentration of the ^{18}F -labeled product is much lower than the detection limit of the LC/MS, the K^{19}F carrier is added to increase the concentration of fluorinated product. However, the addition of the carrier decreases the fluorination yield in the labeling reaction. A different approach to reach the detection limit by concentrating the labeling solution is not feasible. Therefore, an appropriate amount of carrier, $8.6\ \mu\text{mol}\ \text{K}^{19}\text{F}$, was added in the labeling reaction.

Method 3: Precursors are chosen having the same chemical structure, except for a different leaving group, so that they result in the same product, i.e. substitution of the bromo and nitro group leads to the same ^{18}F -labeled product, which is identified by the corresponding retention time on HPLC.

In this work, verification of the ^{18}F -labeled products (some methoxy- or methyl-substituted compounds) were carried out by **Method 2** and **Method 3**.

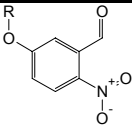
3.2.2 The effect of methoxy substituents on the S_NAr reaction

3.2.2.1 Selection of protective groups for the hydroxyl group

In the case of the nucleophilic aromatic substitution used for radiofluorination, it is particularly important to avoid free $-OH$ or $-NH_2$ groups by means of appropriate protecting groups. The reason is that the reactivity of the $[^{18}F]$ fluoride ion is decreased due to strong interactions of the $[^{18}F]$ fluoride ion with the acidic hydrogens. Acidic hydrogens can be present as impurities i.e. protic solvent residues or traces of unprotected precursor. Because of the fact that the concentration of precursor (0.03 – 0.07 mmol/mL) is much higher than the concentration of the $[^{18}F]$ fluoride ions (0.5 – 1.6 pmol/mL) in the labeling reaction, even an impurity of 0.1 % or less acidic hydrogens is still in large excess with respect to the amount of $[^{18}F]$ fluoride ion. Therefore, the presence of acidic hydrogens has to be avoided in S_NAr with great care. To produce ^{18}F -labeled phenolic amino acids, protection of the phenolic hydroxyl group is essential.

According to the literature, many protective groups are applicable to protect phenol. In this work the protective groups should match the following demands. First, they should be stable towards the labeling reaction conditions (temperature: 100 - 160 °C, pH: 8 - 12) and the conditions used during subsequent synthetic steps. In addition, they should also allow relatively easy deprotection at the last synthetic step. In previous work,⁶⁷ phenol ethers were chosen as protected phenols because of the relatively high stability and selective deprotection under acidic conditions (conc. HI, 150 °C).⁹⁴

Table 3-4. The influence of different ether as protected phenol

	R =					
	-CH ₃ (3-NO ₂)	-C ₂ H ₅ (12-C ₂ H ₅)	-C ₃ H ₇ (12-C ₃ H ₇)	-C ₄ H ₉ (12-C ₄ H ₉)	-Bn (12-Bn)	-CF ₃ (12-CF ₃)
RCY (%)	57 ± 1	63 ± 3	60 ± 2	60 ± 2	50 ± 1	60 ± 1
δ C _{arom} -NO ₂ in ¹³ C NMR (ppm)	141.8	141.6	141.6	141.6	141.9	147.9

Labeling condition: precursor (10 mg), DMF (1 mL), 3.5 % K₂CO₃ (100 μ L) and K2.2.2 (15 mg), at 140 °C, within 30 min.

Maximum RCY is presented.

As shown in Table 3-4, based on the structure of 5-hydroxy-2-nitrobenzaldehyde, the dependence of RCY on differentially-protected phenol hydroxyl was studied. Since

the angle between the benzene ring and the plane of the protective group influences overlap between the lone pairs on the oxygen atom and the π -system of the aromatic ring, the size of alkyl part in the ether could have an effect on this overlap, hence, there will be a changing of the π -electron densities at the *para* carbon atoms, a phenomenon which is verified by ^{13}C NMR chemical shift. However, in Table 3-4, the ^{13}C chemical shift of $\text{NO}_2\text{-C}_{\text{arom}}$ showed no significant difference for compounds **3-NO₂**, **12-C₂H₅**, **12-C₃H₇**, **12-C₄H₉** and **12-Bn** (141.6 - 141.9 ppm). Consequently, RCYs were also not markedly influenced by different type of phenol ether (50 ~ 61 %).

In addition, in the phenol ether, the electron density on the oxygen can be decreased by strong electron-withdrawing $-I$ -effects of alkyl part, such as the trifluoromethyl group. As a consequence, the $+M$ resonance effect on the *para* carbon atoms is reduced. Indeed, in compound **12-CF₃**, the electron density of the *para* carbon atoms bearing the LG was decreased (^{13}C NMR chemical shift of $\text{NO}_2\text{-C}_{\text{arom}} = 147.2$ ppm). However, the RCY was at the same level (60 %) when compared to the RCYs of the other phenol ethers. It is noteworthy that there was a radioactive by-product (RCY = 15 %) in the first 3 minutes of the reaction. This product was proposed to arise from the isotopic exchange (^{18}F for ^{19}F) on the trifluoromethyl group, but was not additionally analyzed.

All of those results indicated that modifying the phenolic precursor with different types of phenol ethers did not clearly increase the RCY. Finally, the methyl ether was chosen as the protection of the phenolic substrate in this study because methoxy compounds are most commonly available or are conveniently synthesized.

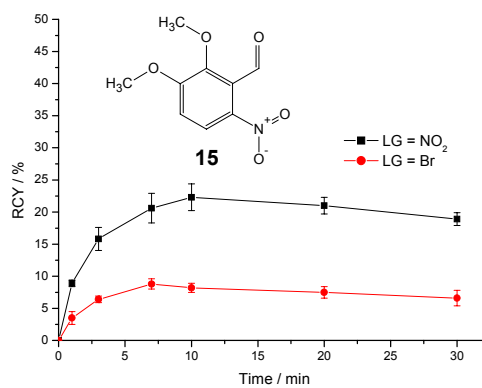
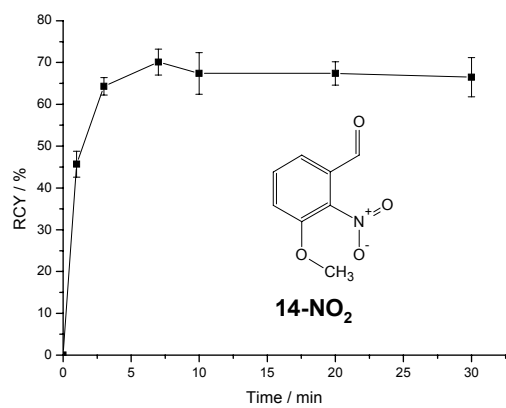
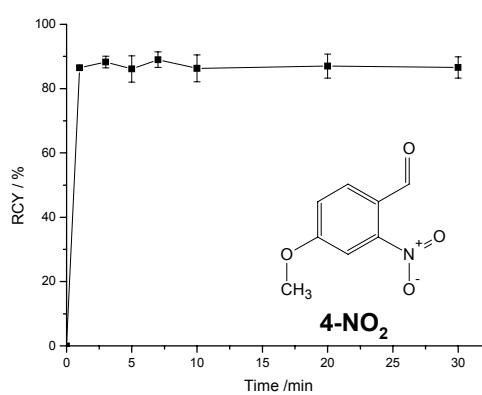
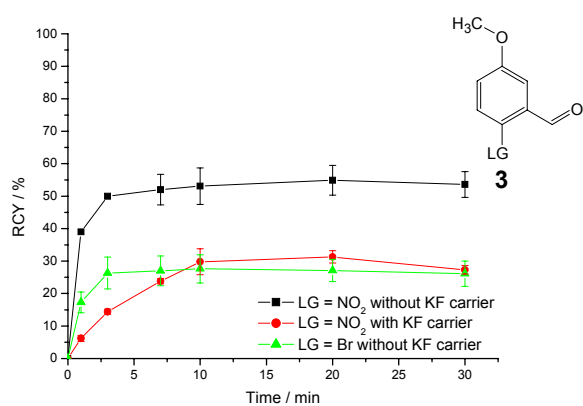
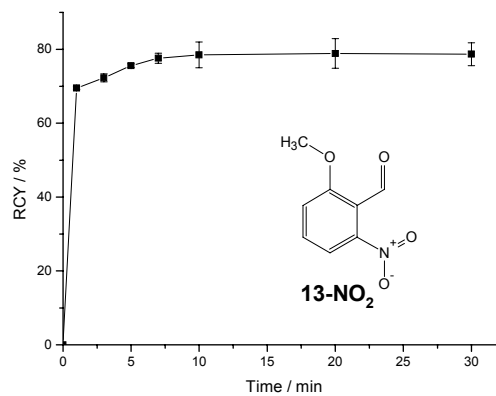
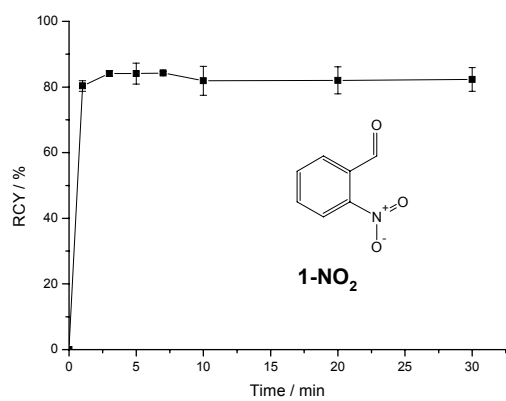
3.2.2.2 Effect of methoxy groups

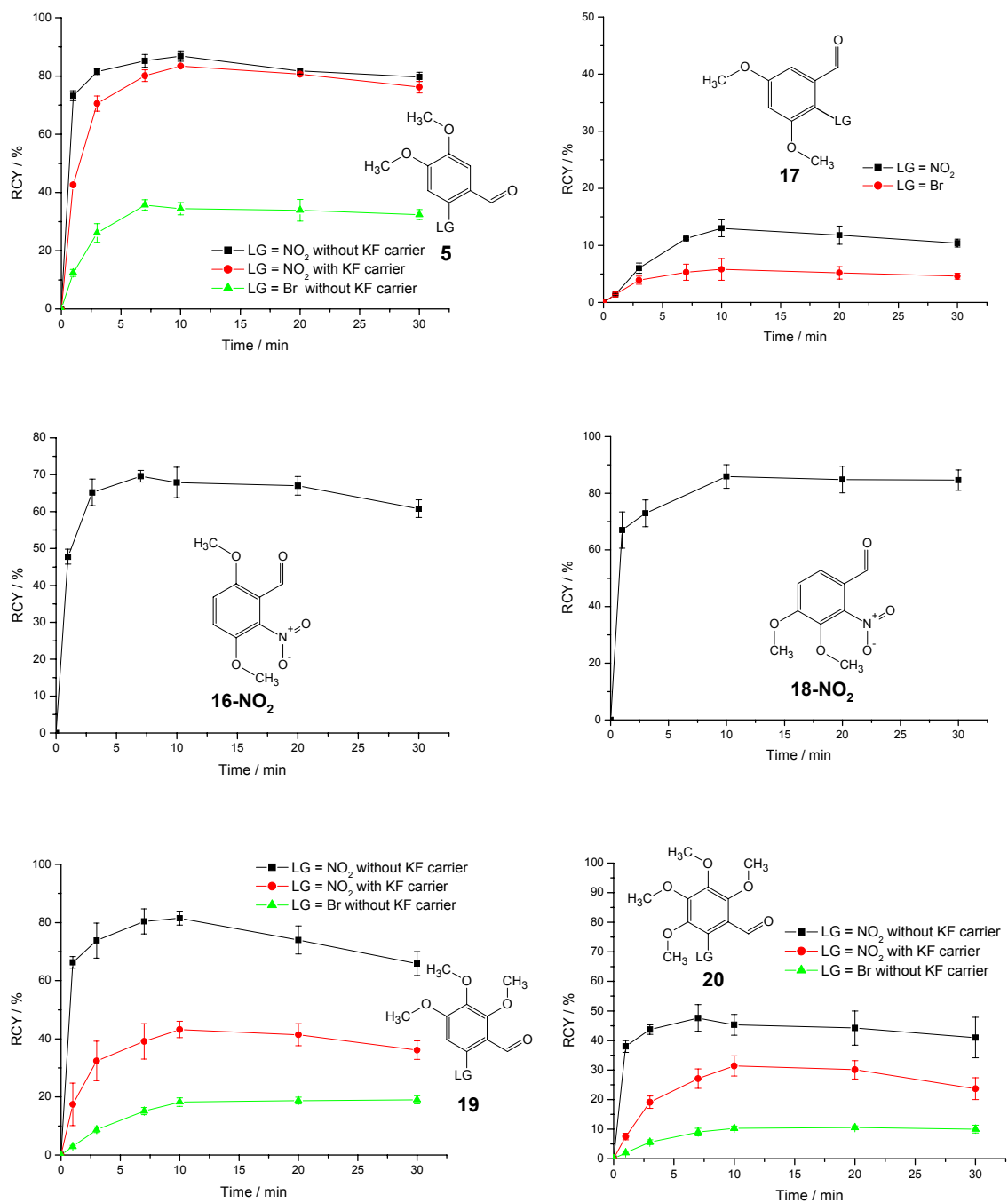
In the case of 5-methoxy-2-nitrobenzaldehyde (**3-NO₂**), a radiochemical yield of 5 % was reported for the substitution of NO_2 by ^{18}F .⁸⁴ This poor RCY may be understood in terms of the strong $+M$ -effect of the $-\text{OCH}_3$ substituent *p*-oriented to the LG. Compared to this result, the radiochemical yields (25 ~ 55 %) obtained for 4,5-dimethoxy-2-nitrobenzaldehyde (**5-NO₂**) as precursor^{95, 96} may be considered to be high. These results prompted a systematic study on the dependency of the RCYs on the number and positions of methoxy groups present in *o*-nitrobenzaldehydes.

The investigations were performed on 11 methoxylated *o*-nitrobenzaldehydes and compared with the RCY of 2-nitrobenzaldehyde (**1-NO₂**) in the nucleophilic

fluorination reaction. The labeling results (time dependence curve) are presented in Figures 3-10.

In all cases, the maximum RCY was normally reached within 5 - 10 min. In substitution patterns **3**, **5**, **13**, **18**, **19** and **20**, carrier ($K^{19}F$) added reactions were carried out. For both reactions (n.c.a. and c.a. nucleophilic fluorination), similar trends of yield curves were observed indicating both reactions proceeded by principally the same substitution mechanism. For compounds **13-NO₂** and **18-NO₂**, only the maximum RCY was checked in this c.a. labeling reaction. In addition, in compounds **3-Br**, **5-Br**, **15-Br**, **17-Br**, **19-Br** and **20-Br**, the nitro substituent was replaced with bromine. Results similar to the nitro compounds were observed; however, due to the poorer qualities of the bromo substituent as a LG, the radiochemical yields were generally much lower.





Labeling condition: precursor (10 mg), DMF (1 mL), 3.5 % K₂CO₃ (100 μL), and K2.2.2 (15 mg) at 140 °C, within 30 min.

Maximum RCY is presented.

Figure 3-10. The dependence of RCY on reaction time for differentially-methoxylated *o*-nitrobenzaldehydes

With **1-NO₂**, a maximum radiochemical yield of 84 % was observed. The derivatives obtained by introduction of an increasing number of methoxy groups to the aromatic ring of **1-NO₂** can be roughly divided in three groups with respect to the maximum incorporation yield of ¹⁸F (Figure 3-11).

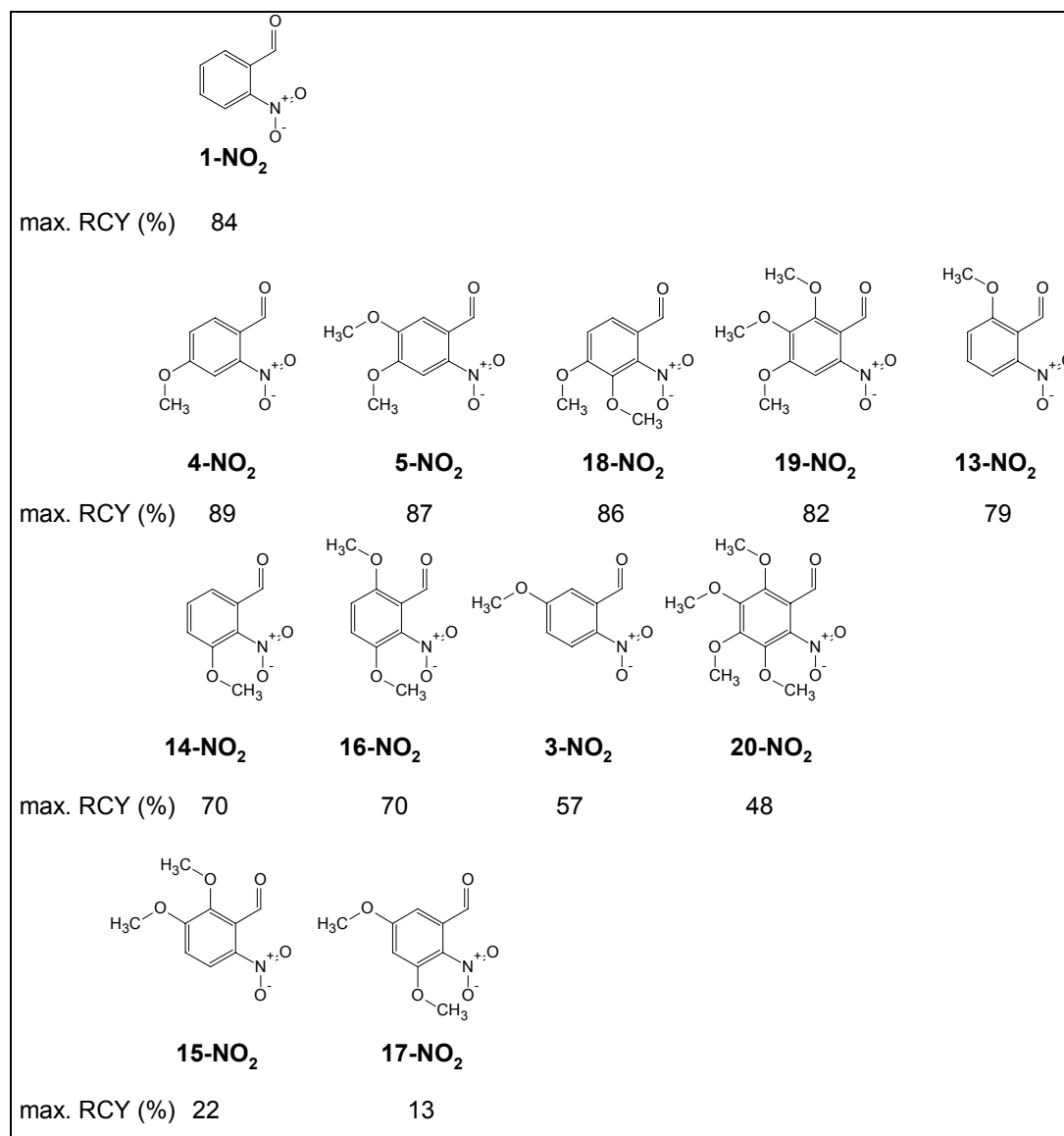


Figure 3-11. Classification of *ortho* nitrobenzaldehyde derivatives by Maximum RCYs

Remarkably high yields close to, or even above, the value for **1-NO₂** were noted for compounds **4-NO₂** (89 %), **13-NO₂** (79 %), **5-NO₂** (87 %), **18-NO₂** (86 %) and **19-NO₂** (82 %). These compounds have a methoxy group at C-4 (*meta* oriented with respect to NO₂) in common. Lower, although still satisfactory, radiochemical yields were found for the fluorination reaction of **16-NO₂** (70 %), **14-NO₂** (70 %), **3-NO₂** (57 %) and **20-NO₂** (48 %). Compound **17-NO₂**, which is substituted with two methoxy groups in the *o*- and *p*-position to the LG showed a significantly lower maximum yield of only 13 %. Similarly, the yield of **15-NO₂** was low (22 %). In this case, the

reason could be the formation of a radioactive by-product of unknown structure accounting for a yield of 15 %.

The electronic influence of methoxy groups on aromatic rings is described by a combination of the electron-donating +M-effect and the electron-withdrawing –I-effect. With respect to the *ortho* and *para* positions relative to the methoxy-substituted carbon atom, the mesomeric effect dominates, and therefore renders nucleophilic attack more difficult. Indeed, both, the 3-methoxy-(**14-NO₂**) and the 5-methoxy-substituted derivative (**3-NO₂**) gave lower yields in comparison to the reference compounds **1-NO₂**. The lowest yield was observed when both positions were simultaneously methoxylated (**17-NO₂**). In contrast, introducing the –OCH₃ group in position 4 (**4-NO₂**) and 6 (**13-NO₂**) (both in the *meta* position to NO₂) did not result in a larger change of the radiochemical yields. For *meta* positions, the electron-withdrawing –I-effect becomes more important, which should result in an increase of the reactivity of the nitro-substituted carbon towards nucleophilic attack. On the other hand, in this substitution pattern the methoxy group suppresses to some extent the activating effect of the *ortho*-formyl substituent by +M-donation (Figure 3-12).

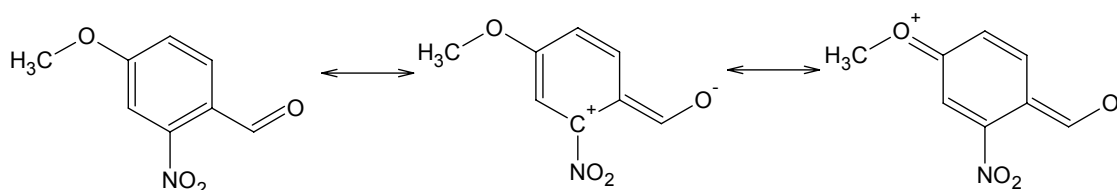


Figure 3-12. Effect of the methoxy group in *para* position to the formyl group

The combined action of both effects may be the reason why such derivatives give more or less the same radiochemical yield as the reference compound **1-NO₂**.

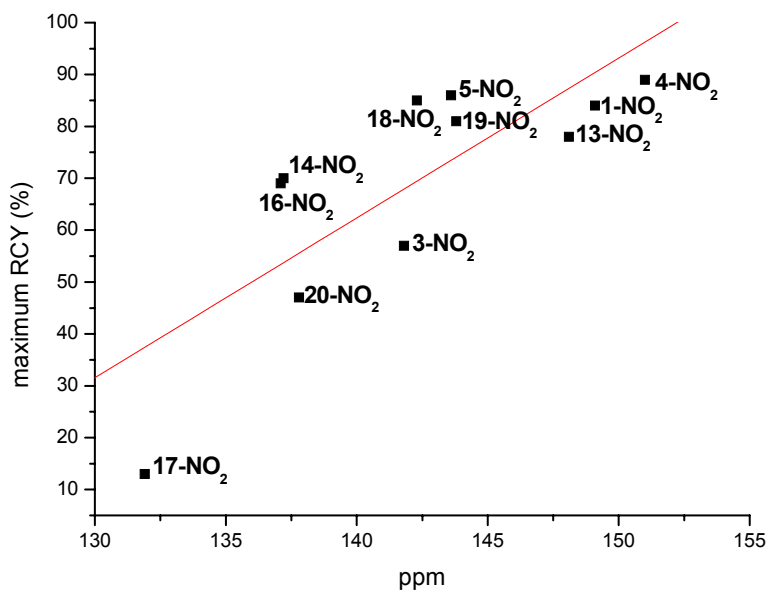
The overall effect of the presence of both *o/p*- and *m*-methoxy groups is difficult to predict because steric effects may additionally become superimposing to the electronic effects.⁸⁴ In particular, steric hindrance works against the +M-effect because the orbital overlap between the lone pair on the oxygen atom and the aromatic π -system becomes disturbed. The total effect of all substituents and the electron density of the carbon atom bearing the leaving group may be derived from the ¹³C NMR chemical shifts of this carbon position.

The ¹³C NMR chemical shift of the nitro-substituted C-atom in the *o*-nitrobenzaldehydes studied (Table 3-5) were in the range between $\delta = 132$ ppm (**17-NO₂**) and 151 ppm (**4-NO₂**).

Table 3-5. ^{13}C NMR chemical shifts of the nitro-substituted carbon and rate constants (k^* , at 1 min) of methoxy-substituted 2-nitrobenzaldehydes

Compounds	$\delta \text{C}_{\text{Arom-NO}_2}$	$k^* \text{ min}^{-1}$	RCY at 1 min
4-NO ₂	151.0	2.00	87 ± 0.6
1-NO ₂	149.1	1.62	80 ± 2
13-NO ₂	148.1	1.19	70 ± 0.4
19-NO ₂	143.8	1.09	66 ± 2
5-NO ₂	143.6	1.32	73 ± 2
18-NO ₂	142.3	1.11	67 ± 6
3-NO ₂	141.8	0.62	46 ± 1
15-NO ₂	139.0	0.09	9 ± 0.5
20-NO ₂	137.8	0.48	38 ± 2
14-NO ₂	137.2	0.61	46 ± 3
16-NO ₂	137.1	0.65	48 ± 2
17-NO ₂	131.9	0.01	1 ± 0.2

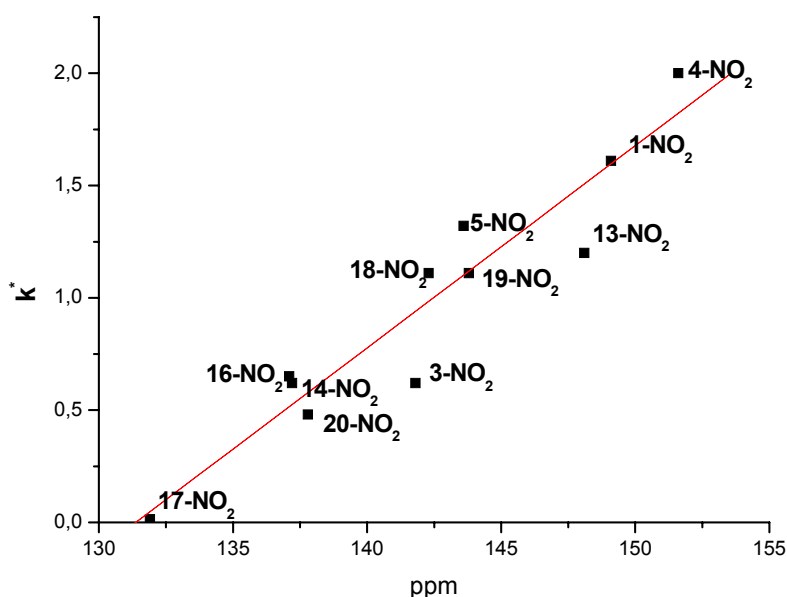
In the reports of Rengan et al.⁸⁷ and Ding et al.,⁸⁴ a correlation of the RCY with the deshielding of the carbon atom bearing leaving group was studied ($R^2 = 0.87$;⁸⁷ $R^2 = 0.53$ ⁸⁴). However, the compounds involved in both reports had different ethers as protected phenols. In addition, DMSO was used as the labeling solvent, which can cause strong competition reactions due to oxidation of aldehydic functions (see paragraph 3.2.1.4). In this work, only the methoxy substituent was used as a protected phenol, and DMF was applied instead of DMSO to avoid oxidative side reactions. The correlation of maximum RCY with the ^{13}C NMR chemical shift of the nitro-substituted C-atom showed a trend but not a good fit ($R^2 = 0.62$) (Figure 3-13). The deshielding of the nitro-substituted carbon atom is considered to be a measure of its electrophilicity. The question is whether such a reactivity parameter may correlate with maximum radiochemical yields or not. In radiofluorination experiments the $[\text{Precursor}] / [^{18}\text{F}]\text{F}^-$ ratios applied are very high. If no product decomposition and side reactions consuming or deactivating $^{18}\text{F}^-$ ion intervene, this should result in complete incorporation of ^{18}F into the reaction product. Only the time needed for the completion of the reaction should vary according to the electrophilicity of the precursor. In reality, however, side reactions and product decomposition contribute to the outcome of a labeling reaction and decrease the yield. These side effects should become more influential as the precursor becomes less reactive. This may explain why the maximum radiochemical yields correlate to some extent with the ^{13}C NMR chemical shift values as reactivity parameter.



Compound 15-NO₂ has been omitted because a radioactive by-product (15 %) of unknown structure was detected.

Figure 3-13. Correlation of maximum RCY with ¹³C NMR chemical shift values

At the beginning of a labeling experiment any competing side effect lowering the yield should be less disturbing. In our experiments, the course of the radiochemical yields was determined over 30 min (Table 3-5, Figure 3-10). The strongest yield increase was generally observed within the first minute. Provided that the ¹³C NMR chemical shifts are reliable measures of the electrophilicities, these values should give a satisfactory correlation with the rate constants (k^*) in this reaction interval. Because only the measurements after 1 min were available, the pseudomonomolecular rate constants derived from the radiochemical yields after 1 min can only be considered as estimates. Yet, the k^* values showed a satisfactory correlation with ¹³C-chemical shifts ($R^2 = 0.89$). (Figure 3-14).



Compound **15-NO₂** has been omitted because a radioactive by-product (15 %) of unknown structure was detected.

Figure 3-14. Correlation between k^* and ^{13}C NMR chemical shift values

As outlined before, the more reactive *o*-nitrobenzaldehyde derivatives with respect to the $\text{S}_{\text{N}}\text{Ar}$ reaction should have a better chance to escape unwanted side reactions and, therefore, attain higher yields in the radiofluorination steps. The precursor molecules **19-NO₂** and **20-NO₂** may illustrate this. **19-NO₂** (δ (C-6) = 144 ppm) was ca. twofold as reactive as **20-NO₂** (δ (C-6) = 138 ppm). The corresponding maximum radiochemical yields were 82 % (**19-NO₂**) and 48 % (**20-NO₂**). It should be emphasized that the yield obtained from the fully substituted derivative **20-NO₂** was still acceptable from a practical point of view, and higher than expected when comparing with **17-NO₂** (13 %, δ (C-6) = 132 ppm).

From the data compiled in Table 3-5 it can be seen that the precursors with chemical shifts of the nitro-substituted carbon atom close to the corresponding value found in **1-NO₂** (δ (C-6) = 149 ppm) give high maximum radiochemical yields, e.g. **4-NO₂** (δ (C-6) = 151 ppm), 89 %; **19-NO₂** (δ (C-6) = 144 ppm), 82 %.

In these cases, because of the high reactivities of the precursors towards the $\text{S}_{\text{N}}\text{Ar}$ reaction, side reactions did not play an important role, and high yields (≥ 80 %) resulted in the radiofluorination. However, for the less reactive precursors exhibiting δ -values in the range of 132 to 137 ppm, a decrease in the radiofluorination yields (13 ~ 70 %) was observed. Because the yields went through a maximum within the reaction interval of 30 min, the reduced yields could not be explained by insufficiently

long reaction times. Obviously, with compounds less prone to the S_NAr reaction, other processes consuming $^{18}F^-$ ion became important.

In the course of our experiments with methoxylated *o*-nitrobenzaldehydes, indications of possible side reactions were indeed obtained. LC/MS measurements revealed the formation of phenolates which could be formed in an S_N2 -like demethylation by attack of F^- at the methoxy group (Figure 3-15).

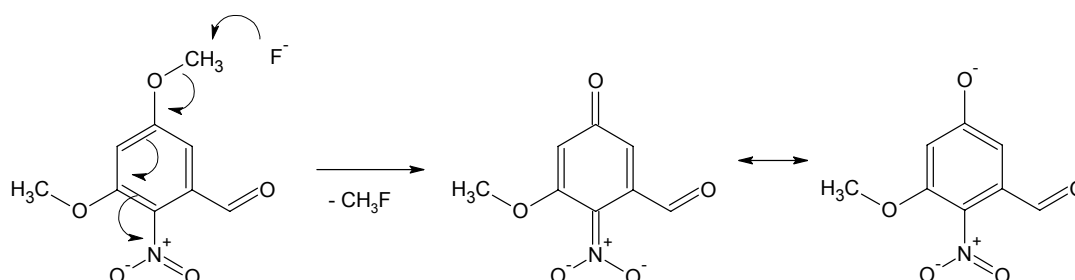


Figure 3-15. Demethylation of methoxy group by S_N2 mechanism

In all cases a HPLC-peak eluting faster than the starting compound with a mass corresponding to the $[M-H]^-$ ion of the phenolic demethylation product could be detected. In ^{19}F -fluorination of 2,3,4-trimethoxy-6-nitrobenzaldehyde (see paragraph 5.2.3.12), the phenolic product was isolated and characterized.

The proximity of a nitro and formyl group in the precursor molecules could give rise to an intramolecular redox process resulting in *o*-nitrosobenzoic acids. If *o*-nitrosobenzoic acids are formed as side products, they deactivate the nucleophilic power of $[^{18}F]$ fluoride ion by interacting with the acidic hydrogens, potentially ending up in strong hydrogen bonds. Such intramolecular redox-processes are well known in photochemistry⁹⁷ and electron-impact induced fragmentation (mass spectrometric *ortho*-effect).⁹⁸ Under these reaction conditions the intramolecular process is initiated by abstraction of the aldehydic hydrogen by an unpaired electron on a nitro oxygen formed by $n-\pi^*$ excitation and ionisation, respectively. An analogous thermal process could be started by intramolecular nucleophilic addition of a nitro oxygen atom to the neighbouring carbonyl group (Figure 3-16).

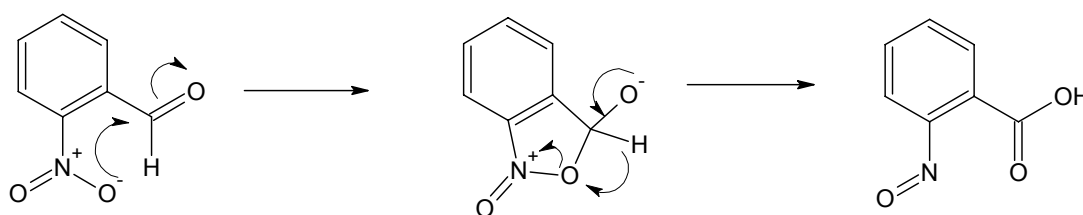


Figure 3-16. The intramolecular redox-processes in *o*-nitrobenzaldehyde

To test a thermal intramolecular redox reaction as a possible side reaction intervening in our labeling experiments, *o*-nitrobenzaldehyde was heated under conditions identical with the labeling experiments except that no fluoride ion was present. On heating in DMF in the presence of the K₂CO₃-crown ether complex, a blueish colour built up. Subsequent LC/MS analysis indicated the formation of an isomeric compound eluting faster than the starting compound. The mass spectrum (ACPI (-) mode) exhibited strong [M-H]⁻ (m/z 150) and [M-H-CO₂]⁻ (m/z 106) ions. In contrast, the negative ion mass spectrum of the starting compound was dominated by the radical anion M^{•-} at m/z 151. The blue colour (typical for C-nitroso compounds) and the mass spectral data are in accordance with the formation of *o*-nitrosobenzoic acid.

In summary, for the nucleophilic aromatic fluorination of methoxylated *o*-nitrobenzaldehydes by [¹⁸F]fluoride ion, a correlation has been found between the downfield shift of the nitro-substituted aromatic carbon atom in the ¹³C NMR spectrum and the reaction rate at the beginning of the reaction. Side reactions and product decomposition decrease the radiochemical yields to some extent as the reaction proceeds, and become relevant in the cases of less reactive precursor molecules.

4-Methoxy-2-nitrobenzaldehyde (**4-NO₂**), 4,5-dimethoxy-2-nitrobenzaldehyde (**5-NO₂**) and 3,4-dimethoxy-2-nitrobenzaldehyde (**18-NO₂**) are potential candidates for the syntheses of ¹⁸F-labeled tyrosine and DOPA, respectively, when the aldehydic function is utilized for connecting the aromatic substructure with the amino acid residue. All the three *o*-nitrobenzaldehyde precursors gave high maximum radiochemical yields (> 85 %). Even the threefold and fourfold methoxylated precursors **19-NO₂** and **20-NO₂** reacted in remarkably good yields to furnish the corresponding ¹⁸F-labeled products (82 % and 48 %, respectively).

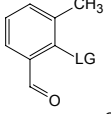
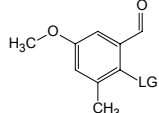
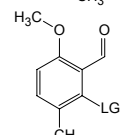
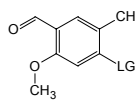
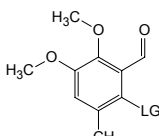
3.2.3 The effect of methyl substituent on S_NAr reaction

In a further approach towards the final goal of synthesizing ¹⁸F-labeled aromatic amino acids, the radiofluorination of compounds having a methyl group to mimic the protected glycine residue was examined.

3.2.3.1 Dependence of RCY on LG

Methyl-substituted precursors, modeling [¹⁸F]fluorophenylalanine, [¹⁸F]fluorotyrosine and [¹⁸F]FDOPA, were labeled with ¹⁸F via S_NAr. The radiochemical yields were dependent on different LGs such as nitro, fluoro, bromo and chloro groups (Table 3-6).

Table 3-6. RCYs of the precursors modeling ¹⁸F-labeled aromatic amino acids (i.e. effect of different leaving groups)

Substitution pattern	LG				Modeling
	NO ₂	F	Cl	Br	
6 	48 ± 5 % ^a	79 ± 3 % ^a	62 ± 9 % ^a	52 ± 2 % ^a	[¹⁸ F]fluoro phenylalanine
8 	3 ± 1 % ^a	75 ± 2 % ^a	14 ± 3 % ^a	10 ± 2 % ^a	[¹⁸ F]fluoro- <i>m</i> -tyrosine
9 	52 ± 6 % ^b	85 ± 5 % ^b	9 ± 2 % ^b	29 ± 2 % ^b	[¹⁸ F]fluoro- <i>p</i> -tyrosine
10 	69 ± 8 % ^b	80 ± 8 % ^b	32 ± 3 % ^b	36 ± 5 % ^b	[¹⁸ F]fluoro- <i>p</i> -tyrosine
11 	1 ± 1 % ^b	76 ± 6 % ^b	3 ± 1 % ^b	3 ± 2 % ^b	[¹⁸ F]FDOPA

Labeling condition: precursor (10 mg), DMF (1 mL), 3.5 % K₂CO₃ (100 μL) and K2.2.2 (15 mg), within 30 min. **a**: 140 °C, **b**: 120 °C⁷³.

Maximum RCY is presented.

For all of these compounds (Table 3-6), the RCYs were highest for the fluoro substituent as a LG. As a general tendency, the bromo and chloro substituent as the LG led to similar labeling results, which are usually lower than the RCYs in the precursor with a nitro substituent as a LG.⁸³ However, in Table 3-6 the RCYs of the nitro compounds varied from high (**10-NO₂**, 69 %) to low (**11-NO₂**, 1 %). For substitution patterns **6**, **8** and **11**, the nitro precursors showed even lower RCYs than

the bromo or chloro precursors. In addition, the maximum RCY was normally reached within 5 min to 10 min, except for **11-F**, where the maximum RCY was reached after 30 min.

3.2.3.2 Influence of the methyl group

In paragraph 3.2.2, for the precursors bearing a different number of methoxy groups in different substitution patterns, the correlation between the pseudomonomolecular rate constants k^* (determined from the RCY at $t = 1$ min) and the ^{13}C NMR chemical shifts of the carbon atom with the LG ($-\text{NO}_2$) was described.

Whereas for methoxylated *o*-nitrobenzaldehydes the plot exhibited a satisfactory fit ($R^2 = 0.89$, Figure 3-14), this was not the case for the corresponding precursors bearing a methyl group (**6-NO₂**, **7-NO₂**, **8-NO₂**, **9-NO₂**, **10-NO₂** and **11-NO₂**). The data were plotted as (k^* vs δ , $R^2 = 0.27$) (Figure 3-17).

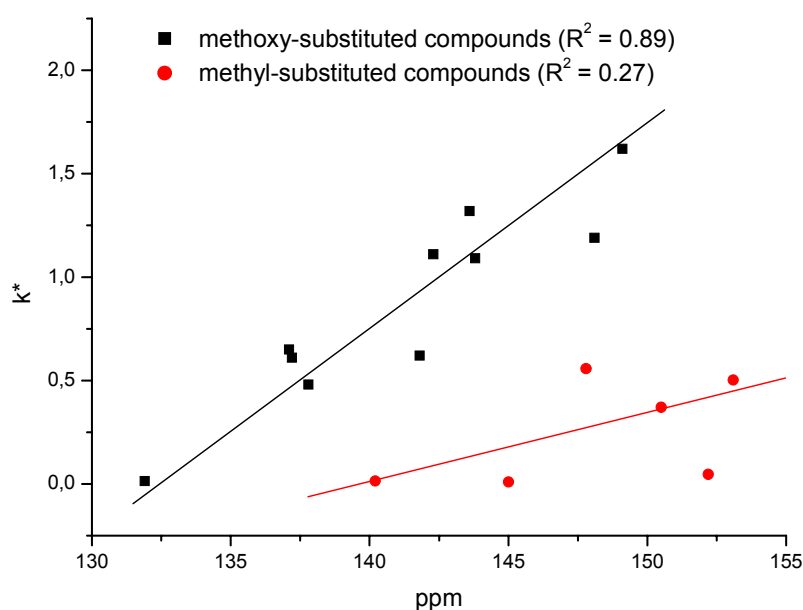
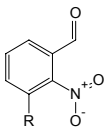
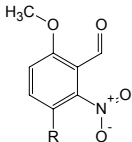
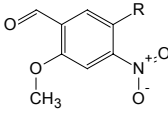
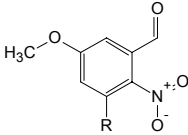
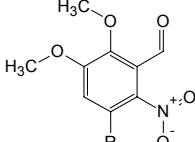


Figure 3-17. Correlation between k^* (1 min) and (δ) ^{13}C NMR chemical shifts of the carbon atom substituted by LG

This poor correlation for the compounds with a methyl group seems to be caused by the influence of the methyl group. Kilbourn et al.⁸⁷ suspected that the ^{18}F fluoride ion was deactivated by the methyl group, but did not propose a mechanism.

In order to explain this observation, the problem was approached systematically by comparing methyl-substituted compounds with their analogues. Compounds carrying either a hydrogen atom or a methoxy group in the position of the methyl group were chosen for comparison. The radiochemical yields are presented in Table 3-7.

Table 3-7. RCYs of model compounds with hydrogen, methoxy or methyl *ortho* to NO₂

Substitution patterns					
R = H	84 ± 0.3 % ^a (1-NO ₂)	79 ± 4 % ^a (13-NO ₂)	82 ± 2 % ^a	57 ± 1% ^a (3-NO ₂)	22 ± 2 % ^a (15-NO ₂)
R = -OMe	70 ± 3 % ^a (14-NO ₂)	70 ± 2 % ^a (16-NO ₂)	--	13 ± 2 % ^a (17-NO ₂)	--
R = Me	48 ± 5 % ^a (6-NO ₂)	52 ± 6 % ^a (9-NO ₂)	69 ± 8 % ^b (10-NO ₂)	3 ± 1 % ^a (8-NO ₂)	1 ± 1 % ^b (11-NO ₂)

Labeling condition: precursor (10 mg), DMF (1 mL), 3.5 % K₂CO₃ (100 μL) and K2.2.2 (15 mg), within 30 min. **a:** 140 °C, **b:** 120 °C⁷³

Maximum RCY is presented.

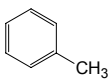
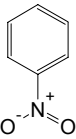
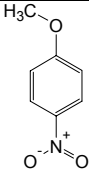
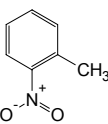
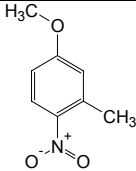
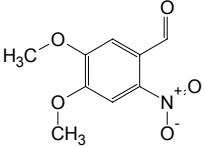
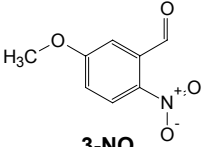
The introduction of a methyl group or a methoxy group in the *ortho* position to the nitro group always decreased the RCY, but the extent of yield decrease was different. This by itself is not surprising as the methyl group increases the electron density of the aromatic ring through a +I-effect, hence reducing its reactivity towards nucleophilic attack. However, a methoxy group exhibits a stronger electronic effect (+M-effect) and, hence, towards nucleophilic attack the reactivity of the reactive center should be reduced even more. Therefore, the reduction of the RCY by the methoxy group should be more than that by the methyl group. Surprisingly, the methoxy group in the position of the methyl group showed a much weaker negative effect on the RCY. Therefore, it can be concluded that electronic effects did not have the main influence in decreasing the RCY.

Following the literature by Rengan et al.,⁸⁷ competition experiments were carried out in order to determine which group or substitution pattern can be related to the decrease in RCY. **5-NO₂** and **3-NO₂** with a known RCY were labeled in the presence of competitive compounds bearing methyl, nitro and methoxy substituents, either one of them or in combination (Table 3-8).

Neither the addition of toluene, nor that of nitrobenzene and nitro anisole, influenced the labeling results. However, compounds with a methyl group *ortho* to the nitro group, i.e. *o*-nitrotoluene and 5-methoxy-2-nitrotoluene, seemed to have a negative effect on the RCY.

Since the RCY was not decreased in the presence of toluene and nitrobenzene, a particular intramolecular interaction between the methyl and nitro group was taken into consideration.

Table 3-8. ^{18}F -substitution in the presence of toluene or nitrobenzene derivatives

Precursor for ^{18}F -substitution	Competitive compounds					
	None					
 5-NO₂	87 ± 2 %	82 ± 0.4 %	84 ± 1 %	85 ± 4 %	55 ± 5 %	69 ± 3 %
 3-NO₂	57 ± 1 %	58 ± 1 %	59 ± 1 %	59 ± 1 %	38 ± 1 %	26 ± 7 %

Labeling condition: precursor (10 mg), DMF (1 mL), 3.5 % K_2CO_3 (100 μL) and K2.2.2 (15 mg), at 140 °C, within 30 min. 1 Molar eqv. competitive compound was added simultaneously with precursor.

Maximum RCY is presented.

For a better understanding of the reaction process, LC/MS analysis was used to monitor the labeling reaction. Interestingly, when the competitive compound *o*-nitrotoluene was used, the LC/MS analysis results showed that an unknown compound with the mass peak 302 (ACPI (+) mode) was detected in the case of **5-NO₂** and another compound with the mass peak 272 (ACPI (+) mode) was detected in the case of **3-NO₂**.

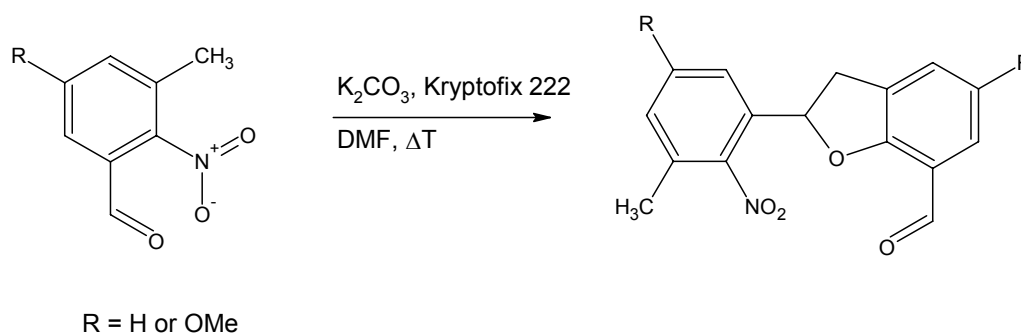


Figure 3-18. Condensation reaction of precursors containing *o*-nitrotoluene structure

Similarly, in the LC/MS analysis of the labeling solution of precursors (with the *o*-nitrotoluene substitution pattern in Table 3-6), a compound hinting at a mass of $(2 \times M_{(\text{precursor})} - 47)$ was always observed. Two precursors (**6-NO₂** and **8-NO₂**) were chosen as an example in order to synthesize the detected by-product and characterize it. The results showed that this side reaction was a condensation

reaction between two precursor molecules (Figure 3-18, Figure 3-19), and details were described in another work.⁷³

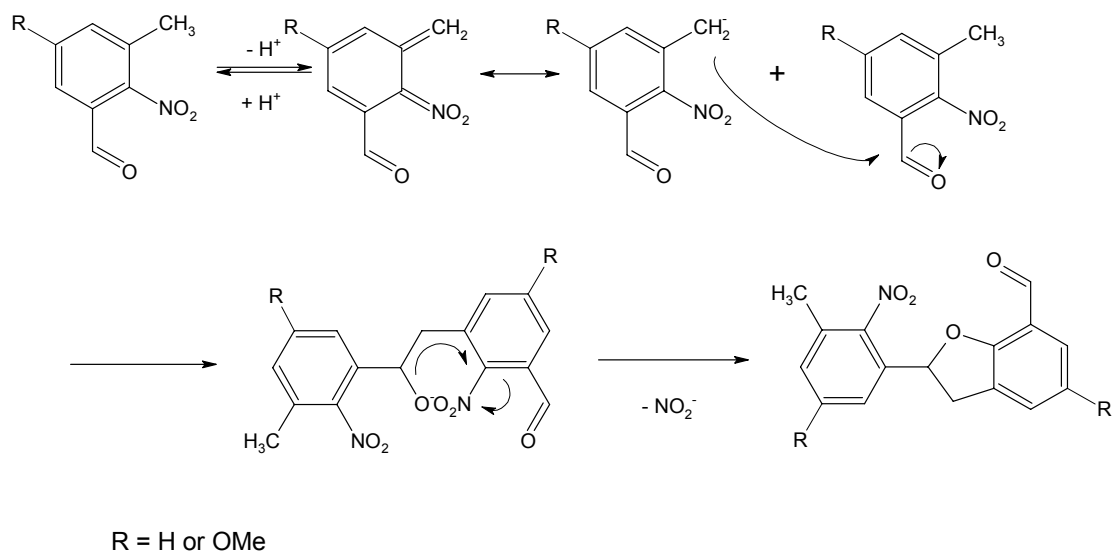


Figure 3-19. The mechanism for condensation reaction during S_NAr

Therefore, in the labeling reaction with the competitive compound *o*-nitrotoluene (Table 3-8), the formation of the unknown compounds can also be explained by the condensation side reaction (Figure 3-20)

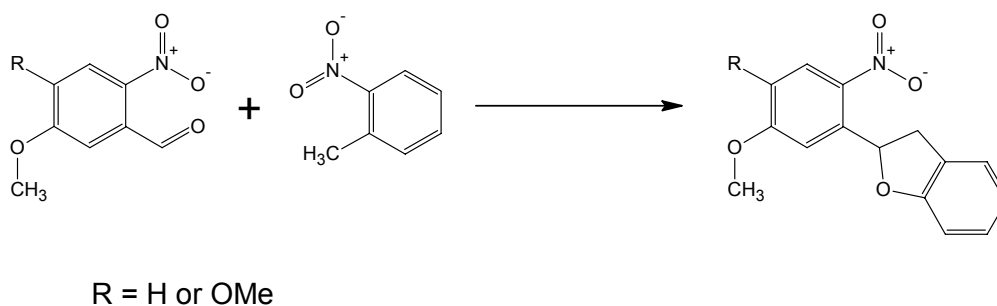


Figure 3-20. Condensation reaction of precursors with competitive compound

This condensation side reaction can reduce the RCY in the following ways:

- 1) The concentration of precursor can be decreased by coupling between two precursor molecules.
- 2) The acidic protons formed in the first step of the condensation reaction (Figure 3-19) can also deactivate the $^{18}F^-$ ion.

Due to the mechanism of the condensation reaction,⁷³ it can be also explained why the RCYs for **9-NO₂** and **10-NO₂** are better than for **8-NO₂** and **11-NO₂** (Table 3-6). In **9-NO₂** and **10-NO₂**, the methoxy substituent is *para/ortho* to the methyl substituent, thus, the ability of the methyl group to abstract a proton is decreased by the +M-effect and the nucleophilic substitution remains the dominating reaction. However,

in **8-NO₂** and **11-NO₂**, the methoxy group in the *p*-position to the LG decreases the reactivity towards S_NAr because of its strong +M-effect. Therefore, the condensation reaction becomes the dominant reaction. Moreover, this side reaction was only observed for methyl-substituted compounds with NO₂ as the LG, not for precursors with Br, Cl and F as the LG.

In summary, for compounds bearing a methyl group the RCY is clearly dependent on the LG and the substitution pattern. The isotopic exchange (¹⁸F/¹⁹F) always proceeds easily and in good yield, and the fluorodenitration is strongly influenced by the described condensation side reaction. In the case of the precursor with lower reactivity, this side reaction becomes dominant, hence resulting in low RCYs.

3.2.3.3 Attempts to improve the RCY of methyl-substituted precursors

As described above, in the labeling reaction of nitro substituted compounds (**8-NO₂** modeling [¹⁸F]fluoro-*m*-tyrosine and **11-NO₂** modeling [¹⁸F]FDOPA) the RCYs dropped significantly because of the strongly competitive side reaction. Due to the high interest in [¹⁸F]fluoro-*m*-tyrosine and [¹⁸F]FDOPA for clinical applications, attempts to improve the RCY of **8-NO₂** and **11-NO₂** (Table 3-6) have been made as follows.

Changing the reaction parameters was taken into consideration for suppressing the side reaction, i.e. reaction solvents (DMF, DMSO, DMAc), temperature (120 - 160 °C) and the type of base (Ce₂CO₃, K₂C₂O₄ or K₂CO₃/K₂C₂O₄). The data presented in Table 3-9 showed that the change of reaction parameters had very little effect on RCY. Moreover, the condensation by-product was still observed by LC/MS analysis of reaction solution (at 1 min). All these results indicate that the side reaction cannot be depressed by changing the reaction parameters.

Table 3-9. Labeling reaction of **8-NO₂** with different reaction parameters

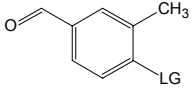
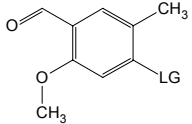
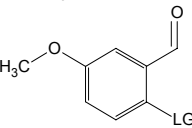
Solvent	Temperature (°C)	Base	RCY (%)
DMF	160	K ₂ CO ₃	3 ± 0.1
DMF	140	K ₂ CO ₃	3 ± 1
DMF	120	K ₂ CO ₃	0.6 ± 0.2
DMF	140	Ce ₂ CO ₃	2 ± 0.6
DMF	140	K ₂ C ₂ O ₄	2 ± 0.8
DMF	140	K ₂ CO ₃ /K ₂ C ₂ O ₄ =1/33	1 ± 0.1
DMF	140	K ₂ CO ₃ /K ₂ C ₂ O ₄ =1/1	0.8 ± 0.1
DMSO	140	K ₂ CO ₃	2 ± 0.2
DMAc	140	K ₂ CO ₃	2 ± 0.6

Labeling condition: precursor (10 mg), solvent (1 mL), base (25 μmol) and K2.2.2 (15 mg).

Maximum RCY is presented.

The side reaction takes place when $-\text{NO}_2$ is used as the leaving group. In paragraph 3.2.1.3, it was been mentioned that the trimethylammonium triflate group has a similar reactivity as the nitro group. Therefore, the effect of the trimethylammonium triflate as the LG was studied with substitution patterns **3**, **7** and **10** (Table 3-10).

Table 3-10. The comparison of NO_2 and $\text{N}^+\text{Me}_3\text{TfO}^-$ as LG in substitution patterns **3**, **6** and **7**

Substitution patterns	LG = NO_2	LG = $\text{N}^+\text{Me}_3\text{TfO}^-$
7 	$8 \pm 1 \%$	$69 \pm 1 \%$
10 	$69 \pm 8 \%^{73}$	$92 \%^{99}$
3 	$57 \pm 1 \%$	$35 \pm 4 \%$

Labeling condition: precursor (10 mg), DMF (1 mL), 3.5 % K_2CO_3 (100 μL) and K2.2.2 (15 mg), at 140 $^\circ\text{C}$, within 30 min.

Maximum RCY is presented.

For substitution patterns **7** and **10**, the RCYs were increased obviously when the trimethylammonium triflate substituent was used as a LG instead of the nitro substituent. However, in the case of substitution pattern **3**, the trimethylammonium triflate substituent as the LG showed a lower RCY than the nitro substituent as the LG. In the LC/MS analysis of the labeling reaction solution (**3-N⁺Me₃TfO⁻** and **7-N⁺Me₃TfO⁻**), the condensation by-product was not observed, whereas another by-product, 4-(dimethylamino)-3-methylbenzaldehyde ((ACPI (+) mode), $[\text{M}+\text{H}]^+$, m/z 163) or 2-(dimethylamino)-5-methoxybenzaldehyde ((ACPI (+) mode), $[\text{M}+\text{H}]^+$, m/z 180), was detected. According to the literature,¹⁰⁰ demethylation can take place for the trimethylammonium triflate precursor during the ^{18}F -labeling reaction (Figure 3-21).

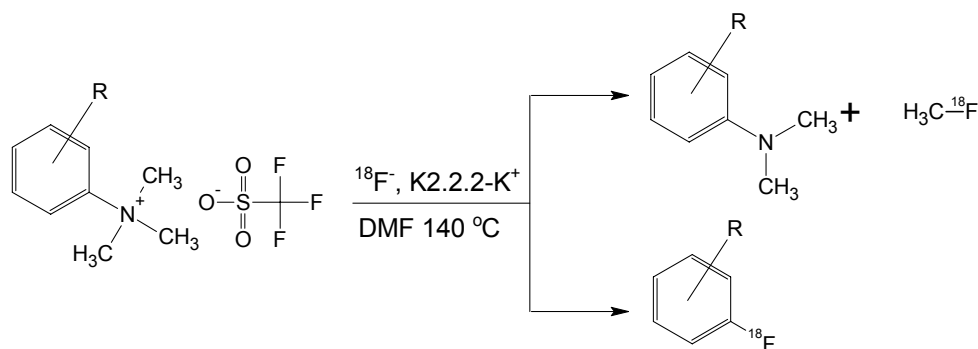
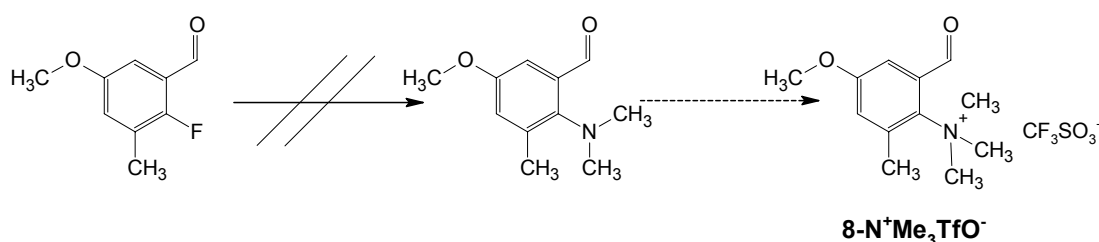


Figure 3-21. Demethylation of the precursor with $\text{N}^+\text{Me}_3\text{TfO}^-$ as LG

Nevertheless, high RCYs (69 % and 92 %) were obtained in the case of **7-N⁺Me₃TfO⁻** and **10-N⁺Me₃TfO⁻**. This indicated that nucleophilic substitution was still the dominant reaction, while the demethylation seemed to have little effect. In the case of **3-N⁺Me₃TfO⁻**, the methoxy substituent *para* to the LG could accelerate the rate of demethylation reaction by the +M-effect (Figure 3-21). This may explain why **3-N⁺Me₃TfO⁻** showed a lower RCY than **3-NO₂** (35 % and 57 %, respectively). As discussed above, RCY was decreased from 57 % (**3-NO₂**) to 3 % (**8-NO₂**) by the effect of the condensation side reaction, which starts with the deprotonation of the methyl substituent. Comparing the RCY decrease from **3-NO₂** to **3-N⁺Me₃TfO⁻** and from **3-NO₂** to **8-NO₂**, it was found that the demethylation side reaction shows a less negative effect. Therefore, a promising RCY could be obtained by using the trimethylammonium triflate substituent as the LG in the model compounds for [¹⁸F]fluoro-*m*-tyrosine and [¹⁸F]FDOPA.

During this work, the synthesis of **8-N⁺Me₃TfO⁻** failed because the intermediate product 2-(dimethylamino)-5-methoxy-3-methylbenzaldehyde cannot be synthesized by a nucleophilic substitution with dimethylamine on 2-fluoro-5-methoxy-3-methylbenzaldehyde, whereas, this synthetic route works very well for compounds **3-N⁺Me₃TfO⁻** and **7-N⁺Me₃TfO⁻**.



It is planned to synthesize **8-N⁺Me₃TfO⁻** by an alternative pathway (Figure 3-22) outside the scope of this thesis.

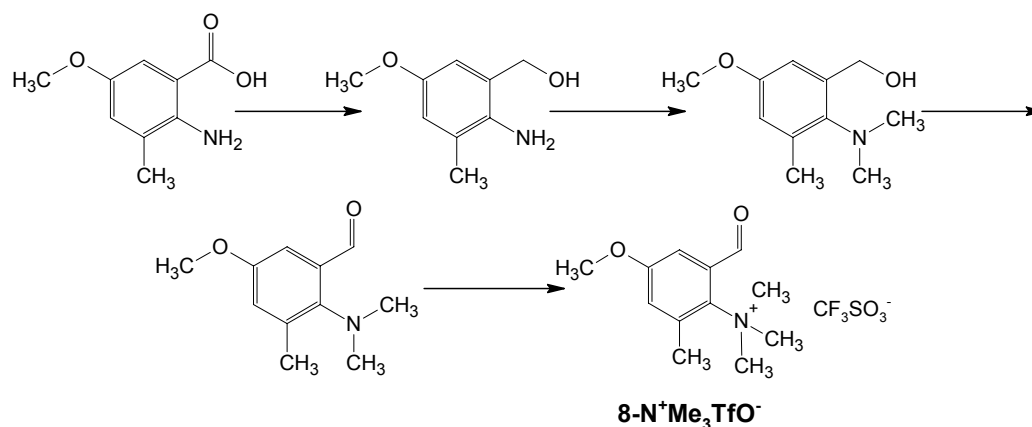


Figure 3-22. An alternative synthetic route for **8-N⁺Me₃TfO⁻**

3.2.4 The effect of a second formyl substituent on the S_NAr reaction

As described in paragraph 1.4.3, among many auxiliary substituents for activating S_NAr , the aldehydic function is one of the best choices for the syntheses of ^{18}F -labeled aromatic amino acids. This is because the aldehydic function can be catalytically removed by decarbonylation or used as starting point for the synthetic addition of the amino acid residue to the aromatic part of the molecule. Moreover, the results in paragraph 3.2.1 showed that the aldehydic function is efficient for improving the RCY, especially when it is located *ortho* or *para* to the LG. Therefore, in this paragraph two aldehydic functions were introduced in the precursor molecule to improve the RCY further.

3.2.4.1 Effect of a second formyl substituent on the maximum RCY

In the syntheses of methyl-substituted model compounds for ^{18}F -labeled aromatic amino acids, the second aldehydic function can be added on the benzene ring depending on the structure of the model compounds. In the case of [^{18}F]fluorophenylalanine and [^{18}F]fluoro-*p*-tyrosine, the second aldehydic group can be introduced *para* to the LG. In the case of [^{18}F]fluoro-*m*-tyrosine and [^{18}F]FDOPA, the second aldehydic group can be only introduced in the *meta* position to the LG (Figure 3-23).

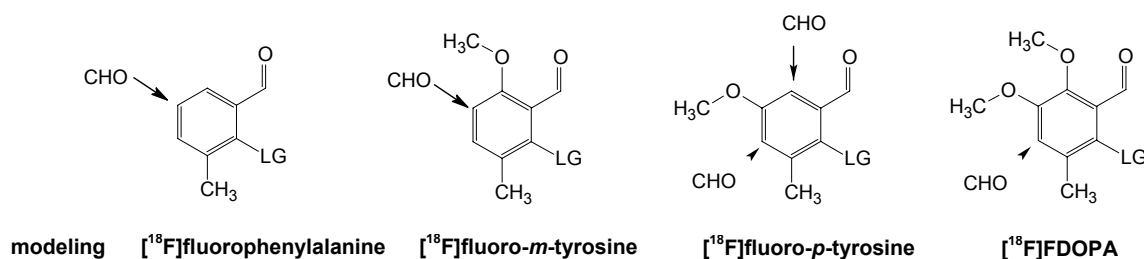


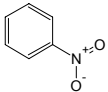
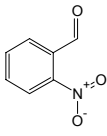
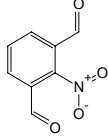
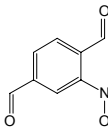
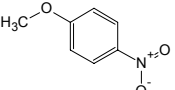
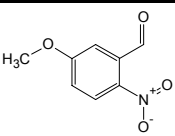
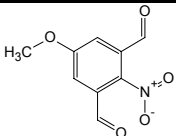
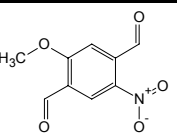
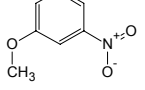
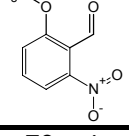
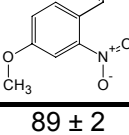
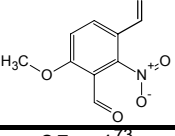
Figure 3-23. Dialdehyde function substituted model compounds aiming at ^{18}F -labeled aromatic amino acids

The discussion about the effect of aldehydic functions on the RCYs started from the compounds without the methyl substituent. Based on the structure of nitrobenzene, 3-nitroanisole and 4-nitroanisole, the aldehydic functions were added *ortho*, *meta* or *para* to the nitro group (Table 3-11).

The presented data in Table 3-11 showed that a maximum RCY of more than 80 % was achieved for compounds **21-NO₂**, **23-NO₂** and **25-NO₂**, which had two aldehydic functions, both *ortho* to the LG. In the case of **1-NO₂**, **13-NO₂** and **4-NO₂**, high maximum RCYs (79 ~ 89 %) were already observed, therefore the maximum RCY

was not improved further when the second aldehydic function was included (84 % for **21-NO₂** and 87 % for **23-NO₂**). However, in the case of **3-NO₂** the maximum RCY (57 %) was not as high as **1-NO₂**, **13-NO₂** and **4-NO₂** because the reactivity of this precursor was decreased by the strong +M-effect of the methoxy substituent *para* to the nitro group. For this kind of substitution pattern, a second aldehydic function *ortho* to the nitro group enhanced the maximum RCY to 80 % (**23-NO₂**).

Table 3-11. The maximum RCY of the precursors with non, mono or dialdehydic function

	Nonaldehydic compound	Monoaldehydic compound	Dialdehydic compound	
				
RCY(%)	1 ± 0.1	84 ± 0.3 (1-NO₂)	84 ± 3 (21-NO₂)	60 ± 3 (22-NO₂)
				
RCY(%)	0	57 ± 1 (3-NO₂)	80 ± 0.6 (23-NO₂)	32 ± 1 (24-NO₂)
		 		
RCY(%)	--	79 ± 4 (13-NO₂)	89 ± 2 (4-NO₂)	85 ± 1 ³ (25-NO₂)

Labeling condition: precursor (10 mg), DMF (1 mL), 3.5 % K₂CO₃ (100 μL) and K2.2.2 (15 mg), at 140 °C, within 30 min.

Maximum RCY is presented.

Interestingly, the dialdehydes **22-NO₂** and **24-NO₂** showed even lower maximum RCYs than monoaldehydes **1-NO₂** and **3-NO₂**. This special RCY decrease might be caused by an oxidation reaction of the dialdehydic precursor, especially when both aldehydic functions are *para* to each other. That increases the risk of oxidation of the aldehyde to benzoic acid due to the strong electron withdrawing effect. Indeed, in the LC/MS analysis of the labeling solution of **22-NO₂** (labeling condition was same as in Table 3-11 but in the absence of ¹⁸F⁻ ion), a relative polar by-product was formed in the first minute of reaction time and the mass spectrum (ACPI (-) mode) exhibits strong ions [M-H]⁻ (m/z 194) and [M-H-CO₂]⁻ (m/z 150). This information indicates that the by-product is a benzoic acid derivative. However, a source of oxygen for oxidation was not known in this experiment. In addition, in the same LC/MS analysis

of the labeling solution of **21-NO₂**, no benzoic acid derivative by-product was detected.

In order to avoid this kind of oxidation in the case of **22-NO₂**, the labeling reaction was performed at a lower temperature (Figure 3-24). However, lower RCYs were observed at 120 °C or 100 °C, and the benzoic acid derivative could still be detected within the first minute of the reaction time by LC/MS analysis.

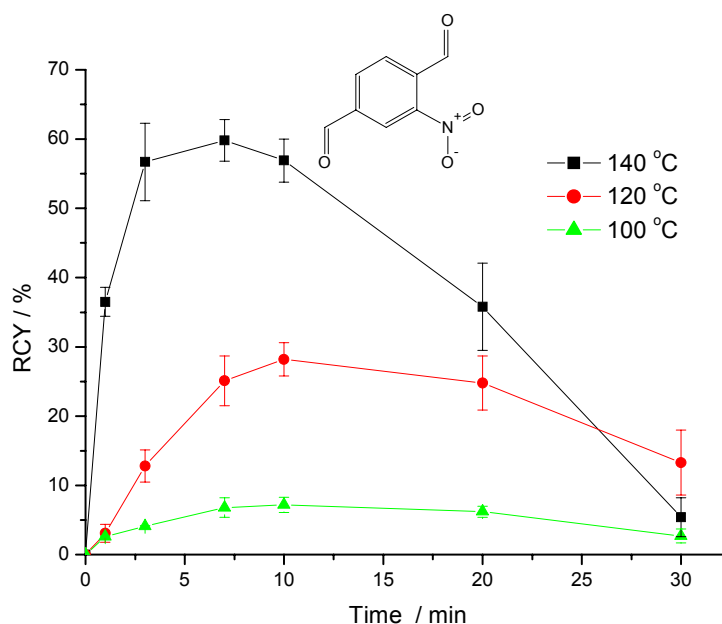


Figure 3-24. ¹⁸F-labeling reaction of **22-NO₂** at different temperature

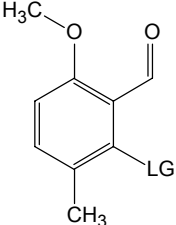
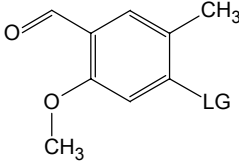
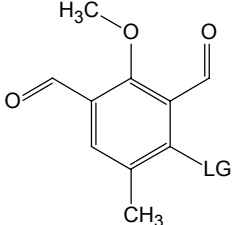
Therefore, the maximum RCY of the monoaldehydic compound can be improved by the introduction of a second aldehydic function, but this should meet the following conditions:

- 1) The reactivity of the monoaldehyde is not very high (maximum RCY ≤ 60 %).
- 2) The second aldehydic function should be introduced *ortho* or *para* to the LG.

According to the above requirements, for improving RCYs of monoaldehyde with a methyl substituent and a halogen as the LG (**9-Cl**, **9-Br** and **10-Cl**, **10-Br**), the second aldehydic function should be introduced *para* to the LG (**26-Cl** and **26-Br**).⁷³

The RCY data presented in Table 3-12 showed that the maximum RCYs were enhanced by introduction of the second aldehydic function.

Table 3-12. Comparison of RCY in monoaldehydic and dialdehydic compounds with a methyl substituent and a halogen as leaving group⁷³

			
LG = Cl	9 ± 2 % (9-Cl)	32 ± 3 % (10-Cl)	85 ± 3 % (26-Cl)
LG = Br	29 ± 2 % (9-Br)	36 ± 5 % (10-Br)	79 ± 4 % (26-Br)

Labeling condition: precursor (10 mg), DMF (1 mL), 3.5 % K₂CO₃ (100 μL) and K2.2.2 (15 mg), at 120 °C, within 30 min.

Maximum RCY is presented.

3.2.4.2 Reaction Kinetics in ¹⁸F-labeling of dialdehydic compounds

For **22-NO₂**, the time dependence curves at 140 °C (Figure 3-25) showed that the RCY reached a maximum value (85 %) within the first minute, and then dropped to only 1 % after 20 min. This indicates that the labeled dialdehydic compounds are not stable under the labeling conditions. In order to avoid decomposition of the labeled product, the labeling reaction of **22-NO₂** was performed at lower temperatures. It was found that the decomposition of the labeled product was depressed by decreasing the reaction temperature. At 60 °C the decomposition of the product was almost stopped (RCY = 80 % at 30 min), yet the substitution reaction proceeded very fast (maximum RCY = 85 % at 1 min). Surprisingly, even at room temperature the relatively high maximum RCY (78 %) was still observed at 7 min.

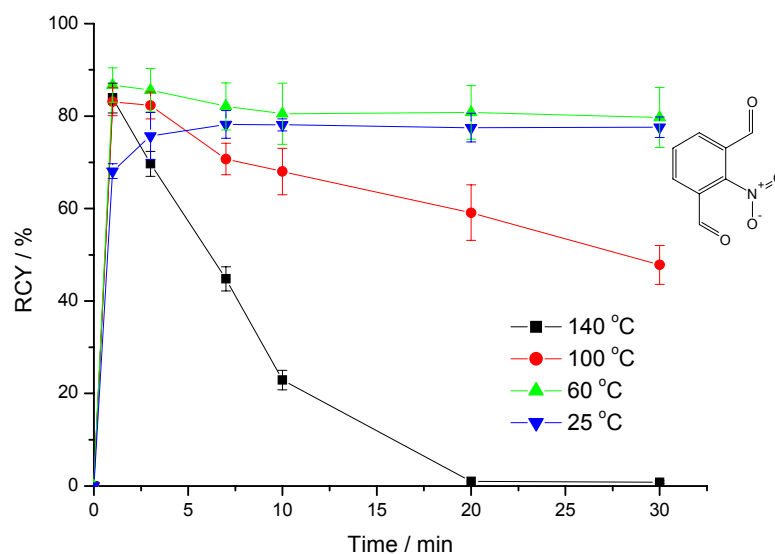


Figure 3-25. Time dependence curves in the radiolabeling of **22-NO₂** at different temperatures

In contrast, for **1-NO₂**, the time dependence curves (25 - 140 °C) showed that the labeled product had a high stability under the labeling conditions, but the reactivity of the precursor and reaction rates were decreased at lower temperatures. At 25 °C, the RCY was only 10 % after the 30 min labeling reaction (Figure 3-26).

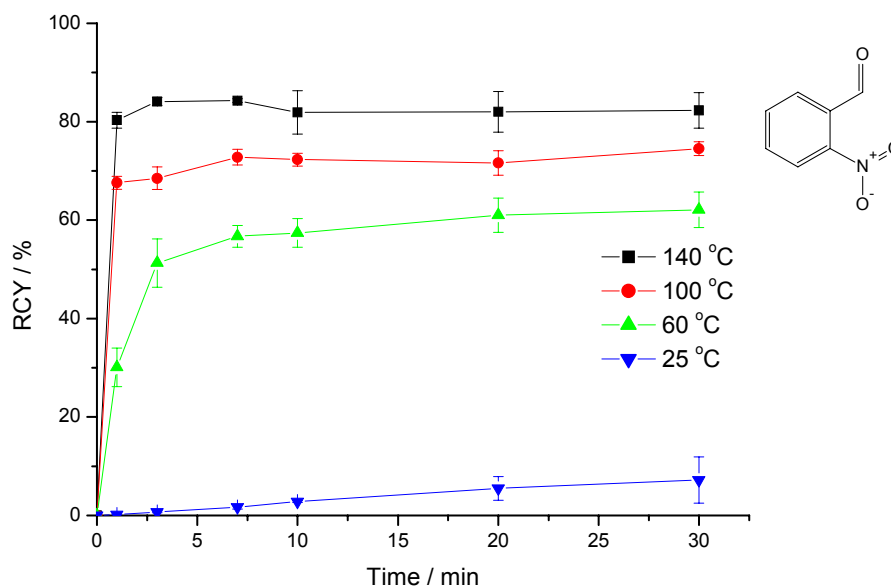


Figure 3-26. Time dependence curves in the radiolabeling of 1-NO₂ at different temperatures

This S_NAr reaction was also performed at a lower temperature for methyl-substituted model compound **26-Cl**.⁷³ The time dependence curves are presented in Figure 3-27. Although the Cl substituent as the LG decreased the reactivity of the precursor, the maximum RCY (30 %) was still found at 25 °C after a 30 min labeling reaction.

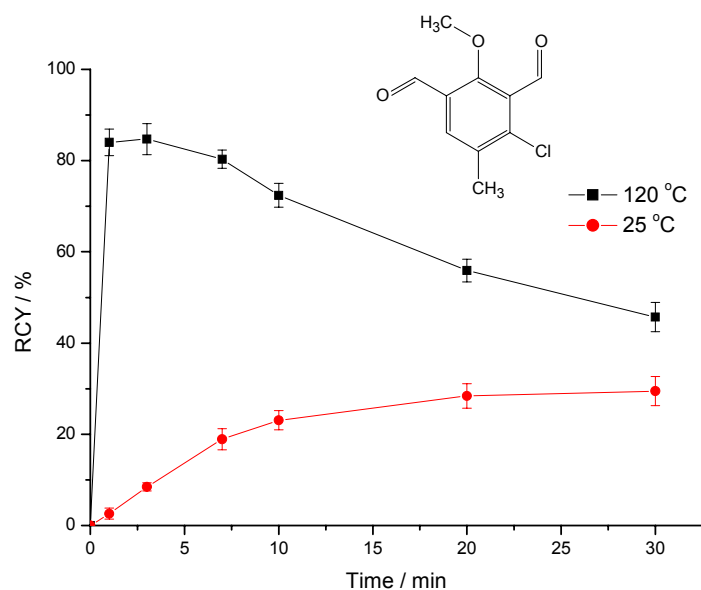


Figure 3-27. Time dependence curves in the radiolabeling of 26-Cl⁷³ at different temperatures

As generally expected, the introduction of a second aldehydic function in the *o/p* position to the LG improves the maximum RCY of precursors with low reactivity and accelerates the reaction rates significantly, i.e. even at room temperature **21-NO₂** was labeled in a good yield of 79 % within 10 min. However, introduction of a second aldehydic function in the *meta* orientation to the LG decreases the maximum RCY compared to the monoaldehyde, the reason is the rapid formation of a benzoic acid derivative in the radiolabeling.

3.3 Decarbonylation of the ^{18}F -labeled benzaldehydes

In order to realize the syntheses of ^{18}F -labeled aromatic amino acids by the newly-developed synthetic strategy (see Figure 2-2), the electron withdrawing substituent that is able to activate the aromatic nucleophilic substitution should be removable after the introduction of the ^{18}F . Among many EWGs, the formyl group was chosen due to the possibility of an easy catalytic removal as was principally demonstrated.^{35, 101} However, in these approaches, it was not pursued further, and the multi-substituted model compounds (similar to [^{18}F]FDOPA) had not yet been studied. In this paragraph, the conditions of the decarbonylation reaction were studied with the model compounds for [^{18}F]fluoro-*m*-tyrosine, and those conditions were applied in decarbonylations of multi-substituted monoaldehydes or dialdehydes modeling ^{18}F -labeled aromatic amino acids.

3.3.1 Decarbonylation of model compounds with monoaldehydic substituent

Decarbonylation was tested on multi-substituted benzenes as model compounds, such as **8-F**, **9-F**, **9-NO₂**, **9-Cl**, **9-Br** and **11-F**, aiming at the syntheses of [^{18}F]fluoro-*m*-tyrosine, [^{18}F]fluoro-*p*-tyrosine and [^{18}F]FDOPA (Figure 3-28). The best reaction conditions were to be determined for an efficient and fast removal of the carbonyl function.

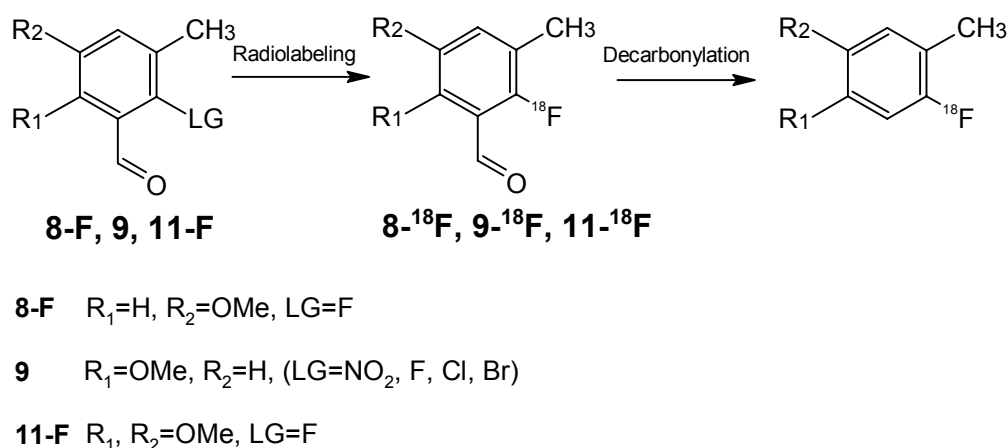


Figure 3-28. Radiochemical syntheses of model compounds for [^{18}F]fluoro-*m*-tyrosine, [^{18}F]fluoro-*p*-tyrosine and [^{18}F]FDOPA

3.3.1.1 Selection of catalyst

Decarbonylation reactions are usually performed by two kinds of catalysts: Wilkinson's catalyst $\text{RhCl}(\text{PPh}_3)_3$ or a palladium / carbon catalyst. It was found that in the syntheses of [^{18}F]fluoroarenes using the corresponding fluorobenzaldehydes, the rhodium complex offered quite a few advantages with respect to reaction rates and mild conditions in comparison to the palladium / carbon catalyst.¹⁰¹

The decarbonylation reaction by Wilkinson's catalyst $\text{RhCl}(\text{PPh}_3)_3$ has been established as an efficient method to remove the carbonyl function.^{102, 103}

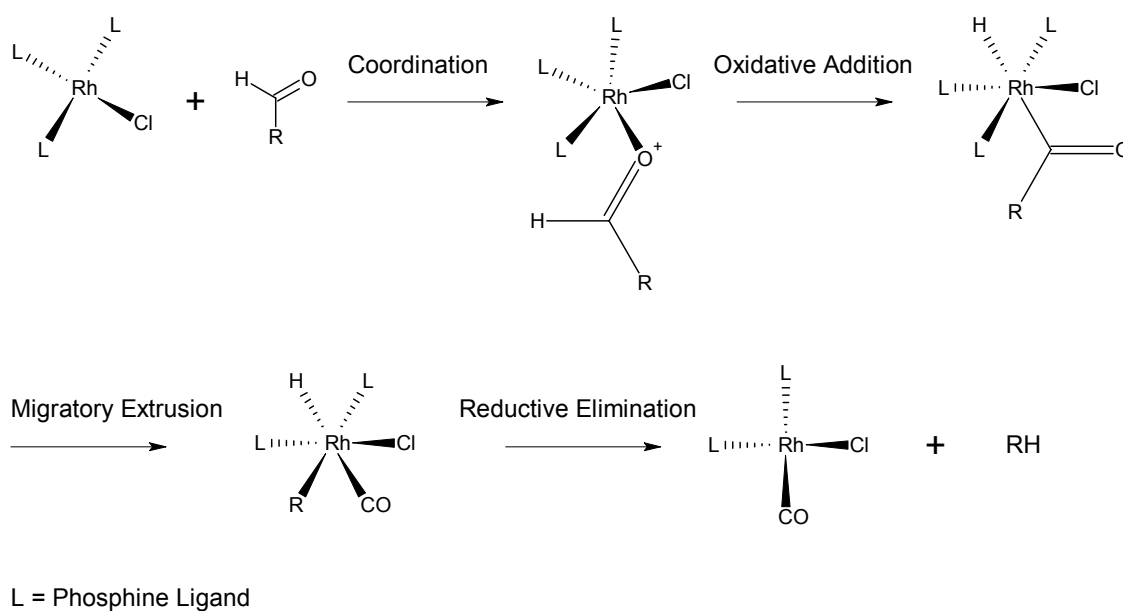


Figure 3-29. The mechanism of decarbonylation by rhodium catalyst

According to the reported mechanism,^{104, 105} the rhodium-catalyzed decarbonylation comprises four elementary steps: (i) coordination of the aldehyde, (ii) oxidative addition of the aldehydic C-H to form a rhodium-acyl complex, (iii) migratory extrusion of carbon monoxide, (iv) reductive elimination of the product. (Figure 3-29).

In the following text, $\text{RhCl}(\text{PPh}_3)_3$ was chosen for a systematic study to optimize the decarbonylation yields of compound **8- ^{18}F** .

3.3.1.2 Solvent dependence

In the literature, dioxane, 1,2-dichloroethane, benzene and toluene are commonly recommended as solvents to achieve the decarbonylation of aldehydes with $\text{RhCl}(\text{PPh}_3)_3$.^{35, 106, 107} Sterically hindered aldehydes require higher temperatures for decarbonylation by the rhodium complex. However, at higher temperatures, large amounts of the catalyst are transformed to a precipitating brick red dimeric complex of di- μ -chloro-tetrakis(triphenylphosphine)dirhodium. According to Ohno and Tsuji,

the active rhodium species is stabilized sufficiently in benzonitrile to suppress dimer formation.¹⁰⁷ Therefore, particular interest was now focused on the application of benzonitrile as the solvent for the decarbonylation.

The decarbonylation of **8-¹⁸F** was performed in DMSO, dioxane, toluene, DMF and benzonitrile with 2 molar equivalents of the rhodium complex (with regard to the precursor) at 150 °C (Figure 3-30). After 20 min of reaction time, the following yields were obtained: 65 ± 1 % (DMSO), 61 ± 1 % (dioxane), 53 ± 2 % (toluene), 30 ± 3 % (DMF) and 81 ± 1 % (benzonitrile). In accordance with the report of Ohno and Tsuji, reaction solutions remained homogeneous in benzonitrile, whereas in the other solvents, precipitation of the brick red complex was observed within the first 5 minutes. Furthermore, TLC analysis revealed the formation of a radioactive polar complex commencing at the beginning of the reaction and resulting in the consumption of 30 ~ 60 % of the ¹⁸F-labeled benzaldehyde after 20 min in all solvents except benzonitrile. In the latter solvent, the radioactive polar by-product was detected in yields < 5 % at the end of the reaction.

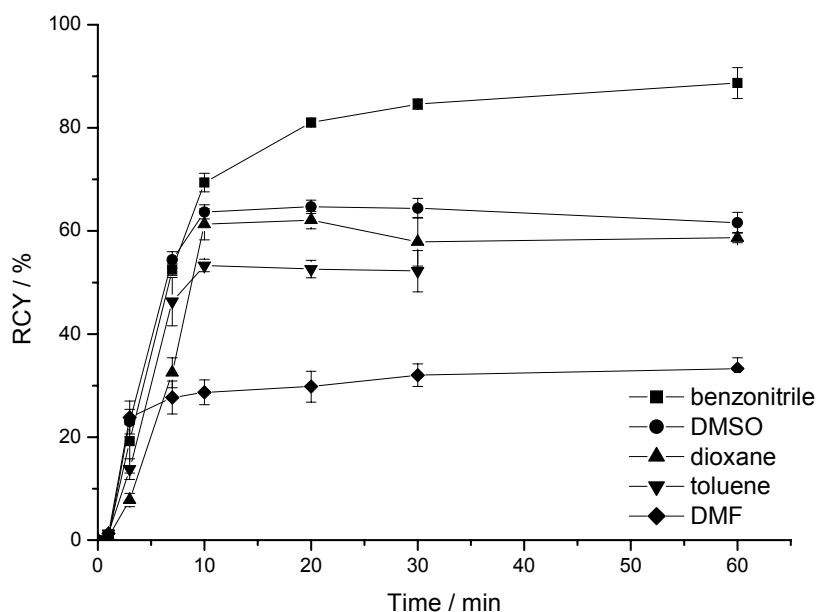


Figure 3-30. Decarbonylation yield of 8-¹⁸F in different solvents with 2 molar eq. catalyst (molar eq. based on quantity of 8-F) at 150 °C

In the case of 2-[¹⁸F]fluoro-4,5-dimethoxy-benzaldehyde (**5-¹⁸F**), a yield of 84 ± 5 % was reported³⁵ for the decarbonylation using 2 molar equivalents of the catalyst in dioxane as solvent at 150 °C after 15 min. Another group,¹⁰⁸ however, using the

same reaction protocol, obtained only 59 % yield as was also observed in our experiments.

The data of Ohno and Tsuji and those presented in this study clearly demonstrate that benzonitrile is the solvent of choice in order to obtain an efficient decarbonylation with Wilkinson's catalyst.

3.3.1.3 Influence of temperature

In the case of decarbonylating $8\text{-}^{18}\text{F}$, the influence of the temperature was evaluated by using 1 mL of benzonitrile as the solvent and 2 molar equivalents of Wilkinson's catalyst. A change of temperature between 100 °C and 180 °C clearly enhanced the decarbonylation yield (Figure 3-31). At 180 °C, the reaction was finished with maximum yield of $89 \pm 1\%$ within 10 min.

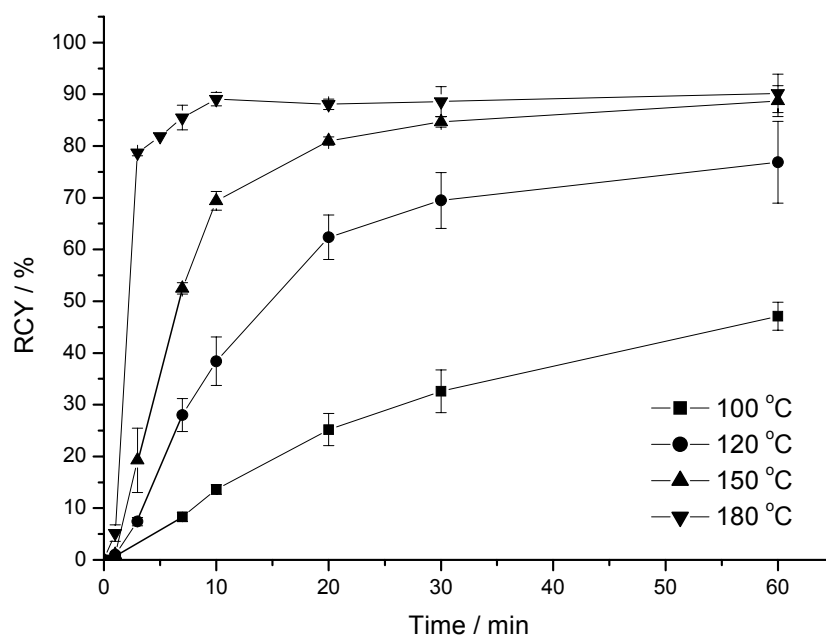


Figure 3-31. Temperature dependence of decarbonylation yield of $8\text{-}^{18}\text{F}$ in 1mL benzonitrile with 2 molar eq.cat (molar eq. based on quantity of 8-F)

3.3.1.4 Effect of catalyst concentration

In a strict definition, a catalyst accelerates a reaction without being consumed. In a homogeneous hydrogenation, the active form of Wilkinson's catalyst ($\text{RhCl}(\text{PPh}_3)_2\text{S}$, S = solvent) enters a catalytic cycle and is regenerated each time. In contrast, in the decarbonylation of aldehydes the active species becomes transformed in a stoichiometric reaction to a rhodium carbonyl complex ($\text{RhCl}(\text{PPh}_3)_2\text{CO}$), which is

unable to mediate further decarbonylation.¹⁰⁹ Therefore, the minimum requirements for the decarbonylation of an aldehyde are equimolar amounts of the rhodium complex.

Compound **8-¹⁸F** was reacted in benzonitrile at 150 °C in the presence of 1, 2 and 3 molar equivalents of RhCl(PPh₃)₃ (molar equivalents of catalyst were based on the quantity of the labeling precursor, Figure 3-32). When 1 molar equivalent catalyst was used, only 4 % of the product was formed after 30 min. When the catalyst concentration was increased, a marked increase of the yield was observed. With 2 molar equivalents of catalyst, the decarbonylation yield was 81 ± 1 % after 20 min, and with 3 molar equivalents the reaction resulted in 90 ± 0.3 % of decarbonylation after 7 min.

As pointed out before, the decarbonylation of aldehydes by Wilkinson's catalyst requires stoichiometric amounts of the complex. When investigating the reaction of **8-¹⁸F** in benzonitrile at 150 °C, a distinct yield dependence of the decarbonylation product on the molar equivalents of the rhodium complex was found (Figure 3-32).

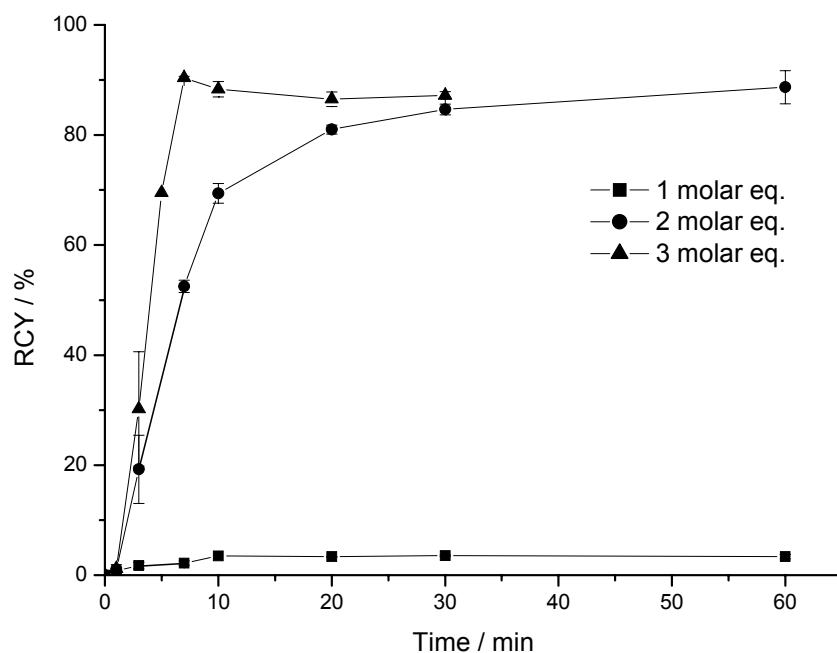


Figure 3-32. Decarbonylation yield of 8-¹⁸F with different catalyst concentrations (molar eq. based on quantity of 8-F) in 1mL benzonitrile at 150 °C

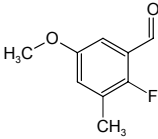
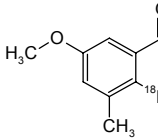
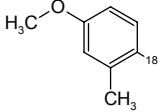
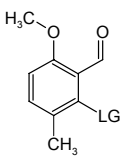
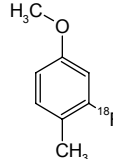
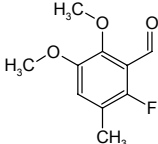
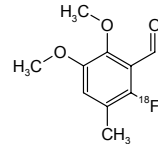
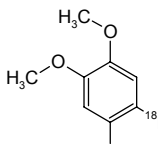
For compound **8-¹⁸F**, maximum decarbonylation yields of 90 ± 0.3 % or 89 ± 1 % were obtained with 3 molar eq. of catalyst at 150 °C, or with 2 molar eq. catalyst at 180 °C in benzonitrile after 10 min, respectively. However, performing the

decarbonylation with 2 molar equivalents of the catalyst in 1 mL benzonitrile at 150 °C facilitated the analytical control of the reaction progress. Therefore, these conditions were chosen for further investigation.

3.3.1.5 *Decarbonylation of multiply-substituted model compounds under optimized condition*

Three kinds of methyl-substituted model compounds were applied with methoxy groups in different positions (Figure 3-28, Table 3-13). The reaction conditions described above were utilized in the decarbonylation of compound **8-¹⁸F**, **9-¹⁸F** and **11-¹⁸F**. After 30 min the decarbonylation yield reached 85 ± 1 % of 4-[¹⁸F]fluoro-3-methylanisole (modeling [¹⁸F]fluoro-*m*-tyrosine). The yield of 3-[¹⁸F]fluoro-4-methylanisole (modeling [¹⁸F]fluoro-*p*-tyrosine) was 87 ± 3 % from **9-F**; 89 ± 1 % from **9-NO₂**; 87 ± 2 % from **9-Cl** and 89 ± 3 % from **9-Br**. For 4,5-dimethoxy-2-[¹⁸F]fluorotoluene (modeling [¹⁸F]FDOPA), the yield was 92 ± 2 %. Thus, the presence of even two methoxy substituents appears to have no effect on the ease of decarbonylation.

Table 3-13. Radiochemical yield of model compounds with substitution patterns (8, 9 and 11) in radiolabeling and decarbonylation

Radiolabeling*		Decarbonylation**				
Precursor	Product	RCY(%) in DMF	RCY(%) in DMSO	Product	Y(%) at 20min	Y(%) at 30min
 8-F	 8-¹⁸F	73 ± 4	--		81 ± 1	85 ± 1
	9-F (LG = F)	85 ± 5	--		87 ± 2	87 ± 3
	9-NO₂ (LG = NO₂)	52 ± 6	33 ± 9		88 ± 2	89 ± 1
	9-Cl (LG = Cl)	9 ± 2	--		85 ± 3	87 ± 2
	9-Br (LG = Br)	29 ± 2	--		85 ± 3	89 ± 3
 11-F	 11-¹⁸F	76 ± 6	--		89 ± 2	92 ± 2

*: 0.05 mmol precursor in 1 mL of labeling solvent at 140 °C.

** : 2 molar eq. RhCl(PPh₃)₃ (based on labeling precursor), 150 °C, 1 mL benzonitrile.

Maximum RCY and decarbonylation yield are presented in the Table.

3.3.2 Decarbonylation of model compounds with dialdehydic functions

In paragraph 3.2.4, the ^{18}F -labeling reaction of the precursor with dialdehydic substituents was discussed. When both aldehydic functions were placed *ortho* or *para* to the nitro group, high RCYs were observed. As important results, it can be seen that both aldehydic groups can be efficiently decarbonylated in one synthetic step.

In this part, based on the optimized decarbonylation conditions of the monoaldehydes, the decarbonylation of dialdehydes was performed in benzonitrile at 120 - 150 °C with different amounts of Wilkinson's catalyst (3 or 4 molar eq. based on the quantity of the labeling precursor), and $23\text{-}^{18}\text{F}$ was chosen as a model compound for this investigation.

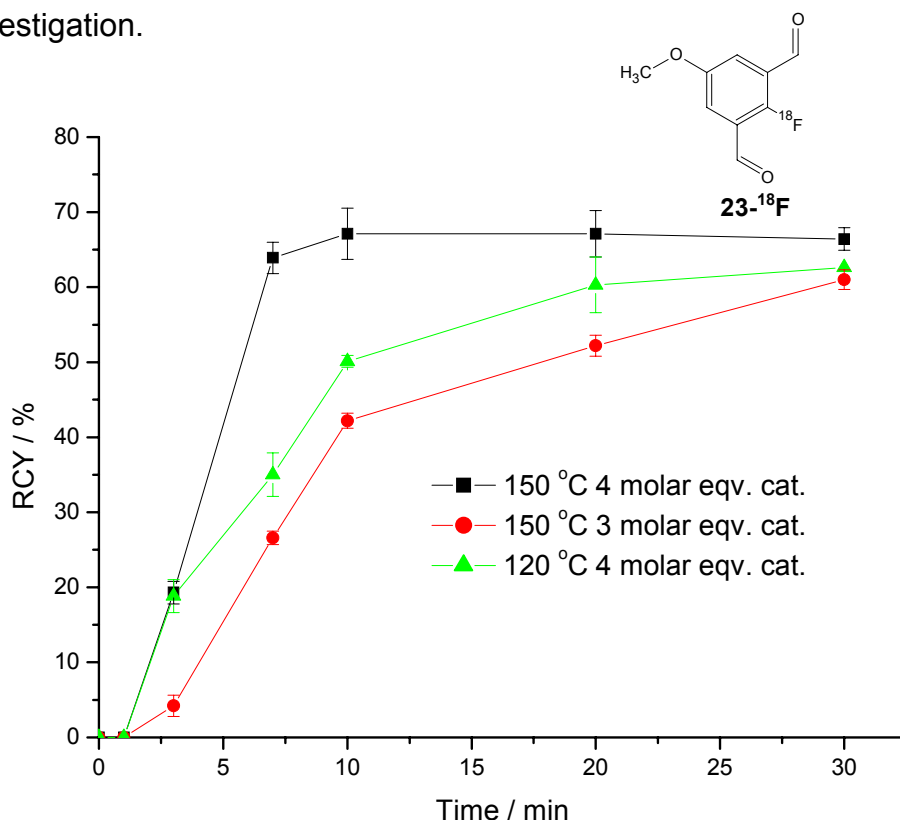


Figure 3-33. Decarbonylation yield of $23\text{-}^{18}\text{F}$ with different catalyst concentrations and temperatures in 1mL benzonitrile

In Figure 3-33, with larger amount of catalyst and at higher temperatures, the yield of decarbonylation was increased. This is in accordance with the study of the decarbonylation of monoaldehydic compounds. For $23\text{-}^{18}\text{F}$, maximum decarbonylation yields of $67 \pm 3\%$ were obtained with 4 molar eq. of catalyst at 150 °C.

3.4 Synthesis of [^{18}F]fluoro-*m*-tyrosine by a new developed strategy

In chapter 2, it was mentioned that ^{18}F -labeled aromatic amino acids can be produced by different strategies. One of these includes three synthetic steps: ^{18}F -labeling reaction, decarbonylation and hydrolysis (see Figure 2-2). In order to facilitate the systematic study on the ^{18}F -labeling reaction (see paragraph 3.2) and decarbonylation (see paragraph 3.3), the experiments were carried out with model compounds in which the position of the molecule that was thought to carry protected amino acid residue was represented by a methyl group. In this part, the complete synthesis of [^{18}F]fluoro-*m*-tyrosine started with a precursor already containing protected amino acid residue. Therefore, the suitable protective group for the glycine residue should meet the following requirements:

- (1) This protective group should not have acidic protons, because they deactivate $^{18}\text{F}^-$ ion by hydrogen bonding.
- (2) The stability of protective groups should be good under the labeling conditions (temperature 100 - 140 °C, pH 8 - 12).
- (3) The precursor containing the protective glycine residue should show high enantiomeric purity, and its deprotection should be possible without partial racemization.

Because of these demands, most protective groups for glycine are ruled out, and the range of options is very narrow. In this work, two kinds of protecting groups were chosen (Figure 3-34).

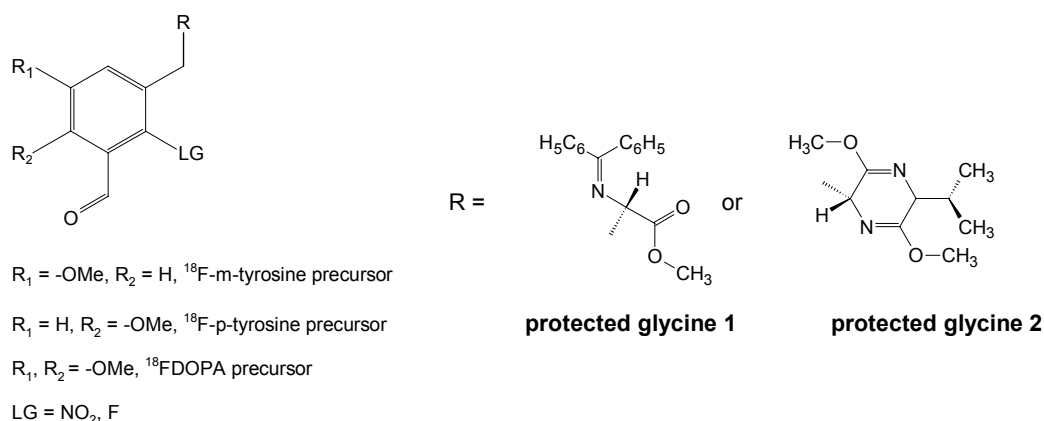
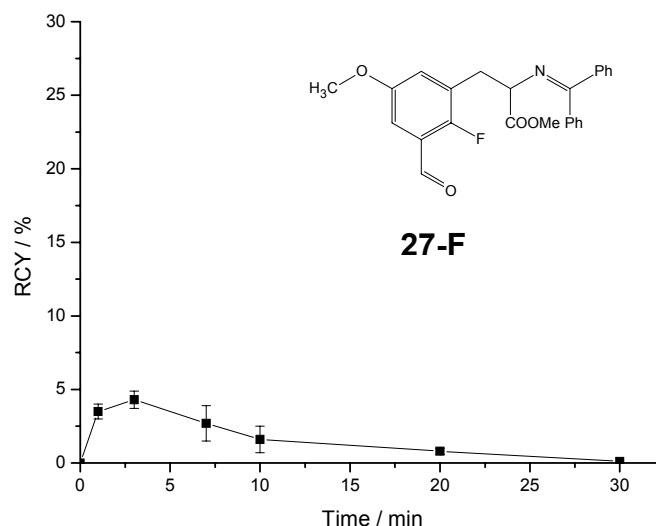


Figure 3-34. The precursors containing protected glycine part for ^{18}F -labeled aromatic amino acids

In the project for [^{18}F]fluoro-*m*-tyrosine, compound **27-F** was obtained by multi-step organic synthesis (see paragraph 3.1.4). The labeling results are presented in Figure 3-35.

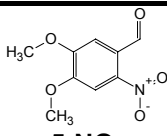
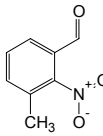


Labeling condition: precursor (10 mg), DMF (1 mL), 3.5 % K_2CO_3 (100 μL) and K2.2.2 (15 mg), at 140 $^\circ\text{C}$, within 30 min.

Figure 3-35. RCY in ^{18}F -labeling reaction of fluoro-*m*-tyrosine precursor containing protected glycine 1

Compared to the RCY (80 %) of model compound **8-F**, the RCY of **27-F** decreased to 5 %. One of the reasons is the decomposition of the protected glycine. Following, a series of test reactions has been performed. At first, some precursors (**5-NO₂** and **6-NO₂**) with known RCYs were labeled in the presence of one molar eq. of protected glycine **1** or protected glycine **2**. It was found that the RCYs were decreased in the case of adding protected glycine **1**, whereas the addition of protected glycine **2** did not show any negative effect on the RCYs. (Table 3-14).

Table 3-14. ^{18}F -labeling reaction in presence of protected glycine derivatives

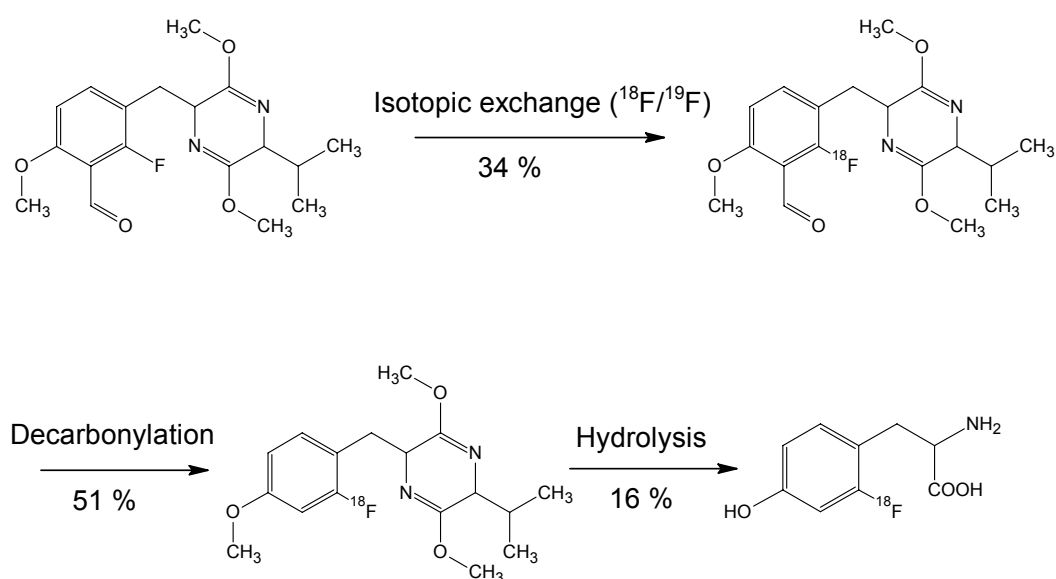
	RCY(%)		
	No addition of protected glycine	With protected glycine 1	With protected glycine 2
 5-NO₂	87 ± 2	30 ± 3	82 ± 3
 6-NO₂	48 ± 5	22 ± 6	45 ± 3

Labeling condition: precursor (10 mg), DMF (1 mL), 3.5 % K_2CO_3 (100 μL) and $\text{K}2.2.2$ (15 mg), 140 °C, within 30 min. Protected glycine derivatives were simultaneously added with molar eq. precursor.

Maximum RCY is presented.

Therefore, protected glycine **2** was a promising option for the ^{18}F -labeling reaction. However, as described in paragraph 3.1.4, the synthesis of compound **28-F** failed in the last synthetic step (formylation).

In another parallel project,⁷³ the complete synthesis of [^{18}F]fluoro-*p*-tyrosine was carried out from compound 2-fluoro-3-[(5-isopropyl-3,6-dimethoxy-2,5-dihydropyrazin-2-yl)methyl]-6-methoxybenzaldehyde (Figure 3-36). The experiment was performed with a small scale of radioactivity (ca. 500 MBq), and the overall yield of three-step radiosynthesis was 2.8 % (d.c.). This is only the first attempt at the synthesis, and the RCY could be improved after further optimization of every single step.

Figure 3-36. The entire synthesis for [^{18}F]fluoro-*p*-tyrosine⁷³

In summary, the pilot study on the synthesis of [^{18}F]fluoro-*p*-tyrosine proved that the type of protection for amino acid (protected glycine **2**) is suitable for syntheses of ^{18}F -labeled aromatic amino acids by this three-step strategy (^{18}F -labeling, decarbonylation and hydrolysis). The further optimization of the organic synthesis of the precursor for [^{18}F]fluoro-*m*-tyrosine (**28-F**) and radiochemical synthesis of [^{18}F]fluoro-*p*-tyrosine has not been undertaken within the scope of this thesis.

3.5 Automated synthesis of n.c.a. [^{18}F]FDOPA via nucleophilic aromatic substitution

As mentioned in the introduction (paragraph 1.5), a reliable, efficient and safe PET radiopharmaceutical production needs the development of automated radiochemical synthesis systems. For PET studies [^{18}F]FDOPA is used mostly for clinical investigations of cerebral disorders such as Parkinson's disease. Therefore, research is directed towards developing commercial production methods that can be applied to large scale production suitable for multi-medicinal analyses.

The preparation of [^{18}F]FDOPA can be accomplished by either electrophilic or nucleophilic procedures, but both of them have limitations. For the electrophilic syntheses, the main disadvantage is the low specific activity of the product (Table 3-15), as this can limit the utility of [^{18}F]FDOPA. Moreover, since F_2 (as carrier) is added in the production of [^{18}F] F_2 , the maximum substitution yield can only reach 50 %. In addition, selective electrophilic radiofluorination on the benzene ring is performed by fluorodemetalation, but this method brings the risk of potentially toxic metals in the final dose.

Table 3-15. [^{18}F]FDOPA production from the literature reports

Type of Fluorination	[^{18}F]FDOPA Product		
	Yield	Radioactivity	Specific activity
$\text{S}_{\text{N}}\text{Ar}^{110}$	23 ± 6 % ^a	32 ± 8.5 mCi	835 ± 280 mCi/ μmol
$\text{S}_{\text{N}}\text{Ar}^{111}$	6.5 ~ 13.6 % ^b	105 ± 35 mCi	2000 mCi/ μmol
$\text{S}_{\text{N}}\text{Ar}^{108}$	2 % ^a	---	5400 mCi/ μmol
$\text{S}_{-\text{E}}^{111}$	8.2 % ^b	16-19 mCi	0.07 mCi/ μmol
$\text{S}_{-\text{E}}^{113}$	8.3 % ^b	3 mCi	0.12 mCi/ μmol
$\text{S}_{-\text{E}}^{114}$	9 % ^b	9 mCi	0.22 mCi/ μmol
$\text{S}_{-\text{E}}^{115}$	8 % ^b	4.8 mCi	0.68 mCi/ μmol
$\text{S}_{-\text{E}}^{116}$	26 % ^a	23-27 mCi	0.12 mCi/ μmol

$\text{S}_{\text{N}}\text{Ar}$: Nucleophilic aromatic substitution, $\text{S}_{-\text{E}}$: Electrophilic substitution

a: decay corrected, **b**: decay uncorrected

Nucleophilic methods using no-carrier-added [^{18}F]fluoride ion have the potential to provide a higher specific activity and higher absolute yields. Several groups have attempted to synthesize [^{18}F]FDOPA by this more promising method (Figure 3-37).

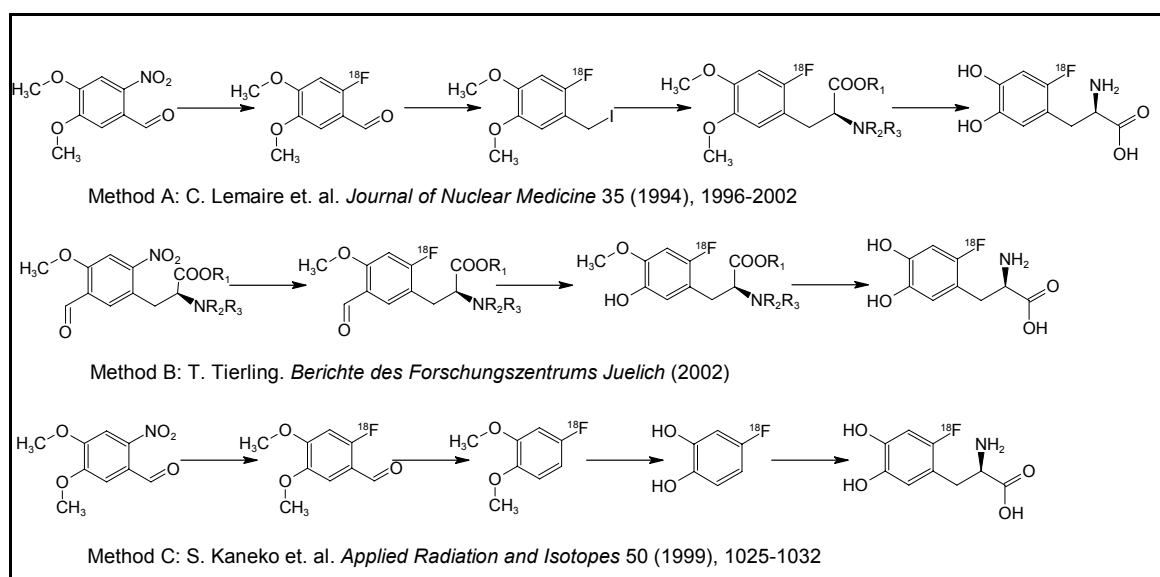


Figure 3-37. The strategies for synthesis of [^{18}F]FDOPA via $\text{S}_{\text{N}}\text{Ar}$ ^{99, 108, 110}

In method A, the amino acid residue is introduced in the aromatic part after the ^{18}F -labeling reaction. Lemaire, C. and co-workers have reported a chiral catalytic phase-transfer procedure in which 90 ~ 98 % enantiomeric purity of L-[^{18}F]FDOPA can be provided. However, there are still three synthetic steps after incorporating ^{18}F into the precursor. This complex multi-step synthesis makes automated production more difficult. Only one semi-automated synthesis of [^{18}F]FDOPA by this method has been accomplished.¹¹¹ In method B, the protecting amino acid residue has been already included in the precursor molecule before the ^{18}F -labeling reaction. Therefore, the radiochemical synthesis was simplified. However, the lower enantiomeric purity of L-[^{18}F]FDOPA (80 %) was obtained because of the basic conditions in the labeling procedure.⁹⁹ So method B is not considered for automated synthesis. In the method C, an enzymatic synthesis for building amino acid chains was developed, but the low radiochemical yield and complicated synthetic procedure became the limitation in this method.

In summary, when transferring the multi-step synthesis of [^{18}F]FDOPA to a completely automated synthesis, the main problem is to have the remote controlled system functioning in a reliable way. Therefore, in this paragraph an improved automated synthesis of n.c.a. [^{18}F]FDOPA via nucleophilic aromatic substitution is studied. According to the above discussion about nucleophilic substitution methods, method A was chosen for developing the [^{18}F]FDOPA production. Based on the program (GE Medical Systems), the synthesis procedure was brought into automation and a synthetic module was built in the laboratory of radiopharmacy

department (Figure 3-38). The complete synthesis can be divided into four parts: fluorination, reductive iodination, alkylation and hydrolysis. The improvement of the automated synthesis was focused on chemical optimization (increased radiochemical yields for every single synthetic step) and technical optimization (e. g. to prevent marked radioactivity losses during the entire process).

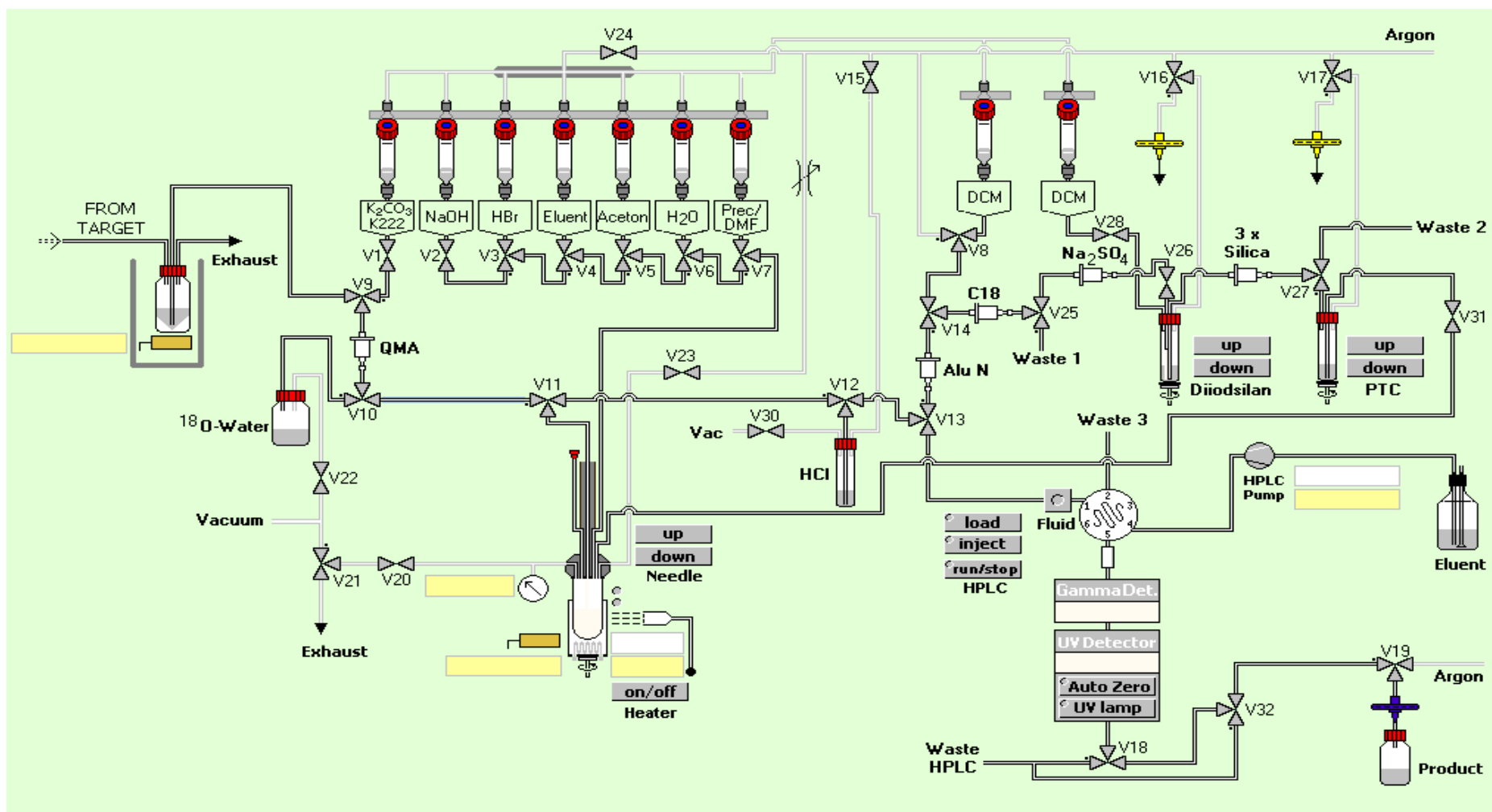


Figure 3-38. Scheme for the automated synthesis of $[^{18}\text{F}]$ FDOPA via $\text{S}_{\text{N}}\text{Ar}$

3.5.1 Fluorination

The first step of the entire synthesis is ^{18}F -fluorination of precursor 4,5-dimethoxy-2-nitrobenzaldehyde (**5-NO₂**). The optimized labeling reaction conditions were discussed in paragraph 3.2.1 and directly applied in the automated synthesis. The precursor was labeled with activated nucleophilic $^{18}\text{F}^-$ ion at 140 °C in DMF for 10 min, and **5-¹⁸F** was obtained in RCY of $71 \pm 4 \%$ ($n = 40$). This is clearly better than the reported results in DMSO ($23 \sim 55 \%$).^{35, 84, 95, 96, 108, 110, 117}

After the labeling reaction, the solution was cooled down and transferred into a vessel with 10 mL of water. It was found that there was always some radioactivity left on the wall of the labeling reactor, even after washing with water. Therefore, the relationship between reactor material and radioactivity loss during the transferring was investigated. In Table 3-16, when a glassy carbon reactor was used, the radioactivity loss during this step can be reduced to 2 % compared to normal glass (16 %). In the literature,⁸⁹ the influence of different reactor materials (polycarbonate, pyrex, Teflon and glassy carbon) on ^{18}F -labeling reactions has been reported. When the polycarbonate vessel was used, there was no radioactivity loss on the wall of vessel, however, a much lower RCY was observed. In this study, with the glassy carbon vessel, satisfying results were obtained for both RCY and radioactivity loss. Therefore, no further optimization of reactor material was developed.

Table 3-16. Effect of material of labeling reactor in fluorination

Material of labeling reactor	Normal glass	Glassy carbon
Radioactivity loss	$16 \pm 6 \%$, $n = 10$	$2.0 \pm 0.7 \%$, $n = 10$

Optimized fluorination conditions: $^{18}\text{F}^-$, K₂.2.2-K⁺, 5 mg precursor in 1 mL DMF at 140 °C for 10 min. Before the next synthetic step, the radiochemical pure **5-¹⁸F** has to be separated from the labeling reaction solution. This separation was performed by a combination of three different kinds of cartridges. A Sep-Pak[®] Light Alumina N cartridge can be used to removed the residual $^{18}\text{F}^-$ ion in the labeling reaction; a Sep-Pak[®] Plus C18 cartridge was used for trapping **5-¹⁸F** and this product was eluted with DCM; the utility of an Na₂SO₄ cartridge is to absorb the water traces in the DCM eluent of **5-¹⁸F** because the following reductive iodination reaction is very sensitive to water. After purification by cartridges. the radiochemical purity of the **5-¹⁸F** ($\geq 95 \%$) was found by radio-TLC analysis.

3.5.2 Reductive iodination

The second step is to convert 2-[¹⁸F]fluoro-4,5-dimethoxybenzaldehyde (**5-¹⁸F**) to 2-[¹⁸F]fluoro-4,5-dimethoxybenzyl iodide via reductive iodination by using the newly prepared diiodosilane (Figure 3-39). In this reaction, a strong deviation of the yield was observed. The reason might be that the newly prepared diiodosilane is extremely unstable, even at room temperature, it can decompose very fast.¹¹⁸ Therefore, the effect of the storage time for diiodosilane on the reductive iodination yield was investigated (in Table 3-17). When the freshly prepared diiodosilane was used immediately, a reproducible and high yield was obtained. In the automatic synthesis, the iodine was loaded in the iodination vessel before starting the whole synthesis. Phenylsilane and ethyl acetate were introduced into this vessel just before the C18 cartridge trapping **5-¹⁸F** was eluted by DCM. After 10 seconds of stirring at room temperature, the diiodosilane was formed and the DCM eluent came in immediately.

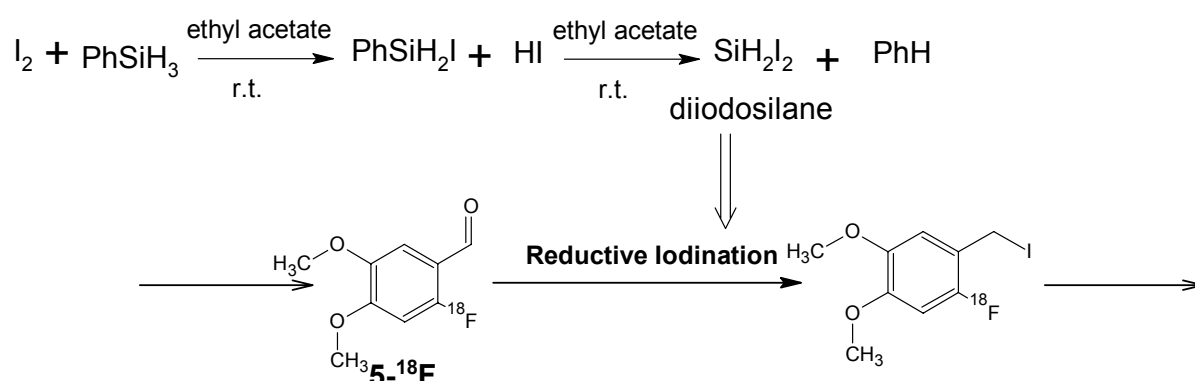


Figure 3-39. Reductive iodination in automatic synthesis of [¹⁸F]FDOPA

Table 3-17. Effect of the storage time for newly prepared diiodosilane on the yield in reductive iodination

Diiodosilane Preparation *	3 h	1 h	10 min	0 min
Yield	23 % n = 1	53 ± 12 % n = 9	62 ± 12 % n = 16	78 ± 4 % n = 23

Optimized reductive iodination condition: Fresh diiodosilane (250 μL phenylsilane 250 mg I₂ and 15 μL ethylacetate mixed at r.t.) with **5-¹⁸F** stirred for 10 min at r.t.

*: The storage time of newly prepared diiodosilane.

Because the following alkylation reaction can be disturbed by diiodosilane, which was used in excess in the reductive iodination reaction, [¹⁸F]fluorobenzyl iodide had to be purified. This purification was also performed by cartridges. Different types of

cartridge were tested (Table 3-18). The results showed that the alkylation yield was strongly affected by the purification of the [^{18}F]fluorobenzyl iodide (yield in range of 42 % ~ 78 %). The combination of different types of cartridges was examined. The silica cartridge was used for trapping the iodinated product and the other cartridge was used for trapping the excessive iodination reagents. The utility of basic type Sep-Pak[®] cartridge (diol (**D**) or NH_2 (**A**)) showed a better yield in the alkylation reaction than did the acidic type Sep-Pak[®] cartridge (Accell CM (**CM**)). However, the value of standard deviation in the alkylation yields was very large. In fact, when the diiodosilane or phenylsilane passed through the silica cartridge, they decomposed. Thus, only the Sep-Pak[®] Plus silica cartridges were used for further optimization in the purification, and different numbers of silica cartridges were tested. The results showed that the stable and highest alkylation yields (78 ± 4 %, $n = 23$) were obtained when three silica cartridges were used. In practice, the reductive iodination reaction solution passed through three combined silica cartridges, and then the cartridges were dried under a stream of argon for 5 min. Finally, the [^{18}F]fluorobenzyl iodide trapped on the cartridge was eluted with DCM (7 mL). During the purification, the radioactivity loss of iodinated product was less than 5 %. In addition, the radiochemical purity of iodinated product was more than 95 % by Radio-TLC analysis.

Table 3-18. Purification of [^{18}F]fluorobenzyl iodide by cartridges and yields in alkylation

Reductive iodination solution							
Cartridge1	S	CM	D	A	A	S	S
Cartridge2	---	S	S	S	A	S	S
Cartridge3	---	---	---	---	S	---	S
Alkylation *							
Yield	42 ± 6 % $n = 3$	47 % $n = 1$	56 % $n = 1$	60 % $n = 1$	53 ± 22 % $n = 5$	60 ± 8 % $n = 20$	78 ± 6 % $n = 15$

S = Sep-Pak[®] Plus Silica, **CM** = Sep-Pak[®] Accell Plus CM, **A** = Sep-Pak[®] Light NH_2 , **D** = Sep-Pak[®] Light Diol

*: 250 mg CsOH, 40 mg PTC and 45 mg glycinate with 2-[^{18}F]fluoro-4,5-dimethoxybenzyl iodide stirred for 10 min at r.t.

3.5.3 Alkylation

The third step is to couple the 2-[^{18}F]fluoro-4,5-dimethoxybenzyl iodide with the protected glycine derivative by enantioselective synthesis. In practice, the ^{18}F -labeled alkylation product was synthesized in a two-phase mixture containing ^{18}F -labeled benzyl iodide, *N*-(diphenylmethylene)glycine *tert*-butyl ester, PTC (*O*-allyl-*N*-(9-anthracenylmethyl)cinchonidinium)⁶⁴ and cesium hydroxide in DCM. In the literature, this enantioselective catalytic phase-transfer alkylation is conducted

at $-78\text{ }^{\circ}\text{C}$ and high enantioselectivity is observed ($> 95\%$). However, this low temperature is not feasible for automated radiosynthesis. In radiochemistry, the reaction kinetics can be different from those in normal organic chemistry because of the extremely low concentration of the educt (at subnanomolar levels). In particular, Lemaire, C. et al. has reported that high enantiomeric purity ($> 90\%$) can be achieved even at $20\text{ }^{\circ}\text{C}$ as reaction temperature in this enantioselective synthesis.⁶⁴ Therefore, in this study the alkylation reaction was carried out at room temperature in DCM, and the optimization of the amount of alkylation reagent was studied. In Table 3-19, when the ratio of reagents was fixed, the yield was improved by increasing the amount of reagent (from 43 % to 70 %). If larger amounts of reagents were used, continuously higher yields were observed. However, more reagent will cause difficulty in the filtration step before the preparative HPLC separation. Therefore, in the automated synthesis, 250 mg of CsOH, 40 mg of PTC and 45 mg of *N*-(diphenylmethylene)glycine *tert*-butyl ester were loaded in the alkylation vessel, and when the DCM eluent from the silica cartridges reached this vessel, the reaction solution was stirred at room temperature for 10 min. The reaction mixture was passed through a filter back into the fluorination reactor for the next step.

Table 3-19. Optimization for the amount of reagent in alkylation

Amount of alkylation reagent			Yield
CsOH	PTC	glycine <i>tert</i> -butyl ester	
100 mg	15 mg	20 mg	43 %, n = 1
200 mg	30 mg	40 mg	70 \pm 8 %, n = 8
250 mg	40 mg	45 mg	78 \pm 6 %, n = 15

3.5.4 Hydrolysis

In the entire synthesis, the last synthetic step is the hydrolysis for cleaving the protected groups in the molecule of ^{18}F -labeled alkylation product. In the literature,^{64, 66, 96, 110, 111} this step was usually performed under acidic conditions i.e. 57 % HI at $150\text{ }^{\circ}\text{C}$ for 10 min. However, in our case, a lower hydrolysis yield (37 %) was obtained under the reported conditions. With 48 % HBr and KI, a better yield of 76 % was achieved. Furthermore, the crude [^{18}F]FDOPA product from hydrolysis reaction had to be purified by HPLC. In practice, the [^{18}F]FDOPA which was obtained by using HI as the hydrolysis reagent was not stable (Table 3-20). A reason might be that the trace impurities still remain in the product solution even after HPLC purification.

Table 3-20 Comparison of different reagent in the hydrolysis reaction

Reagent in Hydrolysis	57 % HI	48 % HBr and KI
Yield in Hydrolysis	37 ± 9 % n = 3	76 ± 10 % n = 12
Stability of [¹⁸ F]FDOPA	Decomposed 0.5 h after EOS	7 h after EOS Radiochemical purity > 90 %

Optimized hydrolysis condition: 500 µL of 48 % HBr and 10mg KI at 150 °C for 10 min

In the automatic synthesizer, after the hydrolysis the reaction solution was adjusted to pH = 2-3 by adding 6 N NaOH, this mixed solution was introduced into a preparative HPLC. Before the purification on HPLC, a filtration step was necessary for removing the fine precipitates in the solution. However, the entire synthesis was often blocked because the filter was plugged by this solution. Therefore, several different types of filters were tested (Table 3-21). The best filtration was achieved with a microglass fiber filter (diameter 13 mm, pore size 1.6 µm).

Table 3-21. Filtration test before preparative HPLC

Filter	CN (Milipore)		PTFE (CS)		micro glass fiber (WHATMAN)	
	pore size	diameter	pore size	diameter	pore size	diameter
	2.5 µm	3 mm	0.45 µm	13 mm	1.6 µm	13 mm
Filtration	blocked		> 10 min		< 2 min	

3.5.5 Overall synthesis

After optimization for every single synthetic step, the complete four-step synthesis of [¹⁸F]FDOPA was primarily performed with small scale radioactivity (200-400 MBq) in the automatic synthesizer (Figure 3-40).

According to the optimized yield for the single steps, the calculated yield for the final product should be 32 % (d.c.), but in the real synthesis (n = 17), 20 ± 4 % (d.c.) of [¹⁸F]FDOPA was found. That means that there might be about 10 % radioactivity loss during the synthetic steps.

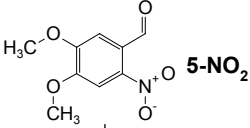

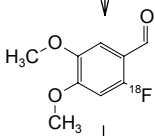

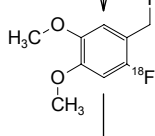

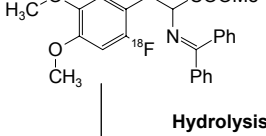

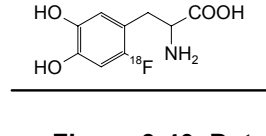
	Accumulated Yield (Calculated)	Radiochemical purity	Yield (Found)
 5-NO ₂			
 18F-Fluorination RCY = 71 %			
 5- ¹⁸ F	71 %	> 95 %	
 Reductive Iodination Y = 78 %			
	55 %	> 95 %	
 Alkylation Y = 78 %			
	43 %		
 Hydrolysis Y = 75 %			
	32 %	> 95 %	20 %, n = 17

Figure 3-40. Data of single synthetic step in the [¹⁸F]FDOPA automatic synthesis

The large scale production of [¹⁸F]FDOPA was carried out five times in the improved automated synthesizer. The reaction parameters are presented in Table 3-22.

Table 3-22. Reaction parameter in the production of [¹⁸F]FDOPA by an automatic synthesizer

Irradiation	120 min; 35 μA
Reaction time	120 min
Yield	c.a. 20 % (d.c.)
[¹⁸F]FDOPA at EOS	9064 ± 3076 MBq (n = 5)
Radiochemical purity	95 % (7 h after EOS > 90 %)
specific activity	ca. 50 GBq/μmol at EOS
enantiomeric excess (ee %)	95 %

All other quality parameters were according to Ph. Eur.

In conclusion, the routine production of n.c.a. [¹⁸F]FDOPA, suitable for multimedicinal analyses, was synthesized reliably in an automated synthesizer via a 4-step procedure including nucleophilic aromatic substitution.

4 SUMMARY

The objective in this work was to develop a new strategy aimed at the syntheses of n.c.a. (no-carrier-added) ^{18}F -labeled aromatic amino acids via nucleophilic aromatic substitution ($\text{S}_{\text{N}}\text{Ar}$). The reason for choosing a $\text{S}_{\text{N}}\text{Ar}$ reaction to introduce ^{18}F is that the electrophilic aromatic substitution method cannot provide labeling products with high specific activities as needed for clinical PET applications. Fluorine-18 (n.c.a.) is easily and efficiently produced at a cyclotron via the $^{18}\text{O}(\text{p},\text{n})^{18}\text{F}$ nuclear reaction yielding the radionuclide as $[\text{}^{18}\text{F}]\text{fluoride}$ ion. That implies that the nucleophilic substitution is used as the only type of reaction for labeling with fluorine-18. However, since the amino acids of clinical interest are principally not suited to undergo $\text{S}_{\text{N}}\text{Ar}$ due to their phenolic structure, this has been a challenging task for more than two decades. Therefore, this study emphasized the evaluation of $\text{S}_{\text{N}}\text{Ar}$ on aromatic compounds multiply-substituted with both electron withdrawing and electron donating groups. Consequently, the study focused on the following parts:

- A systematic investigation on nucleophilic aromatic substitution using a variety of model compounds exhibiting different substitution patterns with both +M and -M substituents.
- Evaluation of decarbonylation of the ^{18}F -labeled arenes, as it is an important intermediate synthetic step in the syntheses of ^{18}F -labeled aromatic amino acids.
- A pilot study to suggest a new synthetic strategy for ^{18}F -labeled aromatic amino acids i.e. the precursor includes the protected amino acid residue (Figure 2-2).
- An improved automated synthesis of $[\text{}^{18}\text{F}]\text{FDOPA}$ by a reported synthetic strategy, i.e. n.c.a. ^{18}F -labeling and subsequent addition of the amino acid residue (Figure 2-1).

The first part of the thesis dealt with the integrated effects of three different types of substituents on the benzene ring in the nucleophilic aromatic ^{18}F -fluorination. The first type of substituent was the leaving group, i.e. NO_2 , F, Br, Cl and $\text{N}^+\text{Me}_3\text{TfO}^-$. The second type of substituent was the aldehydic function as an auxiliary group for decreasing the electron density of the reactive center. The third type of substituent was the methoxy or methyl group. The methoxy group was used as masked phenolic

hydroxyl group and the methyl group was used for mimicking the protected amino acid residue.

For n.c.a. ^{18}F -labeling, the reaction conditions were determined by using model compounds with only two substituents (leaving group and aldehydic function, see paragraph 3.2.1). As had previously been observed, DMF was superior to DMSO, which is usually used as the solvent for the labeling reaction. Partial DMSO-mediated oxidation of the aldehydes could be identified as a reason for the poor yields obtained in this solvent. For the precursors 2-bromobenzaldehyde (**1-Br**), 2-nitrobenzaldehyde (**1-NO₂**) and 4-nitrobenzaldehyde (**2-NO₂**), 95 %, 10 % and 55 % of the precursor was oxidized in DMSO after 3 min of reaction time, resulting in RCYs of 1 %, 68 % and 40 %, respectively. However, in DMF less than 5 % of these three precursors were oxidized after 3 min of reaction time, and higher RCYs of 73 % (**1-Br**), 84 % (**1-NO₂**) and 81 % (**2-NO₂**) were observed.

In case of the nucleophilic ^{18}F -fluorination of methoxylated *o*-nitrobenzaldehydes, twelve different compounds were studied (see paragraph 3.2.2). Most surprisingly, the RCYs were not decreased with increasing numbers of methoxy substituents. The threefold and fourfold methoxylated precursors (**19-NO₂** and **20-NO₂**) showed even better RCYs (82 % and 48 %, respectively) than some of the mono- or di-methoxylated precursors. Additionally, the $\text{S}_{\text{N}}\text{Ar}$ reaction remained dominant in most cases, although some side reactions, such as demethylation and intramolecular redox-processes of the precursor, were observed. These observations prompted further studies to evaluate the dependence of $\text{S}_{\text{N}}\text{Ar}$ reaction rates (determined at one minute of reaction) on the deshielding of the particular carbon atom bearing $-\text{NO}_2$ (chemical shifts of ^{13}C NMR). The correlation ($R^2 = 0.89$) illustrated the influences originated by the methoxy substituents on the substitution reaction.

In the study of the model compounds with the methyl substituent (see paragraph 3.2.3), a strong competition reaction, i.e. condensation reaction, was observed if the precursor contained the *o*-nitrotoluene structure. When the precursor showed lower reactivity towards the $\text{S}_{\text{N}}\text{Ar}$ reaction (methoxy substituent *para* to the nitro group), this side reaction became the dominant process, resulting in low RCYs. Although this side reaction does not take place for the precursors with halogens as leaving groups, the RCYs for halogen precursor were relatively low except in case of isotopic exchange. The increase of RCY from 7 % (**7-NO₂**) to 69 % (**7-N⁺Me₃TfO⁻**)

showed that $N^+Me_3TfO^-$ as a leaving group was a promising option for avoiding condensation side reactions while maintaining a high RCY.

Throughout this study, the aldehydic function was used as an auxiliary group in order to facilitate the S_NAr reaction. For gaining a more intensive effect, compounds with two aldehydic functions were studied (see paragraph 3.2.4). When both aldehydic functions were located in the *ortho/para* position to the LG, the RCYs were always high (> 80 %) and the reaction rates were improved significantly, so that **21-NO₂** was labeled in an RCY of 78 %, even at room temperature within 10 min.

When aiming at the development of a new strategy for syntheses of ^{18}F -labeled aromatic amino acids, the aldehydic function as a necessary auxiliary group has to be removed fast and efficiently after ^{18}F -labeling. The decarbonylation of ^{18}F -labeled aromatic substrates was therefore studied in detail (see paragraph 3.3). It was found that the reaction could be carried out smoothly without by-products in benzonitrile by using Wilkinson's catalyst. A fast decarbonylation was achieved with higher concentrations of the catalyst or at higher temperatures. Decarbonylation of the multi-substituted compound **11- ^{18}F** (modeling [^{18}F]FDOPA) or dialdehydic substituted compound **23- ^{18}F** (modeling [^{18}F]fluoro-*m*-tyrosine) was efficiently performed in good yields of 89 % and 67 % under the optimized conditions i.e. using 1 mL of benzonitrile with 2 molar eq. of catalyst (based on the amount of $-CHO$) at 150 °C within 20 min.

Thus far, all the information from these results guided the further studies on the syntheses of ^{18}F -labeled aromatic amino acids (see paragraph 3.4). Compound **27-F** with a protected glycine residue (glycine derivative **1**) was taken as an example for testing the synthesis of [^{18}F]fluoro-*m*-tyrosine by the newly-developed synthetic strategy (^{18}F -labeling, decarbonylation and hydrolysis). In the ^{18}F -labeling, a low RCY (4 %) was obtained because of decomposition of the protected glycine residue. An alternative protected glycine residue (glycine derivative **2**) was used in another parallel project for the synthesis of [^{18}F]fluoro-*p*-tyrosine by the same strategy, and a pilot experiment showed that the RCY of ^{18}F -labeling was improved to 40 %, after the other two step synthesis, [^{18}F]fluoro-*p*-tyrosine was achieved with an overall yield of 3 %. This result proved the three-step synthetic strategy to be suitable for syntheses of ^{18}F -labeled aromatic amino acids. However, in the case of the precursor with low reactivity ([^{18}F]fluoro-*m*-tyrosine and [^{18}F]FDOPA), further optimization of the organic synthesis of the precursor has to be performed out of the scope of this thesis.

In the last part, an automated synthesis of [^{18}F]FDOPA over four steps (fluorination, reductive iodination, alkylation and hydrolysis), as described in the literature, was brought into routine application for the first time. Every single synthetic step was optimized in detail (see paragraph 3.5). In this improved automated synthesis, 9064 ± 3076 MBq of [^{18}F]FDOPA could be produced within 120 min of production time from EOB ($n = 5$). The radiochemical purity and enantiomeric excess were both 95 %. The specific activity was ca. 50 GBq/ μmol at EOS.

5 EXPERIMENTAL

5.1 General

Chemicals and solvents for organic synthesis and ^{18}F -radiochemical synthesis were obtained from the following companies: Aldrich (Germany), Sigma (Germany), Riedel-de Haën (Germany), Fluka (Germany), Merck (Germany), Lancaster (England), ABCR (England). The chemicals were reagent grade or better and were directly used in the synthesis without further purification.

The fluorination reactor in the automated synthesis of [^{18}F]FDOPA: Glassy carbon reactor (HTW, Germany) and Normal glass reactor (GE Medical Systems, USA).

Cartridge: Sep-Pak[®] Light QMA, Sep-Pak[®] Light Alumina N, Sep-Pak[®] Plus C18, Sep-Pak[®] Accell Plus CM, Sep-Pak[®] Light NH_2 , Sep-Pak[®] Light Diol, Sep-Pak[®] Plus Silica were obtained from Waters (USA). Na_2SO_4 cartridge (38 mm, 2.2 GM) was purchased from VARIAN (Germany).

Thin-layer chromatography (**TLC**) was carried out with silica gel plates (Polygram[®] Silica G/UV₂₅₄, 8 × 4 cm, Macherey Nagel, Germany) visualized under an UV-lamp (254 nm).

The employed high performance liquid chromatography (**HPLC**) consists of a Hewlett-Packard Model 1050 equipped with an UV/Vis detector.

Middle pressure liquid chromatography system (**MPLC**, Büchi, Switzerland) was applied for the purification in the organic synthesis. Silica gel 60 (0.040 – 0.063 mm, Merck) or reverse phase material (POLYGOPREP 60-50, C18, MN, Germany) was used as immobile phase. Eluents were mixtures of petroleum ether (60/90 °C) and ethyl acetate or water and acetonitrile (given as v/v ratio).

LC/MS measurements were performed on a quadrupole LC/MS (Agilent Technologies, Model 6120) with an HPLC (Agilent Technologies, Model 1200). All solvents (methanol and water) were of HPLC-grade purity.

Melting points (**m.p.**) were determined using Gallenkamp device (MPG 350, USA) and were uncorrected.

IR spectra were carried out on spectrum-one FT-IR spectrometer (Perkin-Elmer, Boston, USA).

MS spectra were measured by using Triple Stage Quadrupole TSQ 70 Finnigan MAT – Massenspektrometer (Finnigan-MAT, Bremen, Germany).

^1H NMR, **^{13}C NMR** and **^{19}F NMR** were carried out on Avance 400 (Bruker, USA) operating at 400 or 100 MHz. For measurements, as internal standards the deuterated solvents were used (DMSO- d_6 : $\delta = 2.49$ in ^1H and $\delta = 39.5$ in ^{13}C ; CDCl_3 : $\delta = 7.25$ in ^1H and $\delta = 77.0$ in ^{13}C). The chemical shift δ in ppm was referred to the internal standard.

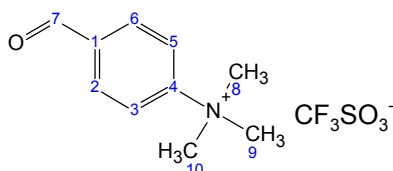
5.2 Organic syntheses of precursors and standards for S_NAr with $[^{18}F]$ fluoride ion

5.2.1 Model compounds as building blocks for ^{18}F -labeled aromatic amino acids

5.2.1.1 4-Formylphenyl-trimethylammonium triflate ($2-N^+Me_3TfO^-$)

To a stirred solution of *p*-dimethylaminobenzaldehyde (1.00 g, 6.71 mmol) in DCM (15 mL) was added methyl trifluoromethanesulfonate (0.88 mL, 7.78 mmol). The solution was stirred for 3 h at room temperature under argon. The suspension was filtered and the obtained solid product was crystallized from methanol and diisopropylether (20:80, v/v) to give 0.95 g $2-N^+Me_3TfO^-$ as grey crystals (39 %).

4-Formylphenyl-trimethylammonium triflate



m.p. 111 - 112 °C (reported¹¹⁹ 108 - 110 °C).

1H NMR (DMSO- d_6 , 400 MHz)

δ (ppm) = 10.10 (s, 1H, H -(C-7)), 8.17 (dd, $^4J_{H,H} = 7.2$ Hz, $^3J_{H,H} = 9.1$ Hz, 4H, H_{arom}), 3.64 (s, 9H, -N-(CH_3)₃).

^{13}C NMR (DMSO- d_6 , 100 MHz)

δ (ppm) = 56.9, 121.7, 130.9, 136.7, 151.0, 192.1.

MS-FAB (70 eV)

m/z : 164 ($[M]^+$, $C_{10}H_{14}NO$, 100 %), 154 (38 %), 136 ($[M - CO]^+$, $C_9H_{14}N$, 32 %), 107 (11 %).

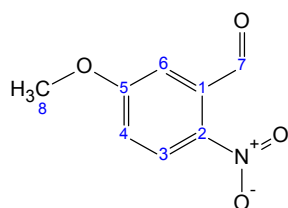
IR

$\bar{\nu}/cm^{-1}$ (T %): 3046 (93 %), 2941 (93 %), 2835 (92 %), 2298 (98 %), 1701 (97 %), 1609 (96 %), 1497 (80 %), 1483 (84 %), 1474 (84 %), 1457 (88 %), 1416 (88 %), 1368 (86 %), 1317 (91 %), 1252 (28 %), 1223 (41 %), 1195 (63 %), 1160 (48 %), 1119 (71 %), 1099 (52 %), 1078 (56 %), 1051 (51 %), 1025 (29 %), 984 (53 %), 958 (67 %), 940 (69 %), 909 (70 %), 890 (85 %), 848 (64 %), 818 (65 %), 757 (77 %), 744 (92 %), 710 (89 %).

5.2.1.2 5-Methoxy-2-nitrobenzaldehyde (3-NO₂)

To a stirred suspension of 5-hydroxy-2-nitrobenzaldehyde (3.99 g, 23.89 mmol) and K₂CO₃ (3.18 g, 23.04 mmol) in DMF (40 mL), MeI (1.49 mL, 23.92 mmol) was added dropwise at 0 °C. After this addition, the suspension was stirred at room temperature and monitored by TLC. The starting compound was completely reacted after 3 h, the resulting mixture was poured into 100 mL water and extracted with diethyl ether (3 × 50 mL). The combined organic layers were washed with 100 mL water and dried over Na₂SO₄. After evaporation of solvent, the residue was purified by using MPLC (petroleum ether / ethyl acetate, 1:1) to yield 3.77 g **3-NO₂** as yellow crystal (87 %).

5-Methoxy-2-nitrobenzaldehyde



m.p. 81 - 82 °C (reported¹²⁰ 83 °C).

¹H NMR (CDCl₃, 250 MHz)

δ (ppm) = 10.46 (s, 1H, H-(C-7)), 8.13 (d, ³J_{H,H} = 9.1 Hz, 1H, H-(C-3) or H-(C-4)), 7.30 (s, 1H, H-(C-6)), 7.13 (d, ³J_{H,H} = 9.1 Hz, 1H, H-(C-3) or H-(C-4)), 3.94 (s, 3H, H-(C-8)).

¹³C NMR (CDCl₃, 60 MHz)

δ (ppm) = 55.6, 113.5, 118.9, 127.5, 134.6, 142.5, 164.3, 188.8.

HRMS (EI)

m/z measured: 181.03488 ([M]⁺, C₈H₇NO₄).

m/z calculated: 181.037486.

MS-EI (70 eV)

m/z: 181 ([M]⁺, C₈H₇NO₄, 10 %), 180 ([M - H]⁺, C₈H₆NO₄, 29 %), 163 ([M - H₂O]⁺, C₈H₅NO₃, 5 %), 151 ([M - NO]⁺, C₈H₇O₃, 41 %), 133 ([M - H₂O - NO]⁺, C₈H₅O₂, 21 %), 123 (32 %), 108 (65 %), 95 (54 %), 77 ([C₆H₅]⁺, 24 %), 64 (37 %), 63 ([C₅H₃]⁺, 100 %), 52 ([C₄H₄]⁺, 21 %), 49 (14 %).

IR

$\bar{\nu}$ /cm⁻¹ (T %): 3102 (81 %), 2982 (82 %), 2946 (79 %), 2845 (82 %), 2666 (83 %), 2166 (87 %), 1922 (87 %), 1689 (37 %), 1609 (77 %), 1580 (29 %), 1499 (31 %), 1479 (47 %), 1459 (61 %), 1442 (47 %), 1419 (51 %), 1390 (45 %), 1326 (24 %), 1286 (25 %), 1233 (29 %), 1187 (41 %), 1159 (33 %), 1079 (39 %), 1024 (38 %),

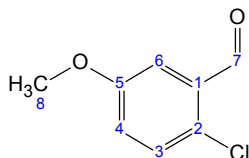
1001 (48 %), 963 (66 %), 929 (27 %), 892 (28 %), 847 (31 %), 834 (22 %), 771 (52 %), 741 (23 %), 688 (42 %), 667 (45 %).

5.2.1.3 2-Chloro-5-methoxybenzaldehyde (3-Cl)

To a stirred suspension of 4-chloro-3-methylanisole (4.00 g, 25.64 mmol) in CCl_4 (20 mL) were added N-bromosuccinimide (5.00 g, 28.09 mmol) and a catalytic amount of AIBN (0.11 g). The reaction was refluxed for 1 h, the reaction suspension was filtered off and the filtrate was evaporated to afford 5.80 g crude 4-chloro-3-bromomethylanisole, which was used directly in the next synthesis step without further purification.

A stirred suspension of crude 4-chloro-3-bromomethylanisole (5.80 g), DMSO (30 mL) and Na_2CO_3 (5.30 g, 50.00 mmol) was heated to 50 °C under argon overnight. Then this reaction suspension was cooled down and partitioned between diethyl ether (200 mL) and water (100 mL). The organic layer was separated, dried over Na_2SO_4 and reduced to crude product. After purification by using MPLC (petroleum ether / ethyl acetate, 1:1), 1.60 g **3-Cl** was obtained as white substance (36 % based on 4-chloro-3-methylanisole).

2-Chloro-5-methoxybenzaldehyde



m.p. 62 - 63 °C (reported¹²¹ 62 - 64 °C).

¹H NMR (CDCl_3 , 250 MHz)

δ (ppm) = 10.41 (s, 1H, H -(C-7)), 7.71 (d, $^4J_{H,H} = 3.3$ Hz, 1H, H -(C-6)), 7.30 (d, $^3J_{H,H} = 8.8$ Hz, 1H, H -(C-3)), 7.07 (dd, $^4J_{H,H} = 3.3$ Hz, $^3J_{H,H} = 8.8$ Hz, 1H, H -(C-4)), 3.82 (s, 3H, H -(C-8)).

¹³C NMR (CDCl_3 , 60 MHz)

δ (ppm) = 55.7, 111.9, 122.7, 129.6, 131.4, 132.9, 158.6, 189.6.

MS-EI (70 eV)

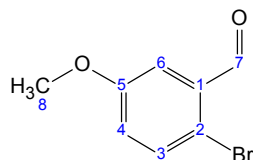
m/z : 172 ($[\text{M}]^+$, $\text{C}_8\text{H}_7^{37}\text{ClO}_2$, 29 %), 169 ($[\text{M} - \text{H}]^+$, $\text{C}_8\text{H}_6^{35}\text{ClO}_2$, 100 %), 155 ($[\text{M} - \text{OH}]^+$, $\text{C}_8\text{H}_6^{37}\text{ClO}$, 22 %), 141 (17 %), 126 (10 %), 99 (13 %), 98 (3 %), 77 ($[\text{C}_6\text{H}_5]^+$, 10 %), 63 ($[\text{C}_5\text{H}_3]^+$, 12 %), 62 (4 %).

IR

$\bar{\nu}/\text{cm}^{-1}$ (T %): 3099 (86 %), 3076 (86 %), 3010 (79 %), 2979 (84 %), 2944 (78 %), 2890 (79 %), 2844 (78 %), 2766 (86 %), 2042 (89 %), 1894 (87 %), 1694 (48 %), 1679 (31 %), 1603 (53 %), 1573 (43 %), 1475 (40 %), 1443 (50 %), 1417 (50 %), 1396 (44 %), 1300 (54 %), 1281 (37 %), 1243 (44 %), 1195 (31 %), 1170 (46 %), 1137 (54 %), 1122 (53 %), 1069 (48 %), 1017 (43 %), 931 (22 %), 889 (57 %), 867 (40 %), 821 (25 %), 756 (38 %), 687 (69 %), 660 (29 %).

5.2.1.4 2-Bromo-5-methoxybenzaldehyde (3-Br)

To a stirred solution of 3-methoxybenzaldehyde (3.00 mL, 24.62 mmol) in CHCl_3 (40 mL, absolved) bromine (1.89 mL, 3.69 mmol) was introduced slowly over 20 min. Following, the reaction solution was stirred at room temperature for 0.5 h. The resulting solution was poured into diethyl ether (100 mL) and the mixture was washed with $\text{Na}_2\text{S}_2\text{O}_3$ (2 × 50 mL) and 50 mL water. The organic layer was separated and dried over Na_2SO_4 . After evaporation of the solvent under reduced pressure, the crude product was purified by using MPLC (petroleum ether / ethyl acetate, 1:1). 4.37 g **3-Br** was obtained (82 %).

2-Bromo-5-methoxybenzaldehyde

m.p. 77 °C (reported¹²² 75 - 76 °C).

¹H NMR (CDCl₃, 400 MHz)

δ (ppm) = 10.30 (s, 1H, *H*-(C-7)), 7.50 (*d*, ³*J*_{H,H} = 8.6 Hz, 1H, *H*-(C-3)), 7.39 (*d*, ⁴*J*_{H,H} = 3.3 Hz, 1H, *H*-(C-6)), 7.02 (*dd*, ³*J*_{H,H} = 8.7 Hz, ⁴*J*_{H,H} = 3.1 Hz, 1H, *H*-(C-4)), 3.83 (s, 3H, *H*-(C-8)).

¹³C NMR (CDCl₃, 100 MHz)

δ (ppm) = 55.7, 112.6, 117.9, 123.1, 133.9, 134.5, 159.2, 191.7.

MS-EI (70 eV)

m/z: 216 ([*M*]⁺, C₈H₇⁸¹BrO₂, 95 %), 215 ([*M* - H]⁺, C₈H₆⁸¹BrO₂, 87 %), 214 ([*M*]⁺, C₈H₇⁷⁹BrO₂, 100 %), 213 ([*M* - H]⁺, C₈H₇⁷⁹BrO₂, 90 %), 185 ([*M* - CHO]⁺, C₇H₆⁷⁹BrO, 14 %), 170 (10 %), 143 (11 %), 134 ([*M* - H^{79/81}Br]⁺, C₈H₇O₂, 6 %), 106 (12 %), 77 ([C₆H₅]⁺, 5 %), 63 ([C₅H₃]⁺, 15 %), 50 (2 %).

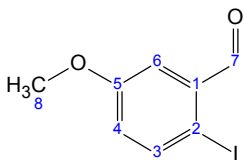
IR

$\bar{\nu}/\text{cm}^{-1}$ (T %): 3094 (81 %), 3073 (81 %), 3007 (73 %), 2943 (73 %), 2875 (64 %), 2842 (72 %), 2745 (79 %), 2580 (82 %), 2069 (82 %), 1895 (82 %), 1673 (25 %), 1599 (50 %), 1569 (40 %), 1469 (36 %), 1440 (50 %), 1417 (46 %), 1382 (42 %), 1366 (65 %), 1300 (47 %), 1278 (29 %), 1241 (39 %), 1198 (30 %), 1169 (42 %), 1134 (52 %), 1116 (58 %), 1060 (43 %), 1012 (39 %), 931 (17 %), 864 (27 %), 819 (17 %), 753 (37 %), 684 (63 %).

5.2.1.5 2-Iodo-5-methoxybenzaldehyde (3-I)

To a vigorous stirring suspension of I_2 (4.06 g, 15.98 mmol) in CHCl_3 (50 mL) were added dropwise 3-methoxybenzyl alcohol (2.00 mL, 16.11 mmol) and CF_3COOAg (3.56 g, 16.11 mmol) under argon within 30-40 min. The reaction mixture was stirred at room temperature for 20 h. The resulting suspension was filtered and the filter cake was washed with CHCl_3 (50 mL), the CHCl_3 solution was concentrated and purified by using MPLC (petroleum ether / ethyl acetate, 1:1) to afford 2.03 g 2-iodo-5-methoxybenzyl alcohol (48 %).

2-Iodo-5-methoxybenzyl alcohol (1.79 g, 6.78 mmol) and PDC (5.00 g, 13.3 mmol) were suspended in DCM (20 mL). The reaction mixture was stirred at room temperature for 2 h. The resulting mixture was filtered and DCM was evaporated. To the residue diethyl ether (100 mL) was given and the mixture was put in an ultrasonic bath. The suspension was filtered and the filtrate solution was washed by 1 N HCl (50 mL) to remove pyridinium. The diethyl ether solution was dried over Na_2SO_4 and evaporated. The residue was purified by using MPLC (petroleum ether / ethyl acetate, 1:1) to give 1.50 g **3-I** as white crystals (84 % based on 2-iodo-5-methoxybenzyl alcohol).

2-Iodo-5-methoxybenzaldehyde

m.p. 115 - 116 °C (reported¹²³ 114 - 115 °C).

¹H NMR (CDCl₃, 250 MHz)

δ (ppm) = 10.01 (s, 1H, *H*-(C-7)), 7.77 (d, ³*J*_{H,H} = 8.5 Hz, 1H, *H*-(C-3)), 7.40 (d, ⁴*J*_{H,H} = 3.1 Hz, 1H, *H*-(C-6)), 6.91 (dd, ³*J*_{H,H} = 8.7 Hz, ⁴*J*_{H,H} = 3.0 Hz, 1H, *H*-(C-4)), 3.83 (s, 3H, *H*-(C-8)).

^{13}C NMR (CDCl₃, 60 MHz)

δ (ppm) = 56.1, 90.1, 114.1, 123.9, 136.2, 141.5, 160.8, 196.1.

MS-EI (70 eV)

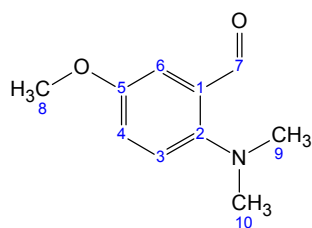
m/z : 262 ([M]⁺, C₈H₇IO₂, 100 %), 233 ([M – CHO]⁺, C₇H₆IO, 7 %), 203 (2 %), 147 (4 %), 134 ([M – HI]⁺, C₈H₆O₂, 17 %), 107 (3 %), 106 (13 %), 77 ([C₆H₅]⁺, 6 %), 63 ([C₅H₃]⁺, 10 %), 62 (3 %).

IR

$\bar{\nu}$ /cm⁻¹ (T %): 3322 (78 %), 3068 (78 %), 3004 (72 %), 2976 (75 %), 2937 (71 %), 2860 (69 %), 2838 (70 %), 2743 (75 %), 2573 (78 %), 1980 (80 %), 1897 (79 %), 1667 (38 %), 1592 (47 %), 1562 (41 %), 1465 (39 %), 1412 (46 %), 1381 (44 %), 1298 (46 %), 1276 (30 %), 1242 (39 %), 1197 (35 %), 1166 (42 %), 1131 (53 %), 1111 (58 %), 1052 (40 %), 1006 (42 %), 931 (25 %), 864 (29 %), 818 (26 %), 748 (38 %), 682 (54 %).

**5.2.1.6 5-Methoxy-2-trimethylammoniumbenzaldehyde triflate
(3-N⁺Me₃TfO⁻)****5-Methoxy-2-dimethylaminobenzaldehyde**

2-Fluoro-5-methoxybenzaldehyde (1.42 g, 9.22 mmol), dimethylamine hydrochloride (1.10 g, 13.50 mmol) and K₂CO₃ (1.80 g, 13.04 mmol) were stirred and heated under reflux in a mixture of DMSO (20 mL) and water (8 mL). After there was no 2-fluoro-5-methoxybenzaldehyde left as checked by TLC (petroleum ether / ethyl acetate, 5:1), the saturated aqueous K₂CO₃ solution (100 mL) was added to cooled reaction solution. This mixture was extracted with diethyl ether (2 × 50 mL). The organic layer was dried over Na₂SO₄. After evaporation of solvent, the residue was purified by using MPLC (petroleum ether / ethyl acetate, 5:1) and 0.97 g 5-methoxy-2-dimethylaminobenzaldehyde was obtained as yellow oil (59 %).

5-Methoxy-2-dimethylaminobenzaldehyde **^1H NMR (DMSO-d₆, 250 MHz)**

δ (ppm) = 10.24 (s, 1H, H-(C-7)), 7.21 (m, 3H, H_{arom}), 3.75 (s, 3H, H-(C-8)), 2.82 (s, 6H, H-(C-9) and H-(C-10)).

¹³C NMR (DMSO-d₆, 60 MHz)

δ (ppm) = 46.1, 55.4, 79.1, 111.5, 120.6, 122.0, 128.2, 150.6, 154.2, 190.7.

MS-EI (70 eV)

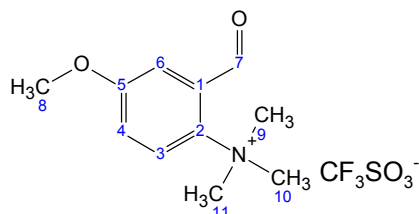
m/z : 179 ($[M]^+$, C₁₀H₁₃NO₂, 100 %), 164 ($[M - CH_3]^+$, C₉H₁₀NO₂, 56 %), 150 (21 %), 136 (21 %), 121 (23 %), 118 (9 %), 65 (6 %), 44 (2 %).

IR

$\bar{\nu}$ /cm⁻¹ (T %): 2944 (85 %), 2834 (79 %), 2789 (86 %), 1676 (32 %), 1607 (76 %), 1572 (87 %), 1494 (25 %), 1453 (56 %), 1415 (59 %), 1381 (61 %), 1301 (57 %), 1275 (34 %), 1234 (45 %), 1185 (63 %), 1164 (59 %), 1151 (44 %), 1089 (72 %), 1034 (35 %), 950 (66 %), 937 (65 %), 926 (63 %), 869 (68 %), 822 (57 %), 774 (55 %), 729 (90 %), 687 (53 %).

5-Methoxy-2-trimethylammoniumbenzaldehyde triflate

To a stirred solution of 5-methoxy-2-dimethylaminobenzaldehyde (0.97 g, 5.42 mmol) in DCM (10 mL) was added methyl trifluoromethanesulfonate (1.10 mL, 9.73 mmol). The solution was stirred for 3 h at room temperature under argon. The reaction solvent was concentrated and the residue was crystallized in a mixture of diisopropylether and DCM (1:10, v/v). 1.40 g **3-N⁺Me₃TfO⁻** was obtained as white crystals (78 %).

5-Methoxy-2-trimethylammoniumbenzaldehyde triflate

m.p. 112 - 113 °C (reported⁷² 114 - 115 °C).

¹H NMR (DMSO-d₆, 400 MHz)

δ (ppm) = 10.19 (s, 1H, H -(C-7)), 8.00 (d, ³ $J_{H,H}$ = 8.7 Hz, 1H, H -(C-3)), 7.87 (d, ⁴ $J_{H,H}$ = 3.5 Hz, 1H, H -(C-6)), 7.46 (dd, ⁴ $J_{H,H}$ = 3.5 Hz, ³ $J_{H,H}$ = 8.5 Hz, 1H, H -(C-4)), 4.00 (s, 3H, H -(C-8)), 3.71 (s, 9H, -N-(CH₃)₃).

¹³C NMR (DMSO-d₆, 100 MHz)

δ (ppm) = 56.3, 57.0, 118.7, 124.3, 126.0, 131.1, 137.0, 160.1, 193.0.

MS-FAB (70 eV)

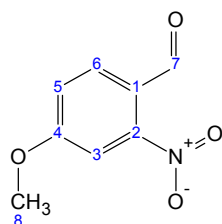
m/z : 194 ($[M]^+$, C₁₁H₁₆NO₂, 100 %), 179 ($[M - CH_3]^+$, C₁₀H₁₃NO₂, 14 %), 164 (8 %), 150 (6 %), 136 (8 %).

IR

$\bar{\nu}/\text{cm}^{-1}$ (T %): 3085 (93 %), 3045 (92 %), 2985 (94 %), 2951 (94 %), 2851 (95 %), 2287 (96 %), 1700 (67 %), 1686 (62 %), 1609 (89 %), 1585 (61 %), 1493 (77 %), 1462 (82 %), 1447 (82 %), 1407 (86 %), 1309 (83 %), 1255 (17 %), 1221 (37 %), 1203 (70 %), 1146 (31 %), 1082 (86 %), 1029 (18 %), 956 (72 %), 942 (75 %), 922 (52 %), 901 (64 %), 830 (51 %), 770 (69 %), 754 (65 %), 690 (84 %), 660 (83 %).

5.2.1.7 4-Methoxy-2-nitrobenzaldehyde (4-NO₂)

4-Bromo-3-nitroanisole (1.75 g, 7.54 mmol) and THF (80 mL, absolved) were added to a dried flask while stirring under argon stream. The solution was cooled down to -78 °C, and phenyllithium (4.00 mL, 7.60 mmol, 1.9 M in dibutyl ether) was added dropwise. Then the reaction mixture was stirred at -70 - -90 °C for 2 h and DMF (1.50 mL, 21.63 mmol) was added dropwise. After this addition the reaction solution was kept stirring at -70 - -90 °C for another 1 h and was allowed to reach 0 °C within 1 h. This mixture was quenched by adding acetic acid (5 mL, concentrated) and partitioned between diethyl ether (100 mL) and water (50 mL). The organic layer was washed with saturated NaHCO₃ solution (50 mL), water (50 mL) and brine (50 mL), dried over Na₂SO₄ and concentrated to afford a crude product, which was purified by using MPLC (petroleum ether / ethyl acetate, 9:1) to yield 0.90 g **4-NO₂** as yellow crystals (65 %).

4-Methoxy-2-nitrobenzaldehyde

m.p. 95 - 96 °C (reported¹²⁴ 96 - 97 °C).

¹H NMR (DMSO-d₆, 400 MHz)

δ = 10.28 (s, 1H, H-(C-7)), 7.96 (d, ³J_{H,H} = 8.5 Hz, 1H, H-(C-5) or H-(C-6)), 7.50 (d, ⁴J_{H,H} = 2.6 Hz, 1H, H-(C-3)), 7.22 (d, ³J_{H,H} = 8.8 Hz, 1H, H-(C-5) or H-(C-6)), 3.95 (s, 3H, H-(C-8)).

¹³C NMR (DMSO-d₆, 100 MHz)

δ = 56.3, 109.5, 119.1, 123.4, 131.4, 151.6, 163.7, 186.9.

HRMS (EI)

m/z measured: 181.03411 ($[M]^+$, $C_8H_7NO_4$).

m/z calculated: 181.037486.

MS-EI (70 eV)

m/z : 181 ($[M]^+$, $C_8H_7NO_4$, 4 %), 151 ($[M - NO]^+$, $C_8H_7O_3$, 100 %), 134 (21 %), 119 (4 %), 108 (18 %), 106 (26 %), 95 (22 %), 92 (12 %), 77 ($[C_6H_5]^+$, 8 %), 63 ($[C_5H_3]^+$, 23 %), 50 (3 %).

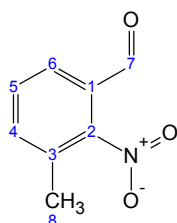
IR

$\bar{\nu}/\text{cm}^{-1}$ (T %): 3104 (85 %), 3066 (82 %), 2945 (84 %), 2841 (85 %), 1679 (56 %), 1600 (59 %), 1564 (77 %), 1524 (41 %), 1500 (56 %), 1458 (74 %), 1435 (70 %), 1403 (79 %), 1353 (52 %), 1320 (60 %), 1282 (54 %), 1241 (38 %), 1200 (65 %), 1184 (52 %), 1140 (59 %), 1067 (48 %), 1025 (44 %), 963 (78 %), 910 (56 %), 897 (47 %), 825 (29 %), 775 (57 %), 758 (54 %), 698 (76 %), 675 (73 %), 655 (62 %).

5.2.2 Methyl-substituted model compounds**5.2.2.1 3-Methyl-2-nitrobenzaldehyde (6- NO_2)**

The compound 1-bromo-3-methyl-2-nitrobenzene was formylated by the analogous method described in the preparation of **4- NO_2** (see paragraph **5.2.1.7**).

Phenyl lithium (6.29 mL, 10.06 mmol, 1.6 M in dibutyl ether solution) and 1-bromo-3-methyl-2-nitrobenzene (2.00 g, 9.26 mmol) in THF (50 mL) were stirred for 2 h at -70 - -90 °C under argon. Then piperidine-1-carbaldehyde (1.20 mL, 10.72 mmol) was added dropwise and the solution was allowed to reach room temperature within 1 h. After workup and purification by using MPLC (petroleum ether / ethyl acetate, 3:1), 1.00 g **6- NO_2** was obtained (66 %) as slightly yellow crystals.

3-Methyl-2-nitrobenzaldehyde

m.p. 62 - 64 °C (reported¹²⁵ 59 - 61 °C).

 ^1H NMR (CDCl_3 , 250 MHz)

δ (ppm) = 9.93 (s, 1H, H -(C-7)), 7.59 (dd, $^3J_{H,H} = 9.2$ Hz, $^3J_{H,H} = 9.2$ Hz, 1H, H -(C-5)), 7.57 (d, $^3J_{H,H} = 9.0$ Hz, 2H, H -(C-4) and H -(C-6)), 2.38 (s, 3H, H -(C-8)).

¹³C NMR (CDCl₃, 60 MHz)

δ (ppm) = 16.9, 127.6, 128.6, 130.7, 131.0, 137.0, 150.5, 186.9.

MS-FAB (70 eV)

m/z: 166 ([M + H]⁺, C₈H₈NO₃, 100 %), 154 (89 %), 136 ([M + H – NO]⁺, C₈H₈O₂, 97 %), 107 (34 %), 89 (43 %), 77 ([C₆H₅]⁺, 56 %), 65 (22 %).

IR

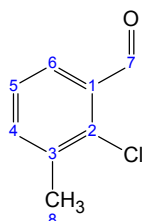
$\bar{\nu}$ /cm⁻¹ (T %): 2869 (89 %), 2758 (94 %), 1701 (33 %), 1604 (57 %), 1585 (78 %), 1527 (20 %), 1463 (61 %), 1433 (68 %), 1368 (30 %), 1320 (80 %), 1304 (76 %), 1262 (47 %), 1233 (49 %), 1174 (66 %), 1131 (88 %), 1073 (85 %), 1044 (66 %), 960 (52 %), 853 (39 %), 782 (27 %), 758 (40 %), 744 (55 %), 724 (64 %).

5.2.2.2 2-Chloro-3-methylbenzaldehyde (6-Cl)

6-Cl was synthesized by bromination and oxidation according to the above mentioned procedure for **3-Cl** (see paragraph 5.2.1.3).

2-Chloro-1,3-dimethylbenzene (4.85 g, 34.64 mmol), N-bromosuccinimide (6.77 g, 38.03 mmol) and a catalytic amount of AIBN (0.11 g) in CCl₄ (50 mL) were refluxed for 1 h. 6.70 g Crude 2-chloro-3-bromomethyltoluene was obtained and used directly in the next synthesis step.

A stirred suspension of 6.70 g crude 2-chloro-3-bromomethyltoluene, DMSO (30 mL) and Na₂CO₃ (6.50 g, 61.32 mmol) was heated to 50 °C under argon overnight. After workup and purification by using MPLC, 1.60 g **6-Cl** (33 % based on 2-chloro-1,3-dimethylbenzene) was obtained as white crystals.

2-Chloro-3-methylbenzaldehyde

m.p. 36 - 37 °C (reported¹²⁶ 37 °C).

¹H NMR (DMSO-d₆, 400 MHz)

δ (ppm) = 10.37 (s, 1H, *H*-(C-7)), 7.67 (*m*, 2H, *H*-(C-4) and *H*-(C-6)), 7.41 (*dd*, ³*J*_{H,H} = 7.4 Hz, ³*J*_{H,H} = 7.4 Hz, 1H, *H*-(C-5)), 2.38 (s, 3H, *H*-(C-8)).

¹³C NMR (DMSO-d₆, 100 MHz)

δ (ppm) = 19.3, 127.2, 127.2, 132.2, 136.4, 136.7, 137.4, 190.3.

MS-EI (70 eV)

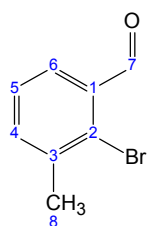
m/z : 156 ($[M]^+$, $C_8H_6^{37}ClO$, 26 %), 154 ($[M]^+$, $C_8H_7^{35}ClO$, 64 %), 153 ($[M - H]^+$, $C_8H_6^{35}ClO$, 100 %), 127 ($[M - CHO]^+$, $C_7H_6^{37}Cl$, 11 %), 125 ($[M - CHO]^+$, $C_8H_6^{35}Cl$, 30 %), 118 (2 %), 101 (2 %), 99 (4 %), 91 (11 %), 89 (20 %), 75 (3 %), 65 (4 %), 63 ($[C_5H_3]^+$, 10 %), 40 (5 %), 39 (6 %).

IR

$\bar{\nu}/cm^{-1}$ (T %): 3346 (83 %), 2986 (78 %), 2921 (83 %), 2876 (75 %), 2745 (83 %), 1952 (83 %), 1891 (84 %), 1831 (85 %), 1747 (90 %), 1701 (68 %), 1678 (14 %), 1578 (39 %), 1452 (38 %), 1421 (68 %), 1378 (28 %), 1286 (78 %), 1242 (26 %), 1169 (54 %), 1107 (65 %), 1046 (30 %), 1012 (58 %), 978 (71 %), 916 (42 %), 781 (12 %), 714 (33 %), 703 (29 %).

5.2.2.3 2-Bromo-3-methylbenzaldehyde (6-Br)

The synthesis of **6-Br** was similar to preparation of **6-Cl** (see paragraph 5.2.2.2). After bromination by N-bromosuccinimide, 2-bromo-1,3-dimethylbenzene (4.38 g, 23.68 mmol) gave 6.47 g crude 2-bromo-3-bromomethylanisole which was directly oxidized in DMSO in the presence of Na_2CO_3 . After workup and purification by using MPLC (petroleum ether / ethyl acetate, 5:1), 2.50 g **6-Br** was obtained as white crystals (53 % based on 2-bromo-1,3-dimethylbenzene).

2-Bromo-3-methylbenzaldehyde

m.p. 53 - 54 °C (reported¹²⁷ 53 - 54 °C).

 1H NMR (DMSO- d_6 , 400 MHz)

δ (ppm) = 10.29 (s, 1H, H -(C-7)), 7.66 (m, 2H, H -(C-4) and H -(C-6)), 7.44 (dd, $^3J_{H,H} = 7.6$ Hz, $^3J_{H,H} = 7.6$ Hz, 1H, H -(C-5)), 2.42 (s, 3H, H -(C-8)).

 ^{13}C NMR (DMSO- d_6 , 100 MHz)

δ (ppm) = 22.3, 127.4, 127.8, 128.3, 133.6, 136.6, 139.3, 192.3.

MS-EI (70 eV)

m/z : 200 ($[M]^+$, $C_8H_7^{81}BrO$, 68 %), 199 ($[M - H]^+$, $C_8H_6^{81}BrO$, 95 %), 198 ($[M]^+$, $C_8H_7^{79}BrO$, 69 %), 197 ($[M - H]^+$, $C_8H_7^{79}BrO$, 100 %), 172 (3 %), 171 ($[M - CHO]^+$,

C₇H₆⁸¹Br, 22 %), 170 (4 %), 169 ([M – CHO]⁺, C₇H₇⁷⁹Br, 24 %), 118 ([M – H^{79/81}Br]⁺, C₈H₆O, 5 %), 98 (2 %), 91 (12 %), 89 (23 %), 74 (2 %), 63 (12 %), 39 (5 %).

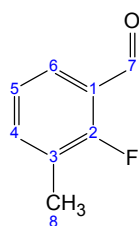
IR

$\bar{\nu}$ /cm⁻¹ (T %): 3340 (80 %), 2982 (74 %), 2867 (71 %), 2735 (80 %), 1952 (81 %), 1889 (82 %), 1825 (83 %), 1725 (87 %), 1696 (52 %), 1674 (17 %), 1584 (70 %), 1572 (39 %), 1449 (43 %), 1418 (65 %), 1373 (32 %), 1280 (75 %), 1263 (76 %), 1238 (31 %), 1168 (52 %), 1105 (61 %), 1031 (35 %), 1006 (49 %), 977 (68 %), 911 (39 %), 779 (13 %), 701 (41 %), 689 (34 %).

5.2.2.4 2-Fluoro-3-methylbenzaldehyde (6-F)

To a stirred solution of *t*-BuOK (1.00 g, 8.93 mmol) in dry THF (20 mL) *n*-BuLi (5.70 mL, 9.12 mmol, 1.6 M in hexane) was added dropwise at -80 °C under argon. After 5 min further stirring, 1-fluoro-2-methylbenzene (1.00 g, 9.09 mmol) was introduced and the reaction was carried out for 2 h at -80 °C. DMF (0.80 mL, 10.04 mmol) was added dropwise, then the solution was allowed to reach room temperature within 1 h. This reaction solution was quenched by adding acetic acid (5 mL, concentrated) and the resulting mixture was added into diethyl ether (100 mL). This solution was washed with saturated aqueous NaHCO₃ solution (50 mL), water (50 mL) and brine (50 mL) respectively, then the organic layer was dried over Na₂SO₄ and concentrated to afford a yellow oil, which was purified by using MPLC (petroleum ether / ethyl acetate, 4:1) to yield 0.77 g **6-F** (62 %) as white crystals.

2-Fluoro-3-methylbenzaldehyde



m.p. 36 - 37 °C.

¹H NMR (DMSO-d₆, 400 MHz)

δ (ppm) = 10.22 (s, 1H, *H*-(C-7)), 7.63 (*m*, 2H, *H*_{arom}), 7.27 (*m*, 1H, *H*_{arom}), 2.28 (*d*, ⁴*J*_{H,F} = 2.0 Hz, 3H, *H*-(C-8)).

¹³C NMR (DMSO-d₆, 100 MHz)

δ (ppm) = 13.7 (*d*, ³*J*_{C,F} = 3.6 Hz, C-8), 123.6 (*d*, ²*J*_{C,F} = 8.8 Hz, C-1 or C-3), 124.5 (*d*, ³*J*_{C,F} = 3.7 Hz, C-4 or C-6), 125.8 (*d*, ²*J*_{C,F} = 16.1 Hz, C-1 or C-3), 126.7 (*d*, ⁴*J*_{C,F} =

1.5 Hz, C-5), 137.9 (*d*, $^3J_{C,F}$ = 6.6 Hz, C-4 or C-6), 161.9 (*d*, $^1J_{C,F}$ = 256.2 Hz, C-2), 188.1 (*d*, $^3J_{C,F}$ = 6.6 Hz, C-7).

HRMS (EI)

m/z measured: 138.04527 ($[M]^+$, C₈H₇FO).

m/z calculated: 138.048085.

MS-EI (70 eV)

m/z: 138 ($[M]^+$, C₈H₇FO, 53 %), 137 ($[M - H]^+$, C₈H₆FO, 53 %), 109 ($[M - CHO]^+$, C₇H₆F, 40 %), 89 (3 %), 83 (12 %), 63 ($[C_5H_3]^+$, 3 %), 39 (2 %).

IR

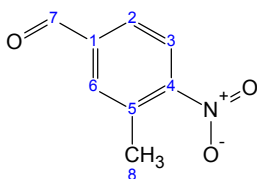
$\bar{\nu}/\text{cm}^{-1}$ (T %): 2861 (93 %), 2759 (95 %), 1697 (34 %), 1678 (49 %), 1615 (68 %), 1585 (52 %), 1474 (53 %), 1397 (59 %), 1382 (78 %), 1307 (90 %), 1252 (30 %), 1228 (77 %), 1194 (43 %), 1164 (89 %), 1090 (87 %), 1074 (84 %), 1006 (93 %), 953 (91 %), 922 (68 %), 820 (69 %), 780 (41 %), 760 (42 %), 721 (48 %), 684 (79 %).

5.2.2.5 3-Methyl-4-nitrobenzaldehyde (7-NO₂)

The solution of 3-methyl-4-nitrobenzoic acid (4.50 g, 24.86 mmol) in THF (40 mL) was stirred in ice bath and 1 N BH₃·THF (60 mL, 60 mmol) was added slowly into this solution. The ice bath was removed and the reaction solution was kept stirring for 36 h. Methanol (50 mL) was added slowly to quench the reaction. The mixture was filtered and the filtrate was evaporated under reduced pressure. The residue was dissolved in ethyl acetate (100 mL) and washed with water (25 mL). Then the organic layer was separated, dried over Na₂SO₄, and evaporated to afford 4.20 g crude (3-methyl-4-nitrophenyl)methanol as yellow solid. This crude product was used directly in the next synthesis step without further purification.

(3-Methyl-4-nitrophenyl)methanol was oxidised to **7-NO₂** by PDC according to the procedure described in the preparation for **3-I** (see paragraph 5.2.1.5). 4.20 g Crude (3-methyl-4-nitrophenyl)methanol gave 3.12 g **7-NO₂** (76 % based on 3-methyl-4-nitrobenzoic acid) after purification by using MPLC (petroleum ether / ethyl acetate, 5:1).

3-Methyl-4-nitrobenzaldehyde



m.p. 72 - 74 °C (reported¹²⁸ 68 °C).

¹H NMR (DMSO-d₆, 250 MHz)

δ (ppm) = 10.07 (s, 1H, *H*-(C-7)), 8.13 (d, ³*J*_{H,H} = 8.3 Hz, 1H, *H*-(C-2) or *H*-(C-3)), 8.00 (s, 1H, *H*-(C-6)), 7.94 (d, ³*J*_{H,H} = 8.4 Hz, 1H, *H*-(C-2) or *H*-(C-3)), 2.54 (s, 3H, *H*-(C-8)).

¹³C NMR (DMSO-d₆, 60 MHz)

δ (ppm) = 18.9 (C-8), 125.0 (H-C_{arom}), 128.0 (H-C_{arom}), 133.3 (C-5), 133.6 (H-C_{arom}), 138.4 (C-1), 152.2 (C-4), 192.2 (C-7).

MS-EI (70 eV)

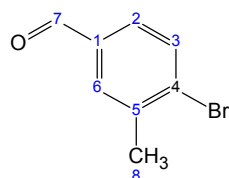
m/z: 165 ([M]⁺, C₈H₇NO₃, 9 %), 148 ([M – OH]⁺, C₈H₆NO₂, 100 %), 120 ([M – OH – CO]⁺, C₇H₆NO, 7 %), 106 (6 %), 92 (23 %), 91 (21 %), 77 ([C₆H₅]⁺, 12 %), 65 (50 %), 51 (10 %), 39 (16 %).

IR

$\bar{\nu}$ /cm⁻¹ (T %): 3378 (88 %), 3104 (83 %), 3078 (85 %), 3042 (86 %), 2996 (87 %), 2857 (82 %), 2744 (86 %), 1916 (90 %), 1782 (93 %), 1699 (60 %), 1606 (71 %), 1586 (74 %), 1511 (40 %), 1458 (73 %), 1416 (73 %), 1382 (60 %), 1358 (47 %), 1306 (59 %), 1270 (72 %), 1226 (61 %), 1148 (56 %), 1082 (69 %), 1038 (77 %), 1007 (69 %), 963 (64 %), 952 (68 %), 889 (69 %), 831 (36 %), 757 (58 %), 734 (45 %), 694 (66 %), 678 (64 %).

5.2.2.6 4-Bromo-3-methylbenzaldehyde (7-Br)

The synthesis of **7-Br** was similar to the preparation of **7-NO₂** (see paragraph 5.2.2.5). 4-Bromo-3-methylbenzoic acid (2.10 g, 9.77 mmol) gave 2.20 g crude (4-bromo-3-methylphenyl)methanol. This intermediate was directly oxidized by using PDC and 1.14 g **7-Br** (58 % based on 4-bromo-3-methylbenzoic acid) was obtained as yellow oil after purification by using MPLC (petroleum ether / ethyl acetate, 5:1).

4-Bromo-3-methylbenzaldehyde**¹H NMR (DMSO-d₆, 400 MHz)**

δ (ppm) = 9.95 (s, 1H, *H*-(C-7)), 7.85 (d, ⁴*J*_{H,H} = 1.3 Hz, 1H, *H*-(C-6)), 7.83 (d, ³*J*_{H,H} = 7.9 Hz, 1H, *H*-(C-3)), 7.64 (dd, ³*J*_{H,H} = 8.3 Hz, ⁴*J*_{H,H} = 1.7 Hz, 1H, *H*-(C-2)), 2.42 (s, 3H, *H*-(C-8)).

¹³C NMR (DMSO-d₆, 100 MHz)

δ (ppm) = 22.3, 128.4, 131.1, 131.5, 133.1, 135.4, 138.5, 192.4.

MS-EI (70 eV)

m/z : 200 ($[M]^+$, C₈H₇⁸¹BrO, 62 %), 199 ($[M - H]^+$, C₈H₆⁸¹BrO, 97 %), 198 ($[M]^+$, C₈H₇⁷⁹BrO, 64 %), 197 ($[M - H]^+$, C₈H₇⁷⁹BrO, 100 %), 172 (4 %), 171 ($[M - CHO]^+$, C₇H₆⁸¹Br, 26 %), 170 (4 %), 169 ($[M - CHO]^+$, C₇H₇⁷⁹Br, 30 %), 118 ($[M - H^{79/81}Br]^+$, C₈H₆O, 2 %), 91 (8 %), 89 (18 %), 74 (2 %), 63 (11 %), 39 (5 %).

IR

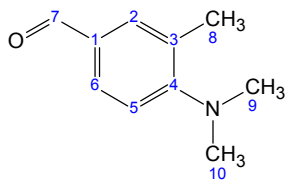
$\bar{\nu}/\text{cm}^{-1}$ (T %): 3378 (99 %), 2954 (96 %), 2923 (96 %), 2833 (92 %), 2722 (94 %), 1698 (32 %), 1686 (34 %), 1590 (43 %), 1568 (51 %), 1469 (75 %), 1445 (78 %), 1410 (87 %), 1383 (68 %), 1365 (72 %), 1291(72 %), 1279 (78 %), 1227 (50 %), 1164 (80 %), 1153 (70 %), 1140 (84 %), 1024 (27 %), 948 (51 %), 924 (54 %), 892 (78 %), 815 (48 %), 775 (45 %), 736 (38 %), 699 (77 %), 673 (81 %), 666 (82 %).

5.2.2.7 3-Methyl-4-trimethylammoniumbenzaldehyde triflate (7-N⁺Me₃TfO⁻)

The synthetic procedure was the same as described in the preparation of 3-N⁺Me₃TfO⁻ (see paragraph 5.2.1.6)

3-Methyl-4-dimethylaminobenzaldehyde

4-Fluoro-3-methylbenzaldehyde (0.95 g, 6.88 mmol), dimethylamine hydrochloride (1.40 g, 17.28 mmol) and K₂CO₃ (2.37 g, 17.17 mmol) were stirred in a mixture of DMSO (50 mL) and water (20 mL) and refluxed for 12 h. After workup and purification by using MPLC (petroleum ether / ethyl acetate, 5:1), 0.84 g 3-methyl-4-dimethylaminobenzaldehyde was obtained as yellow oil (68 %).

3-Methyl-4-dimethylaminobenzaldehyde**¹H NMR (DMSO-d₆, 400 MHz)**

δ = 9.79 (s, 1H, H -(C-7)), 7.65 (m, 2H, H_{arom}), 7.07 (d, $^3J_{H,H}$ = 8.3 Hz, 1H, H_{arom}), 2.77 (s, 6H, H -(C-9) and H -(C-10)), 2.30 (s, 3H, H -(C-8)).

¹³C NMR (DMSO-d₆, 100 MHz)

δ = 19.2, 59.7, 117.3, 128.9, 129.4, 129.7, 132.4, 157.9, 170.2, 191.2.

MS-EI (70 eV)

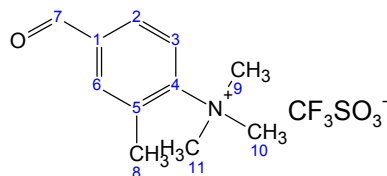
m/z: 163 ($[M]^+$, $C_{10}H_{13}NO$, 100 %), 148 ($[M - CH_3]^+$, $C_9H_{10}NO$, 50 %), 132 (28 %), 118 (14 %), 91 (14 %), 65 (7 %).

IR

$\bar{\nu}/cm^{-1}$ (T %): 2946 (85 %), 2834 (83 %), 2791 (82 %), 2722 (90 %), 1679 (29 %), 1594 (22 %), 1565 (55 %), 1500 (45 %), 1476 (79 %), 1445 (64 %), 1418 (76 %), 1372 (72 %), 1333 (55 %), 1313 (58 %), 1230 (30 %), 1186 (62 %), 1156 (56 %), 1137 (61 %), 1099 (27 %), 1053 (66 %), 1004 (87 %), 956 (43 %), 933 (75 %), 897 (76 %), 821 (48 %), 778 (51 %), 744 (68 %), 731 (60 %), 703 (80 %).

3-Methyl-4-trimethylammoniumbenzaldehyde triflate

To a stirred solution of 3-methyl-4-dimethylaminobenzaldehyde (0.95 g, 5.83 mmol) in DCM (5 mL) was added methyl trifluoromethanesulfonate (0.78 mL, 6.90 mmol). The solution was stirred for 3 h at room temperature under argon. The reaction solvent was concentrated and the residue was crystallized in mixture of diisopropylether and DCM (1:10, v/v). 0.92 g **7-N⁺Me₃TfO⁻** was obtained as white crystals (74 %).

3-Methyl-4-trimethylammoniumbenzaldehyde triflate

m.p. 113 - 115 °C.

¹H NMR (DMSO-d₆, 400 MHz)

δ = 10.06 (s, 1H, *H*-(C-7)), 8.10 (d, $^4J_{H,H}$ = 8.8 Hz, 1H, *H*_{arom}), 7.99 (m, 2H, *H*_{arom}), 3.71 (s, 9H, -N-(CH₃)₃), 2.82 (s, 3H, *H*-(C-8)).

¹³C NMR (DMSO-d₆, 100 MHz)

δ = 22.6 (C-8), 56.5(-N-(CH₃)₃), 122.7 (H-C_{arom}), 128.4 (H-C_{arom}), 132.0 (C-5), 136.2 (H-C_{arom}), 136.6 (C-1), 149.0 (C-4), 192.0 (C-7).

MS-FAB (70 eV)

m/z: 178 ($[M]^+$, $C_{11}H_{16}NO$, 100 %), 164 ($[M - CH_3]^+$, $C_{10}H_{13}NO$, 34 %), 136 ($[M - CH_3 - CO]^+$, $C_9H_{13}NO$, 26 %), 107 (8 %).

IR

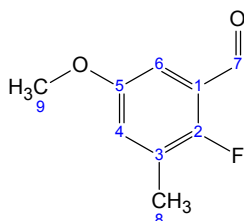
$\bar{\nu}/cm^{-1}$ (T %): 3052 (93 %), 2296 (98 %), 1691 (60 %), 1609 (93 %), 1584 (88 %), 1496 (76 %), 1480 (81 %), 1389 (90 %), 1376 (90 %), 1315 (92 %), 1255 (26 %),

1223 (30 %), 1197 (76 %), 1147 (33 %), 1092 (78 %), 1067 (60 %), 1026 (20 %), 962 (80 %), 947 (58 %), 820 (73 %), 777 (65 %), 756 (72 %), 739 (90 %), 679 (86 %).

5.2.2.8 2-Fluoro-5-methoxy-3-methylbenzaldehyde (8-F)

2.45 g **8-F** was obtained as white crystals (70 %) from 4-fluoro-3-methylanisole (3.00 mL, 17.14 mmol). The synthetic procedure was carried out according to described in the synthesis of **6-F** (see paragraph 5.2.2.4).

2-Fluoro-5-methoxy-3-methylbenzaldehyde



m.p. 41 - 42 °C.

¹H NMR (DMSO-d₆, 400 MHz)

δ (ppm) = 10.18 (s, 1H, *H*-(C-7)), 7.21 (dd, ⁴*J*_{H,H} = 3.3 Hz, ⁴*J*_{H,F} = 6.6 Hz, 1H, *H*-(C-4) or *H*-(C-6)), 7.07 (dd, ⁴*J*_{H,H} = 3.8 Hz, ⁴*J*_{H,F} = 5.1 Hz, 1H, *H*-(C-4) or *H*-(C-6)), 3.76 (s, 3H, -OCH₃), 2.25 (d, ⁴*J*_{H,F} = 2.0 Hz, 3H, *H*-(C-8)).

¹³C NMR (DMSO-d₆, 100 MHz)

δ (ppm) = 13.9 (d, ³*J*_{C,F} = 3.7 Hz, C-8), 55.7 (C-9), 108.7 (d, ³*J*_{C,F} = 2.9 Hz, C-4 or C-6), 123.7 (d, ²*J*_{C,F} = 10.2 Hz, C-1 or C-3), 124.1 (d, ³*J*_{C,F} = 5.9 Hz, C-4 or C-6), 127.2 (d, ²*J*_{C,F} = 18.2 Hz, C-1 or C-3), 155.1 (d, ⁴*J*_{C,F} = 2.2 Hz, C-5), 156.8 (d, ¹*J*_{C,F} = 249.6 Hz, C-2), 187.8 (d, ³*J*_{C,F} = 5.9 Hz, C-7).

HRMS (EI)

m/z measured: 168.05987 ([M]⁺, C₉H₉FO₂).

m/z calculated: 168.058645.

MS-EI (70 eV)

m/z: 168 ([M]⁺, C₉H₉FO₂, 100 %), 153 (3 %), 139 ([M - CHO]⁺, C₈H₈FO, 22 %), 109 (9 %), 97 (7 %), 77 ([C₆H₅]⁺, 4 %), 57 (2 %), 51 ([C₄H₃]⁺, 6 %).

IR

$\bar{\nu}$ /cm⁻¹ (T %): 2941 (92 %), 2860 (92 %), 1690 (32 %), 1600 (65 %), 1478 (41 %), 1444 (70 %), 1399 (52 %), 1382 (76 %), 1333 (56 %), 1290 (55 %), 1232 (52 %), 1200 (34 %), 1149 (45 %), 1055 (43 %), 1010 (81 %), 967 (76 %), 946 (62 %), 857 (58 %), 794 (72 %), 764 (88 %), 705 (64 %), 696 (63 %), 674 (30 %).

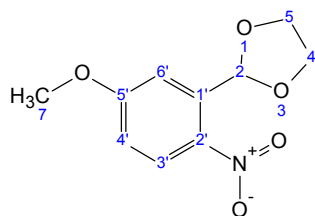
5.2.2.9 5-Methoxy-3-methyl-2-nitrobenzaldehyde (8-NO₂)

Synthetic pathway 1

2-(5-Methoxy-2-nitrophenyl)-1,3-dioxolane

In the Dean-Stark-Trap 5-methoxy-2-nitrobenzaldehyde (3.97 g, 21.93 mmol), ethylene glycol (2.20 mL, 39.49 mmol) and toluene-4-sulfonic acid (0.25 g, 1.32 mmol) were mixed in toluene (55 mL). This solution was refluxed at 130 °C for 6 h. The resulting mixture was washed with 3 % aqueous NaHCO₃ solution (50 mL), then the toluene layer was dried over Na₂SO₄. After evaporation of solvent, the residue was purified by using MPLC (petroleum ether / ethyl acetate, 5:1). The collected product from MPLC was crystallized in diisopropyl ether to yield 4.51 g 2-(5-methoxy-2-nitrophenyl)-1,3-dioxolane as white needle crystal (71 %).

2-(5-Methoxy-2-nitrophenyl)-1,3-dioxolane



m.p. 52 - 54 °C.

¹H NMR (CDCl₃, 250 MHz)

δ (ppm) = 8.04 (*d*, ³*J*_{H,H} = 9.1 Hz, 1H, *H*-(C-3')), 7.29 (*d*, ⁴*J*_{H,H} = 3.0 Hz, 1H, *H*-(C-6')), 6.90 (*dd*, ³*J*_{H,H} = 9.1 Hz, ⁴*J*_{H,H} = 2.8 Hz, 1H, *H*-(C-4')), 6.55 (*s*, 1H, *H*-(C-2)), 4.04 (*m*, 4H, *H*-(C-4) and *H*-(C-5)), 3.89 (*s*, 3H, *H*-(C-7)).

¹³C NMR (CDCl₃, 60 MHz)

δ (ppm) = 55.9 (C-7), 65.3 (C-4 and C-5), 99.5 (C-2), 112.7 (C-6'), 113.9 (C-4'), 127.5 (C-3'), 136.2 (C-1'), 141.5 (C-2'), 163.2 (C-5').

HRMS (EI)

m/z measured: 225.06277 ([M]⁺, C₁₀H₁₁NO₅).

m/z calculated: 225.063696.

MS-FAB (70 eV)

m/z: 226 ([M + H]⁺, C₁₀H₁₂NO₅, 100 %), 208 ([M - OH]⁺, C₁₀H₁₀NO₄, 28 %), 178 (100 %), 164 (12 %), 150 (16 %), 134 (53 %), 121 (46 %), 106 (89 %), 92 (10 %), 73 (18 %), 63 ([C₅H₃]⁺, 14 %), 45 (8 %).

IR

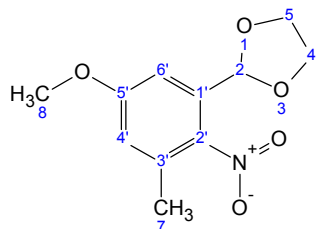
$\bar{\nu}$ /cm⁻¹ (T %): 3122 (84 %), 3105 (86 %), 3081 (85 %), 2974 (83 %), 2948 (81 %), 2897 (73 %), 2839 (86 %), 2617 (90 %), 2479 (91 %), 2055 (92 %), 1941 (90 %),

1812 (93 %), 1736 (94 %), 1689 (94 %), 1603 (61 %), 1589 (50 %), 1504 (49 %), 1489 (41 %), 1473 (54 %), 1466 (55 %), 1457 (55 %), 1417 (80 %), 1392 (49 %), 1317 (38 %), 1286 (39 %), 1240 (41 %), 1192 (41 %), 1177 (38 %), 1153 (59 %), 1133 (70 %), 1100 (46 %), 1058 (29 %), 1026 (36 %), 982 (38 %), 957 (23 %), 938 (29 %), 867 (30 %), 852 (29 %), 841 (34 %), 775 (50 %), 756 (46 %), 721 (47 %), 695 (56 %).

2-(5-Methoxy-3-methyl-2-nitrophenyl)-1,3-dioxolane

To a stirred solution of 2-(5-methoxy-2-nitrophenyl)-1,3-dioxolane (0.30 g, 1.33 mmol) in THF (10 mL, absolute) at -80 °C MeMgBr (1.40 mL, 4.20 mmol, 3 M in diethyl ether) was added dropwise. After 30 min, the solution of KMnO₄ (0.51 g, 3.23 mmol) in water and acetone (10 mL, 1:1, v/v) was introduced into the mixture which was then stirred another 1 h without cooling bath. 0.1 N HCl (25 mL) was added and the mixture was extracted with DCM (2 × 50 mL), the combined extracts were washed, dried over Na₂SO₄ and evaporated to leave a residue, which was subjected by using MPLC (petroleum ether / ethyl acetate, 5:1). 0.12 g 2-(5-methoxy-3-methyl-2-nitrophenyl)-1,3-dioxolane was obtained as yellow oil (39 %).

2-(5-Methoxy-3-methyl-2-nitrophenyl)-1,3-dioxolane



¹H NMR (CDCl₃, 250 MHz)

δ = 7.00 (d, ⁴J_{H,H} = 2.7 Hz, 1H, H-(C-4') or H-(C-6')), 6.74 (d, ⁴J_{H,H} = 2.8 Hz, 1H, H-(C-4') or H-(C-6')), 6.10 (s, 1H, H-(C-2)), 3.99 (m, 4H, H-(C-4) and H-(C-5)), 3.83 (s, 3H, H-(C-8)), 2.33 (s, 3H, H-(C-7)).

¹³C NMR (CDCl₃, 60 MHz)

δ = 18.2 (C-7), 55.6 (C-8), 65.2 (C-4 and C-5), 99.8 (C-2), 109.9 (C-4' or C-6'), 116.6 (C-4' or C-6'), 133.0 (C-3'), 133.3 (C-1'), 134.5 (C-2'), 160.3 (C-5').

MS-FAB (70 eV)

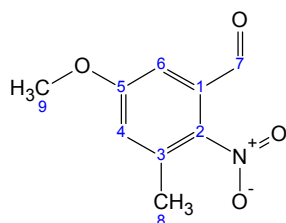
m/z: 240 ([M + H]⁺, C₁₁H₁₄NO₅, 100 %), 219 (18 %), 196 ([M + H - CH₂CH₂O]⁺, C₉H₁₀NO₄, 45 %), 178 (16 %), 163 (18 %), 154 (78 %), 136 (15 %), 120 (25 %), 107 (29 %), 89 (28 %), 77 ([C₆H₅]⁺, 38 %), 73 (35 %), 57 (18 %).

IR

$\bar{\nu}/\text{cm}^{-1}$ (T %): 2967 (90 %), 2892 (88 %), 1735 (96 %), 1595 (54 %), 1521 (35 %), 1468 (64 %), 1360 (49 %), 1332 (56 %), 1316 (59 %), 1283 (56 %), 1233 (74 %), 1195 (61 %), 1167 (47 %), 1123 (50 %), 1096 (33 %), 1052 (58 %), 1022 (53 %), 935 (49 %), 863 (58 %), 840 (45 %), 753 (80 %), 722 (83 %), 678 (80 %).

5-Methoxy-3-methyl-2-nitrobenzaldehyde

To solution of 2-(5-methoxy-3-methyl-2-nitrophenyl)-1,3-dioxolane (0.40 g, 1.67 mmol) in THF (5 mL) was added 1 N HCl (5 mL). This solution was stirred at room temperature overnight. After workup and purification by using MPLC (petroleum ether / ethyl acetate, 5:1), 0.24 g **8-NO₂** was obtained as yellow substance (70 %).

5-Methoxy-3-methyl-2-nitrobenzaldehyde

m.p. 114 - 116 °C.

¹H NMR (CDCl₃, 250 MHz)

δ (ppm) = 9.94 (s, 1H, *H*-(C-7)), 7.23 (s, 1H, *H*-(C-4) or *H*-(C-6)), 6.99 (s, 1H, *H*-(C-4) or *H*-(C-6)), 3.89 (s, 3H, *H*-(C-9)), 2.42 (s, 3H, *H*-(C-8)).

¹³C NMR (CDCl₃, 60 MHz)

δ (ppm) = 18.3 (C-8), 56.0 (C-9), 111.4 (C-4 or C-6), 122.1 (C-4 or C-6), 130.9 (C-1), 134.2 (C-3), 144.9 (C-2), 160.9 (C-5), 187.0 (C-7).

HRMS (EI)

m/z measured: 195.05047 ($[\text{M}]^+$, C₉H₉NO₄).

m/z calculated: 195.053136.

MS-EI (70 eV)

m/z: 195 ($[\text{M}]^+$, C₉H₉NO₄, 11 %), 178 ($[\text{M} - \text{OH}]^+$, C₉H₈NO₃, 6 %), 167 ($[\text{M} - \text{CO}]^+$, C₈H₉NO₃, 5 %), 165 ($[\text{M} - \text{NO}]^+$, C₉H₉O₃, 11 %), 162 (21 %), 149 ($[\text{M} - \text{NO}_2]^+$, C₉H₉O₂, 100 %), 137 (9 %), 134 (16 %), 122 (8 %), 121 (41 %), 107 (9 %), 106 (50 %), 95 (7 %), 78 (10 %), 73 (18 %), 63 ($[\text{C}_5\text{H}_3]^+$, 9 %), 62 (4 %), 51 ($[\text{C}_4\text{H}_3]^+$, 9 %), 39 (6 %).

IR

$\bar{\nu}/\text{cm}^{-1}$ (T %): 2941 (90 %), 1702 (63 %), 1593 (58 %), 1519 (38 %), 1468 (62 %), 1360 (58 %), 1327 (49 %), 1289 (41 %), 1237 (67 %), 1194 (64 %), 1167 (52 %),

1112 (59 %), 1097 (53 %), 1052 (66 %), 1029 (62 %), 966 (69 %), 938 (60 %), 863 (63 %), 841 (51 %), 730 (76 %), 692 (74 %).

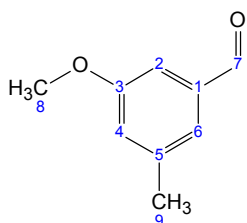
Synthetic pathway 2

3-Methoxy-5-methylbenzaldehyde

3,5-Dimethylphenol (18.00 g, 147.54 mmol) was methoxylated with MeI to give 18.60 g crude 1-methoxy-3,5-dimethylbenzene. The synthetic procedure was the same as described in the preparation of **3-NO₂** (see paragraph 5.2.1.2).

13.00 g Crude 1-methoxy-3,5-dimethylbenzene was brominated with N-bromosuccinimide and the intermediate was submitted to oxidation under basic condition, 3.00 g 3-methoxy-5-methylbenzaldehyde (30 % based on 1-(bromomethyl)-5-methoxy-3-methylbenzene) was obtained after purification by using MPLC (petroleum ether / ethyl acetate, 9:1). The synthetic procedure was the same as described in the synthesis of **3-Cl** (see paragraph 5.2.1.3).

3-Methoxy-5-methylbenzaldehyde



¹H NMR (DMSO-d₆, 400 MHz)

δ (ppm) = 9.92 (s, 1H, *H*-(C-7)), 7.31 (s, 1H, *H*_{arom}), 7.21 (s, 1H, *H*_{arom}), 7.09 (s, 1H, *H*_{arom}), 3.79 (s, 3H, *H*-(C-8)), 2.35 (s, 3H, *H*-(C-9)).

¹³C NMR (DMSO-d₆, 100 MHz)

δ (ppm) = 20.7, 55.3, 110.3, 121.3, 123.1, 137.5, 140.2, 159.7, 192.9.

HRMS (EI)

m/z measured: 150.06764 ([M]⁺, C₉H₁₀O₂).

m/z calculated: 150.068671.

MS-EI (70 eV)

m/z: 150 ([M]⁺, C₉H₁₀O₂, 100 %), 135 ([M - CH₃]⁺, C₈H₇O₂, 1 %), 121 ([M - CHO]⁺, C₇H₆O, 34 %), 105 (6 %), 91 (20 %), 78 (8 %), 77 ([C₆H₅]⁺, 17 %), 63 ([C₅H₃]⁺, 6 %), 51 (7 %), 38 (6 %).

IR

$\bar{\nu}$ /cm⁻¹ (T %): 2940 (91 %), 2841 (90 %), 2731 (94 %), 1696 (32 %), 1594 (45 %), 1465 (58 %), 1385 (63 %), 1330 (54 %), 1292 (24 %), 1261 (85 %), 1232 (92 %),

1193 (67 %), 1155 (45 %), 1148 (45 %), 1064 (44 %), 1005 (80 %), 992 (84 %), 965 (77 %), 935 (80 %), 918 (78 %), 845 (43 %), 770 (92 %), 705 (45 %), 678 (42 %).

5-Methoxy-3-methyl-2-nitrobenzaldehyde

3-Methoxy-5-methylbenzaldehyde (3.00 g, 20.00 mmol) was added to 90 % HNO₃ (10 mL) in several portions while stirring at 0 °C. After 1 h TLC analysis showed that the starting compound was completely converted and there were 3 different kinds of products in the solution. The resulting mixture was poured into water (100 mL) and extracted with diethyl ether (2 × 100 mL). The organic layer was washed with saturated NaHCO₃ solution (2 × 50 mL) and brine (50 mL), dried over Na₂SO₄ and evaporated. After purification by using the MPLC (petroleum ether / ethyl acetate, 5:1), 1.30 g **8-NO₂** (30 %) was obtained as yellow substance.

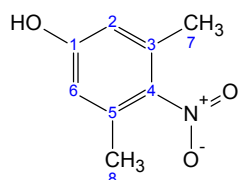
The analytic data (**MS**, **NMR** and **IR**) matched that of **8-NO₂** in synthetic pathway 1.

Synthetic pathway 3

3,5-Dimethyl-4-nitrophenol

Concentrated HCl (30 mL) was added dropwise into a stirred solution of 3,5-dimethylphenol (40.40 g, 331.15 mmol) and NaNO₃ (28.20 g, 331.76 mmol) in diethyl ether (250 mL) and water (250 mL). The solution was kept stirring at room temperature overnight. The resulting mixture was extracted with diethyl ether (2 × 150 mL) and the combined organic extracts were washed with saturated aqueous NaHCO₃ solution (2 × 150 mL), water (2 × 200 mL) and brine (100 mL), then dried over Na₂SO₄ and concentrated to afford a crude mixed product (3,5-dimethyl-4-nitrophenol and 3,5-dimethyl-2-nitrophenol). These two compounds were separated by steam distillation. 15.90 g 3,5-dimethyl-4-nitrophenol was obtained as yellow powder (29 %).

3,5-Dimethyl-4-nitrophenol



m.p. 107 - 108 °C (reported¹²⁹ 107 - 108 °C).

¹H NMR (DMSO-d₆, 400 MHz)

δ (ppm) = 6.59 (s, 2H, *H*-(C-2) and *H*-(C-6)), 2.19 (s, 6H, *H*-(C-7) and *H*-(C-8)).

¹³C NMR (DMSO-d₆, 100 MHz)

δ (ppm) = 17.6, 115.2, 132.0, 143.7, 158.6.

MS-EI (70 eV)

m/z : 167 ($[M]^+$, $C_8H_7NO_4$, 85 %), 150 ($[M - OH]^+$, $C_8H_6NO_3$, 100 %), 137 ($[M - NO]^+$, $C_8H_7O_3$, 11 %), 122 (14 %), 95 (9 %), 91 (26 %), 77 ($[C_6H_5]^+$, 31 %), 65 (8 %).

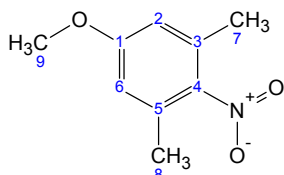
IR

$\bar{\nu}/cm^{-1}$ (T %): 3345 (61 %), 2974 (85 %), 2935 (85 %), 2868 (88 %), 2195 (93 %), 1589 (38 %), 1506 (27 %), 1466 (35 %), 1438 (40 %), 1381 (73 %), 1350 (53 %), 1306 (25 %), 1277 (29 %), 1232 (44 %), 1181 (36 %), 1172 (37 %), 1097 (39 %), 1030 (54 %), 971 (67 %), 868 (56 %), 845 (34 %), 838 (37 %), 764 (66 %), 699 (48 %).

3,5-Dimethyl-4-nitroanisole

The methoxylation of 3,5-dimethyl-4-nitrophenol was similar to the procedure described in the preparation of **3-NO₂** (see paragraph 5.2.1.2).

A mixture of 3,5-dimethyl-4-nitrophenol (1.25 g, 7.49 mmol), K_2CO_3 (1.03 g, 7.46 mmol) and MeI (0.47 mL, 7.55 mmol) was stirred in 40 mL DMF at room temperature for 4 h. After workup and purification by using MPLC (petroleum ether / ethyl acetate, 3:1), 1.13 g 3,5-dimethyl-4-nitroanisole was obtained as a yellow substance (81 %).

3,5-Dimethyl-4-nitroanisole

m.p. 56 - 58 °C (reported¹³⁰ 52 °C).

¹H NMR (DMSO-d₆, 400 MHz)

δ (ppm) = 6.82 (s, 2H, H -(C-2) and H -(C-6)), 3.78 (s, 3H, H -(C-9)), 2.24 (s, 6H, H -(C-7) and H -(C-8)).

¹³C NMR (DMSO-d₆, 100 MHz)

δ (ppm) = 17.6, 55.6, 114.0, 131.8, 144.8, 159.8.

MS-EI (70 eV)

m/z : 181 ($[M]^+$, $C_9H_{11}NO_3$, 95 %), 164 ($[M - OH]^+$, $C_9H_{10}NO_2$, 100 %), 151 ($[M - NO]^+$, $C_9H_{11}O_2$, 19 %), 121 (11 %), 109 (22 %), 91 (35 %), 77 ($[C_6H_5]^+$, 30 %), 65 ($[C_5H_5]^+$, 15 %), 51 ($[C_4H_3]^+$, 6 %).

IR

$\bar{\nu}/cm^{-1}$ (T %): 3022 (88 %), 2974 (85 %), 2942 (80 %), 2842 (87 %), 2623 (92 %), 1802 (95 %), 1716 (94 %), 1594 (40 %), 1505 (27 %), 1479 (41 %), 1441 (58 %),

1422 (65 %), 1379 (59 %), 1355 (44 %), 1325 (34 %), 1295 (45 %), 1189 (45 %), 1168 (45 %), 1108 (48 %), 1057 (55 %), 1040 (66 %), 1004 (53 %), 964 (75 %), 943 (53 %), 850 (50 %), 834 (24 %), 759 (71 %), 703 (56 %).

5-Methoxy-3-methyl-2-nitrobenzaldehyde

According to the procedure described in the preparation of **3-Cl** (see paragraph **5.2.1.3**), **8-NO₂** was synthesized from 3,5-dimethyl-4-nitroanisole (1.02 g, 5.64 mmol) by bromination and following oxidation. After workup and purification by using MPLC (petroleum ether / ethyl acetate, 5:1), 0.33 g **8-NO₂** was obtained (30 % based on 3,5-dimethyl-4-nitroanisole) as slightly yellow needles.

The analytic data (**MS**, **NMR** and **IR**) matched that of **8-NO₂** in synthetic pathway 1.

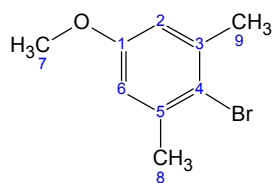
5.2.2.10 2-Bromo-5-methoxy-3-methylbenzaldehyde (**8-Br**)

2-Bromo-5-methoxy-1,3-dimethylbenzene

1-Methoxy-3,5-dimethylbenzene (**5.2.2.9**, synthetic pathway 2) was brominated as described in the preparation of **3-Br** (see paragraph **5.2.1.4**).

1-Methoxy-3,5-dimethylbenzene (3.00 g, 22.06 mmol) and Br₂ (1.25 mL, 24.30 mmol) was stirred in CHCl₃ (50 mL) at room temperature for 0.5 h. After purification by using MPLC (petroleum ether / ethyl acetate, 5:1), 3.90 g 2-bromo-5-methoxy-1,3-dimethylbenzene (85 %) was obtained as colourless oil.

2-Bromo-5-methoxy-1,3-dimethylbenzene



¹H NMR (DMSO-d₆, 400 MHz)

δ (ppm) = 6.78 (s, 2H, *H*-(C-2) and *H*-(C-6)), 3.71 (s, 3H, *H*-(C-7)), 2.31 (s, 6H, *H*-(C-8) and *H*-(C-9)).

¹³C NMR (DMSO-d₆, 100 MHz)

δ (ppm) = 23.4, 55.1, 114.0, 117.2, 138.4, 157.8.

MS-EI (70 eV)

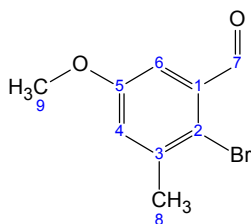
m/z: 217 ([M]⁺, C₉H₁₁⁸¹BrO, 11 %), 216 ([M - H]⁺, C₉H₁₀⁸¹BrO, 94 %), 215 ([M]⁺, C₉H₁₁⁷⁹BrO, 13 %), 214 ([M - H]⁺, C₉H₁₀⁷⁹BrO, 100 %), 201 ([M - CH₃]⁺, C₈H₈⁸¹BrO, 10 %), 199 ([M - CH₃]⁺, C₈H₈⁷⁹BrO, 12 %), 173 ([M - CH₃ - CO]⁺, C₇H₈⁸¹Br, 22 %), 171 ([M - CH₃ - CO]⁺, C₇H₈⁷⁹Br, 24 %), 135 ([M - H^{79/81}Br]⁺, C₉H₁₀O, 22 %), 119 (3 %), 105 (11 %), 91 (23 %), 77 ([C₆H₅]⁺, 6 %).

IR

$\bar{\nu}/\text{cm}^{-1}$ (T %): 2953 (89 %), 2836 (92 %), 1585 (56 %), 1465 (49 %), 1437 (69 %), 1407 (75 %), 1377 (83 %), 1318 (26 %), 1280 (82 %), 1236 (92 %), 1214 (90 %), 1194 (49 %), 1160 (23 %), 1098 (85 %), 1075 (51 %), 1030 (67 %), 1016 (49 %), 997 (71 %), 956 (91 %), 933 (77 %), 851 (58 %), 831 (60 %), 692 (73 %).

2-Bromo-5-methoxy-3-methylbenzaldehyde

According to the procedure described in the preparation of **3-Cl** (see paragraph 5.2.1.3), **8-Br** was synthesized from 2-bromo-5-methoxy-1,3-dimethylbenzene (2.08 g, 9.63 mmol) by bromination and following oxidation. After workup and purification by using MPLC (petroleum ether / ethyl acetate, 5:1), 0.85 g **8-Br** was obtained (39 % based on 2-bromo-5-methoxy-1,3-dimethylbenzene) as white needle crystals.

2-Bromo-5-methoxy-3-methylbenzaldehyde

m.p. 94 - 95 °C.

¹H NMR (DMSO-d₆, 400 MHz)

δ (ppm) = 10.24 (s, 1H, *H*-(C-7)), 7.29 (d, ⁴*J*_{H,H} = 3.1 Hz, 1H, *H*-(C-4) or *H*-(C-6)), 7.14 (d, ⁴*J*_{H,H} = 3.0 Hz, 1H, *H*-(C-4) or *H*-(C-6)), 3.79 (s, 3H, *H*-(C-9)), 2.38 (s, 3H, *H*-(C-8)).

¹³C NMR (DMSO-d₆, 100 MHz)

δ (ppm) = 22.2 (C-8), 55.6 (C-9), 115.1 (C-4 or C-6), 119.2 (C-2), 123.0 (C-4 or C-6), 134.1 (C-1), 140.6 (C-3), 158.3 (C-5), 192.0 (C-7).

HRMS (EI)

m/z measured: 227.98030 ([M]⁺, C₉H₉BrO₂).

m/z calculated: 227.978542.

MS-EI (70 eV)

m/z: 230 ([M]⁺, C₉H₉⁸¹BrO₂, 95 %), 229 ([M - H]⁺, C₉H₈⁸¹BrO₂, 95 %), 228 ([M]⁺, C₉H₉⁷⁹BrO₂, 100 %), 227 ([M - H]⁺, C₉H₈⁷⁹BrO₂, 95 %), 202 (7 %), 201 ([M - CHO]⁺, C₈H₈⁸¹BrO, 25 %), 200 (9 %), 199 ([M - CHO]⁺, C₈H₈⁷⁹BrO, 26 %), 185 (10 %), 157 (6 %), 148 ([M - H^{79/81}Br]⁺, C₉H₈O₂, 7 %), 134 (2 %), 120 (15 %), 105 (8 %), 91 (17 %), 77 ([C₆H₅]⁺, 24 %), 63 ([C₅H₃]⁺, 10 %), 51 ([C₄H₃]⁺, 18 %).

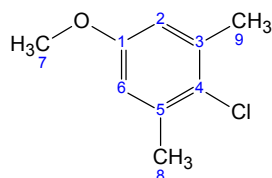
IR

$\bar{\nu}/\text{cm}^{-1}$ (T %): 3339 (87 %), 3071 (81 %), 3016 (79 %), 2978 (76 %), 2938 (77 %), 2888 (75 %), 2841 (78 %), 2604 (85 %), 2166 (88 %), 1762 (90 %), 1674 (32 %), 1587 (46 %), 1578 (49 %), 1461 (40 %), 1428 (49 %), 1386 (42 %), 1375 (33 %), 1311 (26 %), 1283 (37 %), 1231 (47 %), 1198 (43 %), 1158 (24 %), 1101 (70 %), 1074 (32 %), 1020 (45 %), 969 (52 %), 937 (30 %), 881 (51 %), 867 (30 %), 714 (49 %), 687 (53 %).

5.2.2.11 2-Chloro-5-methoxy-3-methylbenzaldehyde (8-Cl)**2-Chloro-5-methoxy-1,3-dimethylbenzene**

4-Chloro-3,5-dimethylphenol was methoxylated according to the procedure described in the synthesis of **3-NO₂** (see paragraph 5.2.1.2).

4-Chloro-3,5-dimethylphenol (13.80 g, 88.46 mmol), K₂CO₃ (14.60 g, 105.80 mmol) and MeI (6.60 mL, 105.97 mmol) were stirred in DMF (100 mL) at room temperature overnight. After workup and purification by using MPLC (petroleum ether / ethyl acetate, 5:1), 14.10 g 2-chloro-5-methoxy-1,3-dimethylbenzene was obtained as colourless oil (94 %).

2-Chloro-5-methoxy-1,3-dimethylbenzene**¹H NMR (DMSO-d₆, 400 MHz)**

δ (ppm) = 6.76 (s, 2H, *H*-(C-2) and *H*-(C-6)), 3.70 (s, 3H, *H*-(C-7)), 2.27 (s, 6H, *H*-(C-8) and *H*-(C-9)).

¹³C NMR (DMSO-d₆, 100 MHz)

δ (ppm) = 20.4, 55.2, 114.1, 124.9, 136.5, 157.3.

MS-EI (70 eV)

m/z: 172 ([M]⁺, C₉H₁₁³⁷ClO, 34 %), 170 ([M]⁺, C₉H₁₁³⁵ClO, 100 %), 157 ([M - CH₃]⁺, C₈H₈³⁷ClO, 9 %), 155 ([M - CH₃]⁺, C₈H₉³⁷ClO, 23 %), 135 ([M - ^{35/37}Cl]⁺, C₉H₁₁O, 38 %), 127 (22 %), 105 (14 %), 91 (21 %), 77 ([C₆H₅]⁺, 10 %), 65 ([C₅H₃]⁺, 7 %), 39 (5 %).

IR

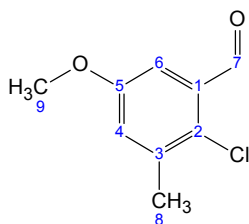
$\bar{\nu}/\text{cm}^{-1}$ (T %): 2953 (88 %), 2837 (91 %), 1715 (96 %), 1592 (57 %), 1471 (52 %), 1438 (72 %), 1413 (76 %), 1377 (87 %), 1322 (29 %), 1281 (82 %), 1237 (91 %),

1194 (50 %), 1160 (21 %), 1082 (62 %), 1039 (44 %), 998 (77 %), 957 (90 %), 936 (79 %), 853 (60 %), 834 (63 %), 697 (73 %).

2-Chloro-5-methoxy-3-methylbenzaldehyde

According to the procedure described in the synthesis of **3-Cl** (see paragraph **5.2.1.3**), 2-chloro-5-methoxy-1,3-dimethylbenzene (5.70 g, 33.14 mmol) was brominated and oxidized. 0.92 g **8-Cl** was obtained (15 % based on 2-chloro-5-methoxy-1,3-dimethylbenzene) as white needle crystals after workup and purification by using MPLC (petroleum ether / ethyl acetate, 5:1).

2-Chloro-5-methoxy-3-methylbenzaldehyde



m.p. 88 - 90 °C.

¹H NMR (DMSO-d₆, 400 MHz)

δ (ppm) = 10.31 (s, 1H, *H*-(C-7)), 7.27 (d, ⁴*J*_{H,H} = 3.1 Hz, 1H, *H*-(C-4) or *H*-(C-6)), 7.15 (d, ⁴*J*_{H,H} = 3.3 Hz, 1H, *H*-(C-4) or *H*-(C-6)), 3.78 (s, 3H, *H*-(C-9)), 2.34 (s, 3H, *H*-(C-8)).

¹³C NMR (DMSO-d₆, 100 MHz)

δ (ppm) = 19.3 (C-8), 55.6 (C-9), 110.6 (C-4 or C-6), 123.1 (C-4 or C-6), 128.2 (C-2), 132.8 (C-3), 138.8 (C-1), 157.7 (C-5), 190.0 (C-7).

HRMS (EI)

m/z measured: 184.028585 ([M]⁺, C₉H₉ClO₂).

m/z calculated: 184.029095.

MS-EI (70 eV)

m/z: 186 ([M]⁺, C₉H₉³⁷ClO₂, 34 %), 185 ([M - H]⁺, C₉H₈³⁷ClO₂, 42 %), 184 ([M]⁺, C₉H₉³⁵ClO₂, 93 %), 183 ([M - H]⁺, C₉H₈³⁵ClO₂, 100 %), 158 (2 %), 157 ([M - CHO]⁺, C₈H₈³⁷ClO, 6 %), 156 (5 %), 155 ([M - CHO]⁺, C₈H₈³⁵ClO, 18 %), 141 (3 %), 127 (2 %), 125 (4 %), 113 (3 %), 99 (2 %), 91 (6 %), 89 (5 %), 77 ([C₆H₅]⁺, 10 %), 63 ([C₅H₃]⁺, 4 %), 51 (6 %), 39 (3 %).

IR

$\bar{\nu}$ /cm⁻¹ (T %): 3345 (90 %), 3074 (85 %), 3019 (82 %), 2982 (80 %), 2941 (80 %), 2891 (78 %), 2844 (83 %), 1766 (92 %), 1678 (38 %), 1594 (50 %), 1463 (42 %), 1450 (53 %), 1433 (46 %), 1388 (44 %), 1376 (46 %), 1315 (33 %), 1284 (39 %),

1229 (53 %), 1196 (50 %), 1159 (30 %), 1081 (45 %), 1036 (38 %), 1013 (64 %), 970 (56 %), 940 (39 %), 884 (58 %), 870 (32 %), 727 (58 %), 695 (56 %).

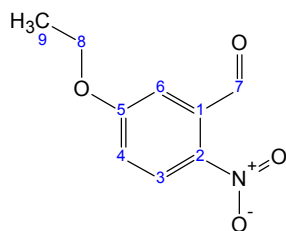
5.2.3 The precursors for further systematic study of nucleophilic aromatic ^{18}F -fluorination

5.2.3.1 5-Ethoxy-2-nitrobenzaldehyde (12-C₂H₅)

Compounds **12-C₂H₅**, **12-C₃H₇** and **12-C₄H₉** were synthesized by the analogous method described in methoxylation of **3-NO₂** (see paragraph 5.2.1.2):

5-Hydroxy-2-nitrobenzaldehyde (0.37 g, 2.22 mmol), K₂CO₃ (0.37 g, 2.68 mmol) and C₂H₅I (0.21 mL, 2.69 mmol) in DMF (5 mL) were stirred at room temperature for 12 h, 0.41 g **12-C₂H₅** (95 %) was obtained after purification by using MPLC (petroleum ether / ethyl acetate, 4:1).

5-Ethoxy-2-nitrobenzaldehyde



m.p. 69 - 70 °C.

^1H NMR (DMSO-d₆, 400 MHz)

δ (ppm) = 10.27 (s, 1H, H-(C-7)), 8.17 (d, $^3J_{\text{H,H}} = 9.1$ Hz, 1H, H-(C-3)), 7.34 (dd, $^3J_{\text{H,H}} = 9.1$ Hz, $^4J_{\text{H,H}} = 2.8$ Hz, 1H, H-(C-4)), 7.21 (d, $^4J_{\text{H,H}} = 3.0$ Hz, 1H, H-(C-6)), 4.24 (q, $^3J_{\text{H,H}} = 7.1$ Hz, 2H, H-(C-8)), 1.37 (t, $^3J_{\text{H,H}} = 7.0$ Hz, 3H, H-(C-9)).

^{13}C NMR (DMSO-d₆, 100 MHz)

δ (ppm) = 14.2 (C-9), 64.7 (C-8), 113.9 (C-6), 118.4 (C-4), 127.2 (C-3), 134.3 (C-1), 141.6 (C-2), 162.8 (C-5), 189.9 (C-7).

MS-EI (70 eV)

m/z : 195 ([M]⁺, C₉H₉NO₄, 16 %), 167 ([M - C₂H₄]⁺, C₇H₅NO₄, 100 %), 150 ([M - C₂H₄ - OH]⁺, C₇H₄NO₃, 12 %), 137 ([M - C₂H₄ - NO]⁺, C₇H₅O₃, 28 %), 123 (29 %), 109 (54 %), 92 (14 %), 81 (50 %), 69 (14 %), 63 ([C₅H₃]⁺, 15 %), 53 (18 %), 39 (16 %).

IR

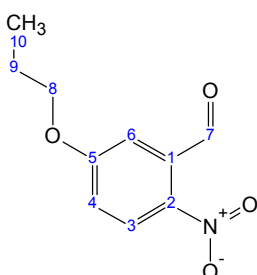
$\bar{\nu}$ /cm⁻¹ (T %): 3107 (96 %), 2986 (90 %), 2939 (93 %), 2899 (93 %), 2661 (98 %), 1693 (44 %), 1579 (38 %), 1512 (30 %), 1486 (63 %), 1473 (62 %), 1425 (72 %),

1386 (56 %), 1327 (22 %), 1285 (22 %), 1232 (19 %), 1161 (57 %), 1111 (68 %), 1079 (48 %), 1070 (43 %), 1034 (41 %), 993 (81 %), 974 (80 %), 882 (59 %), 842 (32 %), 821 (56 %), 766 (77 %), 743 (37 %), 674 (61 %).

5.2.3.2 2-Nitro-5-propoxybenzaldehyde (12-C₃H₇)

5-Hydroxy-2-nitrobenzaldehyde (1.00 g, 5.99 mmol), K₂CO₃ (1.00 g, 7.25 mmol) and C₃H₇I (0.70 mL, 7.23 mmol) in DMF (15 mL) were stirred at room temperature for 48 h, 0.90 g 12-C₃H₇ (72 %) was obtained after purification by using MPLC (petroleum ether / ethyl acetate, 3:1).

2-Nitro-5-propoxybenzaldehyde



m.p. 63 - 65 °C.

¹H NMR (DMSO-d₆, 400 MHz)

δ (ppm) = 10.28 (s, 1H, H-(C-7)), 8.17 (d, ³J_{H,H} = 8.9 Hz, 1H, H-(C-3)), 7.35 (dd, ³J_{H,H} = 8.9 Hz, ⁴J_{H,H} = 2.8 Hz, 1H, H-(C-4)), 7.22 (d, ⁴J_{H,H} = 2.8 Hz, 1H, H-(C-6)), 4.13 (t, ³J_{H,H} = 6.6 Hz, 2H, H-(C-8)), 1.80 (m, 2H, H-(C-9)), 0.99 (t, ³J_{H,H} = 7.3 Hz, 3H, H-(C-10)).

¹³C NMR (DMSO-d₆, 100 MHz)

δ (ppm) = 10.1 (C-10), 21.7 (C-9), 70.4 (C-8), 114.0 (C-6), 118.4 (C-4), 127.2 (C-3), 134.3 (C-1), 141.6 (C-2), 163.0 (C-5), 189.9 (C-7).

MS-EI (70 eV)

m/z: 209 ([M]⁺, C₁₀H₁₁NO₄, 2 %), 167 ([M - C₃H₆]⁺, C₇H₅NO₄, 100 %), 137 ([M - C₃H₆ - NO]⁺, C₇H₅O₃, 18 %), 123 (23 %), 109 (30 %), 92 (6 %), 81 (22 %), 63 ([C₅H₃]⁺, 15 %), 43 (40 %).

HRMS (EI)

m/z measured: 209.07177 ([M]⁺, C₁₀H₁₁NO₄).

m/z calculated: 209.068786.

IR

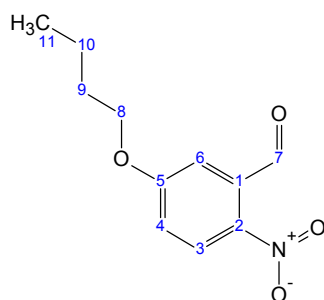
$\bar{\nu}$ /cm⁻¹ (T %): 3106 (96 %), 2969 (85 %), 2939 (87 %), 2881 (88 %), 2660 (97 %), 1695 (49 %), 1579 (38 %), 1512 (33 %), 1484 (65 %), 1471 (67 %), 1425 (72 %),

1385 (60 %), 1327 (25 %), 1284 (24 %), 1231 (22 %), 1162 (59 %), 1071 (46 %), 1042 (77 %), 1013 (71 %), 997 (72 %), 932 (69 %), 916 (71 %), 887 (72 %), 870 (73 %), 846 (39 %), 789 (74 %), 744 (49 %), 674 (65 %).

5.2.3.3 5-Butoxy-2-nitrobenzaldehyde (12-C₄H₉)

5-Hydroxy-2-nitrobenzaldehyde (1.00 g, 5.99 mmol), K₂CO₃ (1.00 g, 7.25 mmol) and C₄H₉I (0.80 mL, 7.25 mmol) in DMF (15 mL) were stirred at room temperature for 48 h, 0.94 g 12-C₄H₉ (70 %) was obtained after purification by using MPLC (petroleum ether / ethyl acetate, 3:1).

5-Butoxy-2-nitrobenzaldehyde



¹H NMR (DMSO-d₆, 400 MHz)

δ (ppm) = 10.27 (s, 1H, H-(C-7)), 8.17 (d, ³J_{H,H} = 9.1 Hz, 1H, H-(C-3)), 7.35 (dd, ³J_{H,H} = 9.1 Hz, ⁴J_{H,H} = 3.0 Hz, 1H, H-(C-4)), 7.22 (d, ⁴J_{H,H} = 3.0 Hz, 1H, H-(C-6)), 4.17 (t, ³J_{H,H} = 6.6 Hz, 2H, H-(C-8)), 1.72 (m, 2H, H-(C-9)), 1.43 (m, 2H, H-(C-10)), 0.94 (t, ³J_{H,H} = 7.5 Hz, 3H, H-(C-11)).

¹³C NMR (DMSO-d₆, 100 MHz)

δ (ppm) = 13.6 (C-11), 18.5 (C-10), 30.3 (C-9), 68.7 (C-8), 114.0 (C-6), 118.4 (C-4), 127.3 (C-3), 134.3 (C-1), 141.6 (C-2), 163.0 (C-5), 189.9 (C-7).

MS-EI (70 eV)

m/z: 223 ([M]⁺, C₁₁H₁₃NO₄, 2 %), 167 ([M - C₄H₈]⁺, C₇H₅NO₄, 100 %), 137 ([M - C₄H₈ - NO]⁺, C₇H₅O₃, 33 %), 123 (53 %), 109 (42 %), 92 (8 %), 81 (24 %), 57 (50 %), 41 (70 %).

HRMS (EI)

m/z measured: 223.08570 ([M]⁺, C₁₁H₁₃NO₄).

m/z calculated: 223.084436.

IR

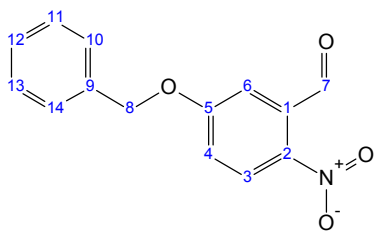
$\bar{\nu}$ /cm⁻¹ (T %): 3106 (96 %), 2960 (81 %), 2936 (84 %), 2874 (85 %), 2662 (97 %), 1695 (52 %), 1579 (42 %), 1513 (36 %), 1485 (68 %), 1467 (69 %), 1425 (74 %), 1385 (62 %), 1327 (24 %), 1282 (24 %), 1242 (35 %), 1233 (31 %), 1162 (62 %),

1124 (88 %), 1071 (49 %), 1022 (72 %), 934 (73 %), 887 (76 %), 873 (74 %), 840 (44 %), 768 (78 %), 746 (50 %), 674 (67 %).

5.2.3.4 5-(Benzyloxy)-2-nitrobenzaldehyde (12-Bn)

A mixture of K_2CO_3 (3.95 g, 28.62 mmol), MeOH (35 mL) and $CHCl_3$ (70 mL) was heated to reflux for 15 min. 5-Hydroxy-2-nitrobenzaldehyde (1.04 g, 6.23 mmol) and BnBr (1.07 g, 6.26 mmol) were added into the reaction solution and it was kept refluxing for 20 h. The reaction mixture was partitioned between diethyl ether (200 mL) and water (200 mL). The diethyl ether layer was separated and washed with saturated $NaHCO_3$ solution (100 mL), water (100 mL) and brine (100 mL). The extracted organic phase was dried over Na_2SO_4 and concentrated to afford a crude product, which was purified by using MPLC (petroleum ether / ethyl acetate, 5:1) to yield 1.12 g **12-Bn** as yellow crystals (70 %).

5-(Benzyloxy)-2-nitrobenzaldehyde



m.p. 77 - 79 °C.

1H NMR (DMSO- d_6 , 400 MHz)

δ (ppm) = 10.28 (s, 1H, H -(C-7)), 8.19 (d, $^3J_{H,H}$ = 8.9 Hz, 1H, H_{arom}), 7.48 (m, 7H, H_{arom}), 5.31 (s, 2H, H -(C-8)).

^{13}C NMR (DMSO- d_6 , 100 MHz)

δ (ppm) = 70.4 (C-8), 114.4 ($H-C_{arom}$), 118.9 ($H-C_{arom}$), 127.2 ($H-C_{arom}$), 127.8 ($H-C_{arom}$), 128.2 ($H-C_{arom}$), 128.5 ($H-C_{arom}$), 134.2 (C-1), 135.7 (C-9), 141.9 (C-2), 162.5 (C-5), 189.8 (C-7).

MS-EI (70 eV)

m/z : 257 ($[M]^+$, $C_{14}H_{11}NO_4$, 26 %), 227 ($[M - NO]^+$, $C_{14}H_{11}O_3$, 36 %), 181 ($[M - C_6H_4]^+$, $C_8H_7NO_4$, 28 %), 163 (14 %), 152 ($[M - C_6H_4 - CHO]^+$, $C_7H_6NO_3$, 90 %), 136 (100 %), 108 (36 %), 91 (99 %), 65 (6 %).

IR

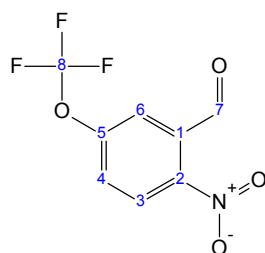
$\bar{\nu}/cm^{-1}$ (T %): 3380 (86 %), 3102 (83 %), 3072 (84 %), 3035 (84 %), 2920 (84 %), 2663 (86 %), 2240 (87 %), 1743 (85 %), 1695 (61 %), 1584 (56 %), 1512 (52 %), 1499 (61 %), 1485 (62 %), 1455 (67 %), 1417 (73 %), 1392 (62 %), 1330 (44 %),

1277 (54 %), 1246 (46 %), 1187 (64 %), 1160 (54 %), 1117 (70 %), 1069 (55 %), 1030 (69 %), 1003 (50 %), 987 (56 %), 961 (65 %), 906 (67 %), 887 (57 %), 842 (42 %), 774 (69 %), 750 (48 %), 734 (37 %), 694 (40 %).

5.2.3.5 2-Nitro-5-(trifluoromethoxy)benzaldehyde (12-CF₃)

3-(Trifluoromethoxy)benzaldehyde (0.50 g, 2.63 mmol) was added portion by portion to a mixture of 100 % HNO₃ (4 mL) and 97 % H₂SO₄ (1 mL) while stirring at 25 °C. Afterward, the reaction solution was kept stirring at 25 °C for 1 h. The resulting mixture was poured into water (100 mL) and extracted with diethyl ether (100 mL). The diethyl ether layer was washed with saturated NaHCO₃ solution (2 × 50 mL) and brine (50 mL). Then the organic phase was separated, dried over Na₂SO₄ and evaporated to give a yellow oil. After purification by using MPLC (petroleum ether / ethyl acetate, 2:1) 0.50 g **12-CF₃** was obtained (81 %).

2-Nitro-5-(trifluoromethoxy)benzaldehyde



¹H NMR (DMSO-d₆, 400 MHz)

δ (ppm) = 10.22 (s, 1H, *H*-(C-7)), 8.32 (d, ³*J*_{H,H} = 8.9 Hz, 1H, *H*-(C-3) or *H*-(C-4)), 7.90 (d, ³*J*_{H,H} = 8.8 Hz, 1H, *H*-(C-3) or *H*-(C-4)), 7.80 (s, 1H, *H*-(C-6)).

¹³C NMR (DMSO-d₆, 100 MHz)

δ (ppm) = 118.4 (C-8), 121.0 (C-8), 121.2 (H-C_{arom}), 125.5 (H-C_{arom}), 127.4 (H-C_{arom}), 133.1 (C-1), 147.2 (C-2), 151.2 (C-5), 188.5 (C-7)

MS-EI (70 eV)

m/z: 235 ([M]⁺, C₈H₄F₃NO₄, 15 %), 205 ([M – NO]⁺, C₈H₄F₃O₃, 100 %), 188 (25 %), 177 ([M – NO – CO]⁺, C₇H₄F₃O₂, 10 %), 160 (40 %), 149 (8 %), 132 (5 %), 110 (21 %), 95 (15 %), 83 (54 %), 69 (40 %), 63 ([C₅H₃]⁺, 46 %), 52 ([C₄H₄]⁺, 8 %), 50 (8 %).

HRMS (EI)

m/z measured: 235.00715 ([M]⁺, C₈H₄F₃NO₄).

m/z calculated: 235.00921.

IR

$\bar{\nu}$ /cm⁻¹ (T %): 3371 (97 %), 3111 (86 %), 3073 (91 %), 2913 (94 %), 2869 (95 %), 2646 (96 %), 2431 (96 %), 2083 (97 %), 1941 (96 %), 1789 (97 %), 1690 (32 %),

1618 (93 %), 1584 (49 %), 1519 (26 %), 1476 (65 %), 1424 (64 %), 1392 (75 %), 1359 (84 %), 1323 (51 %), 1282 (48 %), 1244 (47 %), 1199 (22 %), 1144 (3 %), 1081 (36 %), 1001 (44 %), 986 (33 %), 893 (30 %), 876 (47 %), 846 (22 %), 789 (45 %), 749 (31 %), 707 (41 %), 681 (41 %).

5.2.3.6 2-Methoxy-6-nitrobenzaldehyde (13-NO₂)

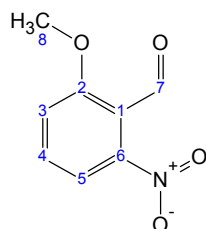
To a stirred solution of hexamethylenetetraamine (3.63 g, 25.92 mmol) in trifluoroacetic acid (35 mL) 3-nitrophenol (3.00 g, 21.58 mmol) was added. The reaction solution was refluxed at 130 °C under argon. After 27 h, TLC analysis showed complete conversion of the starting compound. The reaction solution was cooled down and quenched by adding 6 N HCl (120 mL). After 20 min stirring, the resulting solution was extracted with DCM (2 × 100 mL). The combined organic layer was washed with saturated NaHCO₃ solution (2 × 50 mL), water (50 mL) and brine (50 mL). Then this organic phase was separated and dried over Na₂SO₄. After evaporation of solvent, 1.50 g crude products (2-hydroxy-6-nitrobenzaldehyde and 2-hydroxy-4-nitrobenzaldehyde) were obtained. This crude intermediate compound was directly submitted to the methoxylation. The procedure was the same as described in synthesis of **3-NO₂** (see paragraph 5.2.1.2).

1.45 g Crude intermediate compounds, K₂CO₃ (1.38 g, 10.00 mmol) and MeI (0.62 mL, 9.95 mmol) in DMF (17 mL) were stirred at room temperature for 3 h, two pure products were obtained after purification by using MPLC (petroleum ether / ethyl acetate, 1:1):

0.33 g 2-methoxy-4-nitrobenzaldehyde (9 % based on 3-nitrophenol)

0.59 g 2-methoxy-6-nitrobenzaldehyde (16 % based on 3-nitrophenol)

2-Methoxy-6-nitrobenzaldehyde



m.p. 108 - 109 °C (reported¹³¹ 110 - 111 °C).

¹H NMR (DMSO-d₆, 400 MHz)

δ (ppm) = 10.36 (s, 1H, H-(C-7)), 7.59 (m, 1H, H-(C-4)), 7.42 (d, ³J_{H,H} = 8.1 Hz, 1H, H-(C-3) or H-(C-5)), 7.22 (d, ³J_{H,H} = 8.3 Hz, 1H, H-(C-3) or H-(C-5)), 3.94 (s, 3H, H-(C-8)).

¹³C NMR (DMSO-d₆, 100 MHz)

δ (ppm) = 55.6, 115.4, 116.0, 120.4, 133.5, 148.1, 159.7, 187.6.

HRMS (EI)

m/z measured: 181.03436 ([M]⁺, C₈H₇NO₄).

m/z calculated: 181.037486.

MS-EI (70 eV)

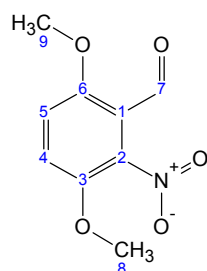
m/z: 181 ([M]⁺, C₈H₇NO₄, 10 %), 163 ([M – H₂O]⁺, C₈H₅NO₃, 10 %), 151 ([M – NO]⁺, C₈H₇O₃, 100 %), 136 (66 %), 133 ([M – H₂O – NO]⁺, C₈H₅O₂, 17 %), 119 (11 %), 108 (41 %), 92 (18 %), 77 ([C₆H₅]⁺, 27 %), 76 (38 %), 63 ([C₅H₃]⁺, 19 %), 50 (6 %), 43 (5 %).

IR

$\bar{\nu}$ /cm⁻¹ (T %): 3092 (86 %), 3034 (87 %), 2954 (86 %), 2879 (82 %), 1959 (88 %), 1706 (42 %), 1609 (67 %), 1527 (34 %), 1468 (50 %), 1437 (59 %), 1388 (73 %), 1353 (42 %), 1309 (62 %), 1269 (37 %), 1208 (57 %), 1190 (58 %), 1162 (51 %), 1048 (38 %), 971 (62 %), 900 (58 %), 833 (50 %), 804 (41 %), 792 (33 %), 733 (30 %).

5.2.3.7 3,6-Dimethoxy-2-nitrobenzaldehyde (16-NO₂)

To a stirred solution of 2,5-dimethoxybenzaldehyde (1.00 g, 6.02 mmol) in AcOH (5 mL) was added 70 % HNO₃ (1-1.5 molar eq. based on 2,5-dimethoxybenzaldehyde) at 0 °C within 5 min and then this reaction solution was kept stirring at room temperature for 1 h. The resulting mixture was poured into water (50 mL) and was extracted with diethyl ether (2 × 50 mL). The combined diethyl ether layer was washed with saturated NaHCO₃ solution (50 mL) and brine (50 mL). Then the organic layer was separated, dried over Na₂SO₄ and concentrated under reduced pressure. 0.53 g **16-NO₂** was obtained as yellow crystals (42 %) after purification by using MPLC (petroleum ether / ethyl acetate, 2:1).

3,6-Dimethoxy-2-nitrobenzaldehyde

m.p. 172 °C (reported¹³² 171 - 172 °C).

¹H NMR (DMSO-d₆, 400 MHz)

δ (ppm) = 10.24 (s, 1H, *H*-(C-7)), 7.67 (d, ³*J*_{H,H} = 9.3 Hz, 1H, *H*-(C-4) or *H*-(C-5)), 7.45 (d, ³*J*_{H,H} = 9.3 Hz, 1H, *H*-(C-4) or *H*-(C-5)), 3.94 (s, 3H, *H*-(C-8) or *H*-(C-9)), 3.85 (s, 3H, *H*-(C-8) or *H*-(C-9)).

¹³C NMR (DMSO-d₆, 100 MHz)

δ (ppm) = 57.2, 57.3, 114.9, 116.0, 121.7, 137.1, 143.7, 155.1, 186.7.

MS-EI (70 eV)

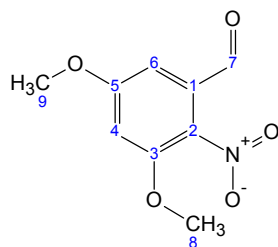
m/z: 211 ([M]⁺, C₉H₉NO₅, 18 %), 194 ([M – OH]⁺, C₉H₈NO₄, 3 %), 176 (5 %), 166 ([M – OH – CO]⁺, C₈H₈NO₃, 100 %), 165 (40 %), 149 (22 %), 136 (41 %), 135 (46 %), 119 (38 %), 107 (23 %), 106 (14 %), 93 (13 %), 77 ([C₆H₅]⁺, 22 %), 65 (25 %), 51 ([C₄H₃]⁺, 12 %), 50 (7 %).

IR

$\bar{\nu}$ /cm⁻¹ (T %): 3099 (92 %), 2946 (92 %), 2898 (90 %), 2844 (92 %), 1893 (96 %), 1691 (67 %), 1611 (81 %), 1577 (84 %), 1535 (57 %), 1488 (61 %), 1450 (66 %), 1443 (70 %), 1432 (66 %), 1399 (83 %), 1368 (74 %), 1269 (46 %), 1186 (59 %), 1087 (64 %), 1049 (62 %), 948 (60 %), 921 (74 %), 824 (58 %), 803 (65 %), 715 (55 %).

5.2.3.8 3,5-Dimethoxy-2-nitrobenzaldehyde (17-NO₂)

3,5-Dimethoxybenzaldehyde (2.00 g, 12.05 mmol) was added to 90 % HNO₃ (10 mL) in several portion while stirring at 0 °C. After this addition, the reaction solution was kept stirring at 0 °C and monitored by TLC. When the starting compound was completely converted, the resulting mixture was poured into water (100 mL) and extracted with diethyl ether (100 mL). The organic layer was washed with saturated NaHCO₃ solution (2 × 50 mL) and brine (50 mL), dried over Na₂SO₄ and concentrated. 0.41 g **17-NO₂** (17 %) was obtained as yellow crystals after separation on the MPLC (petroleum ether / ethyl acetate, 1:1).

3,5-Dimethoxy-2-nitrobenzaldehyde

m.p. 104 - 106 °C (reported¹³³ 104 - 106 °C).

¹H NMR (DMSO-d₆, 400 MHz)

δ (ppm) = 9.92 (s, 1H, H-(C-7)), 6.94 (d, ⁴J_{H,H} = 2.5 Hz, 1H, H-(C-4) or H-(C-6)), 6.75 (d, ⁴J_{H,H} = 2.8 Hz, 1H, H-(C-4) or H-(C-6)), 3.92 (s, 3H, H-(C-8) or H-(C-9)), 3.90 (s, 3H, H-(C-8) or H-(C-9)).

¹³C NMR (DMSO-d₆, 100 MHz)

δ (ppm) = 56.1, 56.8, 104.0, 104.9, 130.6, 133.4, 153.2, 162.1, 186.7.

MS-EI (70 eV)

m/z: 211 ([M]⁺, C₉H₉NO₅, 48 %), 194 ([M – OH]⁺, C₉H₈NO₄, 10 %), 179 (16 %), 164 (97 %), 151 (100 %), 136 (81 %), 123 (43 %), 95 (77 %), 77 ([C₆H₅]⁺, 53 %), 69 (35 %), 51 ([C₄H₃]⁺, 22 %).

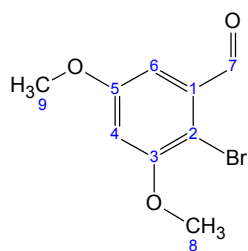
IR

$\bar{\nu}$ /cm⁻¹ (T %): 3094 (91 %), 2989 (89 %), 2953 (86 %), 2847 (83 %), 2746 (92 %), 2652 (93 %), 2060 (95 %), 1700 (24 %), 1590 (36 %), 1529 (24 %), 1492 (62 %), 1458 (32 %), 1430 (53 %), 1386 (58 %), 1369 (46 %), 1334 (22 %), 1311 (20 %), 1231 (44 %), 1198 (23 %), 1185 (41 %), 1166 (27 %), 1118 (45 %), 1112 (45 %), 1031 (50 %), 956 (22 %), 942 (42 %), 931 (43 %), 852 (52 %), 840 (18 %), 831 (19 %), 775 (54 %), 735 (71 %), 695 (55 %).

5.2.3.9 2-Bromo-3,5-dimethoxybenzaldehyde (17-Br)

2-Bromo-3,5-dimethoxybenzaldehyde was synthesized according to the procedure described in the bromination of 3-methoxybenzaldehyde (see paragraph 5.2.1.4).

To a stirred solution of 3,5-dimethoxybenzaldehyde (1.50 g, 9.04 mmol) in dry CHCl₃ (10 mL/mmol) the bromine (0.60 mL, 11.66 mmol) was introduced slowly over 20 min. Then the reaction solution was stirred at room temperature for 0.5 h. After workup and purification by using MPLC (petroleum ether / ethyl acetate, 5:1), 1.86 g **17-Br** was obtained (84 %).

2-Bromo-3,5-dimethoxybenzaldehyde

m.p. 114 - 115 °C (reported¹³⁴ 115 - 116 °C).

¹H NMR (CDCl₃, 250 MHz)

δ (ppm) = 10.24 (s, 1H, *H*-(C-7)), 6.97 (d, ⁴*J*_{H,H} = 2.8 Hz, 1H, *H*-(C-4) or *H*-(C-6)), 6.93 (d, ⁴*J*_{H,H} = 2.7 Hz, 1H, *H*-(C-4) or *H*-(C-6)), 3.89 (s, 3H, *H*-(C-8) or *H*-(C-9)), 3.82 (s, 3H, *H*-(C-8) or *H*-(C-9)).

¹³C NMR (CDCl₃, 60 MHz)

δ (ppm) = 55.8, 56.8, 104.4, 105.7, 107.0, 134.3, 156.9, 159.7, 191.7.

MS-EI (70 eV)

m/z: 246 ([M]⁺, C₉H₉⁸¹BrO₃, 97 %), 245 ([M - H]⁺, C₉H₈⁸¹BrO₃, 46 %), 244 ([M]⁺, C₉H₉⁷⁹BrO₃, 100 %), 243 ([M - H]⁺, C₉H₈⁷⁹BrO₃, 38 %), 217 ([M - CHO]⁺, C₈H₈⁸¹BrO₂, 2 %), 215 ([M - CHO]⁺, C₈H₈⁷⁹BrO₂, 6 %), 202 (15 %), 200 (15 %), 173 (8 %), 157 (3 %), 135 ([M - CHO - H⁸¹Br]⁺, C₈H₇O₂, 5 %), 122 (3 %), 134 (2 %), 106 (18 %), 79 (4 %), 77 ([C₆H₅]⁺, 8 %), 63 ([C₅H₃]⁺, 8 %), 51 (2 %).

IR

$\bar{\nu}$ /cm⁻¹ (T %): 3329 (91 %), 3077 (87 %), 3024 (88 %), 2975 (86 %), 2943 (85 %), 2895 (86 %), 2837 (87 %), 2625 (89 %), 2299 (91 %), 1980 (91 %), 1673 (50 %), 1584 (54 %), 1448 (54 %), 1431 (73 %), 1391 (59 %), 1333 (56 %), 1290 (47 %), 1224 (57 %), 1199 (54 %), 1159 (50 %), 1076 (56 %), 1067 (61 %), 1021 (49 %), 970 (64 %), 918 (57 %), 860 (62 %), 848 (63 %), 832 (55 %), 718 (63 %), 693 (77 %).

5.2.3.10 3,4-Dimethoxy-2-nitrobenzaldehyde (18-NO₂)

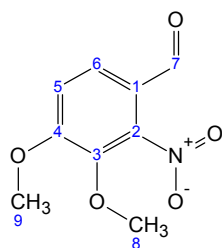
Into the stirred solution of 4-formyl-2-methoxy-3-nitrophenyl benzenesulfonate (2.80 g, 8.31 mmol) in ethanol (70 mL) 2 mL of NaOH aqueous solution (1 g/mL) was added. This solution was refluxed for 0.5 h. After the ethanol was evaporated, 100 mL water was added to the residue and the pH value was adjusted to 6 by adding 2 N HCl. The resulting mixture was extracted with diethyl ether (200 mL) and the separated organic layer was washed with saturated aqueous NaHCO₃ solution (50 mL), water (50 mL) and brine (50 mL) respectively, then dried over Na₂SO₄ and concentrated to afford 0.86 g 4-hydroxy-3-methoxy-2-nitrobenzaldehyde, which was used directly in further synthetic procedure.

The methoxylation of 4-hydroxy-3-methoxy-2-nitrobenzaldehyde was similar to the procedure described in the preparation of **3-NO₂** (see paragraph 5.2.1.2).

0.86 g 4-Hydroxy-3-methoxy-2-nitrobenzaldehyde, K₂CO₃ (0.72 g, 5.22 mmol) and MeI (0.32 mL, 5.14 mmol) were stirred in DMF (15 mL) at room temperature for 2 h. After workup and purification by using MPLC (petroleum ether / ethyl acetate, 1:1),

0.81 g **18-NO₂** was obtained (46 % based on 4-formyl-2-methoxy-3-nitrophenyl benzenesulfonate).

3,4-Dimethoxy-2-nitrobenzaldehyde



m.p. 60 - 62 °C (reported¹³⁵ 58 - 61 °C).

¹H NMR (DMSO-d₆, 400 MHz)

δ (ppm) = 9.79 (s, 1H, *H*-(C-7)), 7.90 (d, ³*J*_{H,H} = 8.6 Hz, 1H, *H*-(C-5) or *H*-(C-6)), 7.51 (d, ³*J*_{H,H} = 8.6 Hz, 1H, *H*-(C-5) or *H*-(C-6)), 4.01 (s, 3H, *H*-(C-8) or *H*-(C-9)), 3.83 (s, 3H, *H*-(C-8) or *H*-(C-9)).

¹³C NMR (DMSO-d₆, 100 MHz)

δ (ppm) = 57.2, 62.0, 114.2, 119.5, 131.3, 140.2, 142.3, 158.1, 188.3.

MS-EI (70 eV)

m/z: 211 ([M]⁺, C₉H₉NO₅, 18 %), 194 ([M - OH]⁺, C₉H₈NO₄, 2 %), 176 (2 %), 166 ([M - OH - CO]⁺, C₈H₈NO₃, 100 %), 165 (43 %), 151 (21 %), 136 (32 %), 135 (38 %), 119 (36 %), 107 (23 %), 93 (14 %), 77 ([C₆H₅]⁺, 34 %), 65 (42 %), 51 ([C₄H₃]⁺, 16 %), 50 (10 %).

IR

$\bar{\nu}$ /cm⁻¹ (T %): 3363 (95 %), 3088 (93 %), 2997 (90 %), 2940 (85 %), 2857 (86 %), 2604 (93 %), 2030 (95 %), 1908 (95 %), 1688 (34 %), 1596 (41 %), 1536 (44 %), 1501 (33 %), 1454 (36 %), 1435 (63 %), 1422 (53 %), 1398 (65 %), 1373 (50 %), 1321 (81 %), 1279 (24 %), 1248 (34 %), 1211 (43 %), 1189 (60 %), 1171 (61 %), 1071 (41 %), 1045 (36 %), 1007 (72 %), 960 (31 %), 901 (45 %), 829 (40 %), 802 (51 %), 780 (64 %), 743 (46 %), 698 (78 %), 663 (72 %).

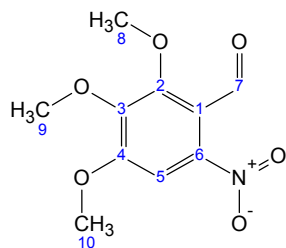
5.2.3.11 2,3,4-Trimethoxy-6-nitrobenzaldehyde (19-NO₂)

The compound 2,3,4-trimethoxybenzaldehyde was nitrated according to the procedure described in the nitration of 2,5-dimethoxybenzaldehyde (see paragraph 5.2.3.7).

2,3,4-Trimethoxybenzaldehyde (2.00 g, 10.20 mmol) and 10 mL mixture of 100 % HNO₃ and 100 % AcOH (50:50) were stirred at 0 °C for 10 min. After workup and

purification by using MPLC (petroleum ether / ethyl acetate, 3:1), 1.62 g **19-NO₂** was obtained as yellow crystals (66 %).

2,3,4,-Trimethoxy-6-nitrobenzaldehyde



m.p. 85 - 86 °C (reported¹³⁶ 80 - 82 °C).

¹H NMR (DMSO-d₆, 400 MHz)

δ (ppm) = 10.12 (s, 1H, H-(C-7)), 7.51 (s, 1H, H-(C-5)), 3.94 (s, 3H, -OCH₃), 3.93 (s, 3H, -OCH₃), 3.86 (s, 3H, -OCH₃).

¹³C NMR (DMSO-d₆, 100 MHz)

δ (ppm) = 57.4, 60.9, 62.7, 104.2, 117.3, 143.8, 144.7, 153.8, 156.7, 187.4.

MS-EI (70 eV)

m/z: 241 ([M]⁺, C₁₀H₁₁NO₆, 34 %), 224 ([M - OH]⁺, C₁₀H₁₀NO₅, 8 %), 211 ([M - NO]⁺, C₁₀H₁₁O₅, 100 %), 196 (99 %), 181 (43 %), 168 (65 %), 153 (56 %), 137 (18 %), 125 (16 %), 123 (14 %), 109 (10 %), 93 (16 %), 77 ([C₆H₅]⁺, 17 %), 66 (13 %), 53 (11 %).

IR

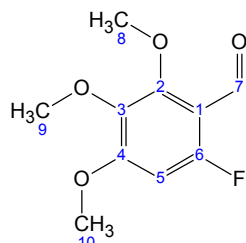
$\bar{\nu}$ /cm⁻¹ (T %): 3081 (85 %), 3018 (88 %), 3000 (88 %), 2946 (78 %), 2866 (84 %), 2752 (89 %), 2642 (90 %), 1946 (93 %), 1704 (51 %), 1607 (79 %), 1560 (84 %), 1521 (55 %), 1485 (51 %), 1454 (59 %), 1429 (76 %), 1389 (61 %), 1323 (51 %), 1301 (41 %), 1253 (49 %), 1207 (57 %), 1196 (59 %), 1119 (33 %), 1048 (52 %), 1030 (54 %), 977 (66 %), 962 (50 %), 918 (50 %), 885 (41 %), 800 (67 %), 766 (45 %), 759 (47 %), 731 (58 %), 675 (62 %).

5.2.3.12 6-Fluoro-2,3,4-trimethoxybenzaldehyde (19-F)

A mixture of KF (0.24 g, 4.14 mmol, spray dried) and Kryptofix 222 (1.16 g, 6.32 mmol) was heated at 140 °C under argon for 20 min, then **19-NO₂** (0.50 g, 2.07 mmol) in DMF (20 mL) was added and the reaction solution was heated for another 15 min. The reaction solution was poured into water (25 mL) and this mixture was extracted with diethyl ether (2 × 25 mL). The combined organic layer was washed with 25 mL of 1 N NaOH (This basic washing solution was kept for isolation of phenolic by-product), water (25 mL) and brine (25 mL), then was dried over Na₂SO₄ and concentrated to afford 0.22 g crude product. After purification by using

MPLC (POLYGOPREP 60-50, C18, CH₃CN / water, 3:7) 0.025 g product was obtained. This product was purified again on preparative HPLC (Luna, phenyl-hexyl 5 μm, 150 mm × 10 mm, Phenomenex, USA; CH₃CN / water, 3:1; 5 mL/min) to give 0.012 g pure **19-F** (1.3 %).

6-Fluoro-2,3,4-trimethoxybenzaldehyde



¹H NMR (CDCl₃, 400 MHz)

δ = 10.21 (s, 1H, H-(C-7)), 6.45 (d, ³J_{H,F} = 8.4 Hz, 1H, H-(C-5)), 3.99 (s, 3H, -OCH₃), 3.90 (s, 3H, -OCH₃), 3.82 (s, 3H, -OCH₃).

¹³C NMR (CDCl₃, 100 MHz)

δ = 56.3 (-OCH₃), 61.1 (-OCH₃), 62.2 (-OCH₃), 96.1 (d, ²J_{C,F} = 26.3 Hz, C-5), 112.0 (d, ²J_{C,F} = 8.8 Hz, C-1), 138.4 (d, ⁴J_{C,F} = 3.7 Hz, C-3), 156.0 (d, ³J_{C,F} = 7.3 Hz, C-2 or C-4), 159.3 (d, ³J_{C,F} = 13.9 Hz, C-2 or C-4), 159.9 (d, ¹J_{C,F} = 259.8 Hz, C-6), 186.3 (d, ³J_{C,F} = 3.7 Hz, C-7).

¹⁹F NMR (CDCl₃, 400 MHz)

117.1 (F-(C-6)).

MS-EI (70 eV)

m/z: 214 ([M]⁺, C₁₀H₁₁FO₄, 100 %), 199 ([M - CH₃]⁺, C₉H₈FO₄, 79 %), 181 ([M - CH₃ - H₂O]⁺, C₉H₆FO₃, 66 %), 171 ([M - CH₃ - CO]⁺, C₈H₈FO₃, 16 %), 153 (30 %), 138 (18 %), 113 (8 %), 97 (8 %), 83 (9 %), 57 (10 %).

HRMS (EI)

m/z measured: 214.06256 ([M]⁺, C₁₀H₁₁FO₄).

m/z calculated: 214.064116.

IR

$\bar{\nu}$ /cm⁻¹ (T %): 2942 (95 %), 1691 (82 %), 1604 (76 %), 1574 (91 %), 1492 (88 %), 1457 (88 %), 1404 (92 %), 1386 (87 %), 1342 (83 %), 1251 (84 %), 1198 (87 %), 1134 (80 %), 1096 (85 %), 1028 (91 %), 989 (88 %), 925 (95 %), 820 (94 %), 800 (92 %).

Phenolic by-product

The basic washing solution was acidified by adding 2 N HCl (50 mL) and extracted with diethyl ether (2 × 50 mL). The ether layer was washed with water (50 mL) and brine (50 mL), dried over Na₂SO₄, and concentrated to afford 0.080 g phenolic by-product. The position of the phenolic hydroxyl substituent was not determined.

¹H NMR (DMSO-d₆, 400 MHz)

δ = 10.13 (s, 1H, -CHO), 7.23 (s, 1H, H_{arom}), 3.92 (s, 3H, -OCH₃), 3.77 (s, 3H, -OCH₃).

¹³C NMR (DMSO-d₆, 100 MHz)

δ = 56.9 (-OCH₃), 60.6 (-OCH₃), 100.9 (C_{arom}-H), 109.9 (C_{arom}-CHO), 138.9 (C_{arom}-NO₂), 145.5 (C_{arom}-OCH₃ or C_{arom}-OH), 154.1 (C_{arom}-OH or C_{arom}-OCH₃), 156.6 (C_{arom}-OCH₃ or C_{arom}-OH), 188.2 (-CHO).

IR

$\bar{\nu}$ /cm⁻¹ (T %): 3095 (84 %), 2948 (75 %), 2850 (81 %), 2324 (91 %), 1632 (45 %), 1508 (35 %), 1460 (54 %), 1445 (49 %), 1416 (56 %), 1389 (35 %), 1317 (38 %), 1283 (33 %), 1250 (21 %), 1203 (29 %), 1139 (18 %), 1035 (42 %), 982 (42 %), 961 (29 %), 896 (32 %), 856 (41 %), 775 (23 %), 728 (32 %), 686 (40 %).

5.2.3.13 6-Bromo-2,3,4-trimethoxybenzaldehyde (19-Br)

5-Bromo-2,3-dimethoxyphenol was synthesized from 5-bromo-2,3-dimethoxybenzaldehyde by baeyer villiger reaction.¹³⁷ A mixture of 30 % H₂O₂ (4 mL) and formic acid (11 mL) with catalytic amount of concentrated H₂SO₄ was stirred at room temperature for 1 h. A solution of 5-bromo-2,3-dimethoxybenzaldehyde (4.05 g, 16.40 mmol) in formic acid (25 mL) was added dropwise in above solution at 0 °C, then the mixture was kept stirring overnight. When TLC analysis indicated complete conversion of the starting compound, the reaction was quenched with water (50 mL) and extracted by diethyl ether (200 mL). The diethyl ether layer was washed by saturated NaHCO₃ (100 mL), and brine (50 mL). The organic phase was separated, dried over Na₂SO₄, and concentrated to afford 5.50 g 5-bromo-2,3-dimethoxyphenol crude product as red oil which was used directly in the next synthesis step.

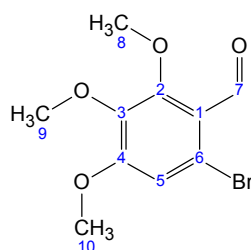
5-Bromo-2,3-dimethoxyphenol was formylated according to the procedure described in formylation of 3-nitrophenol (see paragraph 5.2.3.6).

4.00 g Crude 5-bromo-2,3-dimethoxyphenol and hexamethylenetetramine (2.30 g, 17.22 mmol) were refluxed at 130 °C in trifluoroacetic acid (40 mL) for 4 h. After workup, crude product 6-bromo-2-hydroxy-3,4-dimethoxybenzaldehyde (1.55 g) was

obtained and submitted directly to the methoxylation. The procedure was the same as described in the synthesis of **3-NO₂** (see paragraph 5.2.1.2).

1.55 g Crude 6-bromo-2-hydroxy-3,4-dimethoxybenzaldehyde, K₂CO₃ (0.80 g, 5.80 mmol) and MeI (0.36 mL, 5.78 mmol) were stirred in DMF (20 mL) at room temperature for 3 h. After workup and purification by using MPLC (petroleum ether / ethyl acetate, 2:1), 0.41 g **19-Br** was obtained (13 % based on 5-bromo-2,3-dimethoxybenzaldehyde).

6-Bromo-2,3,4-trimethoxybenzaldehyde



¹H NMR (DMSO-d₆, 400 MHz)

δ (ppm) = 10.09 (s, 1H, H-(C-7)), 7.19 (s, 1H, H-(C-5)), 3.90 (s, 3H, -OCH₃), 3.86 (s, 3H, -OCH₃), 3.76 (s, 3H, -OCH₃).

¹³C NMR (DMSO-d₆, 100 MHz)

δ (ppm) = 56.7, 60.6, 62.4, 113.9, 117.6, 120.9, 141.4, 156.5, 157.8, 188.8.

MS-EI (70 eV)

m/z: 276 ([M]⁺, C₁₀H₁₁⁸¹BrO₄, 93 %), 275 ([M - H]⁺, C₁₀H₁₀⁸¹BrO₄, 32 %), 274 ([M]⁺, C₁₀H₁₁⁷⁹BrO₄, 100 %), 273 ([M - H]⁺, C₁₀H₁₀⁷⁹BrO₄, 18 %), 261 ([M - CH₃]⁺, C₉H₈⁸¹BrO₄, 57 %), 260 (12 %), 259 ([M - CH₃]⁺, C₉H₈⁷⁹BrO₄, 82 %), 258 (37 %), 246 (13 %), 245 (20 %), 244 (17 %), 243 (61 %), 231 (21 %), 230 (36 %), 229 (18 %), 238 (38 %), 215 (38 %), 198 (28 %), 178 (34 %), 165 (8 %), 137 (10 %), 124 (12 %), 109 (23 %), 93 (18 %), 77 ([C₆H₅]⁺, 15 %), 55 (10 %), 43 (24 %).

IR

$\bar{\nu}$ /cm⁻¹ (T %): 2940 (84 %), 2851 (89 %), 2768 (96 %), 2586 (97 %), 1689 (42 %), 1574 (31 %), 1483 (46 %), 1447 (56 %), 1430 (62 %), 1370 (36 %), 1296 (31 %), 1244 (35 %), 1194 (58 %), 1110 (17 %), 1033 (62 %), 1009 (43 %), 961 (58 %), 947 (44 %), 906 (60 %), 818 (59 %), 787 (57 %), 764 (59 %), 717 (72 %).

5.2.3.14 2,3,4,5-Tetramethoxy-6-nitrobenzaldehyde (20-NO₂)

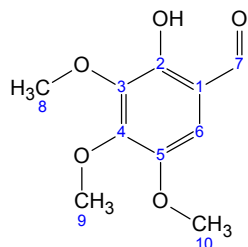
2-Hydroxy-3,4,5-trimethoxybenzaldehyde

2-Hydroxy-3,4,5-trimethoxybenzaldehyde was synthesized by baeyer villiger reaction, the experiment was performed by the synthetic procedure described in

paragraph **5.2.3.13**. 30 % H₂O₂ (15 mL) was added to a stirred solution of 2,3,4-trimethoxybenzaldehyde (7.50 g, 38.26 mmol) in methanol (75 mL) with a catalytic amount of concentrated H₂SO₄ (0.2 mL). The reaction was carried out at room temperature for 2 h. After workup and purification by using MPLC (petroleum ether / ethyl acetate, 2:1) to afford 4.44 g 2,3,4-trimethoxyphenol and used directly in the next synthesis step.

3.40 g 2,3,4-Trimethoxyphenol and Hexamethylentetramine (3.15 g, 22.52 mmol) were refluxed at 130 °C in TFA (20 mL) for 24 h. After extraction with DCM, the crude product was purified by using MPLC (petroleum ether / ethyl acetate, 2:1) to give 2.00 g 2-hydroxy-3,4,5-trimethoxybenzaldehyde as colourless oil (51 % based on 2,3,4-trimethoxyphenol).

2-Hydroxy-3,4,5-trimethoxybenzaldehyde



¹H NMR (DMSO-d₆, 400 MHz)

δ (ppm) = 10.12 (s, 1H, *H*-(C-7)), 7.01 (s, 1H, *H*-(C-6)), 3.87 (s, 3H, -OCH₃), 3.77 (s, 3H, -OCH₃), 3.76 (s, 3H, -OCH₃).

¹³C NMR (DMSO-d₆, 100 MHz)

δ (ppm) = 55.9, 60.7, 60.9, 105.6, 117.1, 141.4, 146.0, 149.0, 150.0, 190.6.

MS-EI (70 eV)

m/z: 212 ([M]⁺, C₁₀H₁₂O₅, 100 %), 197 ([M - CH₃]⁺, C₉H₉O₅, 28 %), 182 ([M - CH₂O]⁺, C₉H₇O₄, 6 %), 169 ([M - CH₃ - CO]⁺, C₈H₄O₄, 23 %), 151 (22 %), 126 (9 %), 111 (10 %), 97 (13 %), 83 (18 %), 69 (35 %), 55 (38 %), 44 (37 %).

IR

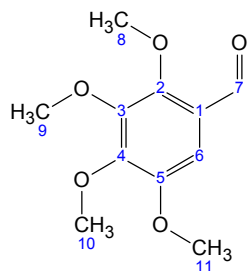
$\bar{\nu}$ /cm⁻¹ (T %): 2947 (73 %), 2841 (82 %), 1639 (43 %), 1585 (72 %), 1488 (48 %), 1453 (41 %), 1431 (41 %), 1393 (39 %), 1319 (23 %), 1272 (23 %), 1217 (62 %), 1198 (49 %), 1189 (52 %), 1139 (20 %), 1096 (25 %), 1031 (28 %), 987 (24 %), 935 (30 %), 896 (31 %), 843 (44 %), 781 (28 %), 732 (28 %).

2,3,4,5-Tetramethoxybenzaldehyde

The synthetic procedure was the same as described in the synthesis of **3-NO₂** (see paragraph **5.2.1.2**).

A mixture of 2-hydroxy-3,4,5-trimethoxybenzaldehyde (1.70 g, 8.02 mmol), K_2CO_3 (1.24 g, 8.99 mmol) and MeI (0.56 mL, 8.99 mmol) was stirred in DMF (30 mL) at room temperature overnight. After extraction with diethyl ether and purification by using MPLC (petroleum ether / ethyl acetate, 2:1), 1.45 g 2,3,4,5-tetramethoxybenzaldehyde was obtained (80 % based on 2-hydroxy-3,4,5-trimethoxybenzaldehyde).

2,3,4,5-Tetramethoxybenzaldehyde



1H NMR (DMSO- d_6 , 400 MHz)

δ (ppm) = 10.17 (s, 1H, H -(C-7)), 7.02 (s, 1H, H -(C-6)), 3.88 (s, 3H, $-OCH_3$), 3.86 (s, 3H, $-OCH_3$), 3.85 (s, 3H, $-OCH_3$), 3.80 (s, 3H, $-OCH_3$).

^{13}C NMR (DMSO- d_6 , 100 MHz)

δ (ppm) = 55.9, 60.8, 61.1, 62.8, 103.7, 123.7, 146.5, 148.8, 149.6, 151.5, 188.4.

MS-EI (70 eV)

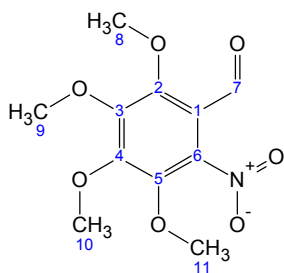
m/z : 226 ($[M]^+$, $C_{11}H_{14}O_5$, 100 %), 211 ($[M - CH_3]^+$, $C_{10}H_8O_5$, 49 %), 193 (23 %), 178 (12 %), 165 (16 %), 140 (10 %), 125 (8 %), 110 (2 %), 97 (6 %), 93 (3 %), 69 (4 %), 53 (4 %).

IR

$\bar{\nu}/cm^{-1}$ (T %): 2940 (83 %), 2844 (89 %), 1679 (45 %), 1591 (65 %), 1481 (57 %), 1467 (41 %), 1412 (41 %), 1385 (45 %), 1338 (35 %), 1280 (61 %), 1252 (68 %), 1213 (62 %), 1197 (51 %), 1127 (28 %), 1076 (22 %), 1034 (46 %), 999 (39 %), 981 (54 %), 924 (59 %), 881 (76 %), 852 (64 %), 787 (83 %), 757 (62 %), 705 (82 %), 686 (82 %).

2,3,4,5-Tetramethoxy-6-nitrobenzaldehyde

2,3,4,5-Tetramethoxybenzaldehyde (0.50 g, 2.21 mmol) and 70 % HNO_3 (0.16 mL, 2.75 mmol) were stirred in acetic acid (5 mL, concentrated) at 0 °C for 10 min, then the ice bath was removed and the reaction solution was stirred for another 1 h at room temperature. After extraction with diethyl ether and purification by using MPLC (petroleum ether / ethyl acetate, 3:1), 0.23 g **20-NO₂** was obtained as yellow crystals (39 % based on 2,3,4,5-tetramethoxybenzaldehyde).

2,3,4,5-Tetramethoxy-6-nitrobenzaldehyde

m.p. 67 - 70 °C.

¹H NMR (DMSO-d₆, 400 MHz)

δ (ppm) = 10.09 (s, 1H, *H*-(C-7)), 4.03 (s, 3H, -OCH₃), 3.98 (s, 3H, -OCH₃), 3.92 (s, 3H, -OCH₃), 3.81 (s, 3H, -OCH₃).

¹³C NMR (DMSO-d₆, 100 MHz)

δ (ppm) = 61.4 (-OCH₃), 61.5 (-OCH₃), 62.6 (-OCH₃), 63.0 (-OCH₃), 115.0 (C-1), 137.8 (C-6), 140.9 (CH₃O-C_{arom}), 148.0 (CH₃O-C_{arom}), 152.7 (CH₃O-C_{arom}), 153.1 (CH₃O-C_{arom}), 186.2 (C-7).

HRMS (EI)

m/z measured: 271.07104 ([M]⁺, C₁₁H₁₃NO₇).

m/z calculated: 271.069167.

MS-EI (70 eV)

m/z: 271 ([M]⁺, C₁₁H₁₃NO₇, 31 %), 254 ([M - OH]⁺, C₁₁H₁₂NO₆, 100 %), 224 (30 %), 211 (82 %), 195 (42 %), 181 (46 %), 167 (27 %), 152 (33 %), 137 (35 %), 127 (19 %), 125 (16 %), 95 (10 %), 93 (8 %), 65 ([C₅H₅]⁺, 5 %), 53 (10 %).

IR

$\bar{\nu}$ /cm⁻¹ (T %): 2998 (87 %), 2952 (77 %), 2876 (80 %), 1692 (26 %), 1591 (60 %), 1537 (39 %), 1465 (28 %), 1444 (48 %), 1404 (32 %), 1383 (29 %), 1364 (29 %), 1336 (17 %), 1267 (44 %), 1194 (44 %), 1125 (34 %), 1082 (22 %), 1054 (21 %), 1011 (17 %), 963 (25 %), 943 (30 %), 901 (47 %), 878 (44 %), 823 (50 %), 787 (54 %), 745 (35 %), 684 (59 %).

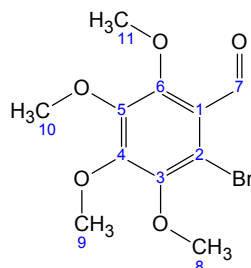
5.2.3.15 2-Bromo-3,4,5,6-tetramethoxybenzaldehyde (20-Br)

20-Br was synthesized by bromination of 2,3,4,5-tetramethoxybenzaldehyde.

Into the solution of 2,3,4,5-tetramethoxybenzaldehyde (0.89 g, 3.94 mmol) in trifluoroacetic acid (5 mL) N-bromosuccinimide (0.84 g, 4.72 mmol) was added over 15 min at 0 °C. The reaction was monitored by TLC. After 0.5 h the starting compound was completely consumed, the reaction was stopped. The resulting

mixture was poured into water and extracted with diethyl ether (100 mL). The organic layer was washed with water (100 mL) and dried over Na₂SO₄. After evaporation of solvent, the residue was purified by using MPLC (petroleum ether / ethyl acetate, 5:1) to yield 0.91 g **20-Br** as yellow oil (75 %).

2-Bromo-3,4,5,6-tetramethoxybenzaldehyde



¹H NMR (DMSO-d₆, 400 MHz)

δ (ppm) = 10.13 (s, 1H, *H*-(C-7)), 3.96 (s, 3H, -OCH₃), 3.85 (s, 3H, -OCH₃), 3.84 (s, 3H, -OCH₃), 3.75 (s, 3H, -OCH₃).

¹³C NMR (DMSO-d₆, 100 MHz)

δ (ppm) = 60.8, 61.1, 61.3, 62.5, 111.7, 123.6, 146.2, 147.1, 151.8, 152.8, 189.5.

MS-EI (70 eV)

m/z: 306 ([M]⁺, C₁₁H₁₃⁸¹BrO₅, 95 %), 305 ([M - H]⁺, C₁₁H₁₂⁸¹BrO₅, 18 %), 304 ([M]⁺, C₁₁H₁₃⁷⁹BrO₅, 100 %), 303 ([M - H]⁺, C₁₁H₁₂⁷⁹BrO₅, 4 %), 291 ([M - CH₃]⁺, C₁₀H₁₀⁸¹BrO₅, 80 %), 290 (12 %), 289 ([M - CH₃]⁺, C₁₀H₁₀⁷⁹BrO₅, 91 %), 288 (18 %), 276 (10 %), 275 (14 %), 274 (16 %), 273 (48 %), 261 (17 %), 260 (14 %), 259 (10 %), 258 (26 %), 246 (23 %), 245 (24 %), 244 (7 %), 243 (22 %), 231 (20 %), 210 ([M - CH₃ - H⁸¹Br]⁺, C₁₀H₉O₅, 10 %), 203 (15 %), 195 (29 %), 167 (17 %), 139 (21 %), 93 (6 %), 83 (14 %), 59 (20 %), 43 (41 %).

IR

$\bar{\nu}$ /cm⁻¹ (T %): 2939 (81 %), 2860 (89 %), 1696 (41 %), 1563 (71 %), 1458 (44 %), 1404 (48 %), 1380 (20 %), 1319 (32 %), 1251 (76 %), 1195 (61 %), 1119 (44 %), 1076 (33 %), 1032 (39 %), 1001 (29 %), 962 (40 %), 938 (43 %), 891 (77 %), 797 (65 %), 765 (71 %).

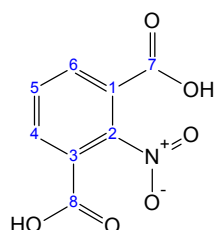
5.2.3.16 2-Nitroisophthalaldehyde (21-NO₂)

2-Nitroisophthalic acid

2-Nitro-1,3-xylene (15.00 g, 99.33 mmol) was added to the solution of KMnO₄ (63.00 g, 39.87 mmol) and KOH (13.20 g, 235.71 mmol) in water (400 mL), and the mixture was refluxed with vigorous stirring for 21 h. Afterward, manganese dioxide in

reaction suspension was filtered off and the filtrate was carefully neutralized with 3 N HCl. This solution was extracted with DCM to remove any monobasic acids, and the water layer was acidified to pH = 2 to precipitate 2-nitroisophthalic acid. After washing with diethyl ether and drying, 12.90 g 2-Nitroisophthalic acid was obtained (63 %).

2-Nitroisophthalic acid



m.p. 313 - 315 °C

¹H NMR (DMSO-d₆, 250 MHz)

δ (ppm) = 8.17 (*d*, ³*J*_{H,H} = 8.0 Hz, 2H, *H*-(C-4) and *H*-(C-6)), 7.80 (*m*, 1H, *H*-(C-5)).

¹³C NMR (DMSO-d₆, 60 MHz)

δ (ppm) = 124.8, 131.1, 134.5, 148.7, 164.0.

MS-EI (70 eV)

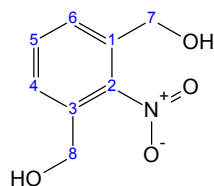
m/z: 211 ([M]⁺, C₈H₅NO₆, 17 %), 194 ([M - OH]⁺, C₈H₄NO₅, 4 %), 181 ([M - NO]⁺, C₈H₅O₅, 20 %), 167 ([M - CO₂]⁺, C₇H₅NO₃, 78 %), 149 ([M - CO₂ - H₂O]⁺, C₇H₃NO₂, 100 %), 147 (66 %), 135 (26 %), 119 (54 %), 107 (22 %), 91 (54 %), 75 (12 %), 63 ([C₅H₃]⁺, 14 %), 45 (10 %), 43 (19 %).

IR

$\bar{\nu}$ /cm⁻¹ (T %): 3405 (79 %), 2870 (70 %), 2825 (69 %), 2658 (70 %), 2534 (68 %), 2004 (89 %), 1954 (90 %), 1811 (90 %), 1694 (38 %), 1604 (44 %), 1556 (28 %), 1467 (72 %), 1413 (41 %), 1376 (51 %), 1306 (54 %), 1268 (32 %), 1166 (45 %), 1068 (66 %), 905 (32 %), 854 (51 %), 837 (54 %), 783 (67 %), 767 (27 %), 735 (63 %), 683 (23 %).

1,3-Dihydroxymethyl-2-nitrobenzene

This compound was synthesized according to the procedure described in the synthesis of (3-methyl-4-nitrophenyl)methanol (see paragraph 5.2.2.5): 2-nitroisophthalic acid (12.90 g, 61.14 mmol) and THF (60 mL) were stirred in an ice bath, 1 N BH₃·THF (300 mL, 300 mmol) was added slowly. The ice bath was removed and the reaction solution was kept stirring for 36 h. To quench the reaction methanol (50 mL) was added slowly. After workup and crystallization from diisopropyl ether, 9.90 g 1,3-dihydroxymethyl-2-nitrobenzene was obtained (90 %).

1,3-Dihydroxymethyl-2-nitrobenzene

m.p. 98 - 99 °C (reported¹³⁸ 100 - 101 °C).

¹H NMR (DMSO-d₆, 250 MHz)

δ (ppm) = 7.55 (*m*, 3H, H_{arom}), 4.53 (*d*, $^4J_{H,H} = 4.4$ Hz, 2H, $H\text{-(C-7)}$ and $H\text{-(C-8)}$).

¹³C NMR (DMSO-d₆, 60 MHz)

δ (ppm) = 59.2, 127.5, 130.7, 134.2, 147.4.

MS-EI (70 eV)

m/z: 165 ($[\text{M} - \text{H}_2\text{O}]^+$, $\text{C}_8\text{H}_7\text{NO}_3$, 46 %), 148 ($[\text{M} - \text{H}_2\text{O} - \text{OH}]^+$, $\text{C}_8\text{H}_6\text{NO}_2$, 100 %), 146 (29 %), 133 (14 %), 120 (38 %), 105 (20 %), 91 (61 %), 77 ($[\text{C}_6\text{H}_5]^+$, 52 %), 63 ($[\text{C}_5\text{H}_3]^+$, 8 %), 51 (13 %), 39 (8 %).

IR

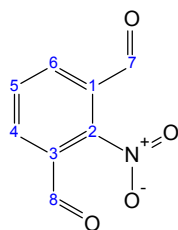
$\bar{\nu}/\text{cm}^{-1}$ (T %): 3202 (60 %), 2925 (72 %), 2862 (75 %), 1967 (90 %), 1909 (91 %), 1828 (91 %), 1709 (92 %), 1602 (82 %), 1580 (83 %), 1517 (26 %), 1470 (64 %), 1444 (66 %), 1429 (63 %), 1352 (41 %), 1322 (48 %), 1286 (63 %), 1255 (62 %), 1235 (58 %), 1173 (69 %), 1063 (33 %), 1040 (32 %), 995 (60 %), 982 (56 %), 912 (74 %), 901 (73 %), 856 (57 %), 794 (39 %), 751 (42 %), 714 (43 %), 664 (41 %).

2-Nitroisophthalaldehyde

1,3-Dihydroxymethyl-2-nitrobenzene was oxidized to **21-NO₂** by PDC using analogy method in the oxidation of 2-iodo-5-methoxybenzyl alcohol (see paragraph **5.2.1.5**).

To the stirred suspension of 1,3-dihydroxymethyl-2-nitrobenzene (0.90 g, 4.92 mmol) and sodium acetate (1.00 g, 12.19 mmol) in DCM (30 mL) in an ice bath, PDC (2.13 g, 5.65 mmol) was introduced slowly over 15 min. When TLC analysis showed that the starting compound was completely converted, the reaction was stopped. After workup, these crude mixture products were purified by using MPLC (DCM containing 1 % MeOH)

0.21 g **21-NO₂** (23 % based on 1,3-dihydroxymethyl-2-nitrobenzene) and 0.49 g 3-(hydroxymethyl)-2-nitrobenzaldehyde (54 % based on 1,3-dihydroxymethyl-2-nitrobenzene) were obtained.

2-Nitroisophthalaldehyde

m.p. 128 - 129 °C

¹H NMR (DMSO-d₆, 250 MHz)

δ (ppm) = 10.01 (s, 2H, *H*-(C-7) and *H*-(C-8)), 8.39 (d, $^3J_{H,H} = 7.9$ Hz, 2H, *H*-(C-4) and *H*-(C-6)), 8.08 (dd, $^3J_{H,H} = 7.9$ Hz, $^3J_{H,H} = 7.9$ Hz, 1H, *H*-(C-5)).

¹³C NMR (DMSO-d₆, 60 MHz)

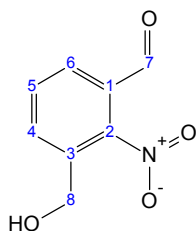
δ (ppm) = 126.9 (C-1 and C-3), 132.2 (C-5), 137.9 (C-4 and C-6), 149.9 (C-2), 188.9 (C-7 and C-8).

MS-EI (70 eV)

m/z: 180 ([M + H]⁺, C₈H₆NO₄, 13 %), 161 ([M – OH]⁺, C₈H₄NO₃, 31 %), 147 (11 %), 133 ([M – OH – CO]⁺, C₇H₄NO₂, 28 %), 119 (6 %), 103 (100 %), 91 (9 %), 77 ([C₆H₅]⁺, 33 %), 65 (29 %), 51 (26 %), 39 (10 %).

IR

$\bar{\nu}$ /cm⁻¹ (T %): 3391 (90 %), 3102 (91 %), 3077 (88 %), 3023 (91 %), 2871 (85 %), 2761 (90 %), 2247 (93 %), 2010 (95 %), 1941 (95 %), 1701 (23 %), 1593 (40 %), 1536 (23 %), 1394 (66 %), 1360 (53 %), 1309 (58 %), 1233 (45 %), 1165 (50 %), 1128 (78 %), 1113 (78 %), 1068 (75 %), 1013 (28 %), 938 (70 %), 863 (74 %), 857 (74 %), 801 (32 %), 773 (45 %), 747 (51 %), 721 (46 %).

3-(Hydroxymethyl)-2-nitrobenzaldehyde**¹H NMR (DMSO-d₆, 250 MHz)**

δ (ppm) = 9.97 (s, 1H, *H*-(C-7)), 7.98 (*m*, 2H, *H*_{arom}), 7.84 (*m*, 1H, *H*_{arom}), 4.56 (d, $^4J_{H,H} = 4.4$ Hz, 2H, *H*-(C-8)).

¹³C NMR (DMSO-d₆, 60 MHz)

δ (ppm) = 58.3, 127.2, 131.5, 131.6, 134.3, 135.0, 146.6, 189.4.

MS-EI (70 eV)

m/z : 182 ($[M + H]^+$, $C_8H_8NO_4$, 3 %), 164 ($[M - OH]^+$, $C_8H_6NO_3$, 7 %), 146 ($[M - OH - H_2O]^+$, $C_8H_6NO_3$, 44 %), 133 (32 %), 118 (34 %), 105 (69 %), 91 (100 %), 77 ($[C_6H_5]^+$, 82 %), 63 ($[C_5H_3]^+$, 10 %), 51 (36 %), 39 (10 %).

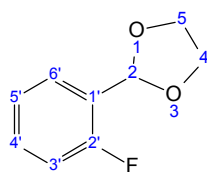
IR

$\bar{\nu}/cm^{-1}$ (T %): 3387 (88 %), 3086 (95 %), 2880 (92 %), 1700 (40 %), 1600 (69 %), 1579 (82 %), 1528 (22 %), 1466 (76 %), 1363 (46 %), 1308 (75 %), 1238 (57 %), 1170 (71 %), 1076 (56 %), 1039 (53 %), 1017 (53 %), 968 (69 %), 919 (76 %), 852 (58 %), 788 (46 %), 754 (59 %), 722 (68 %), 687 (66 %).

5.2.3.17 2-Fluoroisophthalaldehyde (21-F)**2-(2-Fluorophenyl)-1,3-dioxolane**

The synthetic procedure was the same as described in the synthesis of 2-(5-methoxy-2-nitrophenyl)-1,3-dioxolane (see paragraph 5.2.2.9, synthetic pathway 1).

A mixture of 2-fluorobenzaldehyde (5.00 g, 40.32 mmol), ethylene glycol (3.95 mL, 70.72 mmol) and toluene-4-sulfonic acid (0.46 g, 2.35 mmol) in toluene (70 mL) was refluxed in a Dean-Stark-Trap at 130 °C for 6 h. After workup and purification by using MPLC (petroleum ether / ethyl acetate, 5:1), 5.97 g 2-(2-fluorophenyl)-1,3-dioxolane was afforded as colourless oil (81 %).

2-(2-Fluorophenyl)-1,3-dioxolane **1H NMR ($CDCl_3$, 400 MHz)**

δ (ppm) = 7.53 (*m*, 1H, H_{arom}), 7.33 (*m*, 1H, H_{arom}), 7.15 (*m*, 1H, H_{arom}), 7.06 (*m*, 1H, H_{arom}), 6.09 (*s*, 1H, $H-(C-2)$), 4.09 (*m*, 4H, $H-(C-4)$ and $H-(C-5)$).

 ^{13}C NMR ($CDCl_3$, 100 MHz)

δ (ppm) = 65.4 (C-4 and C-5), 98.9 (*d*, $^3J_{C,F} = 5.1$ Hz, C-2), 115.6 (*d*, $^2J_{C,F} = 20.5$ Hz, C-3'), 124.0 (*d*, $^4J_{C,F} = 2.2$ Hz, C-5'), 125.1 (*d*, $^2J_{C,F} = 11.7$ Hz, C-1'), 127.7 (*d*, $^3J_{C,F} = 5.1$ Hz, C-6' or C-4'), 130.8 (*d*, $^3J_{C,F} = 7.3$ Hz, C-6' or C-4'), 161.0 (*d*, $^1J_{C,F} = 249.6$ Hz, C-2').

MS-EI (70 eV)

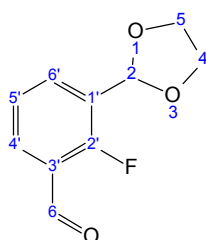
m/z : 168 ($[M]^+$, $C_9H_9FO_2$, 18 %), 167 ($[M - H]^+$, $C_9H_8FO_2$, 100 %), 149 ($[M - F]^+$, $C_9H_9O_2$, 8 %), 137 (11 %), 123 ($[M - H - CH_2CH_2O]^+$, C_7H_4FO , 27 %), 108 (9 %), 95 (5 %), 73 (10 %), 45 (2 %).

IR

$\bar{\nu}/cm^{-1}$ (T %): 2956 (93 %), 2889 (86 %), 1619.47 (79 %), 1593 (84 %), 1490 (65 %), 1458 (68 %), 1398 (72 %), 1300 (90 %), 1276 (77 %), 1232 (58 %), 1185 (68 %), 1153 (81 %), 1112 (58 %), 1071 (30 %), 1030 (61 %), 966 (57 %), 940 (38 %), 874 (83 %), 845 (78 %), 809 (67 %), 756 (16 %).

3-(1,3-Dioxolan-2-yl)-2-fluorobenzaldehyde

According to the procedure described in the preparation of **6-F** (see paragraph **5.2.2.4**), 3-(1,3-Dioxolan-2-yl)-2-fluorobenzaldehyde was prepared by following procedure: To a stirred solution of *t*-BuOK (0.80 g, 7.14 mmol) in THF (20 mL, absolved) *n*-BuLi (4.50 mL, 7.20 mmol, 1.6 M in hexane) was added dropwise at $-78\text{ }^\circ\text{C}$ under argon. After 5 min further stirring, 2-(2-fluorophenyl)-1,3-dioxolane (1.00 g, 5.95 mmol) was added and the reaction was carried out for another 2 h at $-78\text{ }^\circ\text{C}$. DMF (2.00 mL, 26.03 mmol) was added dropwise and the solution was warmed up to room temperature within 1 h. The reaction was quenched by adding acetic acid (5 mL, concentrated). After workup and purification by using MPLC (petroleum ether / ethyl acetate, 5:1), 0.44 g 3-(1,3-dioxolan-2-yl)-2-fluorobenzaldehyde was obtained (37 %).

3-(1,3-Dioxolan-2-yl)-2-fluorobenzaldehyde **^1H NMR (CDCl_3 , 250 MHz)**

δ (ppm) = 10.37 (s, 1H, H -(C-6)), 7.83 (m, 2H, H -(C-4') and H -(C-6')), 7.26 (dd, $^3J_{H,H} = 7.7$ Hz, $^3J_{H,H} = 7.7$ Hz, 1H, H -(C-5')), 6.11 (s, 1H, H -(C-2)), 4.11 (m, 4H, H -(C-4) and H -(C-5)).

 ^{13}C NMR (CDCl_3 , 60 MHz)

δ (ppm) = 65.6 (C-4 and C-5), 98.5 (d, $^3J_{C,F} = 4.8$ Hz, C-2), 124.5 (d, $^3J_{C,F} = 4.7$ Hz, C-6' or C-4'), 126.8 (d, $^2J_{C,F} = 12.4$ Hz, C-1'), 129.6 (d, $^2J_{C,F} = 12.8$ Hz, C-3'), 131.1

(C-5'), 134.2 (*d*, $^3J_{C,F} = 4.8$ Hz, C-6' or C-4'), 162.8 (*d*, $^1J_{C,F} = 211.7$ Hz, C-2'), 186.8 (*d*, $^3J_{C,F} = 4.4$ Hz, C-6).

MS-EI (70 eV)

m/z: 196 ($[M]^+$, C₁₀H₉FO₃, 100 %), 195 ($[M - H]^+$, C₁₀H₈FO₃, 100 %), 167 ($[M - CHO]^+$, C₉H₈FO₂, 19 %), 151 ($[M - H - CH_2CH_2O]^+$, C₈H₄FO₂, 94 %), 140 (18 %), 123 (39 %), 107 (24 %), 101 (18 %), 95 (12 %), 73 (32 %), 59 (28 %), 45 (2 %).

IR

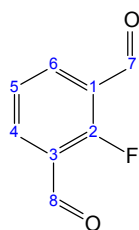
$\bar{\nu}/\text{cm}^{-1}$ (T %): 2968 (93 %), 2891 (86 %), 2767 (96 %), 1692 (39 %), 1617 (62 %), 1588 (75 %), 1460 (70 %), 1398 (58 %), 1299 (87 %), 1249 (54 %), 1218 (68 %), 1198 (63 %), 1166 (84 %), 1098 (32 %), 1026 (62 %), 966 (55 %), 946 (54 %), 907 (71 %), 830 (55 %), 784 (53 %), 762 (60 %), 740 (59 %), 684 (71 %).

2-Fluoroisophthalaldehyde

The dioxolane group in 3-(1,3-Dioxolan-2-yl)-2-fluorobenzaldehyde was cleaved by the same procedure as described in the deprotection of 2-(5-methoxy-3-methyl-2-nitrophenyl)-1,3-dioxolane (see paragraph 5.2.2.9, synthetic pathway 1).

3-(1,3-Dioxolan-2-yl)-2-fluorobenzaldehyde (1.30 g, 6.63 mmol) was stirred in the solution mixture of THF (10 mL) and 1 N HCl (10 mL) at room temperature overnight. After workup and purification by using MPLC (petroleum ether / ethyl acetate, 5:1), 0.61 g 2-fluoroisophthalaldehyde was obtained (61 %).

2-Fluoroisophthalaldehyde



m.p. 92 - 93 °C.

^1H NMR (CDCl₃, 250 MHz)

δ (ppm) = 10.26 (*s*, 2H, *H*-(C-7) and *H*-(C-8)), 8.13 (*m*, 2H, *H*-(C-4) and *H*-(C-6)), 7.55 (*dd*, $^3J_{H,H} = 7.7$ Hz, $^3J_{H,H} = 7.7$ Hz, 1H, *H*-(C-5)).

^{13}C NMR (CDCl₃, 60 MHz)

δ (ppm) = 124.7 (*d*, $^2J_{C,F} = 8.1$ Hz, C-1 or C-3), 125.5 (*d*, $^3J_{C,F} = 4.4$ Hz, C-4 or C-6), 135.2 (*d*, $^4J_{C,F} = 2.9$ Hz, C-5), 164.2 (*d*, $^1J_{C,F} = 270.8$ Hz, C-2), 187.2 (*d*, $^3J_{C,F} = 5.9$ Hz, C-7 or C-8).

HRMS (EI)

m/z measured: 152.02645 ($[M]^+$, $C_8H_5FO_2$).

m/z calculated: 152.027345.

MS-EI (70 eV)

m/z : 152 ($[M]^+$, $C_8H_5FO_2$, 68 %), 151 ($[M - H]^+$, $C_8H_4FO_2$, 100 %), 123 ($[M - CHO]^+$, C_7H_4FO , 6 %), 95 ($[M - CHO - CO]^+$, C_6H_4F , 10 %), 75 (7 %).

IR

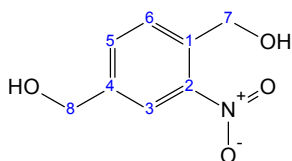
$\bar{\nu}/cm^{-1}$ (T %): 3354 (88 %), 3089 (88 %), 3059 (87 %), 3018 (87 %), 2890 (85 %), 2775 (88 %), 1708 (70 %), 1679 (60 %), 1606 (64 %), 1578 (65 %), 1492 (86 %), 1460 (62 %), 1447 (67 %), 1395 (60 %), 1309 (77 %), 1244 (56 %), 1199 (58 %), 1166 (75 %), 1083 (79 %), 1060 (83 %), 1010 (84 %), 913 (59 %), 828 (69 %), 798 (53 %), 777 (64 %), 724 (65 %), 706 (51 %).

5.2.3.18 2-Nitroterephthalaldehyde (22-NO₂)

The synthetic procedure for this compound was the same as described in the synthesis of **21-NO₂** (see paragraph **5.2.3.16**).

1,4-Dihydroxymethyl-2-nitrobenzene

2-Nitroterephthalic acid (3.82 g 18.10 mmol) and THF (50 mL) were stirred in ice bath, 1 N $BH_3 \cdot THF$ (100 mL, 100 mmol) was added slowly. The ice bath was removed and the reaction solution was kept stirring for 36 h. After workup and crystallization from diisopropylether, 3.15 g 1,4-dihydroxymethyl-2-nitrobenzene was obtained (96 %).

1,4-Dihydroxymethyl-2-nitrobenzene

m.p. 106 - 108 °C.

¹H NMR (DMSO-d₆, 400 MHz)

δ (ppm) = 7.97 (s, 1H, H -(C-3)), 7.77 (d, $^3J_{H,H} = 7.8$ Hz, 1H, H -(C-5) or H -(C-6)), 7.68 (d, $^3J_{H,H} = 7.8$ Hz, 1H, H -(C-5) or H -(C-6)), 4.80 (d, $^4J_{H,H} = 5.2$ Hz, 2H, H -(C-7) or H -(C-8)), 4.59 (d, $^4J_{H,H} = 5.2$ Hz, 2H, H -(C-7) or H -(C-8)).

¹³C NMR (DMSO-d₆, 100 MHz)

δ (ppm) = 59.8 (C-7), 61.5 (C-8), 121.7 (C-3), 128.2 (C-5 or C-6), 131.4 (C-5 or C-6), 136.8 (C-1), 142.9 (C-4), 146.7 (C-2).

MS-EI (70 eV)

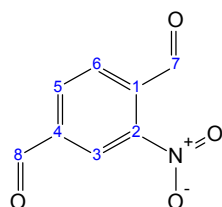
m/z: 166 ([M – H₂O]⁺, C₈H₇NO₃, 35 %), 150 (16 %), 136 ([M – H₂O – CO]⁺, C₇H₇NO₂, 13 %), 120 ([M – H₂O – NO₂]⁺, C₈H₇O, 24 %), 109 (48 %), 92 (50 %), 89 (52 %), 77 ([C₆H₅]⁺, 100 %), 65 (30 %), 50 (38 %), 37 (20 %).

IR

$\bar{\nu}$ /cm⁻¹ (T %): 3228 (59 %), 3088 (70 %), 2923 (78 %), 2857 (79 %), 2035 (90 %), 1932 (90 %), 1810 (91 %), 1715 (90 %), 1625 (89 %), 1567 (81 %), 1521 (43 %), 1488 (61 %), 1424 (56 %), 1334 (42 %), 1295 (49 %), 1253 (62 %), 1225 (65 %), 1213 (63 %), 1189 (60 %), 1146 (78 %), 1080 (64 %), 1018 (23 %), 991 (39 %), 967 (57 %), 905 (57 %), 832 (51 %), 814 (35 %), 748 (41 %), 677 (40 %).

2-Nitroterephthalaldehyde

To a stirred suspension of 1,4-dihydroxymethyl-2-nitrobenzene (1.75 g, 9.51 mmol) and sodium acetate (1.00 g, 12.20 mmol) in DCM (80 mL) at 0 °C, PCC (8.20 g, 38.14 mmol) was introduced slowly over 15 min. The reaction solution was stirred at room temperature for 3 h. After workup, the mixture of products was purified by using MPLC (petroleum ether / ethyl acetate, 2:1) to give 1.10 g **22-NO₂** (64 % based on 3-methyl-4-nitrobenzoic acid).

2-Nitroterephthalaldehyde

m.p. 100 - 101 °C (reported¹³⁹ 96 - 97 °C).

¹H NMR (DMSO-d₆, 400 MHz)

δ (ppm) = 10.31 (s, 1H, *H*-(C-7) or *H*-(C-8)), 10.16 (s, 1H, *H*-(C-7) or *H*-(C-8)), 8.60 (*d*, ⁴*J*_{H,H} = 1.6 Hz, 1H, *H*-(C-3)), 8.37 (*dd*, ⁴*J*_{H,H} = 1.8 Hz, ³*J*_{H,H} = 7.5 Hz, 1H, *H*-(C-5)), 8.06 (*d*, ³*J*_{H,H} = 7.9 Hz, 1H, *H*-(C-6)).

¹³C NMR (DMSO-d₆, 100 MHz)

δ (ppm) = 124.8 (C-6), 130.6 (C-3), 133.9 (C-5), 134.4 (C-1), 139.3 (C-4), 149.3 (C-2), 189.7 (C-7), 191.3 (C-8).

MS-EI (70 eV)

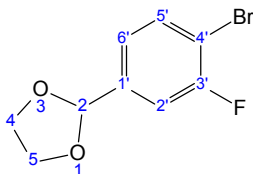
m/z: 180 ([M + H]⁺, C₈H₆NO₄, 28 %), 163 ([M + H – OH]⁺, C₈H₅NO₃, 6 %), 149 ([M – NO]⁺, C₈H₅O₂, 100 %), 133 (5 %), 132 (22 %), 121 (55 %), 103 (100 %), 93 (8 %), 77 ([C₆H₅]⁺, 6 %), 65 (30 %), 51 (20 %), 39 (11 %).

IR

$\bar{\nu}/\text{cm}^{-1}$ (T %): 3396 (91 %), 3367 (91 %), 3082 (83 %), 3058 (88 %), 3041 (89 %), 2933 (88 %), 2868 (74 %), 2742 (91 %), 1983 (95 %), 1811 (96 %), 1690 (10 %), 1615 (78 %), 1566 (57 %), 1528 (22 %), 1483 (39 %), 1416 (60 %), 1391 (47 %), 1376 (76 %), 1351 (19 %), 1313 (52 %), 1267 (36 %), 1181 (17 %), 1140 (61 %), 1068 (67 %), 1009 (71 %), 999 (59 %), 921 (60 %), 911 (47 %), 856 (35 %), 828 (39 %), 794 (22 %), 751 (19 %), 717 (31 %), 670 (54 %).

5.2.3.19 2-Fluoroterephthalaldehyde (22-F)**2-(4-Bromo-3-fluorophenyl)-1,3-dioxolane**

4-Bromo-3-fluorobenzaldehyde (5.50 g, 27.09 mmol) was reacted with ethylene glycol to give 6.20 g 2-(4-bromo-3-fluorophenyl)-1,3-dioxolane (92 %). The experiment was performed by the synthetic procedure described in the synthesis of 2-(2-fluorophenyl)-1,3-dioxolane (see paragraph 5.2.2.9, synthetic pathway 1).

2-(4-Bromo-3-fluorophenyl)-1,3-dioxolane **^1H NMR (DMSO- d_6 , 400 MHz)**

δ (ppm) = 7.73 (*m*, 1H, H_{arom}), 7.39 (*m*, 1H, H_{arom}), 7.23 (*m*, 1H, H_{arom}), 5.75 (*s*, 1H, H -(C-2)), 3.99 (*m*, 4H, H -(C-4) and H -(C-5)).

 ^{13}C NMR (DMSO- d_6 , 100 MHz)

δ (ppm) = 64.9 (C-5 and C-4), 101.3 (*d*, $^4J_{\text{C,F}} = 1.5$ Hz, C-2), 108.6 (*d*, $^2J_{\text{C,F}} = 20.5$ Hz, C-4'), 114.7 (*d*, $^2J_{\text{C,F}} = 23.4$ Hz, C-2'), 124.2 (*d*, $^3J_{\text{C,F}} = 3.7$ Hz, C-5'), 133.5 (C-6'), 140.8 (*d*, $^3J_{\text{C,F}} = 6.6$ Hz, C-1'), 158.1 (*d*, $^1J_{\text{C,F}} = 245.2$ Hz, C-3').

HRMS (EI)

m/z measured: 245.97209 ($[\text{M}]^+$, $\text{C}_9\text{H}_8\text{BrFO}_2$).

m/z calculated: 245.969117.

MS-EI (70 eV)

m/z : 248 ($[\text{M}]^+$, $\text{C}_9\text{H}_8^{81}\text{BrFO}_2$, 100 %), 246 ($[\text{M}]^+$, $\text{C}_9\text{H}_8^{79}\text{BrFO}_2$, 99 %), 227 (6 %), 203 ($[\text{M} - \text{H} - \text{CH}_2\text{CH}_2\text{O}]^+$, $\text{C}_6\text{H}_3^{81}\text{BrFO}$, 28 %), 201 ($[\text{M} - \text{H} - \text{CH}_2\text{CH}_2\text{O}]^+$, $\text{C}_6\text{H}_4^{79}\text{BrFO}$, 27 %), 187 (6 %), 174 (14 %), 167 ($[\text{M} - \text{H}^{79/81}\text{Br}]^+$, $\text{C}_9\text{H}_7\text{FO}_2$, 22 %), 137 (4 %), 123 (10 %), 107 (14 %), 94 (9 %), 73 (12 %), 57 (2 %), 45 (6 %).

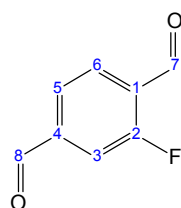
IR

$\bar{\nu}/\text{cm}^{-1}$ (T %): 2956 (93 %), 2888 (85 %), 1726 (97 %), 1581 (83 %), 1483 (68 %), 1424 (67 %), 1397 (71 %), 1277 (81 %), 1241 (73 %), 1165 (59 %), 1135 (84 %), 1082 (35 %), 1039 (51 %), 967 (59 %), 942 (47 %), 873 (50 %), 819 (54 %), 779 (57 %), 739 (79 %), 722 (74 %), 695 (82 %), 667 (75 %).

2-Fluoroterephthalaldehyde

Following the same synthetic procedure as described in the formylation of 4-bromo-3-nitroanisole (see paragraph 5.2.1.7), 2-(4-bromo-3-fluorophenyl)-1,3-dioxolane (2.25 g, 9.07 mmol) gave 3.50 g crude 4-(1,3-dioxolan-2-yl)-2-fluorobenzaldehyde which was directly submitted to hydrolysis without further purification.

3.50 g Crude 4-(1,3-dioxolan-2-yl)-2-fluorobenzaldehyde was stirred in a mixture of THF (10 mL) and 1 N HCl (10 mL) at room temperature overnight. After workup and purification by using MPLC (petroleum ether / ethyl acetate, 3:1), 1.10 g **22-F** was obtained (77 % based on 2-(4-bromo-3-fluorophenyl)-1,3-dioxolane).

2-Fluoroterephthalaldehyde

m.p. 91 - 92 °C.

 ^1H NMR (DMSO- d_6 , 400 MHz)

δ (ppm) = 10.27 (s, 1H, H -(C-8)), 10.07 (d, $^4J_{H,F}$ = 1.5 Hz, 1H, H -(C-7)), 8.05 (m, 1H, H_{arom}), 7.88 (m, 2H, H_{arom}).

 ^{13}C NMR (DMSO- d_6 , 100 MHz)

δ (ppm) = 117.0 (d, $^2J_{C,F}$ = 21.2 Hz, C-3), 125.5 (d, $^3J_{C,F}$ = 3.7 Hz, C-6), 127.4 (d, $^2J_{C,F}$ = 10.3 Hz, C-1), 130.3 (d, $^4J_{C,F}$ = 2.2 Hz, C-5), 141.8 (d, $^3J_{C,F}$ = 5.9 Hz, C-4), 163.3 (d, $^1J_{C,F}$ = 259.1 Hz, C-2), 187.8 (d, $^3J_{C,F}$ = 5.1 Hz, C-7), 191.9 (d, $^4J_{C,F}$ = 2.2 Hz, C-8).

HRMS (EI)

m/z measured: 152.02661 ($[\text{M}]^+$, $\text{C}_8\text{H}_5\text{FO}_2$).

m/z calculated: 152.027345.

MS-EI (70 eV)

m/z: 152 ($[\text{M}]^+$, $\text{C}_8\text{H}_5\text{FO}_2$, 75 %), 151 ($[\text{M} - \text{H}]^+$, $\text{C}_8\text{H}_4\text{FO}_2$, 100 %), 123 ($[\text{M} - \text{CHO}]^+$, $\text{C}_7\text{H}_4\text{FO}$, 40 %), 95 (28 %), 75 (18 %), 50 (6 %).

IR

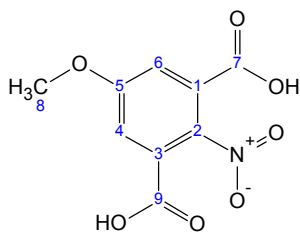
$\bar{\nu}/\text{cm}^{-1}$ (T %): 3372 (90 %), 3114 (90 %), 3081 (87 %), 3062 (86 %), 3044 (82 %), 2885 (83 %), 2847 (83 %), 2778 (88 %), 2742 (88 %), 1992 (92 %), 1936 (93 %), 1802 (93 %), 1723 (86 %), 1682 (33 %), 1615 (65 %), 1577 (62 %), 1492 (65 %), 1430 (49 %), 1401 (60 %), 1384 (51 %), 1314 (51 %), 1280 (80 %), 1259 (57 %), 1238 (56 %), 1185 (48 %), 1133 (46 %), 1104 (58 %), 1002 (82 %), 968 (61 %), 948 (81 %), 897 (65 %), 822 (43 %), 807 (46 %), 750 (28 %), 706 (71 %), 665 (70 %).

5.2.3.20 5-Methoxy-2-nitroisophthalaldehyde (23-NO₂)

The synthetic procedure for this compound was the same as described in the synthesis of **21-NO₂** (see paragraph **5.2.3.16**).

5-Methoxy-2-nitroisophthalic acid

3.00 g 5-methoxy-2-nitroisophthalic acid was produced from 5-methoxy-2-nitro-1,3-xylene (41 %).

5-Methoxy-2-nitroisophthalic acid

m.p. 222 - 224 °C.

¹H NMR (DMSO-d₆, 250 MHz)

δ (ppm) = 7.51 (s, 2H, *H*-(C-4) and *H*-(C-6)), 3.90 (s, 3H, *H*-(C-8)).

¹³C NMR (DMSO-d₆, 60 MHz)

δ (ppm) = 56.5 (C-8), 118.1 (C-4 and C-6), 127.8 (C-1 and C-3), 141.8 (C-2), 159.9 (C-5), 164.3 (C-7 and C-9).

MS-EI (70 eV)

m/z: 241 ([M]⁺, C₉H₇NO₇, 62 %), 225 (4 %), 211 ([M - NO]⁺, C₉H₇O₆, 100 %), 193 ([M - NO - H₂O]⁺, C₉H₅O₅, 3 %), 177 (24 %), 165 (6 %), 149 (18 %), 139 (48 %), 111 (35 %), 93 (42 %), 79 (8 %), 62 (12 %), 53 (6 %).

IR

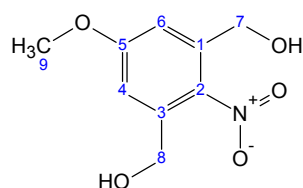
$\bar{\nu}/\text{cm}^{-1}$ (T %): 3607 (81 %), 3396 (82 %), 3096 (80 %), 2389 (81 %), 1903 (83 %), 1715 (59 %), 1673 (67 %), 1589 (60 %), 1552 (47 %), 1466 (62 %), 1456 (62 %), 1441 (61 %), 1373 (60 %), 1325 (63 %), 1267 (49 %), 1192 (46 %), 1152 (52 %),

1091 (52 %), 1033 (53 %), 933 (69 %), 904 (61 %), 891 (47 %), 837 (52 %), 798 (40 %), 764 (64 %), 732 (56 %), 674 (48 %).

5-Methoxy-1,3-dihydroxymethyl-2-nitrobenzene

5-Methoxy-2-nitroisophthalic acid (2.50 g, 10.37 mmol) and THF (20 mL) were stirred in an ice bath, 1 N $\text{BH}_3\cdot\text{THF}$ (65 mL, 65 mmol) was added slowly. The ice bath was removed and the reaction solution was kept stirring for 36 h. After workup and crystallization in diisopropyl ether, 1.45 g 1,3-dihydroxymethyl-2-nitrobenzene was obtained (53 %).

5-Methoxy-1,3-dihydroxymethyl-2-nitrobenzene



m.p. 127 - 129 °C.

^1H NMR (DMSO- d_6 , 400 MHz)

δ = 7.07 (s, 2H, H -(C-4) and H -(C-6)), 4.55 (s, 4H, H -(C-7) and H -(C-8)), 3.85 (s, 3H, H -(C-9)).

^{13}C NMR (DMSO- d_6 , 100 MHz)

δ = 55.7 (C-9), 59.5 (C-7 and C-8), 111.7 (C-4 and C-6), 138.2 (C-1 and C-3), 140.1 (C-2), 160.7 (C-5).

HRMS (EI)

m/z measured: 213.06506 ($[\text{M}]^+$, $\text{C}_9\text{H}_{11}\text{NO}_5$).

m/z calculated: 213.063696.

MS-EI (70 eV)

m/z : 213 ($[\text{M}]^+$, $\text{C}_9\text{H}_{11}\text{NO}_5$, 18 %), 195 ($[\text{M} - \text{H}_2\text{O}]^+$, $\text{C}_9\text{H}_9\text{NO}_4$, 12 %), 178 ($[\text{M} - \text{H}_2\text{O} - \text{OH}]^+$, $\text{C}_9\text{H}_8\text{NO}_3$, 100 %), 149 ($[\text{M} - \text{H}_2\text{O} - \text{NO}_2]^+$, $\text{C}_9\text{H}_9\text{O}_2$, 26 %), 134 (12 %), 121 (43 %), 106 (17 %), 95 (30 %), 77 ($[\text{C}_6\text{H}_5]^+$, 22 %), 65 (17 %), 39 (7 %).

IR

$\bar{\nu}/\text{cm}^{-1}$ (T %): 3206 (62 %), 2944 (83 %), 2256 (96 %), 1707 (94 %), 1594 (55 %), 1511 (63 %), 1409 (29 %), 1327 (19 %), 1280 (25 %), 1231 (47 %), 1193 (56 %), 1165 (47 %), 1109 (37 %), 1050 (41 %), 961 (58 %), 881 (59 %), 864 (58 %), 840 (55 %), 783 (46 %), 764 (40 %), 688 (53 %).

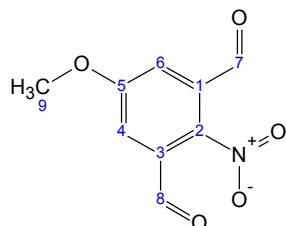
5-Methoxy-2-nitroisophthalaldehyde

To a stirred suspension of 5-methoxy-1,3-dihydroxymethyl-2-nitrobenzene (1.45 g, 6.81 mmol) and sodium acetate (1.00 g, 12.20 mmol) in DCM (30 mL) at 0 °C, PDC

(2.70 g, 7.18 mmol) was introduced slowly over 15 min. After 3 h stirring at room temperature, the reaction mixture was worked up and the crude products was purified by using MPLC (petroleum ether / ethyl acetate, 3:1).

0.33 g **23-NO₂** (22 % based on 5-methoxy-1,3-dihydroxymethyl-2-nitrobenzene) and 0.72 g 5-methoxy-3-(hydroxymethyl)-2-nitrobenzaldehyde (49 % based on 5-methoxy-1,3-dihydroxymethyl-2-nitrobenzene) were obtained.

5-Methoxy-2-nitroisophthalaldehyde



m.p. 152 °C.

¹H NMR (DMSO-d₆, 400 MHz)

δ (ppm) = 10.01 (s, 2H, *H*-(C-7) and *H*-(C-8)), 7.74 (s, 2H, *H*-(C-4) and *H*-(C-6)), 3.98 (s, 3H, *H*-(C-9)).

¹³C NMR (DMSO-d₆, 100 MHz)

δ (ppm) = 56.8 (C-9), 121.1 (C-4 and C-6), 130.4 (C-1 and C-3), 140.3 (C-2), 161.2 (C-5), 189.0 (C-7 and C-8).

HRMS (EI)

m/z measured: 209.03456 ([M]⁺, C₉H₇NO₅).

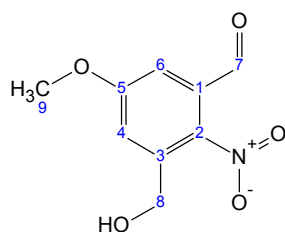
m/z calculated: 209.032396.

MS-EI (70 eV)

m/z: 209 ([M]⁺, C₉H₇NO₅, 5 %), 191 ([M – H₂O]⁺, C₉H₅NO₄, 10 %), 176 ([M – H₂O – CH₃]⁺, C₈H₂NO₄, 6 %), 163 ([M – H₂O – CO]⁺, C₈H₅NO₃, 54 %), 148 ([M – H₂O – CO – CH₃]⁺, C₇H₂NO₃, 9 %), 133 (100), 119 (10 %), 105 (52 %), 92 (22 %), 77 ([C₆H₅]⁺, 19 %), 63 ([C₅H₃]⁺, 66 %), 52 (14 %), 50 (10 %).

IR

$\bar{\nu}$ /cm⁻¹ (T %): 3370 (87 %), 3077 (78 %), 2990 (85 %), 2951 (85 %), 2917 (85 %), 2876 (85 %), 2633 (87 %), 2233 (89 %), 1791 (92 %), 1699 (48 %), 1595 (66 %), 1583 (48 %), 1540 (50 %), 1504 (52 %), 1477 (68 %), 1465 (55 %), 1438 (68 %), 1425 (64 %), 1389 (62 %), 1370 (63 %), 1328 (50 %), 1295 (42 %), 1237 (56 %), 1193 (67 %), 1170 (69 %), 1113 (57 %), 1034 (65 %), 1020 (42 %), 992 (62 %), 966 (65 %), 936 (42 %), 904 (53 %), 885 (32 %), 845 (59 %), 838 (58 %), 781 (74 %), 763 (64 %), 713 (54 %), 683 (58 %).

5-Methoxy-3-(hydroxymethyl)-2-nitrobenzaldehyde**¹H NMR (DMSO-d₆, 400 MHz)**

δ (ppm) = 9.97 (s, 1H, H-(C-7)), 7.44 (d, $^4J_{H,H} = 2.7$ Hz, 1H, H-(C-4) or H-(C-6)), 7.38 (d, $^4J_{H,H} = 2.7$ Hz, 1H, H-(C-4) or H-(C-6)), 4.61 (d, $^4J_{H,H} = 5.1$ Hz, 2H, H-(C-8)), 3.91 (s, 3H, H-(C-9)).

¹³C NMR (DMSO-d₆, 100 MHz)

δ (ppm) = 56.3 (C-8), 58.9 (C-9), 114.5 (C-4 or C-6), 117.8 (C-4 or C-6), 131.4 (C-1), 139.1 (C-2), 140.6 (C-3), 161.1 (C-5), 189.4 (C-7).

MS-EI (70 eV)

m/z : 211 ($[M]^+$, C₉H₉NO₅, 7 %), 194 ($[M - H_2O]^+$, C₉H₇NO₄, 6 %), 176 (14 %), 163 (7 %), 147 (14 %), 134 (48 %), 121 (100 %), 106 (46 %), 92 (42 %), 77 ($[C_6H_5]^+$, 38 %), 63 ($[C_5H_3]^+$, 23 %), 51 (13 %), 39 (11 %).

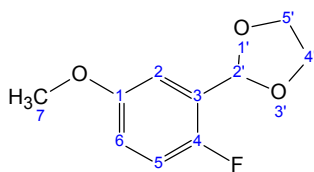
IR

$\bar{\nu}/\text{cm}^{-1}$ (T %): 3513 (79 %), 3369 (80 %), 3079 (83 %), 2987 (87 %), 2949 (84 %), 2847 (87 %), 1693 (43 %), 1585 (35 %), 1500 (34 %), 1463 (42 %), 1422 (50 %), 1393 (45 %), 1359 (58 %), 1320 (34 %), 1284 (15 %), 1229 (48 %), 1195 (50 %), 1162 (52 %), 1108 (31 %), 1064 (30 %), 1031 (31 %), 974 (41 %), 962 (49 %), 936 (38 %), 894 (46 %), 878 (40 %), 844 (35 %), 773 (69 %), 720 (46 %), 704 (47 %), 657 (55 %).

**5.2.3.21 2-Fluoro-5-methoxyisophthalaldehyde (23-F) and
2-fluoro-5-methoxyterephthalaldehyde (24-F)**

3-(1,3-Dioxolan-2-yl)-4-fluoroanisole

3-(1,3-Dioxolan-2-yl)-4-fluoroanisole was synthesized according to described in synthesis of 2-(2-fluorophenyl)-1,3-dioxolane (see paragraph 5.2.2.9, synthetic pathway 1). 2-Fluoro-5-methoxybenzaldehyde (5.80 g, 37.66 mmol) gave 6.74 g 3-(1,3-dioxolan-2-yl)-4-fluoroanisole (90 %).

3-(1,3-Dioxolan-2-yl)-4-fluoroanisole**¹H NMR (DMSO-d₆, 400 MHz)**

δ (ppm) = 7.16 (*m*, 1H, H_{arom}), 6.97 (*m*, 2H, H_{arom}), 5.93 (*s*, 1H, $H-(C-2')$), 4.00 (*m*, 4H, $H-(C-4')$ and $H-(C-5')$), 3.73 (*s*, 3H, $H-(C-7)$).

¹³C NMR (DMSO-d₆, 100 MHz)

δ (ppm) = 55.6 (C-7), 64.8 (C-4' and C-5'), 97.9 (*d*, $^3J_{C,F} = 3.7$ Hz, C-2'), 112.4 (*d*, $^3J_{C,F} = 3.7$ Hz, C-2), 115.9 (*d*, $^3J_{C,F} = 7.3$ Hz, C-6), 116.3 (*d*, $^2J_{C,F} = 22.7$ Hz, C-5), 125.8 (*d*, $^2J_{C,F} = 13.9$ Hz, C-3), 155.2 (*d*, $^4J_{C,F} = 2.2$ Hz, C-1), 155.6 (*d*, $^1J_{C,F} = 240.1$ Hz, C-4).

HRMS (EI)

m/z measured: 198.06757 ($[M]^+$, C₁₀H₁₁FO₃).

m/z calculated: 198.069206.

MS-EI (70 eV)

m/z : 198 ($[M]^+$, C₁₀H₁₁FO₃, 90 %), 197 ($[M - H]^+$, C₁₀H₁₀FO₃, 90 %), 179 ($[M - OH]^+$, C₁₀H₈FO₂, 22 %), 167 (70 %), 153 ($[M - H - CH_2CH_2O]^+$, C₈H₆FO₂, 86 %), 137 (22 %), 126 (55 %), 109 (20 %), 95 (12 %), 83 (14 %), 73 (56 %), 56 (8 %), 43 (18 %).

IR

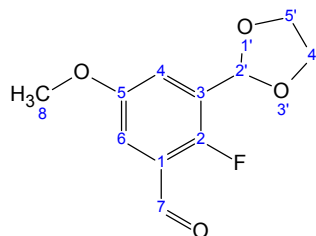
$\bar{\nu}/\text{cm}^{-1}$ (T %): 2957 (90 %), 2890 (87 %), 2838 (93 %), 1598 (91 %), 1496 (37 %), 1466 (73 %), 1431 (73 %), 1400 (68 %), 1302 (77 %), 1273 (60 %), 1253 (80 %), 1199 (41 %), 1160 (47 %), 1114 (74 %), 1068 (37 %), 1032 (43 %), 961 (54 %), 947 (54 %), 879 (65 %), 865 (65 %), 814 (55 %), 753 (78 %), 731 (54 %), 696 (59 %).

4-(1,3-Dioxolan-2-yl)-5-fluoro-2-methoxybenzaldehyde and**3-(1,3-dioxolan-2-yl)-2-fluoro-5-methoxybenzaldehyde**

A solution of 3-(1,3-dioxolan-2-yl)-4-fluoroanisole (4.70 g, 23.74 mmol) and TMEDA (3.6 mL, 23.80 mmol) in THF (100 mL) was chilled to -78 °C in a CO₂/acetone bath. *sec*-BuLi (21.90 mL, 28.49 mmol, 1.3 M in cyclohexane) was added into this cold solution and it was kept stirring for 2 h at -78 °C. DMF (4 mL, 50.20 mmol) was added dropwise. Afterward, the reaction solution was warmed up to room temperature within 1 h and 5 mL water was added to quench the reaction. The reaction mixture was extracted with diethyl ether (2 × 200 mL). The combined organic layer was washed with water (100 mL), saturated NaHCO₃ solution (100 mL), brine

(100 mL) and dried over Na_2SO_4 . After evaporation of the solvent, the residue was purified by using MPLC (petroleum ether / ethyl acetate, 4:1) to yield 0.53 g 4-(1,3-dioxolan-2-yl)-5-fluoro-2-methoxybenzaldehyde (10 %) and 2.00 g 3-(1,3-dioxolan-2-yl)-2-fluoro-5-methoxybenzaldehyde (37 %).

3-(1,3-Dioxolan-2-yl)-2-fluoro-5-methoxybenzaldehyde



m.p. 83 - 85 °C.

^1H NMR (DMSO- d_6 , 400 MHz)

δ (ppm) = 10.19 (s, 1H, H -(C-7)), 7.31 (m, 2H, H -(C-4) and H -(C-6)), 6.02 (s, 1H, H -(C-2')), 4.02 (m, 4H, H -(C-4') and H -(C-5')), 3.80 (s, 3H, H -(C-8)).

^{13}C NMR (DMSO- d_6 , 100 MHz)

δ (ppm) = 55.9 (C-8), 65.0 (C-4' and C-5'), 97.6 (d, $^3J_{\text{C},\text{F}} = 2.9$ Hz, C-2'), 112.3 (d, $^3J_{\text{C},\text{F}} = 2.9$ Hz, C-4), 120.0 (d, $^3J_{\text{C},\text{F}} = 5.1$ Hz, C-6), 124.5 (d, $^2J_{\text{C},\text{F}} = 9.5$ Hz, C-1), 128.0 (d, $^2J_{\text{C},\text{F}} = 13.9$ Hz, C-3), 155.3 (d, $^4J_{\text{C},\text{F}} = 2.2$ Hz, C-5), 156.2 (d, $^1J_{\text{C},\text{F}} = 254.7$ Hz, C-2), 187.4 (d, $^3J_{\text{C},\text{F}} = 5.1$ Hz, C-7).

HRMS (EI)

m/z measured: 226.06312 ($[\text{M}]^+$, $\text{C}_{11}\text{H}_{11}\text{FO}_4$).

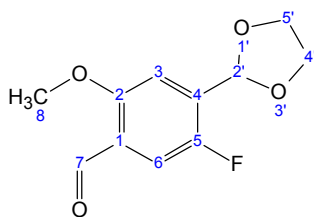
m/z calculated: 226.064116.

MS-EI (70 eV)

m/z: 226 ($[\text{M}]^+$, $\text{C}_{11}\text{H}_{11}\text{FO}_4$, 68 %), 225 ($[\text{M} - \text{H}]^+$, $\text{C}_{11}\text{H}_{10}\text{FO}_4$, 52 %), 198 ($[\text{M} - \text{CO}]^+$, $\text{C}_{10}\text{H}_{11}\text{FO}_3$, 8 %), 181 ($[\text{M} - \text{H} - \text{CH}_2\text{CH}_2\text{O}]^+$, $\text{C}_9\text{H}_6\text{FO}_3$, 98 %), 165 (14 %), 153 (53 %), 141 (8 %), 109 (8 %), 95 (10 %), 73 (100 %), 57 (2 %), 45 (17 %).

IR

$\bar{\nu}/\text{cm}^{-1}$ (T %): 3345 (95 %), 3090 (93 %), 3025 (94 %), 2967 (87 %), 2943 (86 %), 2899 (78 %), 2843 (87 %), 2283 (97 %), 2091 (96 %), 2010 (96 %), 1727 (93 %), 1678 (20 %), 1646 (88 %), 1600 (69 %), 1470 (30 %), 1439 (50 %), 1416 (40 %), 1371 (62 %), 1364 (64 %), 1334 (29 %), 1297 (78 %), 1275 (53 %), 1229 (44 %), 1199 (38 %), 1159 (52 %), 1134 (68 %), 1102 (21 %), 1046 (42 %), 1023 (40 %), 991 (65 %), 963 (56 %), 945 (33 %), 930 (26 %), 905 (40 %), 880 (60 %), 864 (30 %), 814 (77 %), 768 (58 %), 726 (52 %).

4-(1,3-Dioxolan-2-yl)-5-fluoro-2-methoxybenzaldehyde

m.p. 113 - 115 °C.

¹H NMR (DMSO-d₆, 400 MHz)

δ (ppm) = 10.28 (*d*, $^3J_{H,H} = 3.0$ Hz, 1H, *H*-(C-7)), 7.42 (*d*, $^3J_{H,F} = 9.9$ Hz, 1H, *H*-(C-6)), 7.26 (*d*, $^4J_{H,F} = 5.3$ Hz, 1H, *H*-(C-3)), 6.00 (*s*, 1H, *H*-(C-2')), 4.04 (*m*, 4H, *H*-(C-4') and *H*-(C-5')), 3.92 (*s*, 3H, *H*-(C-8)).

¹³C NMR (DMSO-d₆, 100 MHz)

δ (ppm) = 56.6 (C-8), 65.1 (C-4' and C-5'), 97.6 (*d*, $^3J_{C,F} = 2.9$ Hz, C-2'), 112.0 (*d*, $^3J_{C,F} = 3.7$ Hz, C-3), 113.8 (*d*, $^2J_{C,F} = 23.4$ Hz, C-6), 125.3 (*d*, $^3J_{C,F} = 5.9$ Hz, C-1), 132.9 (*d*, $^2J_{C,F} = 14.6$ Hz, C-4), 154.3 (*d*, $^1J_{C,F} = 243.0$ Hz, C-5), 157.7 (*d*, $^4J_{C,F} = 1.5$ Hz, C-2), 188.1 (*d*, $^4J_{C,F} = 1.5$ Hz, C-7).

HRMS (EI)

m/z measured: 226.06256 ($[M]^+$, C₁₁H₁₁FO₄).

m/z calculated: 226.064116.

MS-EI (70 eV)

m/z: 226 ($[M]^+$, C₁₁H₁₁FO₄, 90 %), 225 ($[M - H]^+$, C₁₁H₁₀FO₄, 76 %), 208 ($[M - H_2O]^+$, C₁₁H₈FO₃, 17 %), 203 ($[M - CHO]^+$, C₁₀H₁₀FO₃, 47 %), 181 ($[M - H - CH_2CH_2O]^+$, C₉H₆FO₃, 76 %), 165 (33 %), 153 (48 %), 137 (38 %), 123 (16 %), 109 (22 %), 95 (14 %), 73 (100 %), 57 (7 %), 45 (26 %).

IR

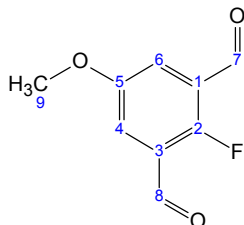
$\bar{\nu}$ /cm⁻¹ (T %): 3347 (95 %), 3054 (92 %), 2967 (87 %), 2901 (81 %), 2879 (81 %), 2770 (93 %), 2277 (97 %), 1980 (96 %), 1678 (40 %), 1622 (69 %), 1590 (90 %), 1488 (43 %), 1466 (40 %), 1419 (42 %), 1400 (33 %), 1384 (43 %), 1281 (53 %), 1235 (52 %), 1202 (61 %), 1187 (45 %), 1155 (28 %), 1117 (61 %), 1068 (27 %), 1024 (55 %), 1002 (28 %), 957 (38 %), 943 (31 %), 891 (21 %), 867 (33 %), 790 (71 %), 723 (40 %), 689 (30 %), 666 (40 %).

2-Fluoro-5-methoxyisophthalaldehyde and**2-fluoro-5-methoxyterephthalaldehyde**

3-(1,3-dioxolan-2-yl)-2-fluoro-5-methoxybenzaldehyde (0.17 g, 0.75 mmol) was hydrolyzed in a mixed solution of 1 N HCl and THF (50:50) to give 0.12 g **23-F** (88 %).

By the same procedure, 4-(1,3-dioxolan-2-yl)-5-fluoro-2-methoxybenzaldehyde (0.20 g, 0.88 mmol) was hydrolyzed in a mixed solution of 1 N HCl and THF (50:50) to give 0.13 g 2-fluoro-5-methoxyterephthalaldehyde (80 %).

2-Fluoro-5-methoxyisophthalaldehyde



m.p. 98 - 100 °C.

¹H-NMR (DMSO-d₆, 400 MHz)

δ (ppm) = 10.22 (s, 2H, *H*-(C-7) and *H*-(C-8)), 7.58 (d, ⁴*J*_{H,F} = 5.3 Hz, 2H, *H*-(C-4) and *H*-(C-6)), 3.85 (s, 3H, *H*-(C-9)).

¹³C-NMR (DMSO-d₆, 100 MHz)

δ (ppm) = 56.2 (C-9), 119.2 (d, ³*J*_{C,F} = 2.9 Hz, C-4 and C-6), 125.5 (d, ²*J*_{C,F} = 9.5 Hz, C-1 and C-3), 155.6 (d, ⁴*J*_{C,F} = 2.2 Hz, C-5), 158.6 (d, ¹*J*_{C,F} = 263.5 Hz, C-2), 187.2 (d, ³*J*_{C,F} = 5.9 Hz, C-7 and C-8).

HRMS (EI)

m/z measured: 182.03754 ([M]⁺, C₉H₇FO₃).

m/z calculated: 182.037906.

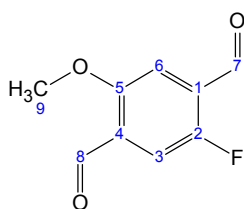
MS-EI (70 eV)

m/z: 182 ([M]⁺, C₉H₇FO₃, 100 %), 153 ([M - CHO]⁺, C₈H₆FO₂, 61 %), 138 (8 %), 125 (10 %), 110 (7 %), 83 (48 %), 71 (22 %), 55 (31 %), 43 (87 %).

IR

$\bar{\nu}$ /cm⁻¹ (T %): 3353 (89 %), 3073 (82 %), 3018 (86 %), 2980 (84 %), 2957 (83 %), 2897 (79 %), 2849 (82 %), 2770 (87 %), 2619 (89 %), 2092 (92 %), 1810 (93 %), 1682 (38 %), 1598 (54 %), 1495 (77 %), 1469 (38 %), 1463 (39 %), 1442 (49 %), 1431 (42 %), 1392 (35 %), 1322 (53 %), 1290 (42 %), 1227 (41 %), 1197 (35 %), 1156 (53 %), 1045 (43 %), 1008 (72 %), 972 (64 %), 945 (39 %), 894 (34 %), 810 (67 %), 724 (56 %), 705 (52 %), 661 (32 %).

2-Fluoro-5-methoxyterephthalaldehyde



m.p. 127 - 128 °C.

¹H NMR (DMSO-d₆, 400 MHz)

δ (ppm) = 10.32 (s, 1H, *H*-(C-7) or *H*-(C-8)), 10.23 (s, 1H, *H*-(C-7) or *H*-(C-8)), 7.58 (s, 1H, *H*-(C-6)), 7.54 (d, ³*J*_{H,F} = 5.5 Hz, 1H, *H*-(C-3)), 3.97 (s, 3H, *H*-(C-9)).

¹³C NMR (DMSO-d₆, 100 MHz)

δ (ppm) = 56.1 (C-9), 112.6 (d, ³*J*_{C,F} = 2.2 Hz, C-6), 115.3 (d, ²*J*_{C,F} = 23.4 Hz, C-3), 128.2 (d, ²*J*_{C,F} = 10.2 Hz, C-1), 128.9 (d, ³*J*_{C,F} = 6.6 Hz, C-4), 157.1 (d, ¹*J*_{C,F} = 251.8 Hz, C-2), 157.4 (d, ⁴*J*_{C,F} = 1.4 Hz, C-5), 187.5 (d, ³*J*_{C,F} = 4.4 Hz, C-7), 188.2 (d, ⁴*J*_{C,F} = 1.4 Hz, C-8).

HRMS (EI)

m/z measured: 182.03624 ([M]⁺, C₉H₇FO₃).

m/z calculated: 182.037906.

MS-EI (70 eV)

m/z: 182 ([M]⁺, C₉H₇FO₃, 92 %), 164 ([M - H₂O]⁺, C₉H₅FO₂, 74 %) 153 ([M - CHO]⁺, C₈H₆FO₂, 30 %), 138 (100 %), 123 (73 %), 121 (56 %), 109 (40 %), 95 (34 %), 83 (26 %), 62 (10 %), 56 (16 %), 48 (10 %).

IR

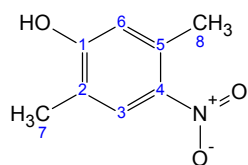
$\bar{\nu}$ /cm⁻¹ (T %): 3365 (91 %), 3109 (90 %), 3052 (83 %), 2995 (89 %), 2960 (81 %), 2929 (83 %), 2871 (73 %), 2769 (84 %), 1998 (92 %), 1726 (78 %), 1697 (53 %), 1683 (43 %), 1619 (80 %), 1581 (87 %), 1478 (53 %), 1465 (50 %), 1414 (46 %), 1402 (38 %), 1390 (41 %), 1296 (52 %), 1279 (44 %), 1234 (53 %), 1200 (55 %), 1190 (47 %), 1166 (59 %), 1131 (36 %), 1072 (67 %), 1040 (78 %), 999 (38 %), 903 (45 %), 883 (39 %), 783 (73 %), 742 (78 %), 710 (81 %), 678 (40 %), 657 (32 %).

5.2.3.22 5-Methoxy-2-nitroterephthalaldehyde (24-NO₂)

2,5-Dimethyl-4-nitrophenol

2,5-Dimethylphenol was nitrated according to the nitration of 3,5-dimethylphenol (see paragraph 5.2.2.9). 2,5-dimethylphenol (5.07 g, 41.56 mmol) gave 2.50 g 2,5-dimethyl-4-nitrophenol (36 %).

2,5-Dimethyl-4-nitrophenol



m.p. 117 - 119 °C (reported¹⁴⁰ 117 - 119 °C).

¹H NMR (DMSO-d₆, 250 MHz)

δ (ppm) = 7.87 (s, 1H, *H*-(C-3) or *H*-(C-6)), 6.74 (s, 1H, *H*-(C-3) or *H*-(C-6)), 2.45 (s, 3H, *H*-(C-7) or *H*-(C-8)), 2.13 (s, 3H, *H*-(C-7) or *H*-(C-8)).

¹³C NMR (DMSO-d₆, 60 MHz)

δ (ppm) = 15.1, 20.6, 117.5, 123.2, 127.7, 133.8, 139.8, 160.4.

MS-EI (70 eV)

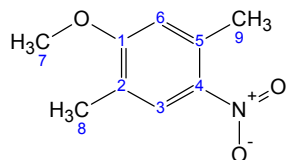
m/z: 167 ([M]⁺, C₈H₉NO₃, 50 %), 150 ([M – OH]⁺, C₈H₈NO₂, 100 %), 122 (30 %), 106 (12 %), 95 (18 %), 91 (41 %), 77 (35 %), 65 (11 %), 50 (11 %).

IR

$\bar{\nu}$ /cm⁻¹ (T %): 3345 (64 %), 2977 (79 %), 2933 (77 %), 2307 (87 %), 1778 (93 %), 1746 (93 %), 1670 (85 %), 1622 (59 %), 1578 (57 %), 1519 (45 %), 1481 (39 %), 1460 (47 %), 1440 (52 %), 1406 (64 %), 1375 (49 %), 1314 (31 %), 1262 (27 %), 1219 (32 %), 1173 (38 %), 1047 (38 %), 1016 (38 %), 903 (53 %), 889 (33 %), 853 (27 %), 785 (57 %), 757 (36 %), 729 (55 %), 712 (52 %).

2,5-Dimethyl-4-nitroanisole

2,5-Dimethyl-4-nitrophenol was methoxylated according to the method described in synthesis of **3-NO₂** (see paragraph 5.2.1.2). 2.30 g 2,5-Dimethyl-4-nitroanisole was obtained (85 %) from 2,5-dimethyl-4-nitrophenol (2.50 g, 14.97 mmol).

2,5-Dimethyl-4-nitroanisole

m.p. 94 - 97 °C (reported¹⁴¹ 91 - 92 °C).

¹H NMR (DMSO-d₆, 400 MHz)

δ (ppm) = 7.88 (s, 1H, *H*-(C-3) or *H*-(C-6)), 6.99 (s, 1H, *H*-(C-3) or *H*-(C-6)), 3.88 (s, 3H, *H*-(C-7)), 2.54 (s, 3H, *H*-(C-8) or *H*-(C-9)), 2.15 (s, 3H, *H*-(C-8) or *H*-(C-9)).

¹³C NMR (DMSO-d₆, 100 MHz)

δ (ppm) = 15.2 (C-8 or C-9), 20.7 (C-8 or C-9), 56.1 (C-7), 113.7 (C-3 or C-6), 124.7 (C-2 or C-5), 126.8 (C-3 or C-6), 134.2 (C-2 or C-5), 140.8 (C-4), 161.0 (C-1).

MS-EI (70 eV)

m/z: 181 ([M]⁺, C₉H₁₁NO₃, 40 %), 164 ([M – OH]⁺, C₉H₁₀NO₂, 100 %), 149 (7 %), 136 (20 %), 109 (28 %), 91 (38 %), 77 (14 %), 65 (8 %), 50 (8 %).

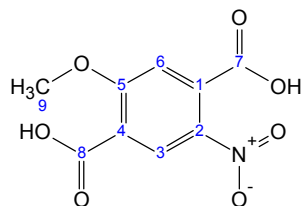
IR

$\bar{\nu}/\text{cm}^{-1}$ (T %): 3056 (89 %), 3009 (88 %), 2974 (83 %), 2932 (75 %), 2849 (84 %), 2736 (90 %), 2593 (90 %), 2514 (90 %), 2321 (91 %), 2052 (91 %), 1980 (92 %), 1802 (93 %), 1725 (93 %), 1643 (89 %), 1618 (57 %), 1572 (49 %), 1513 (42 %), 1496 (33 %), 1473 (51 %), 1462 (49 %), 1441 (49 %), 1394 (73 %), 1372 (60 %), 1334 (32 %), 1322 (26 %), 1255 (15 %), 1197 (54 %), 1175 (40 %), 1062 (25 %), 999 (44 %), 937 (71 %), 898 (42 %), 862 (47 %), 852 (49 %), 787 (46 %), 758 (44 %), 720 (71 %).

Compound 2,5-dimethyl-4-nitroanisole was oxidized to benzoic acid and reduced to benzyl alcohol, then followed by oxidation with PDC to give **24-NO₂**. The synthetic procedure was similar to described in the synthesis of **21-NO₂** (see paragraph 5.2.3.16).

5-Methoxy-2-nitroterephthalic acid

2,5-Dimethyl-4-nitroanisole (2.00 g, 11.05 mmol) gave 1.04 g 5-methoxy-2-nitroterephthalic acid (40 %).

5-Methoxy-2-nitroterephthalic acid**¹H NMR (DMSO-d₆, 400 MHz)**

δ (ppm) = 8.31 (s, 1H, *H*-(C-3) or *H*-(C-6)), 7.14 (s, 1H, *H*-(C-3) or *H*-(C-6)), 3.98 (s, 3H, *H*-(C-9)).

¹³C NMR (DMSO-d₆, 100 MHz)

δ (ppm) = 57.2 (C-9), 112.6 (C-3 or C-6), 117.4 (C-1 or C-4), 127.1 (C-3 or C-6), 134.1 (C-1 or C-4), 138.4 (C-2), 161.6 (C-5), 164.8 (C-7 or C-8), 166.1 (C-7 or C-8).

MS-EI (70 eV)

m/z: 241 ([M]⁺, C₉H₇NO₇, 44 %), 227 (22 %), 212 ([M - CHO]⁺, C₈H₆NO₆, 100 %), 209 (69 %), 194 ([M - CHO - H₂O]⁺, C₈H₄O₄, 26 %), 179 (14 %), 150 (11 %), 135 (8 %), 107 (14 %), 79 (10 %), 63 (14 %).

IR

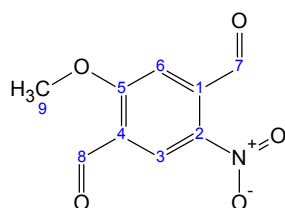
$\bar{\nu}/\text{cm}^{-1}$ (T %): 2852 (71 %), 2638 (74 %), 1695 (32 %), 1620 (56 %), 1567 (52 %), 1531(55 %), 1489 (50 %), 1474 (59 %), 1413 (50 %), 1336 (31 %), 1297 (50 %),

1239 (24 %), 1153 (52 %), 1115 (47 %), 1034 (37 %), 977 (62 %), 926 (56 %), 877 (39 %), 855 (41 %), 789 (47 %), 776 (48 %), 758 (38 %), 741 (39 %), 672 (45 %).

5-Methoxy-2-nitroterephthalaldehyde

5-Methoxy-2-nitroterephthalic acid (1.00 g, 4.15 mmol) was treated with 1 N $\text{BH}_3\cdot\text{THF}$ (20 mL) to give 1.30 g crude 5-methoxy-1,4-dihydroxymethyl-2-nitrobenzene which was submitted to oxidation by PDC. 0.38 g **24-NO₂** was obtained (44 % based on 5-methoxy-2-nitroterephthalic acid).

5-Methoxy-2-nitroterephthalaldehyde



m.p. 149 - 150 °C.

¹H NMR (DMSO-d₆, 400 MHz)

δ (ppm) = 10.34 (s, 1H, *H*-(C-7) or *H*-(C-8)), 10.32 (s, 1H, *H*-(C-7) or *H*-(C-8)), 8.36 (s, 1H, *H*-(C-3) or *H*-(C-6)), 7.52 (s, 1H, *H*-(C-3) or *H*-(C-6)), 4.11 (s, 3H, *H*-(C-9)).

¹³C NMR (DMSO-d₆, 100 MHz)

δ (ppm) = 57.5 (C-9), 113.3 (C-3 or C-6), 124.9 (C-3 or C-6), 125.7 (C-1 or C-4), 138.0 (C-1 or C-4), 141.5 (C-2), 164.4 (C-5), 187.6 (C-7 or C-8), 189.7 (C-7 or C-8).

HRMS (EI)

m/z measured: 209.03132 ($[\text{M}]^+$, C₉H₇NO₅).

m/z calculated: 209.032396.

MS-EI (70 eV)

m/z: 209 ($[\text{M}]^+$, C₉H₇NO₅, 56 %), 195 ($[\text{M} - \text{CH}_3]^+$, C₈H₄NO₅, 14 %), 179 ($[\text{M} - \text{NO}]^+$, C₉H₇O₄, 100%), 151 ($[\text{M} - \text{NO} - \text{CO}]^+$, C₈H₇O₃, 70 %), 135 (56 %), 119 (60 %), 105 (40 %), 91 (28 %), 77 ($[\text{C}_6\text{H}_5]^+$, 45 %), 57 (36 %), 43 (29 %).

IR

$\bar{\nu}/\text{cm}^{-1}$ (T %): 3387 (86 %), 3102 (82 %), 3038 (79 %), 3002 (83 %), 2956 (80 %), 2899 (81 %), 2650 (85 %), 1882 (90 %), 1735 (84 %), 1704 (56 %), 1681 (48 %), 1608 (56 %), 1567 (51 %), 1513 (52 %), 1466 (47 %), 1457 (54 %), 1389 (44 %), 1330 (42 %), 1268 (42 %), 1244 (35 %), 1188 (60 %), 1141 (44 %), 1056 (45 %), 1015 (63 %), 987 (47 %), 941 (47 %), 894 (44 %), 872 (39 %), 817 (51 %), 773 (62 %), 741 (35 %), 690 (61 %).

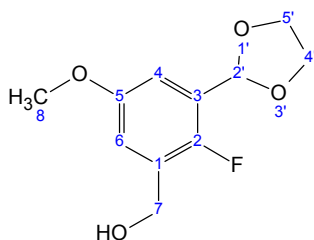
5.2.4 The precursors with protected glycine derivative

5.2.4.1 Methyl *N*-(diphenylmethylene)-2-fluoro-3-formyl-5-methoxyphenylalaninate (27-F)

3-(1,3-Dioxolan-2-yl)-2-fluoro-5-methoxybenzyl alcohol

To a solution of 2-(2-fluoro-5-methoxyphenyl)-1,3-dioxolane (2.00 g, 8.85 mmol) in MeOH (50 mL) in an ice bath, NaBH₄ (0.70 g, 18.92 mmol) was added and the resulting mixture was stirred at room temperature for 3 h. The progress of the reaction was monitored by TLC. After completion of the reaction, AcOH (4 mL, concentrated) was added to adjust pH to 6. Then the reaction solution was poured into water (200 mL) and extracted with DCM (2 × 100 mL). The combined organic layer was washed with saturated NaHCO₃ solution (100 mL) and brine (100 mL), dried over Na₂SO₄. After evaporation of the solvent, the residue was purified by using MPLC (petroleum ether / ethyl acetate, 1:1) and 1.52 g product was obtained as colourless oil (76 %).

3-(1,3-Dioxolan-2-yl)-2-fluoro-5-methoxybenzyl alcohol



¹H NMR (DMSO-d₆, 400 MHz)

δ (ppm) = 7.01 (s, 1H, *H*-(C-4) or *H*-(C-6)), 6.87 (s, 1H, *H*-(C-4) or *H*-(C-6)), 5.93 (s, 1H, *H*-(C-2')), 4.52 (d, ⁴*J*_{H,F} = 5.3 Hz, 2H, *H*-(C-7)), 4.00 (m, 4H, *H*-(C-4') and *H*-(C-5')), 3.73 (s, 3H, *H*-(C-8)).

¹³C NMR (DMSO-d₆, 100 MHz)

δ (ppm) = 55.5 (C-8), 56.7 (d, ³*J*_{C,F} = 4.4 Hz, C-7), 64.8 (C-4' and C-5'), 98.0 (d, ³*J*_{C,F} = 3.7 Hz, C-2'), 110.5 (d, ³*J*_{C,F} = 3.7 Hz, C-4 or C-6), 114.5 (d, ³*J*_{C,F} = 4.4 Hz, C-4 or C-6), 125.5 (d, ²*J*_{C,F} = 13.9 Hz, C-1 or C-3), 130.6 (d, ²*J*_{C,F} = 16.1 Hz, C-1 or C-3), 151.8 (d, ¹*J*_{C,F} = 240.8 Hz, C-2), 154.9 (d, ⁴*J*_{C,F} = 1.5 Hz, C-5).

MS-EI (70 eV)

m/z: 228 ([M]⁺, C₁₁H₁₃FO₄, 85 %), 227 ([M - H]⁺, C₁₁H₁₂FO₄, 74 %), 206 (8 %), 197 ([M - H - CH₂O]⁺, C₁₀H₁₀FO₃, 40 %), 183 ([M - H - CH₂CH₂O]⁺, C₉H₈FO₃, 55 %), 163 (19 %), 156 (64 %), 135 (13 %), 127 (30 %), 112 (13 %), 109 (12 %), 73 (81 %), 71 (100 %), 59 (7 %), 45 (17 %), 43 (32 %).

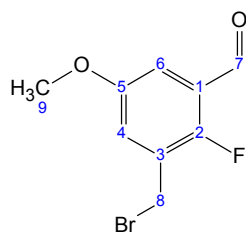
IR

$\bar{\nu}/\text{cm}^{-1}$ (T %): 3421 (89 %), 2950 (89 %), 2891 (85 %), 1707 (95 %), 1606 (86 %), 1472 (55 %), 1442 (72 %), 1396 (61 %), 1325 (67 %), 1246 (81 %), 1194 (46 %), 1154 (61 %), 1100 (29 %), 1045 (47 %), 1026 (51 %), 997 (52 %), 946 (46 %), 859 (53 %), 800 (76 %), 754 (70 %), 728 (71 %), 683 (64 %).

3-(Bromomethyl)-2-fluoro-5-methoxybenzaldehyde

Following the method in the synthesis of **23-F** and **24-F** (see paragraph 5.2.3.21), 3-(1,3-dioxolan-2-yl)-2-fluoro-5-methoxybenzyl alcohol (1.52 g, 6.67 mmol) was hydrolyzed under acidic condition to afford 1.15 g 2-fluoro-3-(hydroxymethyl)-5-methoxybenzaldehyde which was used directly in the further synthesis.

To a solution of 2-fluoro-3-(hydroxymethyl)-5-methoxybenzaldehyde (1.15 g) in 15 mL of dioxane BMDAB (1.82 g, 8.52 mmol) was added. This procedure was carried out under argon. This mixture was kept strong stirring at 70 °C. After completion of the reaction as checked by TLC, the reaction solution was poured into DCM (100 mL). The organic layer was washed with water (50 mL), saturated NaHCO₃ solution (50 mL), brine (50 mL) and dried over Na₂SO₄. After evaporation of solvent, the residue was crystallized in diisopropyl ether to give 1.25 g 3-(bromomethyl)-2-fluoro-5-methoxybenzaldehyde (76 % based on 3-(1,3-dioxolan-2-yl)-2-fluoro-5-methoxybenzyl alcohol).

3-(Bromomethyl)-2-fluoro-5-methoxybenzaldehyde

m.p. 77 - 78 °C.

¹H NMR (DMSO-d₆, 400 MHz)

δ (ppm) = 10.19 (s, 1H, *H*-(C-7)), 7.49 (dd, ⁴*J*_{H,H} = 3.6 Hz, ⁴*J*_{H,F} = 6.1 Hz, 1H, *H*-(C-4) or *H*-(C-6)), 7.26 (dd, ⁴*J*_{H,H} = 3.8 Hz, ⁴*J*_{H,F} = 5.3 Hz, 1H, *H*-(C-4) or *H*-(C-6)), 4.71 (s, 2H, *H*-(C-8)), 3.80 (s, 3H, *H*-(C-9)).

¹³C NMR (DMSO-d₆, 100 MHz)

δ (ppm) = 25.8 (*d*, ³*J*_{C,F} = 4.4 Hz, C-8), 55.9 (C-9), 112.2 (*d*, ³*J*_{C,F} = 3.7 Hz, C-4 or C-6), 123.5 (*d*, ³*J*_{C,F} = 3.7 Hz, C-4 or C-6), 124.5 (*d*, ²*J*_{C,F} = 9.5 Hz, C-1 or C-3), 127.9 (*d*, ²*J*_{C,F} = 16.1 Hz, C-1 or C-3), 155.3 (*d*, ⁴*J*_{C,F} = 2.9 Hz, C-5), 156.1 (*d*, ¹*J*_{C,F} = 254.7 Hz, C-2), 187.3 (*d*, ³*J*_{C,F} = 5.9 Hz, C-7).

MS-EI (70 eV)

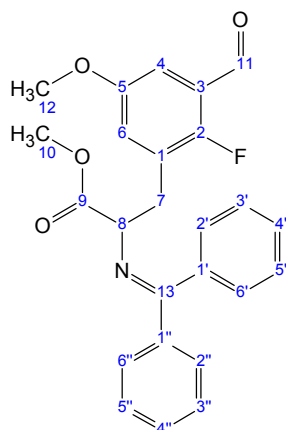
m/z : 248 ($[M]^+$, $C_9H_8^{81}BrFO_2$, 14 %), 246 ($[M]^+$, $C_9H_8^{79}BrFO_2$, 14 %), 167 ($[M - ^{79/81}Br]^+$, $C_9H_8FO_2$, 100 %), 137 (6 %), 123 (6 %), 109 (13 %), 96 (6 %), 57 (2 %), 40 (2 %).

IR

$\bar{\nu}/cm^{-1}$ (T %): 3376 (89 %), 3068 (84 %), 3027 (85 %), 2979 (85 %), 2941 (82 %), 2867 (78 %), 2844 (83 %), 2767 (84 %), 2630 (89 %), 2280 (89 %), 2078 (90 %), 1987 (91 %), 1776 (88 %), 1693 (40 %), 1613 (77 %), 1598 (59 %), 1476 (41 %), 1430 (59 %), 1394 (45 %), 1325 (49 %), 1300 (48 %), 1244 (56 %), 1219 (49 %), 1201 (32 %), 1153 (47 %), 1121 (52 %), 1039 (38 %), 983 (54 %), 949 (46 %), 898 (77 %), 880 (26 %), 798 (68 %), 729 (50 %), 672 (39 %).

Methyl N-(diphenylmethylene)-2-fluoro-3-formyl-5-methoxyphenylalaninate

A solution of lithiumdiisopropylamine (0.85 mL, 1.53 mmol, 1.8 M in THF) in THF (5 mL, absolute) was chilled to $-78\text{ }^\circ\text{C}$ in a CO_2 /acetone bath. To this solution N-(diphenylmethylene)glycine-methylester (0.39 g, 1.52 mmol) dissolved in THF (5 mL, absolute) was added dropwise. Then DMPU (0.18 mL, 1.52 mmol) was added. After 15 min stirring, the solution of 3-(bromomethyl)-2-fluoro-5-methoxybenzaldehyde (0.38 g, 1.53 mmol) in THF (5 mL) was introduced. The reaction mixture was stirred at $-80\text{ }^\circ\text{C}$ for 1 h and was warmed up to $-30\text{ }^\circ\text{C}$ by storing in refrigerator. 100 mL water was added to quench the reaction and the mixture was extracted with diethyl ether ($2 \times 100\text{ mL}$). The combined organic layer was washed with brine ($2 \times 50\text{ mL}$) and dried over Na_2SO_4 . After evaporation of solvent, the residue was purified by using MPLC (petroleum ether / ethyl acetate, 5:1), 0.28 g **27-F** as white powder was obtained (44 %).

Methyl N-(diphenylmethylene)-2-fluoro-3-formyl-5-methoxyphenylalaninate

¹H NMR (DMSO-d₆, 400 MHz)

δ (ppm) = 10.06 (s, 1H, *H*-(C-11)), 7.39 (*m*, 8H, *H*_{arom}), 7.11 (*m*, 1H, *H*_{arom}), 7.07 (*m*, 1H, *H*_{arom}), 6.62 (*m*, 2H, *H*_{arom}), 4.29 (*m*, 1H, *H*-(C-8)), 3.67 (s, 6H, *H*-(C-10) and *H*-(C-12)), 3.25 (*m*, 1H, *H*-(C-7)), 3.17 (*m*, 1H, *H*-(C-7)).

¹³C NMR (DMSO-d₆, 100 MHz)

δ (ppm) = 30.6 (C-7), 31.8 (C-7), 52.2 (C-10), 55.7 (C-12), 64.5 (C-8), 110.2 (*d*, ³*J*_{C,F} = 2.2 Hz, C-4 or C-6), 123.8 (*d*, ²*J*_{C,F} = 10.3 Hz, C-1 or C-3), 124.5 (*d*, ²*J*_{C,F} = 7.3 Hz, C-1 or C-3), 127.1 (*C*_{arom}), 127.2 (*C*_{arom}), 127.2 (*d*, ³*J*_{C,F} = 2.2 Hz, C-4 or C-6), 127.3 (*C*_{arom}), 128.2 (*C*_{arom}), 128.3 (*C*_{arom}), 128.4 (*C*_{arom}), 128.8 (*C*_{arom}), 130.7 (*C*_{arom}), 134.9 (*C*_{arom}), 138.6 (*C*_{arom}), 155.0 (*d*, ⁴*J*_{C,F} = 1.5 Hz, C-5), 156.8 (*d*, ¹*J*_{C,F} = 250.0 Hz, C-2), 170.3 (C-13), 171.0 (C-9), 187.6 (*d*, ³*J*_{C,F} = 5.9 Hz, C-11).

MS-EI (70 eV)

m/z: 420 ([M + H]⁺, C₂₅H₂₃FNO₄, 3 %), 419 ([M]⁺, C₂₅H₂₂FNO₄, 2 %), 360 ([M – COOMe]⁺, C₂₃H₂₂FNO₂, 22 %), 252 (C₁₆H₁₄NO₂, 100 %), 192 (C₁₄H₁₀N, 58 %), 165 (25 %).

HRMS (EI)

m/z measured: 419.15215 ([M]⁺, C₂₅H₂₂FNO₄).

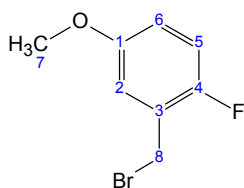
m/z calculated: 419.153261.

IR

$\bar{\nu}$ /cm⁻¹ (T %): 3058 (95 %), 3002 (95 %), 2951 (92 %), 1738 (58 %), 1712 (77 %), 1691 (51 %), 1617 (77 %), 1598 (72 %), 1576 (85 %), 1474 (55 %), 1444 (67 %), 1398 (71 %), 1316 (71 %), 1278 (64 %), 1244 (61 %), 1202 (50 %), 1175 (61 %), 1149 (60 %), 1058 (65 %), 1029 (72 %), 999 (76 %), 982 (74 %), 954 (72 %), 861 (75 %), 801 (74 %), 781 (66 %), 766 (68 %), 695 (33 %).

5.2.4.2 2-(2-Fluoro-5-methoxybenzyl)-5-isopropyl-3,6-dimethoxy-2,5-dihydropyrazine (28-F)**3-(Bromomethyl)-4-fluoroanisole**

Following the method in the synthesis of compound **3-Cl** (see paragraph **5.2.1.3**), 4.50 g 3-(Bromomethyl)-4-fluoroanisole was obtained as colourless oil (55 %) by bromination of 4-fluoro-3-methylanisole (5.26 g, 37.57 mmol) with NBS in CCl₄.

3-(Bromomethyl)-4-fluoroanisole**¹H NMR (DMSO-d₆, 400 MHz)**

δ (ppm) = 7.17 (*m*, 2H, H_{arom}), 6.94 (*m*, 1H, H_{arom}), 4.64 (*s*, 2H, H -(C-8)), 3.73 (*s*, 3H, H -(C-7)).

¹³C NMR (DMSO-d₆, 100 MHz)

δ (ppm) = 27.0, 27.1, 55.6, 115.7, 115.8, 115.9, 116.0, 116.2, 116.4, 125.6, 125.8, 153.3, 155.3, 155.4, 155.7.

MS-EI (70 eV)

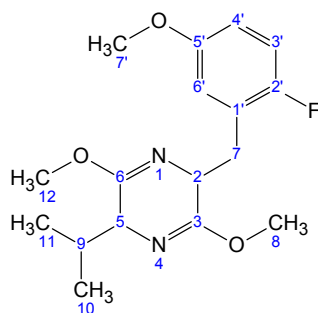
m/z : 220 ($[M]^+$, $C_8H_8^{81}BrFO$, 39 %), 218 ($[M]^+$, $C_8H_8^{79}BrFO$, 39 %), 139 ($[M - ^{81/79}Br]^+$, C_8H_8FO , 100 %), 109 (32 %), 96 (18 %), 83 (6 %), 57 (3 %).

IR

$\bar{\nu}$ /cm⁻¹ (T %): 3004 (95 %), 2958 (93 %), 2836 (93 %), 1737 (98 %), 1613 (93 %), 1596 (90 %), 1497 (22 %), 1463 (69 %), 1422 (66 %), 1321 (77 %), 1283 (59 %), 1256 (86 %), 1221 (35 %), 1208 (23 %), 1155 (55 %), 1100 (82 %), 1033 (38 %), 931 (78 %), 878 (75 %), 853 (75 %), 808 (46 %), 766 (70 %), 725 (61 %), 710 (37 %).

2-(2-Fluoro-5-methoxybenzyl)-5-isopropyl-3,6-dimethoxy-2,5-dihydropyrazine

A solution of (2R)-(-)-2,5-dihydro-3,6-dimethoxy-2-isopropylpyrazine (3.53 g, 19.22 mmol) in THF (40 mL) was chilled to -78 °C in a CO₂/acetone bath. *n*-BuLi (12.00 mL, 19.20 mmol, 1.6 M in hexane) was added into this cold solution and it was kept stirring 15 min at -78 °C. Then the solution of 3-(bromomethyl)-4-fluoroanisole (3.85 g, 17.50 mmol) in THF (15 mL) was added dropwise. Afterward, the reaction was stirred at -78 °C for 2 h. Then the reaction solution was warmed up to room temperature within 1 h and extracted with diethyl ether (2 × 100 mL). The combined organic layer was washed with water (50 mL), saturated NaHCO₃ solution (50 mL), brine (50 mL) and dried over Na₂SO₄. After evaporation of the solvent, the residue was purified by using MPLC (petroleum ether / ethyl acetate, 6:1) to yield 5.20 g **28-F** (91 %) as slightly yellow oil.

2-(2-Fluoro-5-methoxybenzyl)-5-isopropyl-3,6-dimethoxy-2,5-dihydropyrazine**¹H NMR (CDCl₃, 400 MHz)**

δ (ppm) = 6.87 (*m*, 1H, H_{arom}), 6.67 (*m*, 2H, H_{arom}), 4.30 (*m*, 1H, H -(C-2)), 3.72 (*s*, 3H, H -(C-12) or H -(C-8)), 3.71 (*s*, 3H, H -(C-12) or H -(C-8)), 3.65 (*s*, 3H, H -(C-7')), 3.48 (*m*, 1H, H -(C-5)), 3.20 (*m*, 1H, H -(C-7)), 2.99 (*m*, 1H, H -(C-7)), 2.17 (*s*, 1H, H -(C-9)), 0.97 (*d*, $^3J_{H,H} = 6.8$ Hz, 3H, H -(C-10) or H -(C-11)), 0.62 (*d*, $^3J_{H,H} = 6.8$ Hz, 3H, H -(C-10) or H -(C-11)).

¹³C NMR (CDCl₃, 100 MHz)

δ (ppm) = 16.3 (C-10 or C-11), 19.0 (C-10 or C-11), 31.2 (C-7), 33.5 (C-9), 52.1 (C-8 or C-12), 52.2 (C-8 or C-12), 55.6 (C-7'), 56.0 (C-2), 60.3 (C-5), 113.2 (*d*, $^3J_{C,F} = 8.1$ Hz, C-4' or C-6'), 115.3 (*d*, $^2J_{C,F} = 24.9$ Hz, C-3'), 116.7 (*d*, $^3J_{C,F} = 5.1$ Hz, C-4' or C-6'), 125.3 (*d*, $^2J_{C,F} = 17.6$ Hz, C-1'), 154.9 (*d*, $^4J_{C,F} = 2.2$ Hz, C-5'), 156.1 (*d*, $^1J_{C,F} = 237.9$ Hz, C-2'), 162.5 (C-3 or C-6), 164.0 (C-3 or C-6).

MS-EI (70 eV)

m/z : 322 ($[M]^+$, C₁₇H₂₃FN₂O₃, 10 %), 279 ($[M - C_3H_7]^+$, C₁₄H₁₆FN₂O₃, 10 %), 183 (C₉H₁₅N₂O₂, 57 %), 141 (C₈H₁₀FO, 100 %), 109 (6 %), 96 (3 %), 55 (2 %), 43 (4 %).

HRMS (EI)

m/z measured: 322.16812 ($[M]^+$, C₁₇H₂₃FN₂O₃).

m/z calculated: 322.169246.

IR

$\bar{\nu}$ /cm⁻¹ (T %): 2945 (83 %), 2871 (92 %), 2842 (95 %), 1693 (42 %), 1593 (95 %), 1499 (52 %), 1463 (76 %), 1435 (70 %), 1382 (88 %), 1365 (86 %), 1336 (89 %), 1307 (77 %), 1277 (81 %), 1236 (35 %), 1195 (48 %), 1150 (73 %), 1141 (74 %), 1113 (71 %), 1063 (84 %), 1040 (63 %), 1011 (54 %), 917 (89 %), 876 (91 %), 852 (85 %), 804 (75 %), 784 (78 %), 747 (74 %), 722 (67 %), 712 (72 %), 686 (90 %), 660 (88 %).

5.3 Radiosyntheses

5.3.1 Production of [^{18}F]fluoride ion

No-carrier-added (n.c.a.) [^{18}F]fluoride ion was produced at the PET trace cyclotron (General Electric Healthcare, Uppsala, Sweden) via the $^{18}\text{O}(\text{p},\text{n})^{18}\text{F}$ nuclear reaction by irradiating 1.5 mL of > 95 % enriched [^{18}O]water (Rotem, Israel) with 16.5 MeV protons.

5.3.2 ^{18}F -labeling reaction

n.c.a. ^{18}F -fluorination:

A 5 mL glass vial (Supelco, graduated screw top V-Vials[®], autoclavable borosilicate USP Type 1 glass) equipped with triangle stirring bar and a silicone septum sealed lid, into which two needles were stuck, connecting the outlet and the argon gas line, was evacuated and flushed with argon three times. From the aqueous n.c.a. [^{18}F]fluoride solution, 50 to 100 MBq was introduced into this sealed vial containing 100 μL of 3.5 % aqueous K_2CO_3 and 15.0 mg Kryptofix 222. The [^{18}F]fluoride solution was dried for 20 min under a mild stream of argon (ca. 2 mL/min) at 140 °C by azeotropic distillation with acetonitrile (2 \times 1 mL). Then, this reaction vial containing the $[\text{K}2.2.2\text{-K}]^{+18}\text{F}^-$ complex was adjusted to the reaction temperature and 10 mg of precursor dissolved in 1.0 mL of solvent were added into. For Radio-TLC analysis, the reaction samples were withdrawn at 1, 3, 7, 10, 20 and 30 min. For Radio-HPLC analysis, the reaction sample was taken at the reaction time when the maximum RCY was observed by Radio-TLC.

For a number of experiments ($n = 20$), the amount of radioactivity that remained adsorbed in the reaction vial after removing the reaction solution and washing with water (3 \times 3 mL) was determined as 12 ± 8 % (based on the total radioactivity in the vial after labeling).

c.a. ^{18}F fluorination:

The [^{18}F]fluoride solution was introduced into a 5.0 mL sealed vial containing 50 μL of 1 % aqueous K^{19}F , 100 μL of 3.5 % aqueous K_2CO_3 and 15.0 mg Kryptofix 222, the following step was the same as n.c.a. ^{18}F -fluorination.

5.3.3 Decarbonylation of ^{18}F -labeled product with $(\text{Ph}_3\text{P})_3\text{RhCl}$

After ^{18}F -radiolabeling reaction, the reaction solution was cooled down in an ice bath for 2 min and diluted with water (10 mL) and 0.1 N HCl (5 mL). Then this reaction mixture was passed through a combination of cartridges (Sep-Pak[®] Light Alumina N and Sep-Pak[®] Plus C18 in series) and the ^{18}F -labeled product was trapped by the Sep-Pak[®] C18 cartridge. This C18 cartridge was eluted with DCM (4 mL) and the elution passed through a Na_2SO_4 cartridge to a glass vessel. After the solvent was evaporated at 70 °C under argon, the radiochemical pure ^{18}F -labeled product was obtained.

To this residue, 1 mL of decarbonylation solvent was added and the solution was transferred into a sealed vial (same as ^{18}F -labeling reaction vial) containing $\text{RhCl}(\text{PPh}_3)_3$. Then, the mixture was heated in an aluminium block at 100 °C, 120 °C, 150 °C or 180 °C. Aliquots of the solution were taken out at different times for analysis (Radio-TLC and Radio-HPLC, the procedure was the same as that in the ^{18}F -labeling reaction). Amounts of catalyst used are based on quantity of labeling precursor.

5.3.4 Synthesis of [^{18}F]FDOPA by an automatic module

The automated synthesis was carried out in the synthetic module which was built in our laboratory (Figure 3-38). The remote operation was controlled by PC and the operation program was developed from GE Medical Systems. All of the chemicals and solvents were loaded before the [^{18}F]fluoride solution was delivered into the synthetic module.

The automated synthesis procedure was described by following: The [^{18}F]fluoride solution was trapped on a Sep-Pak[®] Light QMA and eluted with 1 mL of solution (containing 900 μL acetonitrile, 100 μL of 3.5 % K_2CO_3 and 15.0 mg Kryptofix 222) into the fluorination reactor. This mixture was dried for 10 min under a stream of argon (ca. 96 bar in vial) at 140 °C by azeotropic distillation with acetonitrile (1 mL). Precursor (5 mg) dissolved in DMF (1 mL) was added to the dry residue of the complex $[\text{K}2.2.2\text{-K}]^{+18}\text{F}^-$. Following, the fluorination reaction vial was kept heating at 140 °C for 10 min. The reaction solution was cooled down to 40 °C and diluted with 15 mL water, then this solution passed through combination of two cartridges (Sep-Pak[®] Light Alumina N and Sep-Pak[®] Plus C18). The Sep-Pak[®] Plus C18 cartridge trapping the ^{18}F -labeled product was washed with DCM (4 mL) and this

eluent was passed through a Na₂SO₄ cartridge into the reductive iodination reaction vial in which the diiodosilane was prepared *in situ* (250 μL phenylsilane, 250 mg I₂ and 15 μL ethylacetate mixed at room temperature.). The reductive iodination reaction was carried out at room temperature for 10 min. Then this iodinated product was trapped on Sep-Pak[®] Plus Silica and eluted with DCM (7 mL) into the next reaction vial in which 250 mg CsOH, 40 mg PTC and 45 mg *N*-(diphenylmethylene)glycine *tert*-butyl ester were loaded. After 10 min alkylation at room temperature, this reaction solution was transferred back into the fluorination reaction vial and DCM was evaporated. Into the residue 48 % HBr (500 μL) containing KI (10 mg) was added and the hydrolysis was performed at 150 °C for 10 min. The reaction mixture was cooled down to 40 °C and NaOH (500 μL, 6 N) was added. The mixed solution was loaded into a HPLC injection loop after on-line filtration through a micro glass fiber filter (WHATMAN). Preparative purification was performed with a precolumn (Phenomenex, Luna, C18 (2), 5μ, 50 mm × 10 mm) and a reverse phase column (Phenomenex, Luna, C18 (2), 5μ, 250 mm × 10 mm) with 0.1 % AcOH and 200 mg/L ascorbic acid in water as an eluent at a flow rate of 5.0 mL/min. The fraction corresponding to [¹⁸F]FDOPA (retention time 9-11 min) was collected and sterile filtered (Millex GV, Millipore, USA).

All of the reaction parameters used above were already optimized results. In the optimization of every single synthetic step, the other reaction parameters were tested (see paragraph 3.5).

5.4 Analytic methods

For examining the identification and purity of the ^{18}F -labeled product both Radio-TLC and Radio-HPLC were used. [^{18}F]Fluorobenzene was a volatile product and not suitable for Radio-TLC, thus this compound was only analysed by Radio-HPLC. In most cases, ^{18}F -labeled compounds were identified by their non-radioactive reference compounds via comparison of the UV-signals with the radioactive signals. In few cases non-radioactive reference compounds were not available, the developed methods (LC/MS analysis for c.a. ^{18}F -fluorination or comparison of the ^{18}F -labeled products from the precursor with the same substitution pattern but different LGs, see paragraph 3.2.1.6) were applied.

5.4.1 Analyses in ^{18}F -labeling reaction and decarbonylation

5.4.1.1 Radio thin layer chromatography

An aliquot of the reaction solution (1-5 μL) was given on a silica gel plate (Polygram® Silica G/UV₂₅₄, 8 × 4 cm, Macherey&Nagel, Germany) and this plate was developed in the appropriate solvent mixture. The radioactive spots were quantitatively assessed by means of electronic autoradiography (Instant Imager, Canberra Packard, USA). The R_f values are listed in Table 5-1 (^{18}F -fluorination) and in Table 5-2 (decarbonylation) along with solvent system (given as v/v ratios). The size of the TLC plate and the location of the reference standard were marked by radioactive spots on the plate, thus a correlation between radioactive labeled product and non-radioactive standards was assured.

5.4.1.2 Radio high performance liquid chromatography

Radio-HPLC was performed on the same system as described in paragraph 5.1 for non-radioactive HPLC. For the measurement of radioactivity, the outlet of the UV/Vis detector was connected to a NaI(Tl)-scintillation detector. The aliquots of ^{18}F -labeling reaction solution (10 μL) were analyzed by reverse phase Radio-HPLC using an appropriate column and acetonitrile / water in various concentration ratios containing 0.1 % KF as mobile phase. KF was added to the eluent as carrier in order to assure radioactive [^{18}F]fluoride ions to be eluted as a sharp peak ($k' = 1.0$). The flow rate was varied from 1 to 2 mL/min. All measurements were performed at room temperature. Individual k' -values of the reference compounds and retention times of

^{18}F -labeled products are given in Table 5-1 (^{18}F -fluorination) and in Table 5-2 (decarbonylation).

The data of compounds **1-F**, **1-Cl**, **2-F**, **2-Cl** and **2-Br** are presented in a previous report,⁶⁷ and the data of compounds with substitution pattern **5**, **9** and **10** are shown in a parallel work.⁷³

For more precise control of RCY, during Radio-HPLC analysis the ^{18}F -labeled product fraction was collected and measured by means of a gamma-counter (1480 Wallac WIZARD 3", PerkinElmer, USA). The radiochemical yield was calculated by relating the radioactivity of the product peak with the amount of radioactivity injected into the column.

Table 5-1. R_f and R_t for the reference compounds and ^{18}F -labeled products in ^{18}F -fluorination

Precursors	R_f (Radio-TLC) *		R_t (Radio-HPLC)		k'
	$[^{19}\text{F}]$ fluoro standard	^{18}F -labeled product	$[^{19}\text{F}]$ fluoro standard(min)	^{18}F -labeled product (min)	
1-NO ₂	0.69	0.69	7.49	8.02 ^a	2.94
1-Br	0.69	0.69	7.49	8.01 ^a	2.94
1-N ⁺ Me ₃ TfO ⁻	0.69	0.69	7.49	8.05 ^b	2.94
2-NO ₂	0.63	0.63	7.21	7.73 ^b	2.79
3-NO ₂	0.68	0.68	8.82	9.36 ^b	3.64
3-F	0.68	0.68	8.74	9.29 ^b	3.6
3-Cl	0.68	0.68	8.72	9.29 ^b	3.58
3-Br	0.68	0.68	8.82	9.37 ^b	3.64
3-I	0.68	0.68	8.77	9.33 ^b	3.61
3-N ⁺ Me ₃ TfO ⁻	0.68	0.68	5.68	5.94 ^c	2.93
4-NO ₂	0.61	0.61	7.94	8.47 ^b	3.17
6-NO ₂	0.71	0.71	10.55	10.98 ^b	4.55
6-F	0.71	0.71	10.61	11.04 ^b	4.58
6-Cl	0.71	0.71	10.54	10.94 ^b	4.54
6-Br	0.71	0.71	10.58	11.00 ^b	4.56
7-NO ₂	0.67	0.67	8.51	8.91 ^b	3.47
7-F	0.67	0.67	8.51	--	--
7-N ⁺ Me ₃ TfO ⁻	0.67	0.67	8.58	9.03 ^b	3.51
8-NO ₂	0.65	0.65	11.76	12.23 ^b	5.18
8-F	0.65	0.65	11.85	12.33 ^b	5.23
8-Cl	0.65	0.65	11.77	12.27 ^b	5.19
8-Br	0.65	0.65	5.76	6.00 ^d	2.84
12-C ₂ H ₅	--	0.72	--	12.63 ^b	--
12-C ₃ H ₇	--	0.72	--	17.03 ^b	--
12-C ₄ H ₉	--	0.72	--	20.55 ^b	--
12-CF ₃	--	0.67	--	16.49 ^b	--
12-Bn	--	0.63	--	27.72 ^b	--
13-NO ₂	0.44	0.44	6.44	7.00 ^b	2.38
14-NO ₂	0.59	0.59	7.75	8.28 ^b	3.07
15-NO ₂	0.40	0.40	10.45	10.74 ^e	5.96
15-Br	0.40	0.40	10.45	10.78 ^e	5.96
16-NO ₂	0.26	0.26	--	9.71 ^e	--
17-NO ₂	0.61	0.61	--	17.86 ^e	--
17-Br	0.61	0.61	--	17.87 ^e	--
18-NO ₂	--	0.30	--	9.48 ^e	--
19-NO ₂	0.52	0.52	7.49	8.05 ^b	2.94
19-Br	0.52	0.52	7.49	8.05 ^b	2.94
20-NO ₂	0.54	0.54	--	10.15 ^b	--
20-Br	0.54	0.54	--	10.16 ^b	--
21-NO ₂	0.51	0.51	7.56	7.98 ^f	2.97
22-NO ₂	0.49	0.49	8.93	9.18 ^g	4.91
23-NO ₂	0.70	0.70	7.70	8.11 ^h	4.13
24-NO ₂	0.48	0.48	8.78	9.19 ^h	4.85
27-F	0.45	0.45	5.56	5.81 ^d	2.70
3-nitrobenzaldehyde	0.58	0.58	15.40	15.83 ⁱ	9.19
nitrobenzene	--	--	10.11	10.52 ^j	5.74
4-nitroanisole	0.79	0.79	10.16 ⁱ	--	5.77

*: Petroleum ether / ethyl acetate (3:1, v/v). Except the case of **23-NO₂**: Petroleum ether / ethyl acetate (1:1, v/v).

a Column: C18, 5 μm , 250 mm \times 4.6 mm (Luna, Phenomenex, USA). Eluent: acetonitrile / water (50:50) containing 0.1 % acetic acid and 0.1 % KF. Flow rate: 1 mL/min. UV: at 254 nm.

b Column: C18, 5 μm , 250 mm \times 4.6 mm (Luna, Phenomenex, USA). Eluent: acetonitrile / water (50:50) containing 0.1 % KF. Flow rate: 1 mL/min. UV: at 254 nm.

c Column: phenylhexyl, 5 μm , 250 mm \times 4.6 mm (Luna, Phenomenex, USA). Eluent: acetonitrile / water (40:60) containing 0.1 % KF. Flow rate: 2 mL/min. UV: at 254 nm.

d Column: C18, 5 μm , 250 mm \times 4.6 mm (Luna, Phenomenex, USA). Eluent: acetonitrile / water (50:50) containing 0.1 % KF. Flow rate: 2 mL/min. UV: at 254 nm.

e Column: C18, 5 μm , 250 mm \times 4.6 mm (Luna, Phenomenex, USA). Eluent: acetonitrile / water (30:70) containing 0.1 % KF. Flow rate: 2 mL/min. UV: at 254 nm.

f Column: C18, 5 μm , 250 mm \times 4.6 mm (Luna, Phenomenex, USA). Eluent: acetonitrile / water (40:60) containing 10 mM Na_2HPO_4 and 0.1 % KF. Flow rate: 1 mL/min. UV: at 254 nm.

g Column: phenylhexyl, 5 μm , 250 mm \times 4.6 mm (Luna, Phenomenex, USA). Eluent: acetonitrile / water (20:80) containing 10 mM Na_2HPO_4 and 0.1 % KF. Flow rate: 2 mL/min. UV: at 254 nm.

h Column: C18, 5 μm , 250 mm \times 4.6 mm (Luna, Phenomenex, USA). Eluent: acetonitrile / water (30:70) containing 10 mM Na_2HPO_4 and 0.1 % KF. Flow rate: 2 mL/min. UV: at 254 nm.

i Column: phenylhexyl, 5 μm , 250 mm \times 4.6 mm (Luna, Phenomenex, USA). Eluent: acetonitrile / water (20:80) containing 0.1 % KF. Flow rate: 2 mL/min. UV: at 254 nm.

j Column: C18, 5 μm , 250 mm \times 4.6 mm (Luna, Phenomenex, USA). Eluent: acetonitrile / water (40:60) containing 0.1 % KF. Flow rate: 2 mL/min. UV: at 254 nm.

Table 5-2. R_f and R_t for the reference compounds and ^{18}F -labeled products in decarboxylation

Precursors	R_f (Radio-TLC)*		R_t (Radio-HPLC)		k'
	^{19}F fluoro standard	^{18}F -labeled product	^{19}F fluoro standard(min)	^{18}F -labeled product (min)	
4- ^{18}F fluoro-3-methylanisole	0.70	0.70	8.12	8.40 ^a	4.41
3- ^{18}F fluoro-4-methylanisole	0.77	0.77	8.97	9.20 ^a	4.98
5-dimethoxy-2- ^{18}F fluorotoluene	0.57	0.57	7.04	7.28 ^a	3.69
4- ^{18}F fluoro-anisole	0.79	0.79	12.17	12.61 ^b	5.41

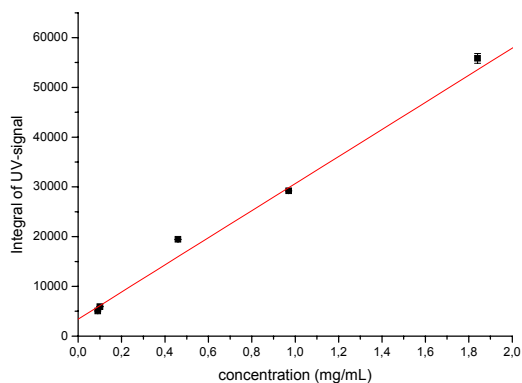
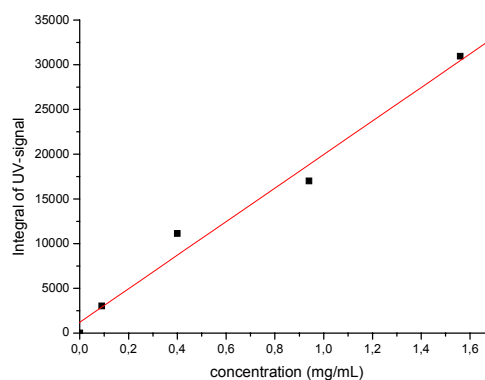
*: Petroleum ether / ethyl acetate (3:1, v/v)

a Column: C18, 5 μm , 250 mm \times 4.6 mm (Luna, Phenomenex, USA). Eluent: acetonitrile / water (50:50). Flow rate: 2 mL/min. UV: at 254 nm.

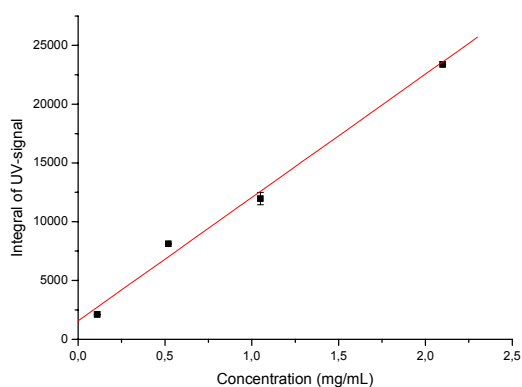
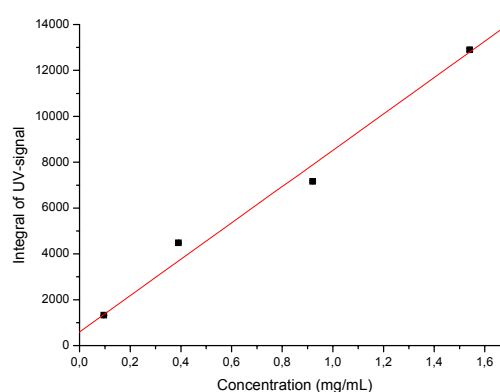
b Column: C18, 5 μm , 250 mm \times 4.6 mm (Luna, Phenomenex, USA). Eluent: acetonitrile / water (50:50). Flow rate: 1 mL/min. UV: at 254 nm.

In Table 5-1 and Table 5-2, The time delay between UV/Vis detector and Radioactive detector: 0.2-0.3 min at 1 mL/min, 0.4-0.6 min at 2 mL/min.

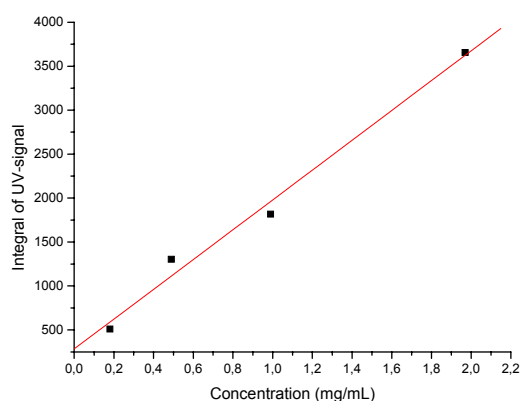
In addition, in the analyses of the oxidation by-products by using DMSO as solvent in labeling reaction (see paragraph 3.2.1.4), the integral of UV-signals obtained by the UV/Vis detector was proportional to the benzoic acids or benzaldehydes. The measured peak-areas were fitted by linear regression as functions of the amount of reference compounds and led to straight lines, which were used for calibration (Figure 5-1).

4-nitrobenzaldehyde (2-NO₂)

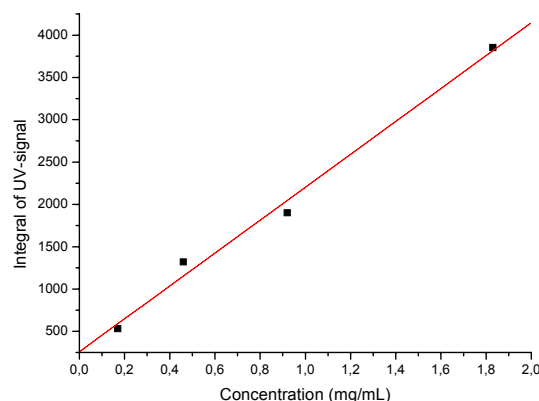
4-nitrobenzoic acid

2-nitrobenzaldehyde (1-NO₂)

2-nitrobenzoic acid



2-bromobenzaldehyde (1-Br)



2-bromobenzoic acid

Figure 5-1. Integral of the UV-peak as a function of the quantity of benzoic acids or benzaldehydes

Column: Luna C18, 5 μ m, 250 mm \times 4.6 mm, (Luna, Phenomenex, USA). Flow rate: 1 mL/min. Eluent: acetonitrile / water (50:50) containing 0.1 % acetic acid. UV: at 280 nm.

1-NO₂: R_t (6.86 min), k' (2.61). 2-Nitrobenzoic acid: R_t (4.24 min), k' (1.23).

2-NO₂: R_t (6.65 min), k' (2.50). 4-Nitrobenzoic acid: R_t (4.85 min), k' (1.55).

1-Br: R_t (11.44 min), k' (5.02). 2-Bromobenzoic acid: R_t (5.13 min), k' (1.70).

5.4.1.3 LC/MS

For identification of product in the c.a. ^{18}F -labeling reaction (see paragraph 3.2.1.6, Method 2):

The reaction sample from the c.a. labeling reaction was separated by Radio-HPLC at first. The fraction (50 μL) corresponding to the ^{18}F -labeled product was injected into the LC/MS system. A HP ODS (100 \times 2.1 mm, 5 μ) column was used. Eluent was methanol / water (40:60) buffered with ammonium acetate (144 mg/L). Compounds **3-NO₂**, **5-NO₂**, **16-NO₂**, **18-NO₂**, **19-NO₂** and **20-NO₂** were identified by this method, the mass peaks in LC/MS analysis are listed in Table 5-3.

Table 5-3. Identification of fluorinated products by LC/MS in c.a. ^{18}F -fluorination

Precursors	3-NO ₂	5-NO ₂	16-NO ₂	18-NO ₂	19-NO ₂	20-NO ₂
Mass peak (ACPI (+) mode)	M+1,M+15	M+1,M+15	M+1,M+15	M+1,M+15	M+1	M+1

For the detection of by-product in the labeling reaction:

The reaction sample (10 μL) from the labeling reaction (with or without addition of [^{18}F]fluoride ion) was directly injected into the LC/MS system.

A Phenomenex Luna (100 \times 2.0 mm, 5 μ) C18 (2) column was used. Eluent was a gradient from 100 % water to 100 % methanol (within 30 min) buffered with ammonium acetate (144 mg/L).

5.4.1.4 GC/MS

In the ^{18}F -labeling reaction with DMSO as solvent, the dimethylsulfide formed by oxidation (see paragraph 3.2.1.4) was analyzed by means of GC/MS (Hewlett-Packard 5890 Series II Plus). Samples were taken from the gas phase above the reaction solution at 30 min reaction time. Column: Chrompack Poraplot Q (27.5 m \times 0.32 mm); He-flow: 9.6 mL/min; temperature program: 10 $^{\circ}\text{C}/\text{min}$ from 85 $^{\circ}\text{C}$ to 200 $^{\circ}\text{C}$. R_f (dimethylsulfide): 8.29 min.

5.4.2 Analyses in the automated synthesis of [^{18}F]FDOPA

Radiochemical yields of the intermediate radioactive products were confirmed by radio-TLC. An aliquot of the intermediate product solution was applied to silica gel plates (Polygram[®] Silica G/UV₂₅₄, 8 \times 4 cm, Macherey&Nagel, Germany) and development was carried out with solvent (petroleum ether / ethyl acetate, 2:1), the R_f values were 0.59, 0.73, 0.58 for compounds 2-fluoro-4,5-dimethoxybenzaldehyde, 1-fluoro-2-(iodomethyl)-4,5-dimethoxybenzene, methyl N-(diphenylmethylene)-

2-fluoro-5-methoxy-O-methyltyrosinate, respectively. All of these reference compounds were provided by my colleague Michael Übele.

Determination of radiochemical purity of [^{18}F]FDOPA were carried out with a reverse phase column (Phenomenex, Luna, C18 (2), 5 μ , 250 mm \times 4.6 mm, eluent: water containing 0.1 % AcOH and 200 mg/L ascorbic acid, flow rate: 1 mL/min). The enantiomeric excess of [^{18}F]FDOPA was checked by a chiral column (Chirosil, 5 μ , 150 \times 4.6 mm, eluent: methanol / Water (85:15) containing 6 mM AcOH, flow rate: 0.6 mL/min). The retention time was 8.69 min ([^{18}F]FDOPA on the reverse phase column) and 7.67 min ([^{18}F]fluoro-L-DOPA on the chiral column).

6 REFERENCES

- (1) M. E. Van Dort, A. Rehemtulla, B. D. Ross, *Current Computer-Aided Drug Design*, **2008**, 4 (1), 46-53.
- (2) S. Konemann, M. Weckesser, *Recent Results in Cancer Research*, **2008**, 170, 243-253.
- (3) V. Sobhan, R. Soumendranath, *Nucl. Med. Commun.*, **2008**, 29 (1), 4-10.
- (4) D. S. Boss, R. V. Olmos, M. Sinaasappel, Jan H. M. Schellens, *The Oncologist*, **2008**, 13 (1), 25-38.
- (5) R. Myers, *Nucl. Med. Biol.*, **2001**, 28 (5), 585-593.
- (6) S. M. Qaim, *Radiochim. Acta*, **2001**, 89, 223-232.
- (7) H. H. Coenen, *Der Nuklearmediziner*, **1994**, 17, 203-214.
- (8) H. J. Ache, *Angew. Chem.*, **1972**, 84, 234-254.
- (9) M. S. Judenhofer, H. F. Wehrl, D. F. Newport, C. Catana, S. B. Siegel, M. Becker, A. Thielscher, M. Kneilling, M. P. Lichy, M. Eichner, K. Klingel, G. Reischl, S. Widmaier, M. Roecken, R. E. Nutt, H.-J. Machulla, K. Uludag, S. R. Cherry, C. D. Claussen, B. J. Pichler, *Nat. Med. (New York, NY, U.S.)*, **2008**, 14(4), 459-465.
- (10) L. S. Cai, S. Y. Lu, V. W. Pike, *Eur. J. Org. Chem.*, **2008**, 2853-2873.
- (11) F. F. Knapp, S. Mirzadeh, *Eur. J. Nucl. Med.*, **1994**, 21, 1151-1165.
- (12) E. E. Kim, D. J. Yang, F. C. Wong, *Current Medical Imaging Reviews*, **2008**, 4 (1), 63-69.
- (13) M. J. Welch, C. S. Redvanly (Eds.), *Hand book of radiopharmaceuticals: radiochemistry and applications*, John Wiley & Sons, Ltd, **2003**.
- (14) G. Stöcklin, *Eur. J. Nucl. Med.*, **1992**, 19, 527-551.
- (15) S. M. Qaim, G. Stöcklin, *Radiochim. Acta*, **1983**, 34, 25-40.
- (16) M. Guillaume, A. Luxen, B. Nebeling, M. Argentini, J. C. Clark, V. W. Pike, *Appl. Radiat. Isot.*, **1991**, 42, 749-762.
- (17) E. Hess, S. Takács, B. Scholten, F. Tárkányi, H. H. Coenen, S. M. Qaim, *Radiochim. Acta*, **2001**, 89, 357-362.
- (18) Medcylopaedia, internet site: www.medcylopaedia.com.
- (19) H. H. Coenen, *Ersnt Schering Research Foundation Workshop*, **2007**, 62, 15-50.
- (20) J. A. Wilkinson, *Chem. Rev.*, **1992**, 92, 505-519.
- (21) V. Casella, T. Ido, A. P. Wolf, J. S. Fowler, R. R. MacGregor, T. J. Ruth, *J. Nucl. Med.*, **1980**, 21, 750-757.
- (22) R. D. Nerinckx, R. M. Lambrecht, A. P. Wolf, *Int. J. Appl. Radiat. Isot.*, **1978**, 29, 323-327.

- (23) C.-Y. Shiue, P. A. Salvadori, A. P. Wolf, *J. Nucl. Med.*, **1982**, 23 (10), 899-903.
- (24) J. M. Muchowski, M. C. Venuti, *J. Org. Chem.*, **1980**, 45, 4798-4801.
- (25) S. Sood, G. Firnau, E. S. Garnett, *Int. J. Appl. Radiat. Isot.*, **1983**, 34 (4), 743-745.
- (26) F. Oberdorfer, E. Hofmann, M.-B. Wolfgang, *J. Labelled Compds. Radiopharm.*, **1968**, 4 (1), 999-1005.
- (27) J. Bergman, O. Solin, *Nucl. Med. Biol.*, **1997**, 24, 677-683.
- (28) H. H. Coenen, S. M. Moerlein, *J. Fluorine Chem.*, **1987**, 36, 63-75.
- (29) U. Berndt, C. Stanetty, T. Wanek, C. Kuntner, J. Stanek, M. Berger, M. Bauer, G. Henriksen, H.-J. Wester, H. Kvaternik, P. Angelberger, C. Noe, *J. Labelled Compds. Radiopharm.*, **2008**, 51, 137-145.
- (30) P. Wasserscheid, T. Welton (Eds), *Ionic liquids in synthesis*, John Wiley & Sons, Ltd, **2003**.
- (31) D. W. Kim, C. E. Song, D. Y. Chi, *J. Am. Chem. Soc.*, **2002**, 124, 10278-10279.
- (32) D. W. Kim, C. E. Song, D. Y. Chi, *J. Org. Chem.*, **2003**, 68, 4281-4285.
- (33) C. B. Murray, G. Sandford, S. R. Korn, *J. Fluorine Chem.*, **2003**, 123, 81-84.
- (34) M. A. Carroll, V. W. Pike, D. A. Widdowson, *Tetrahedron Lett.*, **2000**, 41, 5393-5396.
- (35) A. Plenevaux, C. Lemaire, A. J. Palmer, P. Damhaut, D. Comar, *Appl. Radiat. Isot.*, **1992**, 43, 1035-1040.
- (36) D. Block, H. H. Coenen, G. Stöcklin, *J. Labelled Compds. Radiopharm.*, **1987**, 24, 1029-1042.
- (37) D. Block, H. H. Coenen, G. Stöcklin, *J. Labelled Compds. Radiopharm.*, **1988**, 25, 201-216.
- (38) M. R. Kilbourn, C. S. Dence, M. J. Welch, C. J. Mathias, *J. Nucl. Med.*, **1987**, 28, 462-470.
- (39) D. Block, H. H. Coenen, G. Stöcklin, *J. Labelled Compds. Radiopharm.*, **1988**, 25, 185-200.
- (40) Y. Shai, K. L. Kirk, M. A. Channing, B. B. Dunn, M. A. Lesniak, R. C. Eastman, R. D. Finn, J. Roth, K. A. Jacobson, *Biochemistry*, **1989**, 28, 4801-4806.
- (41) R. Gail, *Berichte des Forschungszentrums Juelich*, **1995**, Jül-3029, 147.
- (42) B. L. Allain, M. C. Lasne, H. C. Perrio, B. Moreau, L. Barré, *Acta Chem. Scand.*, **1998**, 52, 480-489.
- (43) C.-Y. Shiue, J. S. Fowler, A. P. Wolf, M. Watanabe, C. D. Arnett, *J. Nucl. Med.*, **1985**, 26, 181-186.
- (44) T. Ludwig, J. Ermert, H. H. Coenen, *Nucl. Med. Biol.*, **2002**, 29, 255-262.
- (45) T. Poethko, M. Schottelius, G. Thumshirn, U. Hersel, M. Herz, G. Henriksen, H. Kessler, M. Schwaiger, H.-J. Wester, *J. Nucl. Med.*, **2004**, 45, 892-902.

- (46) H. C. Padgett, J. R. Barrio, N. S. MacDonald, M. E. Phelps, *J. Nucl. Med.*, **1982**, 23, 345-348.
- (47) J. Link, J. Clark, *In Proceeding of the 5th workshop on target and Target Chemistry*, **1994**, 245-248.
- (48) R. Ishiwata, M. Takashashi, M. Shinohara, T. Ido, *J. Labelled Compds. Radiopharm.*, **1982**, 19, 1347-1349.
- (49) T. Ido, R. Iwata, *J. Labelled Compds. Radiopharm.*, **1981**, 18, 244-246.
- (50) K. Suzuki, K. Tamate, T. Nakayama, T. Yamazaki, Y. Kasida, K. Fukushi, Y. Maruyama, H. Maekawa, H. Nakaoko, *J. Labelled Compds. Radiopharm.*, **1982**, 19, 1374-1375.
- (51) G. Blessing, H. H. Coenen, M. Hennes, H. Lipperts, *J. Labelled Compds. Radiopharm.*, **1982**, 19, 1333-1335.
- (52) K. Hamacher, H. H. Coenen, G. Stöckling, *J. Nucl. Med.*, **1986**, 27, 235-238.
- (53) M. R. Kilbourn, J. T. Hood, M. J. Welch, *Int. J. Appl. Radiat. Isot.*, **1984**, 35, 599-602.
- (54) B. W. Wieland, G. O. Hendry, D. G. Schmidt, G. Bida, T. J. Ruth, *J. Labelled Compds. Radiopharm.*, **1986**, 23, 1205-1207.
- (55) E. F. J. de Vries, G. Luurtsema, M. Brussermann, P. H. Elsinga, W. Vaalburg, *Appl. Radiat. Isot.*, **1999**, 51, 389-394.
- (56) R. Krasikova, *Radiochemistry*, **1998**, 40, 364-372.
- (57) C. Crouzel, J. C. Clark, C. Brihaye, B. Langstrom, C. Lemaire, G. J. Meyer, B. Nebeling, S. Stone-Elander, *In Radiopharmaceuticals for Positron Emission Tomography Methodological Aspects*, **1993**, 45-89.
- (58) B. M. Palmer, M. Sajjad, D. A. Rottenberg, *Nucl. Med. Biol.*, **1995**, 22, 241-249.
- (59) P. S. Palscjak, K. Kim, W. Meyer Jr, J. Divel, M. Der, W. C. Eckelman, *Appl. Radiat. Isot.*, **1997**, 48, 345-348.
- (60) B. Dembowski, C. Gonzalez-Lepera, *In Proceeding of the 5th workshop on target and Target Chemistry*, **1994**, 323-329.
- (61) D. M. Jewwet, M. R. Kilbourn, *J. Labelled Compds. Radiopharm.*, **1999**, 42, S873-S874.
- (62) A. A. Wilson, A. Garcia, L. Jin, S. Houle, *Nucl. Med. Biol.*, **2000**, 27, 529-532.
- (63) P. L. Jager, W. Vaalburg, J. Pruim, E. G. E. de Vries, K.-J. Langen, D. A. Piers, *J. Nucl. Med.*, **2001**, 42, 432-445.
- (64) C. Lemaire, S. Gillet, S. Guillouet, A. Plenevaux, J. Aerts, A. Luxen, *Eur. J. Org. Chem.*, **2004**, 2899-2904.
- (65) R. N. Krasikova, V. V. Zaitsev, S. M. Ametamey, O. F. Kuznetsova, O. S. Fedorova, I. K. Mosevich, Y. N. Belokon, S. Vyskocil, S. V. Shatik, M. Nader, P. A. Schubiger, *Nucl. Med. Biol.*, **2004**, 31 (5), 597-603.
- (66) L. Zhang, G. H. Tang, D. Z. Y, X. L. Tang, Y. X. Wang, *Appl. Radiat. Isot.*, **2002**, 57, 145-151.

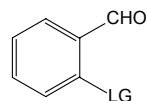
- (67) A. Al-Labadi, *Ph.D. Thesis*, University Tübingen, **2006**.
- (68) A. A. Wilson, R. F. Dannals, H. T. Ravert, H. N. Wagner, *J. Labelled Compds. Radiopharm.*, **1990**, *28* (10), 1189-99.
- (69) J. W. Skiles, M. P. Cava, *J. Org. Chem.*, **1979**, *44* (3), 409-412.
- (70) D. A. Bianchi, M. A. Cipulli, T. S. Kaufman, *Eur. J. Org. Chem.*, **2003**, 4731-4736.
- (71) M. J. Crossley, L. D. Field, A. J. Forster, M. M. Harding, S. Sternhell, *J. Am. Chem. Soc.*, **1987**, *109*, 341-348.
- (72) P. Damhaut, C. Lemaire, A. Plenevaux, C. Brihaye, L. Christiaens, D. Comar, *Tetrahedron*, **1997**, *53* (16), 5785-5796.
- (73) D. Löffler, *Ph.D. Thesis*, University Tübingen, **2008**.
- (74) A. J. Bridges, A. Lee, E. C. Maduakor, C. E. Schwartz, *Tetrahedron Lett.*, **1992**, *49*, 7499-7502.
- (75) M. Małkosza, K. Staliński, *Pol. J. Chem.*, **1999**, *73*, 151-161.
- (76) D. Gaude, R. Le Goaller, J. L. Pierre, *Synth. Commun.*, **1986**, *16* (1), 63-68.
- (77) Y. Ogata, A. Kawasaki, F. Sugiura, *Tetrahedron*, **1968**, *24*, 5001-5010.
- (78) I. W. Harvey, M. D. McFarlane, D. J. Moody, D. M. Smith, *J. Chem. Soc., Perkin Trans. 1*, **1988**, *7*, 1939-1943.
- (79) D. R. Hepburn, H. R. Hudson, *J. Chem. Soc., Perkin Trans. 1*, **1976**, 754-757.
- (80) S. Stone-Elander, N. Elander, *Appl. Radiat. Isot.*, **1993**, *44*, 889-893.
- (81) W. R. Banks, D.-R. Hwang, *Appl. Radiat. Isot.*, **1994**, *45*, 599-608.
- (82) A. Al-Labadi, K.-P. Zeller, H.-J. Machulla, *Radiochim. Acta*, **2006**, *94*, 143-146.
- (83) A. Al-Labadi, K.-P. Zeller, H.-J. Machulla, *J. Radioanal. Nucl. Chem.*, **2006**, *270*, 313-318.
- (84) Y.-S. Ding, C.-Y. Shiue, J. S. Fowler, A. P. Wolf, A. Plenevaux, *J. Fluorine Chem.*, **1990**, *48*, 189-205.
- (85) I. Ekaeva, L. Barre, M. C. Lasne, F. Gourand, *Appl. Radiat. Isot.*, **1995**, *46*, 777-782.
- (86) C. Lemaire, P. Damhaut, A. Plenevaux, R. Cantineau, L. Christiaens, M. Guillaume, *Appl. Radiat. Isot.*, **1992**, *43*, 485-494.
- (87) R. Rengan, P. K. Chakraborty, M. R. Kilbourn, *J. Labelled Compds. Radiopharm.*, **1993**, *33*, 563-572.
- (88) D.-R. Hwang, C. S. Dence, J. Gong, M. J. Welch, *Appl. Radiat. Isot.*, **1991**, *42*, 1043-1047.
- (89) C. Lemaire, M. Guillaume, L. Christiaens, A. J. Palmer, R. Cantineau, *Appl. Radiat. Isot.*, **1987**, *38*, 1033-1038.
- (90) F. W. Sweat, W. W. Epstein, *J. Org. Chem.*, **1967**, *32*, 835-838.
- (91) A. J. Mancuso, D. Swern, *Synthesis*, **1981**, 165-185.

- (92) T. T. Tidwell, *Synthesis*, **1990**, 857-870.
- (93) V. W. Pike; M. J. Kensett; D. R. Turton; S. L. Waters; D. J. Silvester, *Int. J. Appl. Radiat. Isot.*, **1990**, *41* (5), 483-492.
- (94) P. G. M. Wuts, T. W. Greene, *Green's protective groups in organic synthesis*, 4th Ed. **2007**.
- (95) C. Lemaire, M. Guillaume, R. Cantineau, L. Christiaens, *J. Nucl. Med.*, **1990**, *31*, 1247.
- (96) G. N. Reddy, M. Haerberli, H.-F. Beer, A. P. Achubiger, *Appl. Radiat. Isot.*, **1993**, *44*, 645-649.
- (97) J. Michalak, J. Gebicki, T. Baly, *J. Chem. Soc., Perkin Trans. 2*, **1993**, 1321.
- (98) F. Benoit, J. L. Holmes, *Org. Mass Spectrom.*, **1970**, *3*, 993.
- (99) T. Tierling, *Berichte des Forschungszentrums Jülich*, **2002**, Jül-3952.
- (100) H. R. Sun, S. G. DiMugno, *J. Fluorine Chem.*, **2007**, *128* (7), 806-812.
- (101) P. K. Chakraborty, M. Kilbourn, *Appl. Radiat. Isot.*, **1991**, *42*, 1209-1213.
- (102) J. M. O'Connor, J.-N. Ma, *J. Org. Chem.*, **1992**, *57*, 5075-5077.
- (103) F. H. Jardine, *Stud. Inorg. Chem.*, **1991**, *11*, 407-469.
- (104) M. C. Baird, C. J. Nyman, G. Wilkinson, *J. Chem. Soc. A*, **1968**, 348-351.
- (105) D. H. Doughty, L. H. Pignolet, *J. Am. Chem. Soc.*, **1978**, *100*, 7083-7085.
- (106) H. M. Walborsky, L. E. Allen, *J. Am. Chem. Soc.*, **1971**, *93*, 5465-5468.
- (107) K. Ohno, J. Tsuji, *J. Am. Chem. Soc.*, **1968**, *90*, 99-107.
- (108) S. Kaneko, K. Ishiwata, K. Htano, H. Omura, K. Ito, M. Senda, *Appl. Radiat. Isot.*, **1999**, *50*, 1025-1032.
- (109) J. Tsuji, K. Ohno, *Synthesis*, **1969**, 157.
- (110) C. Lemaire, P. Damhaut, A. Plenevaux, D. Comar, *J. Nucl. Med.*, **1994**, *35* (12), 1996-2002.
- (111) A. Najafi, *Nucl. Med. Biol.*, **1995**, *22*, 1996-2002.
- (112) C. W. Chang, H. E. Wang, H. M. Lin, C. S. Chtsai, J. B. Chem, R.-S. Liu, *Nucl. Med. Commun.*, **2000**, *21*, 799-802.
- (113) G. Firnau, R. Chirakal, E. S. Garnett, *J. Nucl. Med.*, **1984**, *25* (11), 1228-1233.
- (114) R. Chirakal, G. Firnau, E. S. Garnett, *J. Nucl. Med.*, **1986**, *27* (3), 417-421.
- (115) M. Diksic, S. Farrokhzad, *J. Nucl. Med.*, **1985**, *26* (11), 1314-1318.
- (116) F. Dollé, S. Demphel, F. Hinnen, D. Fournier, F. Vaufrey, C. Crouzel, *J. Labelled Compds. Radiopharm.*, **1998**, *42*, 101-114.
- (117) Y.-S. Ding, J. S. Fowler, S. J. Gately, S. J. Dewey, A. P. Wolf, A. Plenevaux, *J. Med. Chem.*, **1991**, *34*, 767.
- (118) E. Keinan, D. Perez, *J. Org. Chem.*, **1987**, *52*, 4846-4851.

- (119) A. A. Wilson, R. F. Dannals, H. T. Ravert, H. N. Wagner, *J. Labelled Compds. Radiopharm.*, **1990**, 28 (10), 1189-1199.
- (120) M. Smith, E. Elisberg, M. L. Sherrill, *J. Am. Chem. Soc.*, **1946**, 68, 1301.
- (121) T. Inoi, P. Gericke, W. J. Horton, *J. Org. Chem.*, **1962**, 27, 4597-4601.
- (122) M. Rosillo, G. Dominguez, L. Casarrubios, U. Amador, J. Perez-Castells, *J. Org. Chem.*, **2004**, 69 (6), 2084 - 2093.
- (123) E. Akguen, M. B. Glinski, K. L. Dhawan, T. Durst, *J. Org. Chem.*, **1981**, 46 (13), 2730-2734.
- (124) M. A. Galbershtam, Z. N. Budarina, *Zh. Org. Khim.*, **1969**, 5 (5), 953-956.
- (125) B. T. Phillips, G. D. Hartman, *J. Heterocycl. Chem.*, **1986**, 23 (3), 897-900.
- (126) M. Sreenivasulu, G. S. K. Rao, *Indian J. Chem., Sect. B*, **1989**, 28, 494-495.
- (127) S. Miyano, H. Fukushima, H. Inagawa, H. Hashimoto, *Bull. Chem. Soc. Jpn.*, **1986**, 59, 3285-3286.
- (128) D. M. Doleib, Y. Iskander, *J. Chem. Soc. B*, **1967**, 1154-1158.
- (129) R. J. Bergeron, M. A. Channing, G. J. Gibeily, D. M. Pillor, *J. Am. Chem. Soc.*, **1977**, 99 (15), 5146-5151.
- (130) A. L. Wilds, C. Djerassi, *J. Am. Chem. Soc.*, **1946**, 68, 1862.
- (131) S. M. Kupchan, H. C. Wormser, *J. Org. Chem.*, **1965**, 30, 3792-3800.
- (132) P. Cotellet, J.-P. Catteau, *Synth. Commun.*, **1992**, 22 (14), 2071-2076.
- (133) J.-Y. Chang, M.-F. Yang, C.-Y. Chang, C.-M. Chen, C.-C. Kuo, J.-P. Liou, *J. Med. Chem.*, **2006**, 23, 6412-6415.
- (134) A. K. Sinhababu, R. T. Borchardt, *J. Org. Chem.*, **1983**, 48, 2356-2360.
- (135) J. L. Neumeyer, B. R. Neustadt, K. H. Oh, K. K. Weinhardt, C. B. Boyce, F. J. Rosenberg, D. G. Teiger, *J. Med. Chem.*, **1973**, 16 (11), 1223-1228.
- (136) A.-J. Lin, R. S. Pardini, B. J. Lillis, A. C. Sartorelli, *J. Med. Chem.*, **1974**, 17 (7), 668-672.
- (137) M. Nikaido, R. Aslanian, F. Scavo, P. Helquist, *J. Org. Chem.*, **1984**, 49, 4740-4741.
- (138) M. R. Pavia, W. H. Moos, F. M. Hershenson, *J. Org. Chem.*, **1990**, 55 (2), 560-564.
- (139) P. Ruggli, E. Preiswerk, *Helv. Chim. Acta*, **1939**, 22, 478-495.
- (140) H. E. Albert, W. C. Sears, *J. Am. Chem. Soc.*, **1954**, 76, 4979-4983.
- (141) G. R. Allen, M. J. Weiss, *J. Org. Chem.*, **1965**, 30, 2904-2910.

7 APPENDICES

Table 7-1. ¹⁸F-labeling RCY for precursors with substitution pattern 1



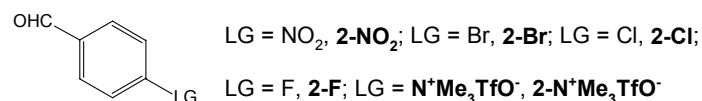
LG = NO₂, **1-NO₂**; LG = Br, **1-Br**;

LG = Cl, **1-Cl**

Nr.	RCY/% (TLC)												RCY/% (HPLC)			
	n	1 min		3 min		7 min		10 min		20 min		30 min		n	Time at max. RCY (TLC)	
		mean	SD	mean	SD	mean	SD	mean	SD	mean	SD	mean	SD		mean	SD
1-NO₂ ^a	5	80.3	1.6	84.1	0.8	84.3	0.4	81.9	4.4	82.0	4.1	82.3	3.6	--	--	--
1-NO₂ ^b	3	67.6	1.3	68.5	2.3	72.8	1.6	72.3	1.3	71.6	2.5	74.5	1.4	--	--	--
1-NO₂ ^c	3	30.1	3.9	51.3	4.9	56.7	2.2	57.4	2.9	61.0	3.5	62.1	3.6	--	--	--
1-NO₂ ^d	3	0.2	0.1	0.7	0.2	1.7	0.4	2.8	0.2	5.5	2.4	7.2	4.7	--	--	--
1-NO₂ ^e	3	64.0	4.5	45.2	3.2	34.2	2.6	31.1	3.8	24.9	2.8	19.7	2.5	--	--	--
1-Br ^e	3	1.2	0.9	1.5	0.5	1.0	0.4	1.3	0.9	1.5	1.1	1.3	0.8	--	--	--
1-Cl ^e	3	0.3	0.3	0.6	0.3	0.2	0.1	0.3	0.1	0.3	0.2	0.1	0.1	--	--	--

Labeling condition: precursor (10 mg), solvent (1 mL), 3.5 % K₂CO₃ (100 μL) and K2.2.2 (15 mg).

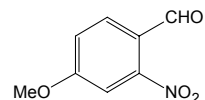
a: DMF, 140 °C; b: DMF, 100 °C; c: DMF, 60 °C; d: DMF, 25 °C; e: DMSO, 140 °C.

Table 7-2. ¹⁸F-labeling RCY for precursors with substitution pattern 2

Nr.	RCY/% (TLC)												RCY/% (HPLC)			
	n	1 min		3 min		7 min		10 min		20 min		30 min		n	Time at max. RCY (TLC)	
		mean	SD	mean	SD	mean	SD	mean	SD	mean	SD	mean	SD		mean	SD
2-NO ₂ ^a	4	12.2	1.2	25.5	1.5	35.0	1.0	39.9	3.0	38.2	3.3	34.3	2.0	--	--	--
2-Br ^a	3	0.5	0.6	0.5	0.4	0.8	0.6	0.4	0.3	0.6	0.4	0.5	0.4	--	--	--
2-Cl ^a	3	0.1	0.1	0.3	0.3	0.3	0.3	0.9	0.7	1.2	0.8	1.1	0.8	--	--	--
2-F ^a	4	55.9	4.3	48.9	4.2	41.4	2.5	36.3	5.5	29.4	5.2	12.2	8.2	--	--	--
2-N ⁺ Me ₃ TfO ⁻ ^b	3	--	--	--	--	--	--	89.3	0.6	--	--	--	--	1	87.6	--

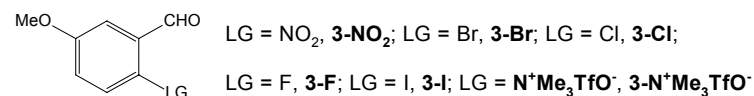
Labeling condition: precursor (10 mg), solvent (1 mL), 3.5 % K₂CO₃ (100 μL) and K2.2.2 (15 mg), at 140 °C.

a: DMSO, b: DMF.

Table 7-3. ¹⁸F-labeling RCY for 4-NO₂

Nr.	RCY/% (TLC)												RCY/% (HPLC)			
	n	1 min		3 min		7 min		10 min		20 min		30 min		n	Time at max. RCY (TLC)	
		mean	SD	mean	SD	mean	SD	mean	SD	mean	SD	mean	SD		mean	SD
4-NO ₂	4	86.5	0.6	88.3	1.8	89.0	2.4	86.3	4.2	87.0	3.7	86.6	3.3	1	85.5	--

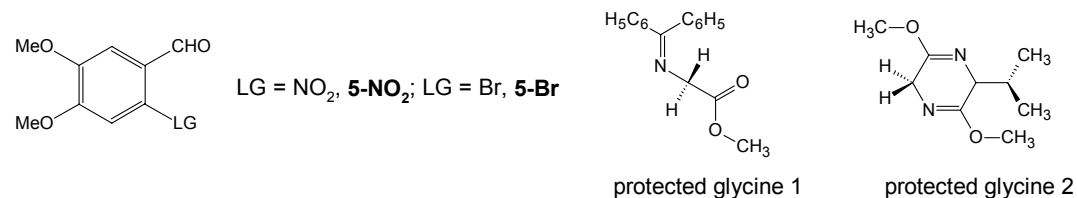
Labeling condition: precursor (10 mg), DMF (1 mL), 3.5 % K₂CO₃ (100 μL) and K2.2.2 (15 mg), at 140 °C.

Table 7-4. ^{18}F -labeling RCY for precursors with substitution pattern 3

Nr.	RCY/% (TLC)												RCY/% (HPLC)			
	n	1 min		3 min		7 min		10 min		20 min		30 min		n	Time at max. RCY (TLC)	
		mean	SD	mean	SD	mean	SD	mean	SD	mean	SD	mean	SD		mean	SD
3-NO₂ ^a	4	46.2	1.2	53.3	1.2	57.4	1.0	53.1	5.6	54.9	4.6	53.6	4.0	2	57.2	5.0
3-NO₂ ^b	3	6.2	0.9	14.4	0.8	23.8	0.8	29.8	4.0	31.3	1.9	27.3	1.3	1	27.7	--
3-NO₂ ^c	3	0.7	0.5	2.2	1.1	2.9	0.3	3.9	0.7	3.5	0.8	2.5	0.5	--	--	--
3-NO₂ ^d	2	31.6	10.0	53.1	7.6	57.6	0.8	56.9	0.3	56.8	1.2	54.1	0.1	1	60.3	--
3-NO₂ ^e	2	41.4	0.2	51.3	0.3	56.1	2.2	58.6	0.9	54.9	3.7	49.8	2.3	2	56.8	2.2
3-NO₂ ^f	2	37.8	1.8	55.4	1.9	59.1	1.0	58.9	0.3	56.8	2.0	56.8	5.0	1	57.7	--
3-NO₂ ^g	2	11.1	2.1	18.9	10.5	29.1	11.8	30.9	8.3	35.5	3.1	37.5	1.2	1	34.7	--
3-NO₂ ^h	2	8.4	1.2	15.1	3.6	20.7	3.6	22.8	3.0	25.8	7.1	25.4	2.6	1	20.2	--
3-Br ^a	4	17.3	3.2	26.3	4.9	27.0	4.6	27.6	4.3	27.1	3.4	26.1	3.9	2	24.8	1.6
3-Cl ^a	4	5.2	2.5	15.8	2.8	24.1	4.4	28.4	3.9	30.6	3.8	28.3	4.3	1	31.4	--
3-F ^a	3	78.4	0.7	82.1	1.5	83.2	2.8	80.9	1.8	75.5	2.4	71.2	2.5	1	76.5	--
3-I ^a	4	3.4	0.9	11.0	2.6	18.4	1.6	17.8	5.1	17.8	3.8	17.8	3.5	1	16.2	--
3-N⁺Me₃TfO⁻ ^a	4	31.4	0.9	35.3	4.1	23.1	3.7	19.2	2.8	15.8	3.9	13.8	1.8	1	32.1	--

Labeling condition: precursor (10 mg), solvent (1 mL), 3.5 % K₂CO₃ (100 μL) and K2.2.2 (15 mg) at 140 °C.

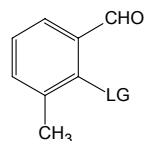
a: DMF; **b:** DMF, c.a. reaction; **c:** DMSO; **d:** DMF, addition of toluene; **e:** DMF, addition of nitrobenzene; **f:** DMF, addition of 4-nitroanisole; **g:** DMF, addition of o-nitrotoluene; **h:** DMF, addition of 4-nitro-3-methylanisole.

Table 7-5. ¹⁸F-labeling RCY for precursors with substitution pattern 5

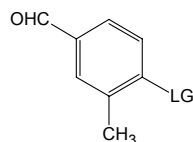
Nr.	RCY/% (TLC)												RCY/% (HPLC)			
	n	1 min		3 min		7 min		10 min		20 min		30 min		n	Time at max. RCY (TLC)	
		mean	SD	mean	SD	mean	SD	mean	SD	mean	SD	mean	SD		mean	SD
5-NO₂	5	73.2	1.7	81.5	1.0	85.2	2.2	86.8	1.8	81.7	1.0	79.7	1.6	1	86.1	--
5-NO₂^a	3	42.6	0.6	70.5	2.6	80.1	2.0	83.4	0.2	80.6	0.7	76.2	2.0	1	80.0	--
5-NO₂^b	4	17.4	2.4	24.9	4.4	25.4	4.4	29.9	3.2	28.1	3.5	23.1	3.4	--	--	--
5-NO₂^c	3	75.8	4.9	78.9	4.1	80.7	3.2	81.5	3.1	76.3	3.2	72.1	3.6	--	--	--
5-NO₂^d	2	68.1	6.5	76.2	3.7	82.2	0.4	82.1	0.5	78.2	1.6	77.4	1.8	1	81.7	--
5-NO₂^e	2	65.3	14.0	73.6	15.1	83.8	1.6	84.4	1.4	80.8	0.1	77.7	1.9	1	86.5	--
5-NO₂^f	2	70.9	4.9	79.7	3.7	82.7	0.7	84.6	4.4	80.6	2.9	77.6	2.2	1	87.5	--
5-NO₂^g	2	35.9	15.0	48.3	7.7	52.3	1.2	54.6	5.3	48.7	7.4	44.9	3.1	1	53.7	--
5-NO₂^h	2	51.4	7.9	63.5	8.6	68.5	5.1	69.2	2.6	65.8	0.1	63.9	2.1	1	70.9	--
5-Br	3	12.4	1.2	26.1	3.2	35.7	1.8	34.4	2.1	33.9	3.7	32.4	1.7	1	36.7	--

Labeling condition: precursor (10 mg), DMF (1 mL), 3.5 % K₂CO₃ (100 μL) and K2.2.2 (15 mg), 140 °C.

a: c.a. reaction; **b:** addition of protected glycine 1; **c:** addition of protected glycine 2; **d:** addition of toluene; **e:** addition of nitrobenzene; **f:** addition of 4-nitroanisole; **g:** addition of o-nitrotoluene; **h:** addition of 4-nitro-3-methylanisole.

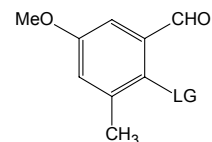
Table 7-6. ¹⁸F-labeling RCY for precursors with substitution pattern 6LG = NO₂, **6-NO₂**; LG = Br, **6-Br**;LG = Cl, **6-Cl**; LG = F, **6-F**

Nr.	RCY/% (TLC)												RCY/% (HPLC)			
	n	1 min		3 min		7 min		10 min		20 min		30 min		n	Time at max. RCY (TLC)	
		mean	SD	mean	SD	mean	SD	mean	SD	mean	SD	mean	SD		mean	SD
6-NO₂	6	--	--	--	--	47.5*	7.1*	48.2	5.3	45.6	4.9	45.0	4.5	2	48.3	2.8
6-NO₂^a	2	--	--	--	--	21.3*	4.5*	21.7	5.5	21.4	7.6	19.1	5.6	--	--	--
6-NO₂^b	2	23.6	5.1	32.7	3.4	38.6	4.3	44.9	2.9	31.6	11.2	31.4	8.8	--	--	--
6-Br	5	17.7	0.9	34.0	4.6	45.0	6.8	51.6	2.0	51.0	3.0	50.0	4.5	1	55.9	--
6-Cl	5	27.6	2.1	43.9	4.6	54.9	8.2	57.8	8.2	61.8	8.8	60.6	8.1	1	64.5	--
6-F	4	45.8	7.7	79.2	2.8	78.7	2.2	75.3	2.2	65.7	2.3	60.5	1.4	2	81.0	1.8

Labeling condition: precursor (10 mg), DMF (1 mL), 3.5 % K₂CO₃ (100 μL) and K2.2.2 (15 mg), 140 °C.*a*: addition of protected glycine 1 (see Table 7-5); *b*: addition of protected glycine 2 (see Table 7-5); *: RCY at 5 min.**Table 7-7.** ¹⁸F-labeling RCY for precursors with substitution pattern 7LG = NO₂, **7-NO₂**; LG = N⁺Me₃TfO⁻, **7-N⁺Me₃TfO⁻**

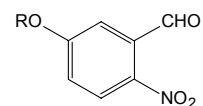
Nr.	RCY/% (TLC)												RCY/% (HPLC)			
	n	1 min		3 min		7 min		10 min		20 min		30 min		n	Time at max. RCY (TLC)	
		mean	SD	mean	SD	mean	SD	mean	SD	mean	SD	mean	SD		mean	SD
7-NO₂	4	4.5	0.7	7.5	0.7	7.5	0.7	5.6	2.0	5.4	2.3	4.0	1.6	--	--	--
7-N⁺Me₃TfO⁻	3	58.2	3.6	68.8	1.3	64.2	5.2	62.6	3.6	54.7	6.1	53.1	7.5	2	69.6	1.4

Labeling condition: precursor (10 mg), DMF (1 mL), 3.5 % K₂CO₃ (100 μL) and K2.2.2 (15 mg), 140 °C.

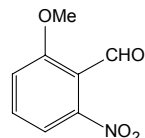
Table 7-8. ¹⁸F-labeling RCY for precursors with substitution pattern 8LG = NO₂, **8-NO₂**; LG = Br, **8-Br**;LG = Cl, **8-Cl**; LG = F, **8-F**

Nr.	RCY/% (TLC)												RCY/% (HPLC)			
	n	1 min		3 min		7 min		10 min		20 min		30 min		n	Time at max. RCY (TLC)	
		mean	SD	mean	SD	mean	SD	mean	SD	mean	SD	mean	SD		mean	SD
8-NO₂ ^a	3	1.0	0.4	1.5	0.4	2.0	0.6	1.6	0.9	2.9	0.8	2.1	0.9	2	3.7	0.2
8-NO₂ ^b	3	0.1	0.1	0.1	0.1	0.4	0.1	0.5	0.1	0.5	0.2	0.6	0.2	--	--	--
8-NO₂ ^c	2	1.4	0.1	1.9	0.2	3.0	0.1	2.6	0.4	0.5	0.2	1.9	0.4	--	--	--
8-NO₂ ^d	2	1.0	0.1	1.7	0	1.1	0.4	1.3	0.4	1.7	0.2	1.4	0.4	--	--	--
8-NO₂ ^e	3	1.2	0.4	1.4	0.7	1.6	1.0	1.7	1.0	1.9	0.6	1.7	1.2	--	--	--
8-NO₂ ^f	2	1.1	0.2	1.6	1.1	1.2	0.7	1.1	0.3	1.6	0.6	1.9	0.6	--	--	--
8-NO₂ ^g	3	0.2	0.2	0.4	0.1	1.5	0.1	1.4	0.3	2.3	0.8	1.7	0.8	--	--	--
8-NO₂ ^h	2	0.3	0.1	0.7	0.4	0.7	0.3	0.6	0.1	1.4	0.1	0.9	0.2	--	--	--
8-NO₂ ⁱ	2	0.1	0.2	0.4	0.2	0.8	0.1	0.6	0.1	0.6	0.1	0.6	0	--	--	--
8-Br ^a	3	3.6	0.2	8.4	1.1	8.6	0.9	9.7	1.5	9.0	0.2	8.4	0.8	1	12.9	--
8-Cl ^a	3	2.0	0.8	4.3	1.7	9.3	2.9	10.3	4.0	13.3	2.9	14.3	3.3	1	17.7	--
8-F ^a	4	60.9	3.6	69.0	1.0	74.6	2.4	73.2	3.1	66.1	2.6	62.2	2.5	3	78.4	3.6

Labeling condition: precursor (10 mg), solvent (1 mL), base (25 μmol) and K₂.2.2 (15 mg).a-e: base = K₂CO₃a: DMF, 140 °C; b: DMF, 120 °C; c: DMF, 160 °C; d: DMSO, 140 °C; e: DMAc, 140 °C; f: DMF, 140 °C, CeCO₃; g: DMF, 140 °C, K₂C₂O₄; h: K₂C₂O₄ / K₂CO₃ = 33:1; i: DMF, 140 °C, K₂C₂O₄ / K₂CO₃ = 1:1.

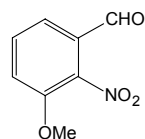
Table 7-9. ¹⁸F-labeling RCY for precursors with substitution pattern 12R = C₂H₅, **12-C₂H₅**; R = C₃H₇, **12-C₃H₇**;R = C₄H₉, **12-C₄H₉**; R = Bn, **12-Bn**; R = CF₃, **12-CF₃**

Nr.	RCY/% (TLC)												RCY/% (HPLC)			
	n	1 min		3 min		7 min		10 min		20 min		30 min		n	Time at max. RCY (TLC)	
		mean	SD	mean	SD	mean	SD	mean	SD	mean	SD	mean	SD		mean	SD
12-C₂H₅	4	42.3	4.0	56.0	1.9	63.1	3.4	61.0	3.6	57.6	1.9	52.7	2.8	2	60.9	0.9
12-C₃H₇	4	48.3	6.5	55.1	4.9	58.9	2.7	60.1	1.9	55.9	1.5	52.1	1.9	1	59.3	--
12-C₄H₉	4	34.4	0.2	56.6	1.6	59.7	2.5	59.6	2.7	56.9	1.2	54.9	2.1	1	61.5	--
12-Bn	3	14.0	2.4	33.1	1.3	46.1	0.5	49.5	0.6	48.6	3.0	46.9	2.3	1	48.3	--
12-CF₃	4	56.1	5.4	59.6	0.8	56.7	2.4	57.6	3.9	52.4	6.2	47.1	7.1	1	61.4	--

Labeling condition: precursor (10 mg), DMF (1 mL), 3.5 % K₂CO₃ (100 μL) and K2.2.2 (15 mg), 140 °C.Table 7-10. ¹⁸F-labeling RCY for 13-NO₂

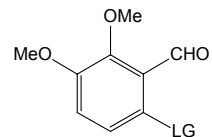
Nr.	RCY/% (TLC)												RCY/% (HPLC)			
	n	1 min		3 min		7 min		10 min		20 min		30 min		n	Time at max. RCY (TLC)	
		mean	SD	mean	SD	mean	SD	mean	SD	mean	SD	mean	SD		mean	SD
13-NO₂	4	69.5	0.4	72.3	1.1	77.6	1.4	78.5	3.5	78.9	4.0	78.7	3.1	1	75.5	--

Labeling condition: precursor (10 mg), DMF (1 mL), 3.5 % K₂CO₃ (100 μL) and K2.2.2 (15 mg), 140 °C.

Table 7-11. ¹⁸F-labeling RCY for 14-NO₂

Nr.	RCY/% (TLC)												RCY/% (HPLC)			
	n	1 min		3 min		7 min		10 min		20 min		30 min		n	Time at max. RCY (TLC)	
		mean	SD	mean	SD	mean	SD	mean	SD	mean	SD	mean	SD		mean	SD
14-NO ₂	4	45.7	3.1	64.3	2.1	70.1	3.1	67.4	5.0	67.4	2.8	66.5	4.7	1	59.2	--

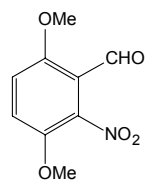
Labeling condition: precursor (10 mg), DMF (1 mL), 3.5 % K₂CO₃ (100 μL) and K2.2.2 (15 mg), 140 °C.

Table 7-12. ¹⁸F-labeling RCY for precursors with substitution pattern 15

LG = NO₂, 15-NO₂; LG = Br, 15-Br

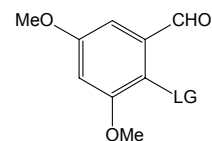
Nr.	RCY/% (TLC)												RCY/% (HPLC)			
	n	1 min		3 min		7 min		10 min		20 min		30 min		n	Time at max. RCY (TLC)	
		mean	SD	mean	SD	mean	SD	mean	SD	mean	SD	mean	SD		mean	SD
15-NO ₂	4	8.9	0.5	15.8	1.8	20.6	2.3	22.3	2.1	21.0	1.3	18.9	1.0	1	21.0	--
15-Br	4	3.5	1.0	6.4	0.5	8.8	0.8	8.2	0.7	7.5	0.9	6.6	1.2	--	--	--

Labeling condition: precursor (10 mg), DMF (1 mL), 3.5 % K₂CO₃ (100 μL) and K2.2.2 (15 mg), 140 °C.

Table 7-13. ¹⁸F-labeling RCY for 16-NO₂

Nr.	RCY/% (TLC)												RCY/% (HPLC)			
	n	1 min		3 min		7 min		10 min		20 min		30 min		n	Time at max. RCY (TLC)	
		mean	SD	mean	SD	mean	SD	mean	SD	mean	SD	mean	SD		mean	SD
16-NO ₂	4	47.8	2.0	65.2	3.6	69.6	1.6	67.9	4.1	67.0	2.5	60.8	2.4	2	76.7	4.0

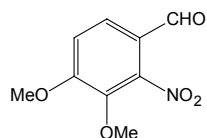
Labeling condition: precursor (10 mg), DMF (1 mL), 3.5 % K₂CO₃ (100 μL) and K2.2.2 (15 mg), 140 °C.

Table 7-14. ¹⁸F-labeling RCY for precursors with substitution pattern 17

LG = NO₂, 17-NO₂; LG = Br, 17-Br

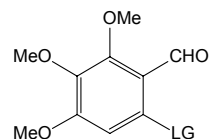
Nr.	RCY/% (TLC)												RCY/% (HPLC)			
	n	1 min		3 min		7 min		10 min		20 min		30 min		n	Time at max. RCY (TLC)	
		mean	SD	mean	SD	mean	SD	mean	SD	mean	SD	mean	SD		mean	SD
17-NO ₂	4	1.4	0.2	6.0	0.9	11.2	0.2	13.0	1.5	11.8	1.6	10.4	0.7	2	17.4	1.7
17-Br	4	1.4	0.4	3.9	0.7	5.3	1.4	5.8	1.9	5.2	1.1	4.6	0.5	1	6.8	--

Labeling condition: precursor (10 mg), DMF (1 mL), 3.5 % K₂CO₃ (100 μL) and K2.2.2 (15 mg), 140 °C.

Table 7-15. ¹⁸F-labeling RCY for 18-NO₂

Nr.	RCY/% (TLC)												RCY/% (HPLC)			
	n	1 min		3 min		7 min		10 min		20 min		30 min		n	Time at max. RCY (TLC)	
		mean	SD	mean	SD	mean	SD	mean	SD	mean	SD	mean	SD		mean	SD
18-NO ₂	4	67.0	6.4	72.9	4.7	70.7	9.7	85.9	4.2	84.8	4.7	84.6	3.6	2	87.0	1.2

Labeling condition: precursor (10 mg), DMF (1 mL), 3.5 % K₂CO₃ (100 μL) and K2.2.2 (15 mg), 140 °C.

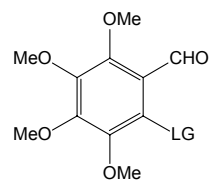
Table 7-16. ¹⁸F-labeling RCY for precursors with substitution pattern 19

LG = NO₂, 19-NO₂; LG = Br, 19-Br

Nr.	RCY/% (TLC)												RCY/% (HPLC)			
	n	1 min		3 min		7 min		10 min		20 min		30 min		n	Time at max. RCY (TLC)	
		mean	SD	mean	SD	mean	SD	mean	SD	mean	SD	mean	SD		mean	SD
19-NO ₂	4	66.3	2.0	73.8	6.0	80.4	4.3	81.5	2.4	74.0	4.8	65.9	4.1	3	79.0	5.9
19-NO ₂ ^a	4	17.4	7.3	32.4	6.8	39.1	6.1	43.2	2.8	41.4	3.8	36.1	3.2	1	44.4	--
19-Br	4	2.9	0.4	8.7	1.0	15.1	1.2	18.2	1.5	18.7	1.2	19.0	1.4	1	18.0	--

Labeling condition: precursor (10 mg), DMF (1 mL), 3.5 % K₂CO₃ (100 μL) and K2.2.2 (15 mg), 140 °C.

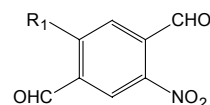
a: c.a. reaction.

Table 7-17. ¹⁸F-labeling RCY for precursors with substitution pattern 20LG = NO₂, **20-NO₂**; LG = Br, **20-Br**

Nr.	RCY/% (TLC)												RCY/% (HPLC)			
	n	1 min		3 min		7 min		10 min		20 min		30 min		n	Time at max. RCY (TLC)	
		mean	SD	mean	SD	mean	SD	mean	SD	mean	SD	mean	SD		mean	SD
20-NO₂	5	38.0	2.0	43.7	1.6	47.6	4.5	45.3	3.5	44.2	5.8	41.0	6.9	3	47.2	5.9
20-NO₂^a	4	7.5	1.1	19.1	2.1	27.1	3.3	31.4	3.4	30.1	3.1	23.7	3.7	1	26.8	--
20-Br	5	2.0	0.5	5.6	0.8	9.0	1.3	10.3	0.7	10.5	0.6	10.0	1.3	1	10.8	--

Labeling condition: precursor (10 mg), DMF (1 mL), 3.5 % K₂CO₃ (100 μL) and K2.2.2 (15 mg), 140 °C.

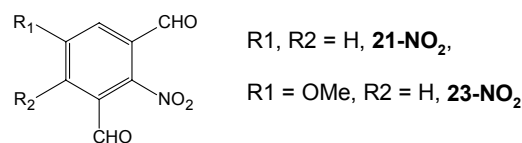
a: c.a. reaction.

Table 7-18. ¹⁸F-labeling RCY for precursors with substitution pattern 22 or 24R1 = H, **22-NO₂**; R1 = OMe, **24-NO₂**

Nr.	RCY/% (TLC)												RCY/% (HPLC)			
	n	1 min		3 min		7 min		10 min		20 min		30 min		n	Time at max. RCY (TLC)	
		Mean	SD	mean	SD	mean	SD	mean	SD	mean	SD	mean	SD		mean	SD
22-NO₂^a	4	36.5	2.1	56.7	5.6	59.8	3.0	56.9	3.1	35.8	6.3	5.4	2.8	3	59.3	5.5
22-NO₂^b	4	3.1	1.3	12.8	2.3	25.1	3.6	28.2	2.4	24.8	3.9	13.3	4.7	--	--	--
22-NO₂^c	3	2.6	0.1	4.1	0.1	6.8	1.4	7.2	1.1	6.2	0.8	2.7	1.0	--	--	--
24-NO₂^a	2	7.7	0.4	16.5	1.8	25.8	4.4	31.9	1.4	29.7	2.4	13.2	0.7	1	29.3	--

Labeling condition: precursor (10 mg), DMF (1 mL), 3.5 % K₂CO₃ (100 μL) and K2.2.2 (15 mg).

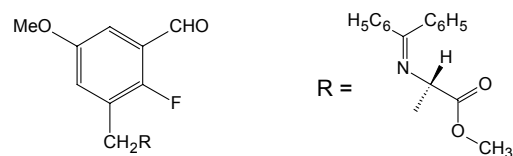
a: 140 °C; b: 120 °C; c: 100 °C.

Table 7-19. ¹⁸F-labeling RCY for precursors with substitution pattern 21 or 23

Nr.	RCY/% (TLC)												RCY/% (HPLC)			
	n	1 min		3 min		7 min		10 min		20 min		30 min		n	Time at max. RCY (TLC)	
		mean	SD	mean	SD	mean	SD	mean	SD	mean	SD	mean	SD		mean	SD
21-NO₂^a	3	83.9	3.2	69.7	2.7	44.8	2.6	22.9	2.1	1.0	0	0.8	0.3	1	84.9	--
21-NO₂^b	3	83.1	3.0	82.3	2.9	70.7	3.4	68.0	5.0	59.1	6.0	47.8	4.2	--	--	--
21-NO₂^c	4	86.7	3.7	85.6	4.7	82.1	5.1	80.5	6.6	80.8	5.8	79.7	6.5	--	--	--
21-NO₂^d	4	68.1	1.6	75.7	5.1	78.2	3.0	78.1	1.3	77.5	3.1	77.6	2.2	2	83.2	0.7
23-NO₂^a	4	75.3	0.5	79.3	0.2	78.3	2.5	79.7	0.6	73.3	1.5	66.3	2.5	2	79.4	0.2

Labeling condition: precursor (10 mg), DMF (1 mL), 3.5 % K₂CO₃ (100 μL) and K2.2.2 (15 mg).

a: 140 °C; b: 100 °C; c: 60 °C; d: 25 °C.

Table 7-20. ¹⁸F-labeling RCY for 27-F

Nr.	RCY/% (TLC)												RCY/% (HPLC)			
	n	1 min		3 min		7 min		10 min		20 min		30 min		n	Time at max. RCY (TLC)	
		mean	SD	mean	SD	mean	SD	mean	SD	mean	SD	mean	SD		mean	SD
27-F	4	3.5	0.5	4.3	0.6	2.7	1.2	1.6	0.9	0.8	0.2	0.1	0	2	4.6	0.3

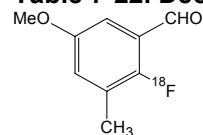
Labeling condition: precursor (10 mg), DMF (1 mL), 3.5 % K₂CO₃ (100 μL) and K2.2.2 (15 mg), 140 °C.

Table 7-21. ¹⁸F-labeling RCY for nitrobenzene, 4-nitroanisole and 3-nitrobenzaldehyde

Precursor	RCY/% (HPLC)		
	n	30 min	
		mean	SD
nitrobenzene	4	1.0	0.1
4-nitroanisole	4	0	--
3-nitrobenzaldehyde	3	7.0*	1.0*

Labeling condition: precursor (10 mg), DMF (1 mL), 3.5 % K₂CO₃ (100 μL) and K2.2.2 (15 mg), at 140 °C, after 30 min, the labeling solution was cooled down and 10 μL of this solution was injected into HPLC.

*: reaction time 10 min.

Table 7-22. Decarbonylation yield for 8-¹⁸F

Nr.	Yield/% (TLC)															Yield/% (HPLC)		
	n	1 min		3 min		7 min		10 min		20 min		30 min		60 min		n	30 min	
		mean	SD	Mean	SD	mean	SD	mean	SD	mean	SD	mean	SD	mean	SD		mean	SD
8-F ^{+,a}	4	0.6	0.3	7.8	1.3	32.5	2.9	61.3	3.0	62.1	1.7	57.9	4.7	58.7	1.0	1	64.5	--
8-F ^{+,b}	4	1.0	0.2	19.2	6.2	52.5	1.1	69.4	1.8	81.0	0.8	84.6	1.0	88.7	3.0	1	92.4	--
8-F ^{+,c}	3	1.3	0	23.8	3.2	27.7	3.2	28.7	2.4	29.8	3.0	32.0	2.2	33.3	2.1	1	25	--
8-F ^{+,d}	3	0.4	0.5	23.0	0.6	54.4	1.6	63.7	1.4	64.7	1.3	64.4	1.9	61.6	2.0	1	57.5	--
8-F ^{+,e}	3	1.3	0.3	13.8	2.0	46.3	4.7	53.3	1.2	52.6	1.7	52.2	4.0	--	--	1	51.8	--
8-F ^{+,f}	3	0.6	0.2	3.1	0.6	8.3	0.9	13.6	0.9	25.2	3.1	32.6	4.1	47.1	2.7	--	--	--
8-F ^{+,g}	4	1.0	0.2	7.4	0.8	28.0	3.2	38.4	4.7	62.4	4.3	69.5	5.4	76.9	7.9	1	72.7	
8-F ^{+,h}	3	5.2	1.6	78.7	0.6	85.5	2.4	89.1	1.3	88.1	1.0	88.6	2.9	90.2	3.7	2	95.5*	0.7
8-F ^{+,i}	2	0.8	0.5	1.7	0.6	2.2	0.4	3.5	0	3.3	0.1	3.5	0.1	3.3	0.4	--	--	--
8-F ^{+,j}	3	1.2	0.7	30.2	10.4	90.4	0.3	88.3	1.4	86.5	1.3	87.2	0.7	--	--	1	94.8**	--

⁺: Precursor for ¹⁸F-labeling reaction.

*: Decarbonylation yield at 10 min, **: Decarbonylation yield at 20 min.

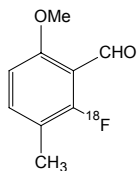
Decarbonylation condition:

a-e: in 1mL solvent with 2 molar eq.catalyst at 150 °C. **a**: dioxan, **b**: benzonitrile, **c**: DMF, **d**: DMSO, **e**: toluene.

f-h: in 1mL benzonitrile with 2 molar eq.catalyst **f**: 100 °C, **g**: 120 °C, **h**: 180 °C.

i-j: in 1mL benzonitrile with X molar eq.catalyst at 150 °C. **i**: 1 molar eq.catalyst, **j**: 3 molar eq.catalyst.

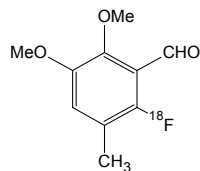
(Amount of the catalyst was based on quantity of labelling precursor)

Table 7-23. Decarbonylation yield for 9-¹⁸F

Nr.	Yield/% (TLC)														Yield/% (HPLC)			
	n	1 min		3 min		7 min		10 min		20 min		30 min		60 min		n	30 min	
		mean	SD	mean	SD	mean	SD	mean	SD	mean	SD	mean	SD	mean	SD		mean	SD
9-F ⁺	3	3.0	1.6	50.7	3.4	75.2	1.2	83.4	2.5	86.5	1.8	86.7	2.5	88.4	2.9	1	92.0	--
9-NO ₂ ⁺	3	1.5	0.9	53.0	4.3	88.8	1.4	88.7	2.8	88.4	1.7	88.9	1.2	89.1	0.6	1	95.0	--
9-Br ⁺	3	4.7	1.5	68.4	1.9	81.0	3.9	82.0	2.9	84.7	2.5	88.7	3.3	88.4	1.6	1	90.8	--
9-Cl ⁺	3	2.6	0.2	55.8	2.9	78.2	2.3	84.7	2.5	85.2	2.5	86.9	2.3	88.0	3.4	--	--	--

+: Precursor with different LG for ¹⁸F-labeling reaction.

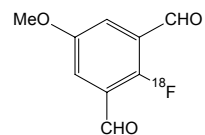
Decarbonylation condition: in 1mL benzonitrile with 2 molar eq.catalyst at 150 °C (Amount of the catalyst was based on quantity of labelling precursor).

Table 7-24. Decarbonylation yield for 11-¹⁸F

Nr.	Yield/% (TLC)														Yield/% (HPLC)			
	n	1 min		3 min		7 min		10 min		20 min		30 min		60 min		n	30 min	
		mean	SD	mean	SD	mean	SD	mean	SD	mean	SD	mean	SD	mean	SD		mean	SD
11-F ⁺	3	3.9	1.4	51.4	2.6	81.1	4.0	84.2	2.6	88.9	2.2	91.8	1.6	92.5	0.6	1	97.0	--

+: Precursor for ¹⁸F-labeling reaction.

Decarbonylation condition: in 1mL benzonitrile with 2 molar eq.cat at 150 °C (Amount of the catalyst was based on quantity of labelling precursor).

Table 7-25. Decarbonylation yield for 23-¹⁸F

Nr.	Yield/% (TLC)														Yield/% (HPLC)			
	n	1 min		3 min		7 min		10 min		20 min		30 min		60 min		n	Time at max. RCY (TLC)	
		mean	SD	mean	SD	mean	SD	mean	SD	mean	SD	mean	SD	mean	SD			
23-NO ₂ ^{+, a}	4	0	0	19.3	1.5	63.9	2.1	67.1	3.4	67.1	3.1	66.4	1.5	--	--	2	66.9	0.2
23-NO ₂ ^{+, b}	3	0	0	18.8	2.2	35.0	2.9	50.1	0.8	60.3	3.7	62.6	0	--	--	1	59.0	--
23-NO ₂ ^{+, c}	2	0	0	4.2	1.4	26.6	0.9	42.2	1.0	52.2	1.4	61.0	1.3	--	--	2	61.5	0.3

+: Precursor for ¹⁸F-labeling reaction.

Decarbonylation condition: 1mL benzonitrile. **a**: 4 molar eq.catalyst at 150 °C; **b**: 4 molar eq.catalyst at 120 °C; **c**: 3 molar eq.catalyst at 150 °C.

(Amount of the catalyst was based on quantity of labelling precursor)

Meine akademische Ausbildung verdanke ich:

X.-N. Liu, H.-J. Machulla, P.-K. Ouyang, G. Reischl, R.-Q. Wei, K.-P. Zeller.

Lebenslauf

Bin Shen

- 15. Mai. 1979** geboren in Nanjing, Provinz Jiangsu, China
- Sep. 1985- Jul.1991** Grundschule im Nanjing
- Sep. 1991- Jul.1997** Mittelschule im Nanjing
- Sep. 1997- Mai. 2001** Studium der Biochemie an der Fakultät für Bioengineering der Nanjing Universität of Technology
- Jul. 2001** Bachelor of Engineering
- Sep. 2001- Mai. 2004** Anfertigung der Arbeit zum Master of Science unter Anleitung von Prof. Dr. X.-N. Liu mit dem Thema „*Studies on the Flexible Immobilization of Papain*“ an der Nanjing Universität of Technology
- Jun. 2004** Master of Engineering
- Feb. 2005- Mai. 2008** Experimenteller Teil der Dissertation in der Sektion Radiopharmazie des Universitätsklinikums der Eberhard-Karls-Universität Tübingen unter Leitung von Prof. Dr. H.-J. Machulla über „*Studies on the Nucleophilic Aromatic ¹⁸F-Fluorination - From Model Compounds to Aromatic Amino Acids -*“
- Feb. 2007- zur Zeit** Anstellung als Wissenschaftlicher Mitarbeiter am Universitätsklinikum Tübingen

